# FINITE STRIP WITH RIGID ENDS AND EDGE NOTCHES

**A THESIS SUBMITTED TO**
**THE GRADUATE SCHOOL OF NATURAL AND APPLIED SCIENCES**
**OF**
**MIDDLE EAST TECHNICAL UNIVERSITY**

**BY**

**DENİZ ERÖZKAN**

**IN PARTIAL FULFILLMENT OF THE REQUIREMENTS**
**FOR**
**THE DEGREE OF MASTER OF SCIENCE**
**IN**
**ENGINEERING SCIENCES**

**AUGUST 2009**

Approval of the thesis:

**FINITE STRIP WITH RIGID ENDS AND EDGE NOTCHES**

submitted by **DENİZ ERÖZKAN** in partial fulfillment of the requirements for the degree of **Master of Science in Engineering Sciences Department, Middle East Technical University** by,

Prof. Dr. Canan Özgen
Dean, **Graduate School of Natural and Applied Sciences** _____

Prof. Dr. Turgut Tokdemir
Head of Department, **Engineering Sciences** _____

Prof. Dr. M. Ruşen Geçit
Supervisor, **Engineering Sciences Dept., METU** _____

**Examining Committee Members**

Prof. Dr. Turgut Tokdemir _____
Engineering Sciences Dept., METU

Prof. Dr. M. Ruşen Geçit _____
Engineering Sciences Dept., METU

Prof. Dr. Ahmet Nedim Eraslan _____
Engineering Sciences Dept., METU

Prof. Dr. M. Polat Saka _____
Engineering Sciences Dept., METU

Assoc. Prof. Dr. Serkan Dağ _____
Mechanical Engineering Dept., METU

**Date: 26.08.2009**

**I hereby declare that all information in this document has been obtained and presented in accordance with academic rules and ethical conduct. I also declare that, as required by these rules and conduct, I have fully cited and referenced all material and results that are not original to this work.**

Name, Last name: Deniz Erözkan

Signature :

## ABSTRACT

### FINITE STRIP WITH RIGID ENDS AND EDGE NOTCHES

Erözkan, Deniz

M.S., Department of Engineering Sciences

Supervisor : Prof. Dr. M. Ruşen Geçit

August 2009, 171 pages

This study considers a symmetrical finite strip with a length of *2L* and a width of *2h* containing two collinear edge cracks located at the center of the strip. Each edge crack has a width *h–a*. Two ends of the finite strip are bonded to two rigid plates through which uniformly distributed axial tensile loads of intensity $p_0$ are applied. The finite strip is assumed to be made of a linearly elastic and isotropic material. For the solution of the finite strip problem, an infinite strip of width *2h* containing two internal cracks of width *b–a* at *y=0* and two rigid inclusions of width *2c* at $y=\pm L$ is considered. When the width of rigid inclusions approach the width of the strip, the portion of the infinite strip between the inclusions becomes identical with the finite strip problem. When the outer edges of the internal cracks approach the edge of the strip, they become edge cracks (notches). Governing equations are solved by using Fourier transform technique and these equations are reduced to a system of three singular integral equations. By using Gauss-Lobatto and Gauss-Jacobi integration formulas, these three singular integral equations are converted to a system of linear algebraic equations which is solved numerically.



Keywords: Finite Strip, Edge Crack, Rigid Inclusion, Stress Intensity Factor.

# ÖZ

## RİJİT UÇLARI VE KENAR ÇENTİKLERİ OLAN SONLU UZUNLUKTAKİ ŞERİT

Erözkan, Deniz
Yüksek Lisans, Mühendislik Bilimleri Bölümü
Tez Yöneticisi : Prof. Dr. M. Ruşen Geçit

Ağustos 2009, 171 sayfa

Bu çalışma, ortasında iki kenar çatlağı (çentik) bulunan *2L* uzunluğunda ve *2h* genişliğinde simetrik, bir şeridi incelemektedir. Çentiklerin herbiri *h–a* genişliğindedir. Şeridin iki ucuna rijit levhalar yapıştırılmıştır. Bu levhalar vasıtasıyla, şeride, eksenel ve $p_0$ şiddetinde düzgün yayılı çekme kuvveti uygulanmaktadır. Şeridin, lineer elastik ve izotrop bir malzemeden imal edildiği kabul edilmektedir. Sonlu uzunluktaki şerit problemi için, *y=0* düzleminde *b–a* genişliğinde iki iç çatlak ve *y*=± *L* düzlemlerinde *2c* genişliğinde iki rijit enklüzyonun bulunduğu, *2h* genişliğinde sonsuz uzunluktaki bir şerit ele alınmaktadır. Rijit enklüzyonların genişliği şeridin genişliğine ulaştığında, enklüzyonlar arasında kalan şerit parçası sonlu uzunlukta bir şerit problemine dönüşmektedir. İç çatlakların dış kenarları şeridin kenarlarına ulaştğında da, iç çatlaklar kenar çatlak (çentik) halini almaktadır. Genel denklemler Fourier dönüşüm tekniği kullanılarak çözülmekte ve bu denklemler üç tekil integral denkleme indirgenmektedir. Bu üç integral denklem Gauss-Lobatto ve Gauss-Jacobi integrasyon formülleri kullanılarak bir lineer cebir denklem takımına çevrilmekte ve sayısal olarak çözülmektedir.

Anahtar Sözcükler: Sonlu Şerit, Çentik, Rijit Enklüzyon, Gerilme Şiddeti Katsayısı.

To My Family,

*Orhan, Naile, Erkan Erözkan*

## ACKNOWLEDGMENTS

I would like to express my gratitude to my advisor Prof. Dr. M. Ruşen Geçit for his inspiring guidance, constant encouragement, generous help and patience at every stage of this thesis.

I would like to thank you my advisory committee members Prof. Dr. Turgut Tokdemir, Prof. Dr. Ahmet N. Eraslan, Prof. Dr. M. Polat Saka and Assoc. Prof. Dr. Serkan Dağ for their suggestions, comments and supports.

Many people guided me throughout this study and I would especially like to mention, Architect Mustafa Kemal Altan, owner of Altan Design & Consultancy Ltd. Co. for his guidance and support.

Further, I must extend thanks to my friends Özge Erdemli, Erkan Doğan and Ayşe Ruşen Ünsal for their supports.

Special thanks to my father, Orhan Erözkan, my mother Naile Erözkan and my brother, Erkan Erözkan for their endless love and emotional support.

## TABLE OF CONTENTS

ABSTRACT.....iv
ÖZ.....v
DEDICATION.....vi
ACKNOWLEDGMENTS.....vii
TABLE OF CONTENTS.....viii
LIST OF FIGURES.....xi
NOMENCLATURE.....xvi

CHAPTER
1. INTRODUCTION..... 1
1.1. Literature Review..... 2
1.2. A Brief Definition of the Problem and the Method of Solution..... 6

2. INFINITE STRIP PROBLEM..... 8
2.1. Formulation of the Problem..... 8
2.1.1. Uniform Solution..... 12
2.1.2. Perturbation Solution..... 13
2.1.2.1. An Infinite Medium Subjected to Arbitrary Symmetric Loads..... 14
2.1.2.2. An Infinite Medium Having Two Collinear Cracks..... 15
2.1.2.3 An Infinite Medium Having Two Rigid Inclusions..... 19
2.1.2.4 General Expressions for Perturbation Problem..... 29
2.1.3 Infinite Strip Problem (Superposition) ..... 30

3. INTEGRAL EQUATIONS..... 36

3.1 Derivation of Integral Equations..... 36

4. SOLUTION OF INTEGRAL EQUATIONS..... 47
4.1 Infinite Strip Having Two Internal Cracks and Two Internal Rigid Inclusions..... 47
4.2 Infinite Strip Having Two Internal Rigid Inclusions (without Cracks)..... 52
4.3 Infinite Strip Having Two Internal Cracks (without Inclusions) ..... 53
4.4 Infinite Strip Having Edge Cracks and Two Internal Rigid Inclusions..... 55
4.5 Finite Strip Having Two Internal Cracks..... 57
4.6 Finite Strip Having Edge Cracks..... 60

5. STRESS INTENSITY FACTORS..... 62
5.1 Stress Intensity Factors at the Edges of the Crack..... 62
5.2 Stress Intensity Factors at the Edges of the Rigid Inclusions and at the Corners of the Finite Strip..... 65

6. RESULTS AND CONCLUSIONS..... 69
6.1 Numerical Results..... 69
6.1.1 Infinite Strip Problem..... 69
6.1.1.1 Two Internal Cracks and Internal Inclusions in an Infinite Strip..... 69
6.1.1.2 Edge Cracks and Internal Inclusions in an Infinite Strip..... 72
6.1.2 Finite Strip Problem..... 73
6.1.2.1 Two Internal Cracks in a Finite Strip..... 73
6.1.2.2 Edge Cracks in a Finite Strip..... 76
6.2 Conclusions..... 78
6.3 Suggestion for Further Studies..... 79
REFERENCES.....139

APPENDICES.....142
A.....142
B.....143
C.....145
D.....148
E.....152
F.....161
G.....171

## LIST OF FIGURES

FIGURES


Figure 1.1 Infinite strip yielding finite strip problem.....7

Figure 2.1 Superposition.....10

Figure 2.2 Schematic representation of general formulation..... 11

Figure 4.1 Geometry of an infinite strip with two internal collinear cracks and two rigid inclusions..... 47

Figure 4.2 Geometry of an infinite strip having two rigid inclusions..... 53

Figure 4.3 Geometry of an infinite strip with two internal symmetrical cracks..... 54

Figure 4.4 Geometry of an infinite strip with two edge cracks and rigid inclusions..... 56

Figure 4.5 Geometry of a finite strip with two internal symmetrical cracks and rigid inclusions.....57

Figure 4.6 Geometry of a finite strip with two edge cracks and rigid inclusions..... 60

Figure 6.1 Normalized Mode I stress intensity factor $\bar{k}_{1a}$ at inner edge of crack when $b/h = 0.9$ $L/h = 0.5$ $c/h = 0.5$ (Plane strain)..... 80

Figure 6.2 Normalized Mode I stress intensity factor $\bar{k}_{1a}$ at inner edge of crack when $a/h = 0.1$ $L/h = 0.5$ $c/h = 0.5$ (Plane strain)..... 81

Figure 6.3 Normalized Mode I stress intensity factor $\bar{k}_{1a}$ at inner edge of crack when $a/h = 0.1$ $b/h = 0.9$ $L/h = 0.5$ (Plane strain)..... 82

Figure 6.4 Normalized Mode I stress intensity factor $\bar{k}_{1a}$ at inner edge of crack when $a/h = 0.1$ $b/h = 0.9$ $\nu = 0.3$ (Plane strain)..... 83

Figure 6.5 Normalized Mode I stress intensity factor $\bar{k}_{1b}$ at outer edge of crack when $b/h = 0.9$ $L/h = 0.5$ $c/h = 0.5$ (Plane strain)..... 84

Figure 6.6 Normalized Mode I stress intensity factor $\bar{k}_{1b}$ at outer edge of crack when $a/h = 0.1$ $L/h = 0.5$ $c/h = 0.5$ (Plane strain)..... 85

Figure 6.7 Normalized Mode I stress intensity factor $\bar{k}_{1b}$ at outer edge of crack when $a/h = 0.1$ $b/h = 0.9$ $L/h = 0.5$ (Plane strain)..... 86

Figure 6.8 Normalized Mode I stress intensity factor $\bar{k}_{1b}$ at outer edge of crack when $a/h = 0.1$ $b/h = 0.9$ $\nu = 0.3$ (Plane strain)..... 87

Figure 6.9 Normalized Mode I stress intensity factor $\bar{k}_{1c}$ at edge of inclusion when $b/h = 0.9$ $L/h = 0.5$ $c/h = 0.5$ (Plane strain)..... 88

Figure 6.10 Normalized Mode I stress intensity factor $\bar{k}_{1c}$ at edge of inclusion when $a/h = 0.1$ $L/h = 0.5$ $c/h = 0.5$ (Plane strain)..... 89

Figure 6.11 Normalized Mode I stress intensity factor $\bar{k}_{1c}$ at edge of inclusion when $a/h = 0.1$ $b/h = 0.9$ $L/h = 0.5$ (Plane strain)..... 90

Figure 6.12 Normalized Mode I stress intensity factor $\bar{k}_{1c}$ at edge of inclusion when $a/h = 0.1$ $b/h = 0.9$ $\nu = 0.3$ (Plane strain)..... 91

Figure 6.13 Normalized Mode II stress intensity factor $\bar{k}_{2c}$ at edge of inclusion when $b/h = 0.9$ $L/h = 0.5$ $c/h = 0.5$ (Plane strain)..... 92

Figure 6.14 Normalized Mode II stress intensity factor $\bar{k}_{2c}$ at edge of inclusion when $a/h = 0.1$ $L/h = 0.5$ $c/h = 0.5$ (Plane strain)..... 93

Figure 6.15 Normalized Mode II stress intensity factor $\bar{k}_{2c}$ at edge of inclusion when $a/h = 0.1$ $b/h = 0.9$ $L/h = 0.5$ (Plane strain)..... 94

Figure 6.16 Normalized Mode II stress intensity factor $\bar{k}_{2c}$ at edge of inclusion when $a/h = 0.1$ $b/h = 0.9$ $\nu = 0.3$ (Plane strain)..... 95

Figure 6.17 Normalized Mode I stress intensity factor $\bar{k}_{1a}$ for edge crack when $L/h = 0.5$ and $c/h = 0.5$ (Plane strain)..... 96

Figure 6.18 Normalized Mode I stress intensity factor $\bar{k}_{1a}$ for edge crack when $a/h = 0.5$ and $L/h = 0.5$ (Plane strain)..... 97

Figure 6.19 Normalized Mode I stress intensity factor $\bar{k}_{1c}$ at edge of inclusion when $L/h = 0.5$ and $c/h = 0.5$ (Plane strain)..... 98

Figure 6.20 Normalized Mode I stress intensity factor $\bar{k}_{1c}$ at edge of inclusion when $a/h = 0.5$ and $L/h = 0.5$ (Plane strain)..... 99

Figure 6.21 Normalized Mode II stress intensity factor $\bar{k}_{2c}$ at edge of inclusion when $L/h = 0.5$ and $c/h = 0.5$ (Plane strain).....100

Figure 6.22 Normalized Mode II stress intensity factor $\bar{k}_{2c}$ at edge of inclusion when $a/h = 0.5$ and $L/h = 0.5$ (Plane strain).....101

Figure 6.23 Normalized Mode I stress intensity factor $\bar{k}_{1a}$ at inner edge of crack in finite strip when $b/h = 0.9$ and $L/h = 1$ (Plane strain)..... 102

Figure 6.24 Normalized Mode I stress intensity factor $\bar{k}_{1a}$ at inner edge of crack in finite strip when $b/h = 0.9$ and $L/h = 0.5$ (Plane strain)..... 103

Figure 6.25 Normalized Mode I stress intensity factor $\bar{k}_{1a}$ at inner edge of crack in finite strip when $a/h = 0.1$ and $L/h = 0.5$ (Plane strain)..... 104

Figure 6.26 Normalized Mode I stress intensity factor $\bar{k}_{1a}$ at inner edge of crack in finite strip when $b/h = 0.9$ and $v = 0.3$ (Plane strain)..... 105

Figure 6.27 Normalized Mode I stress intensity factor $\bar{k}_{1a}$ at inner edge of crack in finite strip when $a/h = 0.1$ and $v = 0.3$ (Plane strain)..... 106

Figure 6.28 Normalized Mode I stress intensity factor $\bar{k}_{1b}$ at outer edge of crack in finite strip when $b/h = 0.9$ and $L/h = 1$ (Plane strain)..... 107

Figure 6.29 Normalized Mode I stress intensity factor $\bar{k}_{1b}$ at outer edge of crack in finite strip when $b/h = 0.9$ and $L/h = 0.5$ (Plane strain)..... 108

Figure 6.30 Normalized Mode I stress intensity factor $\bar{k}_{1b}$ at outer edge of crack in finite strip when $a/h = 0.1$ and $L/h = 0.5$ (Plane strain)..... 109

Figure 6.31 Normalized Mode I stress intensity factor $\bar{k}_{1b}$ at outer edge of crack in finite strip when $b/h = 0.9$ and $v = 0.3$ (Plane strain)..... 110

Figure 6.32 Normalized Mode I stress intensity factor $\bar{k}_{1b}$ at outer edge of crack in finite strip when $a/h = 0.1$ and $v = 0.3$ (Plane strain)..... 111

Figure 6.33 Normalized Mode I stress intensity factor $\bar{k}_{1h}$ at corner of finite strip when $a/h$ = 0.1 and $L/h$ = 1 (Plane strain)..... 112

Figure 6.34 Normalized Mode I stress intensity factor $\bar{k}_{1h}$ at corner of finite strip when $b/h$ = 0.9 and $L/h$ = 1 (Plane strain)..... 113

Figure 6.35 Normalized Mode I stress intensity factor $\bar{k}_{1h}$ at corner of finite strip when $b/h$ = 0.9 and $L/h$ = 0.5 (Plane strain)..... 114

Figure 6.36 Normalized Mode I stress intensity factor $\bar{k}_{1h}$ at corner of finite strip when $a/h$ = 0.1 and $L/h$ = 0.5 (Plane strain)..... 115

Figure 6.37 Normalized Mode I stress intensity factor $\bar{k}_{1h}$ at corner of finite strip when $b/h$ = 0.9 and $v$= 0.3 (Plane strain)..... 116

Figure 6.38 Normalized Mode I stress intensity factor $\bar{k}_{1h}$ at corner of finite strip when $a/h$ = 0.1 and $v$= 0.3 (Plane strain)..... 117

Figure 6.39 Normalized Mode II stress intensity factor $\bar{k}_{2h}$ at corner of finite strip when $a/h$ = 0.1 and $L/h$ = 1 (Plane strain)..... 118

Figure 6.40 Normalized Mode II stress intensity factor $\bar{k}_{2h}$ at corner of finite strip when $b/h$ = 0.9 and $L/h$ = 1 (Plane strain)..... 119

Figure 6.41 Normalized Mode II stress intensity factor $\bar{k}_{2h}$ at corner of finite strip when $b/h$ = 0.9 and $L/h$ = 0.5 (Plane strain)..... 120

Figure 6.42 Normalized Mode II stress intensity factor $\bar{k}_{2h}$ at corner of finite strip when $a/h$ = 0.1 and $L/h$ = 0.5 (Plane strain)..... 121

Figure 6.43 Normalized Mode II stress intensity factor $\bar{k}_{2h}$ at corner of finite strip when $b/h$ = 0.9 and $v$ = 0.3 (Plane strain)..... 122

Figure 6.44 Normalized Mode II stress intensity factor $\bar{k}_{2h}$ at corner of finite strip when $a/h$ = 0.1 and $v$ = 0.3 (Plane strain)..... 123

Figure 6.45 Normalized Mode I stress intensity factor $\bar{k}_{1a}$ for edge crack in finite strip when $L/h$ = 1 (Plane strain)..... 124

Figure 6.46 Normalized Mode I stress intensity factor $\bar{k}_{1a}$ for edge crack in finite strip when $L/h$ = 2 (Plane strain)..... 125

Figure 6.47 Normalized Mode I stress intensity factor $\bar{k}_{1a}$ for edge crack in finite strip when $v$ = 0.3 (Plane strain)..... 126

Figure 6.48 Normalized Mode I stress intensity factor $\bar{k}_{1a}$ for edge crack in finite strip when $\nu$ = 0.45 (Plane strain)..... 127
Figure 6.49 Normalized Mode I stress intensity factor $\bar{k}_{1a}$ for edge crack in finite strip when $\nu$ = 0.3 (Plane strain)..... 128
Figure 6.50 Normalized Mode I stress intensity factor $\bar{k}_{1a}$ for edge crack in finite strip when $a/h$ = 0.1 (Plane strain)..... 129
Figure 6.51 Normalized Mode I stress intensity factor $\bar{k}_{1a}$ for edge crack in finite strip when $a/h$ = 0.5 (Plane strain)..... 130
Figure 6.52 Normalized Mode I stress intensity factor $\bar{k}_{1h}$ at corner of finite strip when $L/h$ = 0.5 (Plane strain)..... 131
Figure 6.53 Normalized Mode I stress intensity factor $\bar{k}_{1h}$ at corner of finite strip when $\nu$ = 0.3 (Plane strain)..... 132
Figure 6.54 Normalized Mode I stress intensity factor $\bar{k}_{1h}$ at corner of finite strip when $\nu$ = 0.3 (Plane strain)..... 133
Figure 6.55 Normalized Mode I stress intensity factor $\bar{k}_{1h}$ at corner of finite strip when $a/h$ = 0.5 (Plane strain)..... 134
Figure 6.56 Normalized Mode II stress intensity factor $\bar{k}_{2h}$ at corner of finite strip when $L/h$ = 0.5 (Plane strain)..... 135
Figure 6.57 Normalized Mode II stress intensity factor $\bar{k}_{2h}$ at corner of finite strip when $\nu$ = 0.3 (Plane strain)..... 136
Figure 6.58 Normalized Mode II stress intensity factor $\bar{k}_{2h}$ at corner of finite strip when $\nu$ = 0.3 (Plane strain)..... 137
Figure 6.59 Normalized Mode II stress intensity factor $\bar{k}_{2h}$ at corner of finite strip when $a/h$ = 0.5 (Plane strain)..... 138

## NOMENCLATURE

| | |
|---|---|
| $2a$ | Distance between inner edges of cracks |
| $2b$ | Distance between outer edges of cracks |
| $2c$ | Width of rigid inclusions |
| $2h$ | Width of strip |
| $2L$ | Distance between rigid inclusions |
| $p_0$ | Uniform intensity of the axial tensile load |
| $x, y, z$ | Rectangular coordinates |
| $u$ , $v$ | Displacement components in $x$- and $y$- directions |
| $\sigma$ , $\tau$ | Normal and shearing stresses |
| $\kappa$ | $(3-4\nu)$ for plane strain and $(3-\nu)/(1+\nu)$ for plane stress |
| $E$ | Young's modulus |
| $\mu$ | Modulus of rigidity |
| $\nu$ | Poisson's ratio |
| $r, t, s, \lambda, \gamma$ | Fourier transform variables |
| $p_1(r)$ | Shearing stress jump on rigid inclusions |
| $p_2(r)$ | Normal stress jump on rigid inclusions |
| $m(t)$ | Crack surface displacement derivative |
| $\alpha$ , $\beta$ | Powers of singularity at the edges of the inclusions and the tip of the crack |
| $\eta$ , $\rho$ | Non-dimensional coordinates on the cracks |

| | |
|---|---|
| $\xi$ , $\varphi$ | Non-dimensional coordinates on the inclusions |
| $G_1(\varphi)$ , $G_2(\varphi)$ | Hölder-continuous functions on the inclusions |
| $Y(\rho)$ | Hölder-continuous function on the cracks |
| $K_{1c}$ , $K_{2c}$ | Mode I and II stress intensity factors at the edge of the internal inclusions |
| $K_{1h}$ , $K_{2h}$ | Mode I and II stress intensity factors at the corners of the finite strip |
| $K_a$ , $K_b$ | Mode I stress intensity factors at the edges of the cracks |
| $\bar{k}_{1a}$ , $\bar{k}_{1b}$ | Normalized Mode I stress intensity factors at the edges of the cracks |
| $\bar{k}_{1c}$ , $\bar{k}_{2c}$ | Normalized Mode I and II stress intensity factors at the edge of the internal inclusions |
| $\bar{k}_{1h}$ , $\bar{k}_{2h}$ | Normalized Mode I and II stress intensity factors at the corners of the finite strip |

# CHAPTER I

# INTRODUCTION

In the past, failures of engineering structures which mostly occured from the cracks situated in the structures revealed the necessity of evaluating the behavior of the cracks. Since the cracks can lower the strength of materials, it becomes mandatory to describe the growth of cracks for all cases according to types of material, loading or geometry. In the view of this observation, fracture mechanics which is concerned with the study of the formation and propagation of cracks in the structures was set forth by Griffith (1920). The Griffith theory explains the failure of brittle materials and has been applied extensively to the fracture of metals, plastics and composites.

A vast and growing field of fracture mechanics provides methods to examine various problems related to cracks in a strip. In many studies the effects of material, loading and geometry on stress distributions and stress intensity factors have been investigated and especially plane cracks occured under tension are widely considered. From the viewpoint of type of the material, most common is the homogeneous and isotropic material. To solve these problems, particular methods are applied for both analytical and numerical calculations. In analytical solution, generally the methods of partial differential equations and singular integral equations are used. Aside from these methods, the principle of superposition which allows reduction of complex systems to simpler cases is used frequently for the solution of problems.

Although a wide variety of strip problems have been studied in the past, a finite and an infinite strip containing two rigid inclusions and two collinear internal and edge cracks located on the center of the strips have not been solved by the method used in this study.

## 1.1 Literature Review

Sneddon and Srivastav (1971) considered the problem of determining the distribution of stress in the vicinity of a Griffith crack in a two-dimensional elastic strip of finite width when pressure is applied to the faces of the crack. It was assumed that the strip is made of elastic material which is both isotropic and homogeneous. In this study, the crack is situated symmetrically at the center of the strip and the problem is reduced to solving a system of coupled equations. The stress intensity factor and the crack energy were determined by solving Fredholm integral equation of the second kind for the case of constant internal pressure.

Cook and Erdoğan (1972) solved the problem of two elastic bonded half planes containing a crack perpendicular to the interface. First the solution of the semi-infinite crack under concentrated wedge loading was obtained and then the problem of a finite crack fully imbedded in one of the half planes was considered. The case of the crack terminating at the interface was separately studied and to derive the integral equations, the Mellin transform in conjuction with dislocations was used.

A semi-infinite strip with fixed end has been solved by Gupta (1973). An infinite strip in which a flat inclusion is situated centrally was reduced to semi-infinite strip by extending the inclusion to the surfaces. Stress singularity at the strip corner was obtained from the singular integral equation by using integral transform technique and then was solved numerically.

Gupta and Erdoğan (1974) investigated the elastostatic problem of an infinite strip with two collinear cracks perpendicular to its sides. The solution of the problem was obtained for various crack geometries and for uniaxial tension which is applied to the strip away from the crack region. The problem was reduced to a singular integral equation with the derivative of the crack surface displacement as the density function.

Krenk (1975) presented a method to deal with an inclined crack in an elastic strip. The method contains the solutions for a cracked plane and an uncracked strip and results in two coupled singular equations with finite interval of integration. In the paper, results were presented for loads according to the technical beam theory.

Gupta (1975) considered a finite strip compressed between two rigid stamps. A homogeneous and isotropic finite strip was analyzed and the problem was formulated in terms of a singular integral equation from which the proper stress singularities at the corners were determined. To determine the stresses along the fixed ends of the strip, the singular integral equation was solved numerically. In the study, the effect of material proporties and strip geometry on the stress intensity factor was presented graphically.

Adams (1980) studied an isotropic, homogeneous semi-infinite elastic strip whose end is bonded to and pressed against an infinite elastic strip which is supported by a pair of symmetrically located, concentrated forces. The solution was reduced to a set of singular integral equations of the second kind by using integral transform techniques. The equations were solved numerically. In this paper, the results show the normal and shear stress distributions and also stress intensity factors for a range of support locations corresponding to various width ratios and material combinations.

Civelek and Erdoğan (1982) examined the basic problem of multiple cracks for an infinite strip by using the method of singular integral equations. The cracks are perpendicular to the boundary. In this study two specific problems were considered. The first is to provide the solution of the interaction problem for multiple edge cracks in a plate or beam subjected to membrane loading or pure bending. The second is an analytical solution for a rectangular plate which is subjected to arbitrary crack surface tractions or concentrated forces.

Geçit (1984) considered the elastostatic antiplane shear problem of two half spaces bonded through an infinite layer all having transverse fatigue cracks. In this paper, the cases of three imbedded cracks, cracks terminating at the interfaces, completely broken layer, and a crack in the layer spreading into the half spaces were investigated. To formulate the problem the Fourier transform was used and by using the mixed type conditions on the crack plane, formulation was reduced to a system of singular integral equations with simple or generalized Cauchy kernels. Numerical results show stress intensity factors and crack opening displacements for material pairs of aluminum-epoxy and steel-aluminum.

Turgut and Geçit (1988) made an analysis of a semi-infinite strip with free sides containing a transverse central crack. Short end of the strip is bonded to a rigid support and the far end is subjected to uniform tension. Solution was obtained by considering an infinite strip which contains a rigid inclusion at the middle and two symmetrical transverse cracks. In the limiting case when the rigid inclusion approaches the sides of the strip, one-half of the infinite strip becomes equivalent to the cracked semi-infinite strip. Formulation was reduced to a system of three singular integral equations and numerical results for stresses, stress intensity factors, probable cleavage angle and strain energy release rate were presented graphically.

Geçit and Turgut (1988) studied the elastostatic plane problem of a finite strip. One end of the strip is bonded to a rigid support and the other is under the action of a uniform tensile load. In the paper, solution for the finite strip was obtained by considering an infinite strip containing a transverse rigid inclusion at the middle and two symmetrically located transverse cracks. When the rigid inclusion and the cracks approach the sides of the infinite strip, the region between one crack and the rigid inclusion becomes equivalent to the finite strip. By using the Fourier transforms, formulation of the problem was reduced to a system of three singular integral equations. Numerical results were presented for stresses and stress intensity factors in graphical form.

The elastostatic plane problem of a semi-infinite strip with free sides bonded to an infinite strip along its short end and subjected to a bending moment at its far end has been considered by Blaibel and Geçit (1989). The semi-infinite problem was solved by the superposition of a simple bending solution due to the load at infinity and a residual solution. Formulation of the problem was reduced to a system of three singular integral equations of the second kind and these integral equations were solved numerically. Numerical results of interface stress distributions and the stress intensity factors at the corners for various geometries and material combinations are presented in graphical form.

Zhou, Bai and Zhang (1999) investigated the problem of determining the stress field in an elastic strip of finite width when the uniform tension is applied to the faces of two collinear symmetrical cracks which are situated within it. In this study Schmidt's method which is suitable for solving the strip's problem of arbitrary width was used. By using the Fourier transform, a mixed boundary value problem was reduced to a set of triple integral equations. For solving these triple integral equations, the crack surface displecement was expanded in a series using Jacobi's polynomials and Schmidt's method was applied.

Yetmez and Geçit (2005) considered a symmetrical finite strip containing a transverse symmetrical crack at the midplane. Two rigid plates are bonded to the ends of the strip through which uniformly distributed axial tension is applied and both edges of the strip are free of stresses. The strip was assumed to be made of a linearly elastic and isotropic material. Solution for this finite strip problem was obtained by means of an infinite strip which contains a crack and two rigid inclusions and which is subjected to uniformly distributed axial tensile loads. By using the Fourier transform, the governing equations were solved and reduced to a system of three singular integral equations which were converted to a system of linear algebraic equations with the help of the Gauss-Jacobi and the Gauss-Lobatto integration formulas. The system was solved numerically and the results of normal and shearing stress distributions and the stress intensity factors were presented in graphical and tabular forms.

## 1.2 A Brief Definition of the Problem and the Method of Solution

A symmetrical finite strip containing two collinear internal cracks located at the center of the strip is considered. The length of the strip is assumed to be $2L$ and the width is $2h$. Each internal crack has a width $b–a$. Two ends of the finite strip are bonded to two rigid plates through which uniformly distributed axial tensile loads of intensity $p_0$ are applied. The finite strip is assumed to be made of a linearly elastic and isotropic material. For the solution of the finite strip problem, an infinite strip of width $2h$ containing two cracks of width $b–a$ at $y=0$ and two rigid inclusions of width $2c$ at $y=\pm L$ are taken into account. When the width of rigid inclusions approach the width of the strip, the portion of the infinite strip between the inclusions becomes identical with the finite strip problem.

Formulation of the infinite strip problem is acquired from the superposition of two subproblems: (i) The uniform solution; an infinite strip subjected to uniform tensile axial loads of intensity $p_0$ with no cracks or inclusions, and (ii) The perturbation solution; an infinite strip containing two internal cracks of width $b–a$ at $y=0$ and two rigid inclusions of width $2c$ at $y=\pm L$ with no load at infinity are considered. In problem (ii), the negative of the stresses obtained in problem (i) at the location of the cracks are applied to the surfaces of the cracks and the negative of the stresses again obtained in problem (i) at the locations of the inclusions are applied to the inclusions.

Perturbation problem is formulated by assembling the general expressions of stresses and displacements for the the following three subproblems: (a) An infinite elastic medium symmetric in both $x$- and $y$-directions with no cracks or inclusions, (b) An infinite elastic medium symmetric in both $x$- and $y$-directions containing two central cracks of width $b–a$, (c) An infinite elastic medium symmetric in both $x$- and $y$-directions containing two rigid inclusions of width $2c$ at $y=\pm L$.

For the solution of these subproblems Fourier transforms are used and expressions obtained by these tranforms are forced to satisfy the boundary conditions. Satisfying the homogeneous boundary conditions at the edges of the strip, the general expressions for an infinite medium become expressions for a strip with free edges. By the use of remaining conditions on the cracks and the inclusions, a system of three singular integral equations is obtained. To obtain numerical results from these integral equations, the system is converted to a system of linear algebraic equations and is solved with a Fortran program.

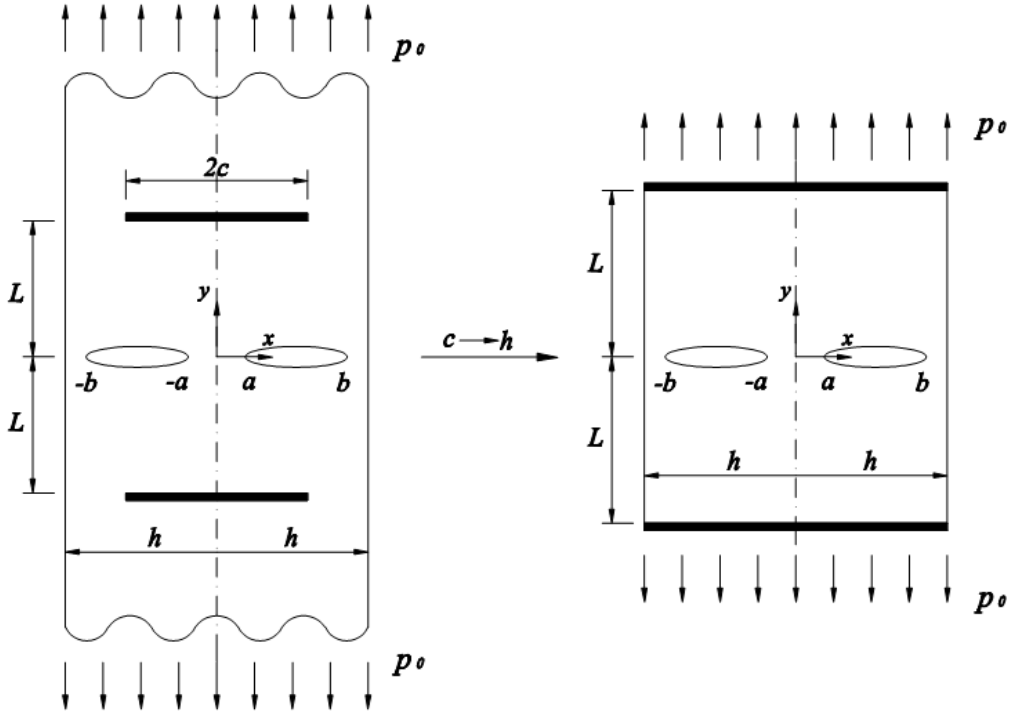


Figure 1.1 Infinite strip yielding finite strip problem

# CHAPTER II

# INFINITE STRIP PROBLEM

## 2.1 Formulation of the Problem

Consider a finite strip of length *2L* and width *2h* with two collinear symmetrical cracks: The ends of the strip are bonded to rigid plates through which uniformly distributed tensile loads are applied. In the problem, symmetry exists in both *x*- and *y*-directions. Formulation for the finite strip is obtained by considering an infinite strip which is assumed to be made from linearly elastic and isotropic material, containing two internal symmetrical cracks at $y=0$ and two rigid inclusions with negligible thickness at $y=\pm L$. Later on the width of the inclusions will approach the width of the strip (Figure 2.1). The infinite strip is loaded at $y=\pm\infty$.

General expressions for the displacements and the stresses for this problem are obtained by superporsition of the following two problems (Figure 2.2):

(i) Uniform solution: An infinite strip loaded at infinity with no cracks or inclusions,

(ii) Perturbation problem: An infinite strip with two cracks and two inclusions. Crack surfaces are subjected to the negative of the stresses obtained in problem (i) at the location of the cracks. The inclusions are subjected to the negative of the displacements obtained in problem (i) at the location of the inclusions.

To solve the perturbation problem, general solutions of the following three subproblems are added as shown in Figure 2.3:

(a) An infinite elastic medium symmetric in both *x*- and *y*-directions with no cracks or inclusions,

(b) An infinite elastic medium symmetric in both *x*- and *y*-directions containing two central cracks of width *b*–*a*,

(c) An infinite elastic medium symmetric in both *x*- and *y*-directions containing two rigid inclusions of width *2c* at $y=\pm L$.

The field equations may be listed in the following form for linearly elastic, isotropic and two-dimensional elasticity problems:

Stress-displacement relations:

$$\sigma_x(x,y)=\frac{\mu}{\kappa-1}\left[(\kappa+1)\frac{\partial u}{\partial x}+(3-\kappa)\frac{\partial v}{\partial y}\right], \tag{2.1a}$$

$$\sigma_y(x,y)=\frac{\mu}{\kappa-1}\left[(3-\kappa)\frac{\partial u}{\partial x}+(\kappa+1)\frac{\partial v}{\partial y}\right], \tag{2.1b}$$

$$\tau_{xy}(x,y)=\mu\left[\frac{\partial u}{\partial y}+\frac{\partial v}{\partial x}\right]. \tag{2.1c}$$

Here, *u*, *v* are the displacement components in *x*- and *y*-directions in rectangular coordinate system, $\mu$ is the modulus of rigidity, $\kappa$=3-4 *v* for plane strain and $\kappa=(3-v)/(1+v)$ for plane stress, *v* being the Poisson's ratio, $\sigma$ and $\tau$ denote the normal and shearing stresses.

Equilibrium equations when the body forces are neglected:

$$\frac{\partial \sigma_x}{\partial x}+\frac{\partial \tau_{xy}}{\partial y}=0,$$

$$\frac{\partial \tau_{xy}}{\partial x}+\frac{\partial \sigma_y}{\partial y}=0. \tag{2.2a,b}$$

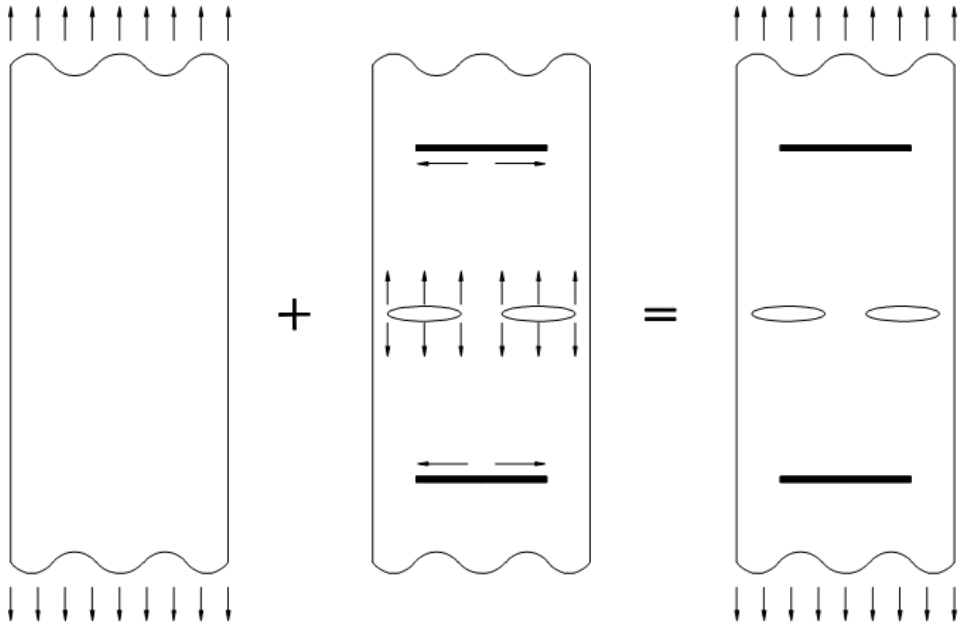

(i) (ii)

Figure 2.1 Superposition

Navier equations (equilibrium equations in terms of the displacements) are expressed in the form:

$$(\kappa+1)\frac{\partial^2 u}{\partial x^2}+(\kappa-1)\frac{\partial^2 u}{\partial y^2}+2\frac{\partial^2 v}{\partial x\partial y}=0\,, \tag{2.3a}$$

$$2\frac{\partial^2 u}{\partial x\partial y}+(\kappa-1)\frac{\partial^2 v}{\partial x^2}+(\kappa+1)\frac{\partial^2 v}{\partial y^2}=0\,. \tag{2.3b}$$

when the body forces are negligible.

For the infinite strip loaded at infinity, boundary conditions may be expressed in the form:

$$\sigma_y(x,\pm\infty) = p_0\,, \qquad (|x| < h)$$

$$\sigma_y(x,0) = 0\,, \qquad (a < |x| < b)$$

$$\sigma_x(\pm h, y) = 0\,, \qquad (|y| < \infty)$$

$$\tau_{xy}(\pm h, y) = 0\,, \qquad (|y| < \infty)$$

$$u(x,L) = 0\,, \qquad (|x| < c)$$

$$v(x,L) = \text{constant.} \qquad (|x| < c). \qquad \text{(2.4a–f)}$$

Note here that due to symmetry, one half of the problem ($0 < y < \infty$) will be solved.

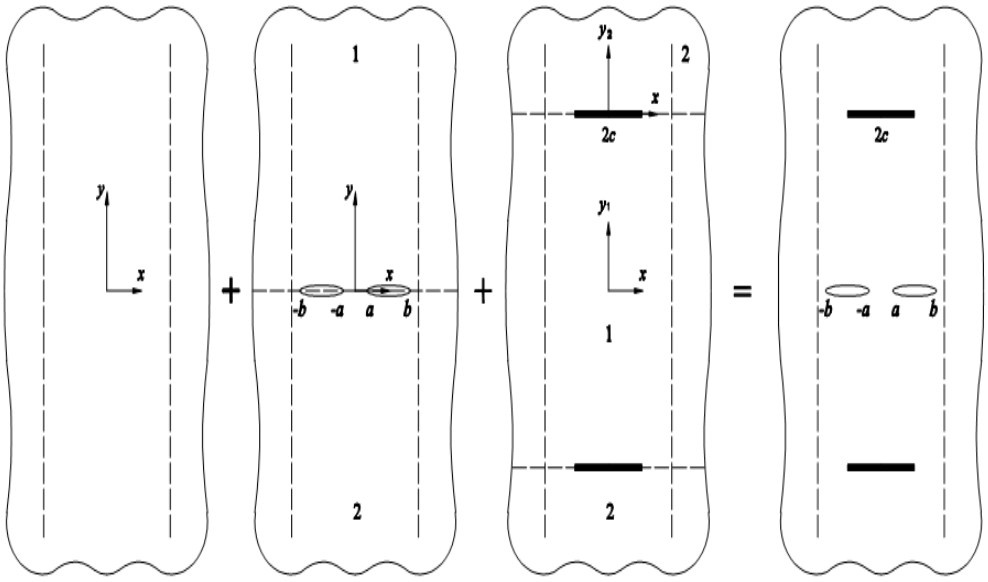


(a) (b) (c)

Figure 2.2 Schematic representation of general formulation.

### 2.1.1 Uniform Solution

For uniform solution, the field equations are to be solved according to following boundary conditions regarding an infinite strip of width *2h*:

$$\sigma_y(x,\infty) = p_0,$$

$$\sigma_x(h,y) = 0,$$

$$\tau_{xy}(h,y) = 0. \qquad \text{(2.5a–c)}$$

Here, Eqs.(2.1) and Eqs.(2.3) become ordinary differential equations for the uniform, uniaxial loading:

$$\frac{d^2u}{dx^2} = 0, \qquad \frac{d^2v}{dy^2} = 0,$$

$$\sigma_x = 0, \qquad \sigma_y = \frac{\mu}{\kappa - 1}\left[(3-\kappa)\frac{du}{dx} + (1+\kappa)\frac{dv}{dy}\right],$$

$$\tau_{xy} = 0. \qquad \text{(2.6a–e)}$$

Solution of Eqs. (2.6) can be obtained easily with necessary symmetry considerations and can be expressed in the form:

$$u^{(i)} = \frac{\kappa - 3}{8\mu} p_0 x, \qquad v^{(i)} = \frac{\kappa + 1}{8\mu} p_0 y,$$

$$\sigma_x^{(i)} = 0, \qquad \sigma_y^{(i)} = p_0, \qquad \text{(2.7a–d)}$$

$$\tau_{xy}^{(i)} = 0\,, \tag{2.7e}$$

in which the superscript (i) refers to the solution for problem (i) in Figure 2.1.

### 2.1.2 Perturbation Solution

For the perturbation solution, an infinite strip of width *2h* having two internal symmetrical cracks of width (*b–a*) at *y=0* and two rigid inclusions of width 2c at $y=\pm L$ is considered. Eqs. (2.3) will be solved subject to the following boundary conditions:

$$\sigma_x(h,y) = 0\,, \qquad \tau_{xy}(h,y) = 0\,,$$

$$\sigma_y(x,\infty) = 0\,, \qquad \tau_{xy}(x,\infty) = 0\,,$$

$$\sigma_y(x,0) = -p_0\,, \qquad \tau_{xy}(x,0) = 0\,, \qquad (a < |x| < b)$$

$$v(x,0) = 0\,, \qquad (0 < |x| < a,\ b < |x| < h)$$

$$\frac{\partial}{\partial x}u(x,L) = -\frac{\kappa-3}{8\mu}p_0\,, \qquad \frac{\partial}{\partial x}v(x,L) = 0\,. \qquad (|x| < c) \tag{2.8a–i}$$

To satisfy all these boundary conditions, sufficient number of unknowns are needed in general expressions for the displacements and stresses. That is why, the general expressions containing required number of unknowns will be acquired by adding the general solutions of three subproblems given in the following three sections.

### 2.1.2.1 An Infinite Medium Subjected to Arbitrary Symmetric Loads

Consider the problem shown in Figure 2.2a, Eq. (2.3a) and Eq. (2.3b) are solved by taking the Fourier cosine transform and Fourier sine transform, respectively, in *y*-direction. Coupled ordinary differential equations acquired from Fourier transforms of Eqs. (2.3) are solved and the inverse transforms are written as follows:

$$u^{(a)}(x,y) = -\frac{2}{\pi}\int_0^\infty \frac{1}{s}\left\{\left[A(s) - \frac{\kappa-1}{2}B(s)\right]\sinh(sx) + B(s)sx\cosh(sx)\right\}\cos(sy)ds,$$

$$v^{(a)}(x,y) = \frac{2}{\pi}\int_0^\infty \frac{1}{s}\left\{\left[A(s) + \frac{\kappa+1}{2}B(s)\right]\cosh(sx) + B(s)sx\sinh(sx)\right\}\sin(sy)ds,$$

(2.9a,b)

$$\frac{d}{dx}u^{(a)}(x,y) = -\frac{2}{\pi}\int_0^\infty \left\{\left[A(s) + \frac{3-\kappa}{2}B(s)\right]\cosh(sx) + B(s)sx\sinh(sx)\right\}\cos(sy)ds,$$

$$\frac{d}{dx}v^{(a)}(x,y) = \frac{2}{\pi}\int_0^\infty \left\{\left[A(s) + \frac{3+\kappa}{2}B(s)\right]\sinh(sx) + B(s)sx\cosh(sx)\right\}\sin(sy)ds\ ,$$

(2.9c,d)

for the displacements and using Eqs.(2.1)

$$\sigma_x{}^{(a)}(x,y) = -\frac{4\mu}{\pi}\int_0^\infty \{A(s)\cosh(sx) + B(s)sx\sinh(sx)\}\cos(sy)ds,$$

$$\sigma_y{}^{(a)}(x,y) = \frac{4\mu}{\pi}\int_0^\infty \{[A(s) + 2B(s)]\cosh(sx) + B(s)sx\sinh(sx)\}\cos(sy)ds,$$

(2.10a,b)

$$\tau_{xy}^{(a)}(x,y)=\frac{4\mu}{\pi}\int_0^{\infty}\left\{\left[A(s)+B(s)\right]\sinh(sx)+B(s)sx\cosh(sx)\right\}\sin(sy)ds\,.$$

(2.10c)

for the stresses. Here *A(s)* and *B(s)* are still unknowns and the superscript (*a*) refers to the general solution for problem (a) shown in Figure 2.2.

### 2.1.2.2 An Infinite Medium Having Two Collinear Cracks

In this part, the infinite medium shown in Figure 2.2b is taken into consideration. Here, Fourier sine transform is applied to Eq. (2.3a) and Fourier cosine transform is applied to Eq. (2.3b) in *x*-direction to acquire the solutions of Eqs. (2.3) for the upper (1) and lower (2) half planes individually. The solutions are then combined at *y=0* such that

$$\sigma_y^1(x,0^+)=\sigma_y^2(x,0^-), \qquad (0<|x|<\infty),$$

$$\tau_{xy}^1(x,0^+)=\tau_{xy}^2(x,0^-)=0, \qquad (0<|x|<\infty),$$

$$u^1(x,0^+)=u^2(x,0^-), \qquad (0<|x|<\infty),$$

$$v^1(x,0^+)=v^2(x,0^-), \qquad (0<|x|<a\,,\ b<|x|<\infty),$$

$$\sigma_y(x,0)=\text{known}, \qquad (a<|x|<b\,). \qquad \text{(2.11a–e)}$$

In the expressions given above, superscript 1 refers to the upper half plane of the strip where superscript 2 refers to the lower half plane.

By using derivative of crack surface displacement *m*(*x*)

$$m(x)=\frac{1}{2}\frac{\partial}{\partial x}\left[v^1(x,0^+)-v^2(x,0^-)\right],\quad (0<x<\infty) \tag{2.12}$$

the stress and displacement expressions for the upper and lower half planes can be obtained in the form given below by taking $m(x)=0$ for ($a<|x|<b$)

$$\sigma_x^{(b1)}(x,y)=\frac{8\mu}{\pi(\kappa+1)}\int_0^\infty\left\{1-\lambda_y\right\}M(\lambda)e^{-\lambda y}\cos(\lambda x)d\lambda,$$

$$\sigma_x^{(b2)}(x,y)=\frac{8\mu}{\pi(\kappa+1)}\int_0^\infty\left\{1+\lambda_y\right\}M(\lambda)e^{\lambda y}\cos(\lambda x)d\lambda,$$

$$\sigma_y^{(b1)}(x,y)=\frac{8\mu}{\pi(\kappa+1)}\int_0^\infty\left\{1+\lambda_y\right\}M(\lambda)e^{-\lambda y}\cos(\lambda x)d\lambda, \tag{2.13a–c}$$

$$\sigma_y^{(b2)}(x,y)=\frac{8\mu}{\pi(\kappa+1)}\int_0^\infty\left\{1-\lambda_y\right\}M(\lambda)e^{\lambda y}\cos(\lambda x)d\lambda,$$

$$\tau_{xy}^{(b1)}(x,y)=\frac{8\mu}{\pi(\kappa+1)}\int_0^\infty\lambda_y M(\lambda)e^{-\lambda y}\sin(\lambda x)d\lambda,$$

$$\tau_{xy}^{(b2)}(x,y)=\frac{8\mu}{\pi(\kappa+1)}\int_0^\infty\lambda_y M(\lambda)e^{\lambda y}\sin(\lambda x)d\lambda, \tag{2.13d–f}$$

$$u^{(b1)}(x,y)=\frac{2}{\pi(\kappa+1)}\int_0^\infty\frac{1}{\lambda}\left\{\kappa-1-2\lambda y\right\}M(\lambda)e^{-\lambda y}\sin(\lambda x)d\lambda,$$

$$u^{(b2)}(x,y)=\frac{2(\kappa-1)}{\pi(\kappa+1)}\int_0^\infty\left\{\frac{1}{\lambda}+\frac{2y}{\kappa-1}\right\}M(\lambda)e^{\lambda y}\sin(\lambda x)d\lambda,$$

(2.14a,b)

$$v^{(b1)}(x,y)=\frac{2}{\pi(\kappa+1)}\int_0^\infty\frac{1}{\lambda}\{-\kappa-1-2\lambda y\}M(\lambda)e^{-\lambda y}\cos(\lambda x)d\lambda\,,$$

$$v^{(b2)}(x,y)=\frac{2}{\pi(\kappa+1)}\int_0^\infty\frac{1}{\lambda}\{\kappa+1-2\lambda y\}M(\lambda)e^{\lambda y}\cos(\lambda x)d\lambda\,, \qquad (2.14c,d)$$

where

$$M(\lambda)=\int_0^\infty m(x)\sin(\lambda x)dx\,, \qquad (2.15)$$

and the superscript (*b*) refers to the problem (b) given in Figure 2.2.

If one uses formulae involving definite integrals in Appendix A by taking Eq. (2.15) into consideration, the expressions of (2.13a–f) and (2.14a–d) are converted into the form

$$\sigma_x^{(b1)}(x,y)=\sigma_x^{(b1)}(x,-y)=\frac{4\mu}{\pi(\kappa+1)}\int_a^b m(t)\left[\frac{t+x}{y^2+(t+x)^2}+\frac{t-x}{y^2+(t-x)^2}-2y^2\left\{\frac{t+x}{\left[y^2+(t+x)^2\right]^2}+\frac{t-x}{\left[y^2+(t-x)^2\right]^2}\right\}\right]dt\,,$$

$$\sigma_y^{(b1)}(x,y)=\sigma_y^{(b1)}(x,-y)=\frac{4\mu}{\pi(\kappa+1)}\int_a^b m(t)\left[\frac{t+x}{y^2+(t+x)^2}+\frac{t-x}{y^2+(t-x)^2}+2y^2\left\{\frac{t+x}{\left[y^2+(t+x)^2\right]^2}+\frac{t-x}{\left[y^2+(t-x)^2\right]^2}\right\}\right]dt\,,$$

$$\tau_{xy}^{(b1)}(x,y)=-\tau_{xy}^{(b1)}(x,-y)=\frac{4\mu}{\pi(\kappa+1)}\int_a^b m(t)y\left[\frac{y^2-(t-x)^2}{\left[y^2+(t-x)^2\right]^2}-\frac{y^2-(t+x)^2}{\left[y^2+(t+x)^2\right]^2}\right]dt, \qquad (2.16a–f)$$

$$\frac{\partial}{\partial x}u^{(b1)}(x,y)=\frac{\partial}{\partial x}u^{(b2)}(x,-y)=\frac{1}{\pi(\kappa+1)}\int_a^b m(t)\Bigg[(\kappa-1)\Bigg\{\frac{t+x}{y^2+(t+x)^2}+\frac{t-x}{y^2+(t-x)^2}\Bigg\}-4y^2\Bigg\{\frac{t+x}{\left[y^2+(t+x)^2\right]^2}+\frac{t-x}{\left[y^2+(t-x)^2\right]^2}\Bigg\}\Bigg]dt\,,$$

$$\frac{\partial}{\partial x}v^{(b1)}(x,y)=\frac{\partial}{\partial x}v^{(b2)}(x,-y)=\frac{1}{\pi(\kappa+1)}\int_a^b m(t)\Bigg[(\kappa+1)y\Bigg\{\frac{1}{y^2+(t-x)^2}-\frac{1}{y^2+(t+x)^2}\Bigg\}+2y\Bigg\{\frac{y^2-(t-x)^2}{\left[y^2+(t-x)^2\right]^2}-\frac{y^2-(t+x)^2}{\left[y^2+(t+x)^2\right]^2}\Bigg\}\Bigg]dt\,.$$

(2.17a–d)

The fact that $m(x)$ is odd can be used to write the expressions given above in more compact form

$$\sigma_x^{(b)}(x,y)=\frac{4\mu}{\pi(\kappa+1)}\int_a^b\Bigg\{\frac{-y^2(x+t)+(x+t)^3}{\left[y^2+(x+t)^2\right]^2}+\frac{y^2(x-t)-(x-t)^3}{\left[y^2+(x-t)^2\right]^2}\Bigg\}m(t)dt\,,$$

$$\sigma_y^{(b)}(x,y)=\frac{4\mu}{\pi(\kappa+1)}\int_a^b\Bigg\{\frac{3y^2(x+t)+(x+t)^3}{\left[y^2+(x+t)^2\right]^2}+\frac{-3y^2(x-t)-(x-t)^3}{\left[y^2+(x-t)^2\right]^2}\Bigg\}m(t)dt\,,$$

$$\tau_{xy}^{(b)}(x,y)=\frac{4\mu}{\pi(\kappa+1)}\int_a^b\Bigg\{\frac{y^3-y(x-t)^2}{\left[y^2+(x-t)^2\right]^2}-\frac{y^3-y(x+t)^2}{\left[y^2+(x+t)^2\right]^2}\Bigg\}m(t)dt\,,\qquad(2.18a–c)$$

$$\frac{\partial}{\partial x}u^{(b)}(x,y)=\frac{1}{\pi(\kappa+1)}\int_a^b\Bigg\{\frac{(\kappa-5)y^2(x+t)+(\kappa-1)(x+t)^3}{\left[y^2+(x+t)^2\right]^2}+\frac{-(\kappa-5)y^2(x-t)-(\kappa-1)(x-t)^3}{\left[y^2+(x-t)^2\right]^2}\Bigg\}m(t)dt\,,\qquad(2.19a)$$

$$\frac{\partial}{\partial x}v^{(b)}(x,y)=\frac{1}{\pi(\kappa+1)}\int_a^b\left\{\frac{(\kappa+3)y^3+(\kappa-1)y(x-t)^2}{\left[y^2+(x-t)^2\right]^2}\right.$$
$$\left.-\frac{(\kappa+3)y^3+(\kappa-1)y(x+t)^2}{\left[y^2+(x+t)^2\right]^2}\right\}m(t)dt\,. \qquad (2.19b)$$

for the upper half.

### 2.1.2.3 An Infinite Medium Having Two Rigid Inclusions

Here, the infinite medium is divided into three sections: A horizontal strip of width 2*L* placed in the middle of the medium called section (1) and two half planes on either side of this strip called section (2) separately. For solving the middle strip and the half planes individually, Navier equations given in (2.3a,b) will be used and the solutions will be matched at $y=\pm L$ such that:

$$u^1(x,y_1=\pm L)=u^2(x,y_2=0)\,,$$

$$v^1(x,y_1=\pm L)=v^2(x,y_2=0)\,. \qquad (2.20a,b)$$

$$u(x,\pm L)=0\,, \qquad (|x|<c)$$

$$v(x,\pm L)=\text{constant.} \quad (|x|<c) \qquad (2.21a,b)$$

Eq. (2.3a) and Eq. (2.3b) are solved by taking the Fourier sine and cosine tranforms in *x*- direction respectively and the solutions of Eqs. (2.3) for the strip and the half planes can be connected at $y=\pm L$ with the help of Eqs. (2.20) and

$$\tau_{xy}^{2}(x, y_2 = 0) - \tau_{xy}^{1}(x, y_1 = \pm L) = p_1(x),$$

$$\sigma_{y}^{2}(x, y_2 = 0) - \sigma_{y}^{1}(x, y_1 = \pm L) = p_2(x), \qquad (2.22a,b)$$

in which $p_1$ and $p_2$ are the jumps in the stresses through the rigid inclusions with negligible thickness and

$$p_1(x) = p_2(x) = 0, (|x| > c). \qquad (2.23)$$

The stress and displacement expressions for the strip and the half planes can then be written in the form

$$\sigma_{x}^{(c1)}(x, y_1) = \frac{1}{\pi(\kappa+1)} \int_0^\infty \Big[ \left\{ SL_{11}^{1}(\gamma, y_1) + SL_{21}^{1}(\gamma, y_1) \right\} P_1(\gamma) + \left\{ SL_{12}^{1}(\gamma, y_1) + SL_{22}^{1}(\gamma, y_1) \right\} P_2(\gamma) \Big] \cos(\gamma x) d\gamma,$$

$$\sigma_{y}^{c1}(x, y_1) = \frac{1}{\pi(\kappa+1)} \int_0^\infty \Big[ \left\{ ST_{11}^{1}(\gamma, y_1) + ST_{21}^{1}(\gamma, y_1) \right\} P_1(\gamma) + \left\{ ST_{12}^{1}(\gamma, y_1) + ST_{22}^{1}(\gamma, y_1) \right\} P_2(\gamma) \Big] \cos(\gamma x) d\gamma,$$

$$\tau_{xy}^{(c1)}(x, y_1) = \frac{1}{\pi(\kappa+1)} \int_0^\infty \Big[ \left\{ SS_{11}^{1}(\gamma, y_1) + SS_{21}^{1}(\gamma, y_1) \right\} P_1(\gamma) + \left\{ SS_{12}^{1}(\gamma, y_1) + SS_{22}^{1}(\gamma, y_1) \right\} P_2(\gamma) \Big] \sin(\gamma x) d\gamma,$$

$$\sigma_{x}^{(c2)}(x, y_2) = \frac{1}{\pi(\kappa+1)} \int_0^\infty \Big[ SL_{11}^{2}(\gamma, y_2) P_1(\gamma) + SL_{12}^{2}(\gamma, y_2) P_2(\gamma) \Big] \cos(\gamma x) d\gamma,$$

(2.24a–d)

$$\sigma_y^{(c2)}(x,y_2)=\frac{1}{\pi(\kappa+1)}\int_0^\infty\Big[ST_{11}^2(\gamma,y_2)P_1(\gamma)+ST_{12}^2(\gamma,y_2)P_2(\gamma)\Big]\cos(\gamma x)d\gamma\,,$$

$$\tau_{xy}^{(c2)}(x,y_2)=\frac{1}{\pi(\kappa+1)}\int_0^\infty\Big[SS_{11}^2(\gamma,y_2)P_1(\gamma)+SS_{12}^2(\gamma,y_2)P_2(\gamma)\Big]\sin(\gamma x)d\gamma\,,$$

(2.24e,f)

$$u^{(c1)}(x,y_1)=\frac{1}{\pi\mu(\kappa+1)}\int_0^\infty\Big[\Big\{DL_{11}^1(\gamma,y_1)+DL_{21}^1(\gamma,y_1)\Big\}P_1(\gamma)+\Big\{DL_{12}^1(\gamma,y_1)+DL_{22}^1(\gamma,y_1)\Big\}P_2(\gamma)\Big]\sin(\gamma x)d\gamma\,,$$

$$v^{(c1)}(x,y_1)=\frac{1}{\pi\mu(\kappa+1)}\int_0^\infty\Big[\Big\{DT_{11}^1(\gamma,y_1)+DT_{21}^1(\gamma,y_1)\Big\}P_1(\gamma)+\Big\{DT_{12}^1(\gamma,y_1)+DT_{22}^1(\gamma,y_1)\Big\}P_2(\gamma)\Big]\cos(\gamma x)d\gamma\,,$$

$$u^{(c2)}(x,y_2)=\frac{1}{\pi\mu(\kappa+1)}\int_0^\infty\Big[DL_{11}^2(\gamma,y_2)P_1(\gamma)+DL_{12}^2(\gamma,y_2)P_2(\gamma)\Big]\sin(\gamma x)d\gamma\,,$$

$$v^{(c2)}(x,y_2)=\frac{1}{\pi\mu(\kappa+1)}\int_0^\infty\Big[DT_{11}^2(\gamma,y_2)P_1(\gamma)+DT_{12}^2(\gamma,y_2)P_2(\gamma)\Big]\cos(\gamma x)d\gamma\,,$$

(2.25a–d)

where

$$P_1(\gamma)=\int_0^c p_1(x)\sin(\gamma x)dx\,,$$

$$P_2(\gamma)=\int_0^c p_2(x)\cos(\gamma x)dx\,,$$

(2.26a,b)

the superscript (*c*) refers to the problem (c) in Figure 2.2 and the expressions of $SL^{k}_{ij}(\gamma,y_i)$, $ST^{k}_{ij}(\gamma,y_i)$, $SS^{k}_{ij}(\gamma,y_i)$, $DL^{k}_{ij}(\gamma,y_i)$ and $DT^{k}_{ij}(\gamma,y_i)$ (i,j,k=1,2) are given in Appendix B. The stress and the displacement expressions can be obtained by substituting Eqs. (2.26) in Eqs. (2.25) with the help of similar manipulations done in 2.1.2.2 and may be expressed as follows:

$$\begin{aligned}\sigma_x^{(c1)}(x,y_1)=\frac{1}{2\pi(\kappa+1)}\int_0^c\Bigg[&\Bigg\{\frac{(1-\kappa)(L+y_1)^2(r-x)-(\kappa+3)(r-x)^3}{\left[(L+y_1)^2+(r-x)^2\right]^2}\\&+\frac{(1-\kappa)(L-y_1)^2(r-x)-(\kappa+3)(r-x)^3}{\left[(L-y_1)^2+(r-x)^2\right]^2}+\frac{(1-\kappa)(L+y_1)^2(r+x)-(\kappa+3)(r+x)^3}{\left[(L+y_1)^2+(r+x)^2\right]^2}\\&+\frac{(1-\kappa)(L-y_1)^2(r+x)-(\kappa+3)(r+x)^3}{\left[(L-y_1)^2+(r+x)^2\right]^2}\Bigg\}p_1(r)\\&+\Bigg\{\frac{(\kappa-1)(L+y_1)^3+(\kappa-5)(r+x)^2(L+y_1)}{\left[(L+y_1)^2+(r+x)^2\right]^2}\\&+\frac{(\kappa-1)(L+y_1)^3+(\kappa-5)(r-x)^2(L+y_1)}{\left[(L+y_1)^2+(r-x)^2\right]^2}\\&+\frac{(\kappa-1)(L-y_1)^3+(\kappa-5)(r+x)^2(L-y_1)}{\left[(L-y_1)^2+(r+x)^2\right]^2}\\&+\frac{(\kappa-1)(L-y_1)^3+(\kappa-5)(r-x)^2(L-y_1)}{\left[(L-y_1)^2+(r-x)^2\right]^2}\Bigg\}p_2(r)\Bigg]dr\,,\end{aligned}\tag{2.27a}$$

$$\begin{aligned}\sigma_y^{(c1)}(x,y_1)=\frac{1}{2\pi(\kappa+1)}\int_0^c\Bigg[&\Bigg\{\frac{(\kappa-5)(L+y_1)^2(r+x)+(\kappa-1)(r+x)^3}{\left[(L+y_1)^2+(r+x)^2\right]^2}\\&+\frac{(\kappa-5)(L-y_1)^2(r+x)+(\kappa-1)(r+x)^3}{\left[(L-y_1)^2+(r+x)^2\right]^2}\\&+\frac{(\kappa-5)(L+y_1)^2(r-x)+(\kappa-1)(r-x)^3}{\left[(L+y_1)^2+(r-x)^2\right]^2}\end{aligned}$$

$$+\frac{(\kappa-5)(L-y_1)^2(r-x)+(\kappa-1)(r-x)^3}{\left[(L-y_1)^2+(r-x)^2\right]^2}\Bigg\}p_1(r)$$

$$+\Bigg\{\frac{-(\kappa+3)(L-y_1)^3-(\kappa-1)(r-x)^2(L-y_1)}{\left[(L-y_1)^2+(r-x)^2\right]^2}$$

$$+\frac{-(\kappa+3)(L-y_1)^3-(\kappa-1)(r+x)^2(L-y_1)}{\left[(L-y_1)^2+(r+x)^2\right]^2}$$

$$+\frac{-(\kappa+3)(L+y_1)^3-(\kappa-1)(r-x)^2(L+y_1)}{\left[(L+y_1)^2+(r-x)^2\right]^2}$$

$$+\frac{-(\kappa+3)(L+y_1)^3-(\kappa-1)(r+x)^2(L+y_1)}{\left[(L+y_1)^2+(r+x)^2\right]^2}\Bigg\}p_2(r)\Bigg]dr\,, \qquad (2.27b)$$

$$\tau_{xy}^{(c1)}(x,y_1)=\frac{1}{2\pi(\kappa+1)}\int_0^c\Bigg[\Bigg\{\frac{(1-\kappa)(L-y_1)^3-(\kappa+3)(L-y_1)(r-x)^2}{\left[(L-y_1)^2+(r-x)^2\right]^2}$$

$$+\frac{(\kappa-1)(L-y_1)^3+(\kappa+3)(L-y_1)(r+x)^2}{\left[(L-y_1)^2+(r+x)^2\right]^2}$$

$$+\frac{(\kappa-1)(L+y_1)^3+(\kappa+3)(L+y_1)(r-x)^2}{\left[(L+y_1)^2+(r-x)^2\right]^2}$$

$$+\frac{(1-\kappa)(L+y_1)^3-(\kappa+3)(L+y_1)(r+x)^2}{\left[(L+y_1)^2+(r+x)^2\right]^2}\Bigg\}p_1(r)$$

$$+\Bigg\{\frac{(\kappa+3)(L-y_1)^2(r+x)+(\kappa-1)(r+x)^3}{\left[(L-y_1)^2+(r+x)^2\right]^2}$$

$$+\frac{-(\kappa+3)(L-y_1)^2(r-x)+(1-\kappa)(r-x)^3}{\left[(L-y_1)^2+(r-x)^2\right]^2}$$

$$+\frac{-(\kappa+3)(L+y_1)^2(r+x)+(1-\kappa)(r+x)^3}{\left[(L+y_1)^2+(r+x)^2\right]^2}$$

$$+\frac{(\kappa+3)(L+y_1)^2(r-x)+(\kappa-1)(r-x)^3}{\left[(L+y_1)^2+(r-x)^2\right]^2}\Bigg\}p_2(r)\Bigg]dr\,, \qquad (2.27c)$$

$$\sigma_x^{(c2)}(x,y_2)=\frac{1}{2\pi(\kappa+1)}\int_0^c\Bigg[\Bigg\{\frac{(1-\kappa)(2L+y_2)^2(r+x)-(\kappa+3)(r+x)^3}{\left[(2L+y_2)^2+(r+x)^2\right]^2}$$
$$+\frac{(1-\kappa)(2L+y_2)^2(r-x)-(\kappa+3)(r-x)^3}{\left[(2L+y_2)^2+(r-x)^2\right]^2}$$
$$+\frac{(1-\kappa)y_2{}^2(r+x)-(\kappa+3)(r+x)^3}{\left[y_2{}^2+(r+x)^2\right]^2}$$
$$+\frac{(1-\kappa)y_2{}^2(r-x)-(\kappa+3)(r-x)^3}{\left[y_2{}^2+(r-x)^2\right]^2}\Bigg\}p_1(r)$$
$$+\Bigg\{\frac{(\kappa-1)(2L+y_2)^3+(\kappa-5)(r+x)^2(2L+y_2)}{\left[(2L+y_2)^2+(r+x)^2\right]^2}$$
$$+\frac{(\kappa-1)(2L+y_2)^3+(\kappa-5)(r-x)^2(2L+y_2)}{\left[(2L+y_2)^2+(r-x)^2\right]^2}$$
$$+\frac{(1-\kappa)y_2{}^3+(5-\kappa)y_2(r+x)^2}{\left[y_2{}^2+(r+x)^2\right]^2}+\frac{(1-\kappa)y_2{}^3+(5-\kappa)y_2(r-x)^2}{\left[y_2{}^2+(r-x)^2\right]^2}\Bigg\}p_2(r)\Bigg]dr,$$

(2.27d)

$$\sigma_y^{(c2)}(x,y_2)=\frac{1}{2\pi(\kappa+1)}\int_0^c\Bigg[\Bigg\{\frac{(\kappa-5)(2L+y_2)^2(r+x)+(\kappa-1)(r+x)^3}{\left[(2L+y_2)^2+(r+x)^2\right]^2}$$
$$+\frac{(\kappa-5)(2L+y_2)^2(r-x)+(\kappa-1)(r-x)^3}{\left[(2L+y_2)^2+(r-x)^2\right]^2}$$
$$+\frac{(\kappa-5)y_2{}^2(r+x)+(\kappa-1)(r+x)^3}{\left[y_2{}^2+(r+x)^2\right]^2}$$
$$+\frac{(\kappa-5)y_2{}^2(r-x)+(\kappa-1)(r-x)^3}{\left[y_2{}^2+(r-x)^2\right]^2}\Bigg\}p_1(r)$$
$$+\Bigg\{\frac{-(\kappa+3)(2L+y_2)^3-(\kappa-1)(2L+y_2)(r+x)^2}{\left[(2L+y_2)^2+(r+x)^2\right]^2}$$

$$+\frac{-(\kappa+3)(2L+y_2)^3-(\kappa-1)(2L+y_2)(r-x)^2}{\left[(2L+y_2)^2+(r-x)^2\right]^2}$$

$$+\frac{(\kappa+3){y_2}^3+(\kappa-1)y_2(r+x)^2}{\left[{y_2}^2+(r+x)^2\right]^2}+\frac{(\kappa+3){y_2}^3+(\kappa-1)y_2(r-x)^2}{\left[{y_2}^2+(r-x)^2\right]^2}\Bigg\}p_2(r)\Bigg]dr,$$

(2.27e)

$$\tau_{xy}^{(c2)}(x,y_2)=\frac{1}{2\pi(\kappa+1)}\int_0^c\Bigg[\Bigg\{\frac{(\kappa-1)(2L+y_2)^3+(\kappa+3)(2L+y_2)(r-x)^2}{\left[(2L+y_2)^2+(r-x)^2\right]^2}$$

$$+\frac{-(\kappa-1)(2L+y_2)^3-(\kappa+3)(2L+y_2)(r+x)^2}{\left[(2L+y_2)^2+(r+x)^2\right]^2}$$

$$+\frac{(\kappa-1){y_2}^3+(\kappa+3)y_2(r-x)^2}{\left[{y_2}^2+(r-x)^2\right]^2}+\frac{-(\kappa-1){y_2}^3-(\kappa+3)y_2(r+x)^2}{\left[{y_2}^2+(r+x)^2\right]^2}\Bigg\}p_1(r)$$

$$+\Bigg\{\frac{-(\kappa+3)(2L+y_2)^2(r+x)-(\kappa-1)(r+x)^3}{\left[(2L+y_2)^2+(r+x)^2\right]^2}$$

$$+\frac{(\kappa+3)(2L+y_2)^2(r-x)+(\kappa-1)(r-x)^3}{\left[(2L+y_2)^2+(r-x)^2\right]^2}$$

$$+\frac{(\kappa+3){y_2}^2(r+x)+(\kappa-1)(r+x)^3}{\left[{y_2}^2+(r+x)^2\right]^2}$$

$$+\frac{-(\kappa+3){y_2}^2(r-x)-(\kappa-1)(r-x)^3}{\left[{y_2}^2+(r-x)^2\right]^2}\Bigg\}p_2(r)\Bigg]dr\,.$$

(2.27f)

$$\frac{\partial}{\partial x}u^{(c1)}(x,y_1)=\frac{1}{2\pi\mu(\kappa+1)}\int_0^c\Bigg[\Bigg\{\frac{(2-\kappa)(L-y_1)^2(r+x)-\kappa(r+x)^3}{\left[(L-y_1)^2+(r+x)^2\right]^2}$$

$$+\frac{(2-\kappa)(L-y_1)^2(r-x)-\kappa(r-x)^3}{\left[(L-y_1)^2+(r-x)^2\right]^2}+\frac{(2-\kappa)(L+y_1)^2(r+x)-\kappa(r+x)^3}{\left[(L+y_1)^2+(r+x)^2\right]^2}$$

$$+\frac{(2-\kappa)(L+y_1)^2(r-x)-\kappa(r-x)^3}{\left[(L+y_1)^2+(r-x)^2\right]^2}\Bigg\}p_1(r)$$

$$+\left\{\frac{(L-y_1)^3-(r-x)^2(L-y_1)}{\left[(L-y_1)^2+(r-x)^2\right]^2}+\frac{(L+y_1)^3-(r-x)^2(L+y_1)}{\left[(L+y_1)^2+(r-x)^2\right]^2}\right.$$

$$\left.+\frac{(L-y_1)^3-(r+x)^2(L-y_1)}{\left[(L-y_1)^2+(r+x)^2\right]^2}+\frac{(L+y_1)^3-(r+x)^2(L+y_1)}{\left[(L+y_1)^2+(r+x)^2\right]^2}\right\}p_2(r)\Bigg]dr\,,$$

(2.28a)

$$\frac{\partial}{\partial x}v^{(c1)}(x,y_1)=\frac{1}{2\pi\mu(\kappa+1)}\int_0^c\Bigg[\Bigg\{\frac{(L-y_1)^3-(L-y_1)(r-x)^2}{\left[(L-y_1)^2+(r-x)^2\right]^2}$$

$$+\frac{(L+y_1)(r-x)^2-(L+y_1)^3}{\left[(L+y_1)^2+(r-x)^2\right]^2}$$

$$+\frac{(L-y_1)(r+x)^2-(L-y_1)^3}{\left[(L-y_1)^2+(r+x)^2\right]^2}+\frac{(L+y_1)^3-(L+y_1)(r+x)^2}{\left[(L+y_1)^2+(r+x)^2\right]^2}\Bigg\}p_1(r)$$

$$+\Bigg\{\frac{(\kappa+2)(L-y_1)^2(r+x)+\kappa(r+x)^3}{\left[(L-y_1)^2+(r+x)^2\right]^2}$$

$$+\frac{-(\kappa+2)(L-y_1)^2(r-x)-\kappa(r-x)^3}{\left[(L-y_1)^2+(r-x)^2\right]^2}$$

$$+\frac{-(\kappa+2)(L+y_1)^2(r+x)-\kappa(r+x)^3}{\left[(L+y_1)^2+(r+x)^2\right]^2}$$

$$+\frac{(\kappa+2)(L+y_1)^2(r-x)+\kappa(r-x)^3}{\left[(L+y_1)^2+(r-x)^2\right]^2}\Bigg\}p_2(r)\Bigg]dr,$$

(2.28b)

$$\frac{\partial}{\partial x}u^{(c2)}(x,y_2)=\frac{1}{2\pi\mu(\kappa+1)}\int_0^c\Bigg[\Bigg\{\frac{(2-\kappa)(2L+y_2)^2(r+x)-\kappa(r+x)^3}{\left[(2L+y_2)^2+(r+x)^2\right]^2}$$

$$+\frac{(2-\kappa)(2L+y_2)^2(r-x)-\kappa(r-x)^3}{\left[(2L+y_2)^2+(r-x)^2\right]^2}+\frac{(2-\kappa){y_2}^2(r+x)-\kappa(r+x)^3}{\left[{y_2}^2+(r+x)^2\right]^2}$$

$$+\frac{(2-\kappa){y_2}^2(r-x)-\kappa(r-x)^3}{\left[{y_2}^2+(r-x)^2\right]^2}\Bigg\}p_1(r)$$

$$+\left\{\frac{(2L+y_2)^3-(r-x)^2(2L+y_2)}{\left[(2L+y_2)^2+(r-x)^2\right]^2}+\frac{(2L+y_2)^3-(r+x)^2(2L+y_2)}{\left[(2L+y_2)^2+(r+x)^2\right]^2}\right.$$
$$\left.+\frac{y_2(r-x)^2-{y_2}^3}{\left[{y_2}^2+(r-x)^2\right]^2}+\frac{y_2(r+x)^2-{y_2}^3}{\left[{y_2}^2+(r+x)^2\right]^2}\right\}p_2(r)\Bigg]dr\,, \qquad (2.28c)$$

$$\frac{\partial}{\partial x}v^{(c2)}(x,y_2)=\frac{1}{2\pi\mu(\kappa+1)}\int_0^c\Bigg[\left\{\frac{(2L+y_2)(r-x)^2-(2L+y_2)^3}{\left[(2L+y_2)^2+(r-x)^2\right]^2}\right.$$
$$+\frac{(2L+y_2)^3-(2L+y_2)(r+x)^2}{\left[(2L+y_2)^2+(r+x)^2\right]^2}+\frac{y_2(r-x)^2-{y_2}^3}{\left[{y_2}^2+(r-x)^2\right]^2}$$
$$\left.+\frac{{y_2}^3-y_2(r+x)^2}{\left[{y_2}^2+(r+x)^2\right]^2}\right\}p_1(r)+\left\{\frac{-(\kappa+2)(2L+y_2)^2(r+x)-\kappa(r+x)^3}{\left[(2L+y_2)^2+(r+x)^2\right]^2}\right.$$
$$+\frac{(\kappa+2)(2L+y_2)^2(r-x)+\kappa(r-x)^3}{\left[(2L+y_2)^2+(r-x)^2\right]^2}$$
$$\left.+\frac{(\kappa+2){y_2}^2(r+x)+\kappa(r+x)^3}{\left[{y_2}^2+(r+x)^2\right]^2}+\frac{-(\kappa+2){y_2}^2(r-x)-\kappa(r-x)^3}{\left[{y_2}^2+(r-x)^2\right]^2}\right\}p_2(r)\Bigg]dr$$
$$(2.28d)$$

These expressions can be rewritten in the more compact form for the middle portion $|y|<L$ owing to reason that $p_1(x)$ is odd and $p_2(x)$ is even:

$$\sigma_x^{(c)}(x,y)=\frac{1}{2\pi(\kappa+1)}\int_{-c}^{c}\Bigg[\left\{\frac{(\kappa-1)(L+y)^2(x-r)+(\kappa+3)(x-r)^3}{\left[(L+y)^2+(x-r)^2\right]^2}\right.$$
$$\left.+\frac{(\kappa-1)(L-y)^2(x-r)+(\kappa+3)(x-r)^3}{\left[(L-y)^2+(x-r)^2\right]^2}\right\}p_1(r)$$
$$+\left\{\frac{(\kappa-1)(L+y)^3+(\kappa-5)(x-r)^2(L+y)}{\left[(L+y)^2+(x-r)^2\right]^2}\right.$$
$$\left.+\frac{(\kappa-1)(L-y)^3+(\kappa-5)(x-r)^2(L-y)}{\left[(L-y)^2+(x-r)^2\right]^2}\right\}p_2(r)\Bigg]dr\,, \qquad (2.29a)$$

$$\sigma_y^{(c)}(x,y)=\frac{1}{2\pi(\kappa+1)}\int_{-c}^{c}\left[\left\{\frac{(5-\kappa)(L+y)^2(x-r)+(1-\kappa)(x-r)^3}{\left[(L+y)^2+(x-r)^2\right]^2}\right.\right.$$
$$\left.+\frac{(5-\kappa)(L-y)^2(x-r)+(1-\kappa)(x-r)^3}{\left[(L-y)^2+(x-r)^2\right]^2}\right\}p_1(r)$$
$$+\left\{\frac{-(\kappa+3)(L+y)^3-(\kappa-1)(x-r)^2(L+y)}{\left[(L+y)^2+(x-r)^2\right]^2}\right.$$
$$\left.\left.+\frac{-(\kappa+3)(L-y)^3-(\kappa-1)(x-r)^2(L-y)}{\left[(L-y)^2+(x-r)^2\right]^2}\right\}p_2(r)\right]dr\,, \qquad (2.29b)$$

$$\tau_{xy}^{(c)}(x,y)=\frac{1}{2\pi(\kappa+1)}\int_{-c}^{c}\left[\left\{\frac{(\kappa-1)(L+y)^3+(\kappa+3)(x-r)^2(L+y)}{\left[(L+y)^2+(x-r)^2\right]^2}\right.\right.$$
$$\left.+\frac{-(\kappa-1)(L-y)^3-(\kappa+3)(x-r)^2(L-y)}{\left[(L-y)^2+(x-r)^2\right]^2}\right\}p_1(r)$$
$$+\left\{\frac{(\kappa+3)(L-y)^2(x-r)+(\kappa-1)(x-r)^3}{\left[(L-y)^2+(x-r)^2\right]^2}\right.$$
$$\left.\left.+\frac{-(\kappa+3)(L+y)^2(x-r)-(\kappa-1)(x-r)^3}{\left[(L+y)^2+(x-r)^2\right]^2}\right\}p_2(r)\right]dr\,, \qquad (2.29c)$$

$$\frac{\partial}{\partial x}u^{(c)}(x,y)=\frac{1}{2\pi\mu(\kappa+1)}\int_{-c}^{c}\left[\left\{\frac{(\kappa-2)(L+y)^2(x-r)+\kappa(x-r)^3}{\left[(L+y)^2+(x-r)^2\right]^2}\right.\right.$$
$$\left.+\frac{(\kappa-2)(L-y)^2(x-r)+\kappa(x-r)^3}{\left[(L-y)^2+(x-r)^2\right]^2}\right\}p_1(r)$$
$$\left.+\left\{\frac{(L+y)^3-(x-r)^2(L+y)}{\left[(L+y)^2+(x-r)^2\right]^2}+\frac{(L-y)^3-(x-r)^2(L-y)}{\left[(L-y)^2+(x-r)^2\right]^2}\right\}p_2(r)\right]dr\,,$$

(2.30a)

$$\frac{\partial}{\partial x}v^{(c)}(x,y)=\frac{1}{2\pi\mu(\kappa+1)}\int_{-c}^{c}\left[\left\{\frac{(x-r)^2(L+y)-(L+y)^3}{\left[(L+y)^2+(x-r)^2\right]^2}\right.\right.$$
$$\left.+\frac{(x-r)^2(L-y)-(L-y)^3}{\left[(L-y)^2+(x-r)^2\right]^2}\right\}p_1(r)+\left\{\frac{-(\kappa+2)(L+y)^2(x-r)-\kappa(x-r)^3}{\left[(L+y)^2+(x-r)^2\right]^2}\right.$$
$$\left.\left.+\frac{(\kappa+2)(L-y)^2(x-r)+\kappa(x-r)^3}{\left[(L-y)^2+(x-r)^2\right]^2}\right\}p_2(r)\right]dr\ . \qquad (2.30b)$$

### 2.1.2.4 General Expressions for Perturbation Problem

To get general expressions for the perturbation problem (ii) indicated in Figure 2.1, general solutions of problems (a), (b) and (c) are to be summed up:

$$\sigma_x^{(ii)}(x,y)=\sigma_x^{(a)}(x,y)+\sigma_x^{(b)}(x,y)+\sigma_x^{(c)}(x,y),$$

$$\sigma_y^{(ii)}(x,y)=\sigma_y^{(a)}(x,y)+\sigma_y^{(b)}(x,y)+\sigma_y^{(c)}(x,y),$$

$$\tau_{xy}^{(ii)}(x,y)=\tau_{xy}^{(a)}(x,y)+\tau_{xy}^{(b)}(x,y)+\tau_{xy}^{(c)}(x,y), \qquad (2.31a–c)$$

$$\frac{\partial}{\partial x}u^{(ii)}(x,y)=\frac{\partial}{\partial x}u^{(a)}(x,y)+\frac{\partial}{\partial x}u^{(b)}(x,y)+\frac{\partial}{\partial x}u^{(c)}(x,y),$$

$$\frac{\partial}{\partial x}v^{(ii)}(x,y)=\frac{\partial}{\partial x}v^{(a)}(x,y)+\frac{\partial}{\partial x}v^{(b)}(x,y)+\frac{\partial}{\partial x}v^{(c)}(x,y). \qquad (2.32a,b)$$

### 2.1.3 Infinite Strip Problem (Superposition)

General expressions for the infinite strip are acquired by the superposition of the uniform solution and the general expressions for the pertubration problem stemmed from 2.1.2.4:

$$\sigma_x = \sigma_x^{(i)} + \sigma_x^{(ii)},$$

$$\sigma_y = \sigma_y^{(i)} + \sigma_y^{(ii)},$$

$$\tau_{xy} = \tau_{xy}^{(i)} + \tau_{xy}^{(ii)}, \qquad (2.33a–c)$$

$$\frac{\partial u}{\partial x} = \frac{\partial}{\partial x} u^{(i)} + \frac{\partial}{\partial x} u^{(ii)},$$

$$\frac{\partial v}{\partial x} = \frac{\partial}{\partial x} v^{(i)} + \frac{\partial}{\partial x} v^{(ii)}. \qquad (2.34a,b)$$

In these expressions being consisted of superposition of the uniform and pertubration solutions, 5 unknowns such as $A$, $B$, $m$, $p_1$, $p_2$ exist. It should also be noted that expressions given in Eqs. (2.31) and Eqs. (2.32) are valid for one quarter of the medium, $0 < x < \infty$ and $0 < y < L$.

To obtain the edges of the strip stress-free, following two boundary conditions must be satisfied:

$$\sigma_x(h, y) = 0,$$

$$\tau_{xy}(h, y) = 0. \qquad (2.35a,b)$$

By substituting Eqs. (2.33a–c) in Eqs. (2.35) and taking integration formulas into account shown in Appendix C, two equations given below can be obtained:

$$A(s)\cosh(sh)+B(s)sh\sin(sh)=\frac{1}{\kappa+1}\int_a^b\left\{s(h+t)e^{-s(h+t)}-s(h-t)e^{-s(h-t)}\right\}m(t)dt$$
$$+\frac{1}{4\mu(\kappa+1)}\left[\int_{-c}^{c}\left\{\kappa+2s(h-r)+1\right\}\cos(sL)e^{-s(h-r)}\ p_1(r)dr\right.$$
$$\left.+\int_{-c}^{c}\left\{\kappa-2s(h-r)-1\right\}\sin(sL)e^{-s(h-r)}p_2(r)dr\right], \qquad (2.36a)$$

$$A(s)\sinh(sh)+B(s)\left[\sin(sh)+sh\cosh(sh)\right]=\frac{-1}{\kappa+1}\int_a^b\left\{\left[1-s(h-t)\right]e^{-s(h-t)}\right.$$
$$\left.+\left[s(h+t)-1\right]e^{-s(h+t)}\right\}m(t)dt$$
$$+\frac{1}{4\mu(\kappa+1)}\left[\int_{-c}^{c}\left\{-\kappa-2s(h-r)+1\right\}\cos(sL)e^{-s(h-r)}\ p_1(r)dr\right.$$
$$\left.+\int_{-c}^{c}\left\{-\kappa+2s(h-r)-1\right\}\sin(sL)e^{-s(h-r)}p_2(r)dr\right]. \qquad (2.36b)$$

When these two equations are solved together, unknowns $A$ and $B$ can be written in terms of the rest of the unkowns functions that are $m$, $p_1$, $p_2$:

$$A(s)=\frac{1}{\kappa+1}\left[\int_a^b m(t)\,f(s)\left\langle e^{-s(h+t)}\left\{e^{sh}\left[-2st(1+2sh)-(2sh)^2\right]+e^{-sh}2st\right\}\right.\right.$$
$$\left.\left.+e^{-s(h-t)}\left\{e^{sh}\left[-2st(1+2sh)+(2sh)^2\right]+e^{-sh}2st\right\}\right\rangle dt\right.$$
$$-\frac{1}{2\mu}\int_{-c}^{c}p_1(r)\,f(s)e^{-s(h-r)}\left\{e^{sh}\left[(1+2sh)(1+\kappa-2sr)+(2sh)^2\right]\right.$$
$$\left.-e^{-sh}\left[1+\kappa-2sr\right]\right\}\cos(sL)dr$$

$$+\frac{1}{2\mu}\int_{-c}^{c} p_2(r)\,f(s)e^{-s(h-r)}\left\{e^{sh}\left[(1+2sh)(1-\kappa-2sr)+(2sh)^2\right]\right.$$
$$\left.-e^{-sh}\left[1-\kappa-2sr\right]\right\}\sin(sL)dr\Big],$$

$$B(s)=\frac{1}{\kappa+1}\Bigg[\int_{a}^{b} m(t)\,f(s)\Big\langle e^{-s(h+t)}\left\{e^{sh}\left[4s(h+t)-2\right]-2e^{-sh}\right\}$$
$$+e^{-s(h-t)}\left\{e^{sh}\left[-4s(h-t)+2\right]+2e^{-sh}\right\}\Big\rangle dt$$
$$+\frac{1}{2\mu}\int_{-c}^{c} p_1(r)\,f(s)e^{-s(h-r)}\left\{e^{sh}\left[2\kappa+4s(h-r)\right]-2e^{-sh}\right\}\cos(sL)dr$$
$$+\frac{1}{2\mu}\int_{-c}^{c} p_2(r)\,f(s)e^{-s(h-r)}\left\{e^{sh}\left[2\kappa-4s(h-r)\right]+2e^{-sh}\right\}\sin(sL)dr\Bigg], \qquad (2.37a,b)$$

in which

$$f(s) = -1/[4sh + e^{2sh} - e^{-2sh}]. \qquad (2.38)$$

The following expressions for the infinite strip problem can be obtained by substituting Eqs. (2.37) in Eqs. (2.33) and Eqs. (2.34) and then rearranging the resulting expressions:

$$\sigma_x(x,y)=\frac{2\mu}{\pi(\kappa+1)}\int_{a}^{b} m(t)\left\{\frac{2y^2(x-t)-2(x-t)^3}{\left[y^2+(x-t)^2\right]^2}\right.$$
$$\left.+\frac{-2y^2(x+t)+2(x+t)^3}{\left[y^2+(x+t)^2\right]^2}+A_1(t,x,y)\right\}dt$$
$$+\frac{1}{2\pi(\kappa+1)}\int_{-c}^{c} p_1(r)\left\{\frac{(\kappa-1)(L+y)^2(x-r)+(\kappa+3)(x-r)^3}{\left[(L+y)^2+(x-r)^2\right]^2}\right.$$
$$\left.+\frac{(\kappa-1)(L-y)^2(x-r)+(\kappa+3)(x-r)^3}{\left[(L-y)^2+(x-r)^2\right]^2}+B_1(r,x,y)\right\}dr$$

$$+\frac{1}{2\pi(\kappa+1)}\int_{-c}^{c} p_2(r)\left\{\frac{(\kappa-1)(L+y)^3+(\kappa-5)(x-r)^2(L+y)}{\left[(L+y)^2+(x-r)^2\right]^2}\right.$$

$$\left.+\frac{(\kappa-1)(L-y)^3+(\kappa-5)(x-r)^2(L-y)}{\left[(L-y)^2+(x-r)^2\right]^2}+C_1(r,x,y)\right\}dr\,, \qquad (2.39a)$$

$$\sigma_y(x,y)=p_0+\frac{2\mu}{\pi(\kappa+1)}\int_a^b m(t)\left\{\frac{6y^2(x+t)+2(x+t)^3}{\left[y^2+(x+t)^2\right]^2}\right.$$

$$\left.+\frac{-6y^2(x-t)-2(x-t)^3}{\left[y^2+(x-t)^2\right]^2}+A_2(t,x,y)\right\}dt$$

$$+\frac{1}{2\pi(\kappa+1)}\int_{-c}^{c} p_1(r)\left\{\frac{(5-\kappa)(L+y)^2(x-r)+(1-\kappa)(x-r)^3}{\left[(L+y)^2+(x-r)^2\right]^2}\right.$$

$$\left.+\frac{(5-\kappa)(L-y)^2(x-r)+(1-\kappa)(x-r)^3}{\left[(L-y)^2+(x-r)^2\right]^2}+B_2(r,x,y)\right\}dr$$

$$+\frac{1}{2\pi(\kappa+1)}\int_{-c}^{c} p_2(r)\left\{\frac{-(\kappa+3)(L+y)^3-(\kappa-1)(x-r)^2(L+y)}{\left[(L+y)^2+(x-r)^2\right]^2}\right.$$

$$\left.+\frac{-(\kappa+3)(L-y)^3-(\kappa-1)(x-r)^2(L-y)}{\left[(L-y)^2+(x-r)^2\right]^2}+C_2(r,x,y)\right\}dr\,, \qquad (2.39b)$$

$$\tau_{xy}(x,y)=\frac{2\mu}{\pi(\kappa+1)}\int_a^b m(t)\left\{\frac{2y^3-2y(x-t)^2}{\left[y^2+(x-t)^2\right]^2}-\frac{2y^3-2y(x+t)^2}{\left[y^2+(x+t)^2\right]^2}+A_3(t,x,y)\right\}dt$$

$$+\frac{1}{2\pi(\kappa+1)}\int_{-c}^{c} p_1(r)\left\{\frac{(\kappa-1)(L+y)^3+(\kappa+3)(x-r)^2(L+y)}{\left[(L+y)^2+(x-r)^2\right]^2}\right.$$

$$\left.+\frac{-(\kappa-1)(L-y)^3-(\kappa+3)(x-r)^2(L-y)}{\left[(L-y)^2+(x-r)^2\right]^2}+B_3(r,x,y)\right\}dr$$

$$+\frac{1}{2\pi(\kappa+1)}\int_{-c}^{c} p_2(r)\left\{\frac{(\kappa+3)(L-y)^2(x-r)+(\kappa-1)(x-r)^3}{\left[(L-y)^2+(x-r)^2\right]^2}\right.$$

$$\left.+\frac{-(\kappa-3)(L+y)^2(x-r)-(\kappa-1)(x-r)^3}{\left[(L+y)^2+(x-r)^2\right]^2}+C_3(r,x,y)\right\}dr\,, \qquad (2.39c)$$

$$\frac{\partial}{\partial x}u(x,y)=\frac{\kappa-3}{8\mu}p_0+\frac{1}{\pi(\kappa+1)}\int_a^b m(t)\left\{\frac{-(5-\kappa)y^2(x+t)-(1-\kappa)(x+t)^3}{\left[y^2+(x+t)^2\right]^2}\right.$$

$$\left.+\frac{(5-\kappa)y^2(x-t)+(1-\kappa)(x-t)^3}{\left[y^2+(x-t)^2\right]^2}+A_4(t,x,y)\right\}dt$$

$$+\frac{1}{2\pi\mu(\kappa+1)}\int_{-c}^{c} p_1(r)\left\{\frac{(\kappa-2)(L+y)^2(x-r)+\kappa(x-r)^3}{\left[(L+y)^2+(x-r)^2\right]^2}\right.$$

$$\left.+\frac{(\kappa-2)(L-y)^2(x-r)+\kappa(x-r)^3}{\left[(L-y)^2+(x-r)^2\right]^2}+B_4(r,x,y)\right\}dr$$

$$+\frac{1}{2\pi\mu(\kappa+1)}\int_{-c}^{c} p_2(r)\left\{\frac{(L+y)^3-(L+y)(x-r)^2}{\left[(L+y)^2+(x-r)^2\right]^2}\right.$$

$$\left.+\frac{(L-y)^3-(L-y)(x-r)^2}{\left[(L-y)^2+(x-r)^2\right]^2}+C_4(r,x,y)\right\}dr\,, \qquad (2.40a)$$

$$\frac{\partial}{\partial x}v(x,y)=\frac{1}{\pi(\kappa+1)}\int_a^b m(t)\left\{\frac{(\kappa-1)y(x-t)^2+(\kappa+3)y^3}{\left[y^2+(x-t)^2\right]^2}\right.$$

$$\left.+\frac{-(\kappa-1)y(x+t)^2-(\kappa+3)y^3}{\left[y^2+(x+t)^2\right]^2}+A_5(t,x,y)\right\}dt$$

$$+\frac{1}{2\pi\mu(\kappa+1)}\int_{-c}^{c} p_1(r)\left\{\frac{(L+y)(x-r)^2-(L+y)^3}{\left[(L+y)^2+(x-r)^2\right]^2}\right.$$

$$\left.+\frac{(L-y)(x-r)^2-(L-y)^3}{\left[(L-y)^2+(x-r)^2\right]^2}+B_5(r,x,y)\right\}dr$$

$$+\frac{1}{2\pi\mu(\kappa+1)}\int_{-c}^{c} p_2(r)\left\{\frac{-\kappa(x-r)^3-(\kappa+2)(x-r)(L+y)^2}{\left[(L+y)^2+(x-r)^2\right]^2}\right.$$

$$\left.+\frac{\kappa(x-r)^3+(\kappa+2)(x-r)(L-y)^2}{\left[(L-y)^2+(x-r)^2\right]^2}+C_5(r,x,y)\right\}dr\,, \qquad (2.40b)$$

in which $A_i$, $B_i$ and $C_i$, ($i$=1–5), are defined in Appendix D.

In these expressions there are still 3 unknowns which are $m$, the crack surface displacement derivative, and $p_1$ and $p_2$, the jumps in the shearing and normal stresses through the rigid inclusions.

To satisfy the requirements of crack surfaces being free of stresses and the displacements such that the inclusions are rigid, following 3 boundary conditions are added to solution:

$$\frac{\partial}{\partial x}u(x,L)=0\,, \qquad (|x|<c),$$

$$\frac{\partial}{\partial x}v(x,L)=0\,, \qquad (|x|<c),$$

$$\sigma_y(x,0)=0\,, \qquad (a<|x|<b). \qquad (2.41a–c)$$

# CHAPTER III

# INTEGRAL EQUATIONS

## 3.1 Derivation of Integral Equations

In this section, the boundary conditions of Eqs. (2.41a–c) are applied to Eqs. (2.40a,b) and (2.39b) and accordingly, three singular integral equations are obtained as given below:

$$\int_{-c}^{c} p_1(r)\left\{\frac{\kappa}{x-r}+\frac{4(\kappa-2)L^2(x-r)+\kappa(x-r)^3}{\left[4L^2+(x-r)^2\right]^2}+k_{11}(x,r)\right\}dr$$

$$+\int_{-c}^{c} p_2(r)\left\{\frac{8L^3-2L(x-r)^2}{\left[4L^2+(x-r)^2\right]^2}+k_{12}(x,r)\right\}dr$$

$$+2\mu\int_{a}^{b} m(t)\left\{\frac{-(5-\kappa)L^2(x+t)-(1-\kappa)(x+t)^3}{\left[L^2+(x+t)^2\right]^2}\right.$$

$$\left.+\frac{(5-\kappa)L^2(x-t)+(1-\kappa)(x-t)^3}{\left[L^2+(x-t)^2\right]^2}+k_{13}(x,t)\right\}dt$$

$$=\frac{\pi}{4}(1+\kappa)(3-\kappa)p_0, \qquad (-c<x<c) \qquad (3.1a)$$

$$\int_{-c}^{c} p_1(r)\left\{\frac{2L(x-r)^2-8L^3}{\left[4L^2+(x-r)^2\right]^2}+k_{21}(x,r)\right\}dr$$

$$+\int_{-c}^{c} p_2(r)\left\{\frac{\kappa}{x-r}+\frac{-\kappa(x-r)^3-4(\kappa+2)L^2(x-r)}{\left[4L^2+(x-r)^2\right]^2}+k_{22}(x,r)\right\}dr$$

$$+2\mu\int_a^b m(t)\left\{\frac{(\kappa-1)L(x-t)^2+(\kappa+3)L^3}{\left[L^2+(x-t)^2\right]^2}\right.$$

$$\left.+\frac{-(\kappa-1)L(x+t)^2-(\kappa+3)L^3}{\left[L^2+(x+t)^2\right]^2}+k_{23}(x,t)\right\}dt=0\,, \qquad (-c<x<c)$$

$$\int_{-c}^{c} p_1(r)\left\{\frac{(\kappa-5)L^2(x-r)+(\kappa-1)(x-r)^3}{\left[L^2+(x-r)^2\right]^2}+k_{31}(x,r)\right\}dr$$

$$+\int_{-c}^{c} p_2(r)\left\{\frac{(\kappa+3)L^3+(\kappa-1)L(x-r)^2}{\left[L^2+(x-r)^2\right]^2}+k_{32}(x,r)\right\}dr$$

$$+2\mu\int_a^b m(t)\left\{\frac{-2}{x+t}+\frac{2}{x-t}+k_{33}(x,t)\right\}dt=\pi(1+\kappa)p_0\,, \qquad (a<x<b)$$

(3.1b,c)

where the kernels $k_{ij}$ ($i, j$ = 1 – 3) are given by

$$k_{ij}(x,r)=\int_0^\infty K_{ij}(x,r,s)ds\,, \quad (j=1,2)$$

$$k_{i3}(x,t)=\int_0^\infty K_{i3}(x,t,s)ds\,, \quad (i=1-3) \qquad \text{(3.2a–i)}$$

in which

$$\begin{aligned}K_{11}(x,r,s)=\Big[&e^{-s(2h-r-x)}\left(\left\{2\kappa-2s(r+x)-2\right\}e^{-2sh}\right.\\&\left.+\left\{\kappa+2s(h-r)\right\}\left\{-\kappa-2s(h-x)+2\right\}-1\right)\\&+e^{-s(2h-r+x)}\left(\left\{2\kappa-2s(r-x)-2\right\}e^{-2sh}\right.\\&\left.+\left\{\kappa+2s(h-r)\right\}\left\{-\kappa-2s(h+x)+2\right\}-1\right)\Big]\times\cos^2(sL)/F(s)\end{aligned}$$

(3.3a)

$$K_{12}(x,r,s)=\Big[e^{-s(2h-r-x)}\Big(\{2+2s(r+x)\}e^{-2sh}$$
$$+\{-\kappa+2s(h-r)\}\{\kappa+2s(h-x)-2\}+1\Big)$$
$$+e^{-s(2h-r+x)}\Big(\{2+2s(r-x)\}e^{-2sh}$$
$$+\{-\kappa+2s(h-r)\}\{\kappa+2s(h+x)-2\}+1\Big)\Big]\times\sin(2sL)/F(s)$$

$$K_{13}(x,t,s)=\Big[e^{-s(2h-t-x)}\Big(\{-\kappa+2s(t+x)+3\}e^{-2sh}$$
$$+\{-1+2s(h-t)\}\{\kappa+2s(h-x)-2\}+1\Big)$$
$$+e^{-s(2h-t+x)}\Big(\{-\kappa+2s(t-x)+3\}e^{-2sh}$$
$$+\{-1+2s(h-t)\}\{\kappa+2s(h+x)-2\}+1\Big)$$
$$+e^{-s(2h+t-x)}\Big(\{\kappa+2s(t-x)-3\}e^{-2sh}$$
$$+\{1-2s(h+t)\}\{\kappa+2s(h-x)-2\}-1\Big)$$
$$+e^{-s(2h+t+x)}\Big(\{\kappa+2s(t+x)-3\}e^{-2sh}$$
$$+\{1-2s(h+t)\}\{\kappa+2s(h+x)-2\}-1\Big)\Big]\times\cos(sL)/F(s)$$

$$K_{21}(x,r,s)=\Big[e^{-s(2h-r-x)}\Big(\{2s(r+x)+2\}e^{-2sh}$$
$$+\{\kappa+2s(h-r)\}\{-\kappa+2s(h-x)-2\}+1\Big)$$
$$+e^{-s(2h-r+x)}\Big(\{-2s(r-x)-2\}e^{-2sh}$$
$$+\{\kappa+2s(h-r)\}\{\kappa-2s(h+x)+2\}-1\Big)\Big]\times\sin(2sL)/2F(s)$$

$$K_{22}(x,r,s)=\Big[e^{-s(2h-r-x)}\Big(\{-2\kappa-2s(r+x)-2\}e^{-2sh}$$
$$+\{\kappa-2s(h-r)\}\{-\kappa+2s(h-x)-2\}-1\Big)$$
$$+e^{-s(2h-r+x)}\Big(\{2\kappa+2s(r-x)+2\}e^{-2sh}$$
$$+\{\kappa-2s(h-r)\}\{\kappa-2s(h+x)+2\}+1\Big)\Big]\times\sin^2(sL)/F(s)$$

(3.3b–e)

$$
\begin{aligned}
K_{23}(x,t,s) = \Big[ & e^{-s(2h-t-x)} \left( \{-\kappa - 2s(t+x) - 3\} e^{-2sh} \right. \\
& \left. + \{1 - 2s(h-t)\} \{-\kappa + 2s(h-x) - 2\} - 1 \right) \\
& + e^{-s(2h-t+x)} \left( \{\kappa + 2s(t-x) + 3\} e^{-2sh} \right. \\
& \left. + \{1 - 2s(h-t)\} \{\kappa - 2s(h+x) + 2\} + 1 \right) \Big] \\
& + e^{-s(2h+t-x)} \left( \{\kappa - 2s(t-x) + 3\} e^{-2sh} \right. \\
& \left. + \{1 - 2s(h+t)\} \{\kappa - 2s(h-x) + 2\} + 1 \right) \Big] \\
& + e^{-s(2h+t+x)} \left( \{-\kappa + 2s(t+x) - 3\} e^{-2sh} \right. \\
& \left. + \{1 - 2s(h+t)\} \{-\kappa + 2s(h+x) - 2\} - 1 \right) \Big] \times \sin(sL)/F(s)
\end{aligned}
$$

$$
\begin{aligned}
K_{31}(x,r,s) = \Big[ & e^{-s(2h-r-x)} \left( \{\kappa - 2s(r+x) - 3\} e^{-2sh} \right. \\
& \left. + \{\kappa + 2s(h-r)\} \{3 - 2s(h-x)\} - 1 \right) \\
& + e^{-s(2h-r+x)} \left( \{\kappa - 2s(r-x) - 3\} e^{-2sh} \right. \\
& \left. + \{\kappa + 2s(h-r)\} \{3 - 2s(h+x)\} - 1 \right) \Big] \times \cos(sL)/F(s)
\end{aligned}
$$

$$
\begin{aligned}
K_{32}(x,r,s) = \Big[ & e^{-s(2h-r-x)} \left( \{\kappa + 2s(r+x) + 3\} e^{-2sh} \right. \\
& \left. + \{\kappa - 2s(h-r)\} \{3 - 2s(h-x)\} + 1 \right) \\
& + e^{-s(2h-r+x)} \left( \{\kappa + 2s(r-x) + 3\} e^{-2sh} \right. \\
& \left. + \{\kappa - 2s(h-r)\} \{3 - 2s(h+x)\} + 1 \right) \Big] \times \sin(sL)/F(s)
\end{aligned}
$$

(3.3f–h)

$$
\begin{aligned}
K_{33}(x,t,s) = \Big[ & e^{-s(2h-t-x)} \left( \{4 + 2s(t+x)\} e^{-2sh} \right. \\
& \left. + \{1 - 2s(h-t)\} \{3 - 2s(h-x)\} + 1 \right) \\
& + e^{-s(2h-t+x)} \left( \{4 + 2s(t-x)\} e^{-2sh} \right. \\
& \left. + \{1 - 2s(h-t)\} \{3 - 2s(h+x)\} + 1 \right) \\
& + e^{-s(2h+t-x)} \left( \{-4 + 2s(t-x)\} e^{-2sh} \right.
\end{aligned}
$$

$$+\{1-2s(h+t)\}\{-3+2s(h-x)\}-1\big)$$
$$+e^{-s(2h+t+x)}\big(\{-4+2s(t+x)\}e^{-2sh}$$
$$+\{1-2s(h+t)\}\{-3+2s(h+x)\}-1\big)\big]/F(s) \qquad (3.3i)$$

and

$$F(s) = 1+4she^{-2sh} - e^{-4sh}. \qquad (3.4)$$

These three singular integral equations, Eqs. (3.1a–c), are to be solved by satisfying the equilibrium conditions for the inclusions and the single-valuedness condition for the crack given below:

$$\int_{-c}^{c} p_1(r)dr = 0,$$

$$\int_{-c}^{c} p_2(r)dr = 0,$$

$$\int_{a}^{b} m(t)dt = 0. \qquad (3.5a–c)$$

Here, it should be mentioned that the solution for the finite strip problem is obtained from the infinite strip problem by considering the limiting case when $c\to h$. In that case, the portion of the infinite strip between two inclusions become a finite strip of length $2L$. When the kernels of the integral equations, Eqs. (3.1) are examined, one can see that there are singular terms in $k_{ij}$ ($i,j$=1–3). These singular terms are due to behavior of $K_{ij}$ ($i,j$=1–3) when $s\to\infty$. If $b < h$ and $c < h$, simple Cauchy kernels of types $1/(t–x)$ and $1/(r–x)$ are the only singular terms. But if $b = h$ or $c = h$, additional singular terms again due to behavior of $K_{ij}$ ($i,j$=1–3) exist. These terms can be detected by giving consideration to the non-vanishing portions of $K_{ij}$ ($i,j$=1–3) as $s\to\infty$:

Let

$$K_{ij\infty} = \lim_{s\to\infty} K_{ij} \qquad \text{(i,j=1–3)} \qquad (3.6)$$

and

$$K_{ijb} = K_{ij} - K_{ij\infty}\,. \qquad \text{(i,j=1–3)} \qquad (3.7)$$

By integrating the expressions of $K_{ij\infty}$, following expressions are obtained which are given in Appendix E:

$$k_{ijs} = \int_0^\infty K_{ij\infty}\,ds \qquad \text{(i,j=1–3)} \qquad (3.8)$$

One has to examine the integrands around $s$ = 0 in addition to singularities in the kernels owing to the non-vanishing integrands in the condition of $s\to\infty$. If integrands around $s$ = 0 are examined, one may point out that $k_{13}(x,t)$ and $k_{31}(x,r)$ need to be calculated carefully. For instance consider $K_{13}(x,t,s)$:

$$K_{13}(x,t,s) = \frac{R_{13}(s,t,x)\cos sL}{1+4she^{-2sh}-e^{-4sh}} \qquad (3.9)$$

According to Adams and Bogy (1975), the integral of $K_{13}(x,t,s)$ can be separated into two parts such as one from *0* to *1* and another from *1* to ∞:

$$\int_0^\infty \frac{R_{13}(s,t,x)\cos sL}{1+4she^{-2sh}-e^{-4sh}}\,ds = \int_0^1 \frac{R_{13}(s,t,x)\cos sL}{1+4she^{-2sh}-e^{-4sh}}\,ds + \int_1^\infty \frac{R_{13}(s,t,x)\cos sL}{1+4she^{-2sh}-e^{-4sh}}\,ds\,. \qquad (3.10)$$

The behavior of $R_{13}$ around $s$ = 0 is as:

$$\lim_{s\to 0} R_{13} = \Phi_{13} = 2(\kappa-3)\,. \qquad (3.11)$$

Due to Eq. (3.11), in the first right hand side expression of Eq. (3.10), $R_{13}$ is rewritten as $R_{13} - \Phi_{13}$ that becomes then unbounded:

$$\int_0^1 \frac{R_{13}(x,t,s)\cos sL}{1+4she^{-2sh}-e^{-4sh}}\,ds = \int_0^1 \frac{R_{13}(x,t,s)-\Phi_{13}}{1+4she^{-2sh}-e^{-4sh}}\cos sL\,ds + \Phi_{13}\int_0^1 \frac{\cos sL}{1+4she^{-2sh}-e^{-4sh}}\,ds \tag{3.12}$$

Although the last integral of Eq. (3.12) is unbounded, this integral is multiplied by

$$\int_a^b m(t)dt \tag{3.13}$$

in Eq. (3.1a) which is equal to zero according to Eq. (3.5c). This means that the singularity at $s = 0$ will be eliminated.

On the other hand, for $K_{31}(x,r,s)$

$$\lim_{s\to 0} R_{31} = \Phi_{31} = 4(1-\kappa) \tag{3.14}$$

is noted. In a similar way given for $K_{13}(x,t,s)$, the unbounded integral will be eliminated as a result of multiplying the unbounded integral in the singular integral equation (3.1c) by

$$\int_{-h}^{h} p_1(r)dr \tag{3.15}$$

which is zero according to Eq. (3.5a).

The unknown functions $p_1$, $p_2$ are expected to be singular at the ends $x = \pm c$ where the other unknown function $m$ is expected to be singular at the ends $x=\pm a, \pm b$. To determine the singularities of these unknown functions, the

singular integral equations (3.1) can be examined around the end points mentioned above by applying the complex technique given in Muskhelishvili (1953). For this purpose, write

$$p_i(r) = p_i^*(r)/(c^2 - r^2)^{\alpha}\,, \qquad (i=1,2,\quad c < h) \qquad 0 < \mathrm{Re}(\alpha) < 1$$

$$p_i(r) = p_i^*(r)/(h^2 - r^2)^{\alpha}\,, \qquad (i=1,2,\quad c = h) \qquad 0 < \mathrm{Re}(\alpha) < 1$$

$$m(t) = m^*(t)/(b-t)^{\gamma}(t-a)^{\beta}\,, \qquad 0 < \mathrm{Re}(\gamma, \beta) < 1 \qquad (3.16a–c)$$

Here, $\alpha$, $\gamma$ and $\beta$ are unknown constants and $p_1^*(r)$, $p_2^*(r)$ and $m^*(t)$ are Hölder-continuous functions in the respective intervals [-$c$, $c$] and [$a$, $b$].

Muskhelishvili's (1953) technique is applied for evaluating the integrals containing singular terms near the end points:

$$\frac{1}{\pi}\int_{-c}^{c}\frac{p_i(r)}{r-x}dr = \frac{p_i^*(-c)\cot\pi\alpha}{\left[2c(x+c)\right]^{\alpha}} - \frac{p_i^*(c)\cot\pi\alpha}{\left[2c(x-c)\right]^{\alpha}} + p_{i1}^*(x) \qquad (i=1,2)$$

$$\frac{1}{\pi}\int_{-h}^{h}\frac{p_i(r)}{r-x}dr = \frac{p_i^*(-h)\cot\pi\alpha}{\left[2h(x+h)\right]^{\alpha}} - \frac{p_i^*(h)\cot\pi\alpha}{\left[2h(x-h)\right]^{\alpha}} + p_{i1}^*(x)\,, \qquad (i=1,2)$$

$$\frac{1}{\pi}\int_{-h}^{h}\frac{p_i(r)}{r-(2h-x)}dr = \frac{-p_i^*(h)}{(2h)^{\alpha}\sin\pi\alpha}\frac{1}{(h-x)^{\alpha}} + p_{i2}^*(x)\,, \qquad (i=1,2)$$

$$\frac{1}{\pi}\int_{-h}^{h}\frac{p_i(r)}{r-(2h+x)}dr = \frac{-p_i^*(h)}{(2h)^{\alpha}\sin\pi\alpha}\frac{1}{(h+x)^{\alpha}} + p_{i3}^*(x)\,, \qquad (i=1,2)$$

(3.17a–d)

$$\frac{1}{\pi}\int_{a}^{b}\frac{m(t)}{t-x}dt = \frac{m^*(a)\cot\pi\beta}{(b-a)^{\gamma}(x-a)^{\beta}} - \frac{m^*(b)\cot\pi\gamma}{(b-a)^{\beta}(b-x)^{\gamma}} + m^{**}(x) \qquad (3.18)$$

In the equations above, $p_{ij}^{*}(x)$ ($i$=1,2; $j$=1–3) and $m^{**}(x)$ are all bounded everywhere excluding the end points. In the situation of substituting these three equations in Eqs. (2.34), the following characteristic equations for $\alpha$ and $\beta$ are deduced from the complex function technique outlined in Muskhelishvili (1953) and the procedure described in Cook and Erdogan (1972):

$$\cot \pi\alpha = 0, \qquad (c < h)$$

$$2\kappa \cos \pi\alpha + 4(\alpha - 1)^2 - \kappa^2 - 1 = 0, \qquad (c = h)$$

$$\cot \pi\beta = 0, \qquad (0 < a)$$

$$\cot \pi\gamma = 0, \qquad (b < h)$$

$$2(1-\gamma)^2 - 1 - \cos \pi\gamma = 0. \qquad (b = h) \qquad \text{(3.19a–e)}$$

Eq. (3.19a) gives $\alpha$ = 1/2 for the tip of an internal rigid inclusion. Eqs. (3.19c,d) give $\beta$ = 1/2, $\gamma$ = 1/2 for the tips of an internal crack. Eq. (3.19e) gives $\gamma$ = 1 which is unacceptable. Therefore, $m(x)$ does not have a power singularity at the end $x = h$ (at the corner of an edge crack with a free boundary). Note here that Eqs. (3.19a–e) are in agreement with the previous results Gupta (1973, 1975), Gecit and Turgut (1988), Artem and Gecit (2002), Yetmez and Gecit (2005), Toygar and Gecit (2006), Kaman and Gecit (2006).

It should also be considered that the following relations are used when obtaining Eqs. (3.19).

$$\frac{h \pm x}{(2h - r \pm x)^2} = \pm(h \pm x)\frac{d}{dx}\left(\frac{1}{2h - r \pm x}\right), \qquad \text{(3.20a)}$$

$$\frac{2(h\pm x)^2}{(2h-r\pm x)^3}=(h\pm x)^2\frac{d^2}{dx^2}\left(\frac{1}{2h-r\pm x}\right). \tag{3.20b}$$

The system of equations shown in Eqs. (3.1) can be put into the form of the following singular integral equations:

$$\begin{aligned}
&\frac{1}{\pi}\int_{-c}^{c}p_1(r)\left[\frac{1}{r-x}+k_{11s}(r,x)+\int_0^\infty K_{11b}(s,r,x)ds\right]dr\\
&+\frac{1}{\pi}\int_{-c}^{c}p_2(r)\left[k_{12s}(r,x)+\int_0^\infty K_{12b}(s,r,x)ds\right]dr\\
&+\frac{1}{\pi}\int_{a}^{b}4\mu m(t)\left[k_{13s}(t,x)+\int_0^\infty K_{13b}(s,t,x)ds\right]dt=\frac{(\kappa+1)(\kappa-3)}{4\kappa}p_0\,, \qquad (|x|<c)
\end{aligned}$$

$$\begin{aligned}
&\frac{1}{\pi}\int_{-c}^{c}p_1(r)\left[k_{21s}(r,x)+\int_0^\infty K_{21b}(s,r,x)ds\right]dr\\
&+\frac{1}{\pi}\int_{-c}^{c}p_2(r)\left[\frac{1}{r-x}+k_{22s}(r,x)+\int_0^\infty K_{22b}(s,r,x)ds\right]dr\\
&+\frac{1}{\pi}\int_{a}^{b}4\mu m(t)\left[k_{23s}(t,x)+\int_0^\infty K_{23b}(s,t,x)ds\right]dt=0\,, \qquad (|x|<c)
\end{aligned}$$

$$\begin{aligned}
&\frac{1}{\pi}\int_{-c}^{c}p_1(r)\left[k_{31s}(r,x)+\int_0^\infty K_{31b}(s,r,x)ds\right]dr\\
&+\frac{1}{\pi}\int_{-c}^{c}p_2(r)\left[k_{32s}(r,x)+\int_0^\infty K_{32b}(s,r,x)ds\right]dr\\
&+\frac{1}{\pi}\int_{a}^{b}4\mu m(t)\left[\frac{1}{t-x}+\frac{1}{t+x}+k_{33s}(t,x)+\int_0^\infty K_{33b}(s,t,x)ds\right]dt=-(\kappa+1)P_0\,, \quad (a<x<b)
\end{aligned} \tag{3.21a–c}$$

for an infinite strip with two rigid inclusions at $y=\pm L$ and two collinear cracks at $y=0$.

As it is mentioned before, kernels of Eqs. (3.21), $k_{ijs}$ and $K_{ijb}$ ($i$, $j$=1–3) are defined in Appendix E.

# CHAPTER IV

# SOLUTION OF INTEGRAL EQUATIONS

## 4.1 Infinite Strip Having Two Internal Cracks and Two Internal Rigid Inclusions

Consider an infinite strip having two internal collinear and symmetrical cracks which are located on *x*-axis, from *a* to *b* and from *–a* to *–b*. The infinite strip contains also two rigid inclusions at $y=\pm L$ and each of them has a width of *2c*. Both ends of this infinite strip are subjected to uniformly distributed axial tensile loads of intensity $p_0$ shown in Figure 4.1.

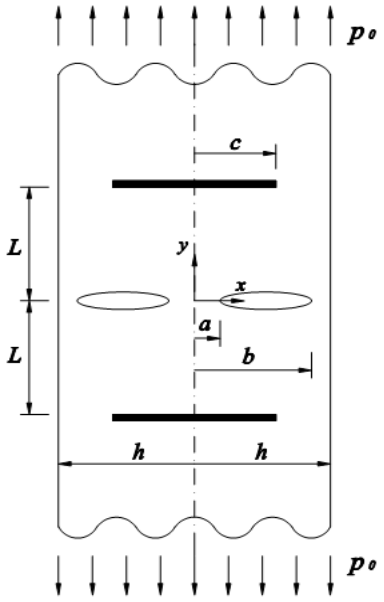


Figure 4.1 Geometry of an infinite strip with two internal collinear cracks and two rigid inclusions.

Non-dimensional variables for the cracks $\eta$ and $\rho$ are defined as

$$x = \frac{b-a}{2}\eta + \frac{b+a}{2}, \qquad (a < x < b, -1 < \eta < 1)$$

$$t = \frac{b-a}{2}\rho + \frac{b+a}{2}, \qquad (a < t < b, -1 < \rho < 1) \qquad (4.1a,b)$$

and the non-dimensional variables for the inclusions $\xi$ and $\varphi$ are defined as

$$x = c\xi, \qquad (-c < x < c, -1 < \xi < 1)$$

$$r = c\varphi. \qquad (-c < r < c, -1 < \varphi < 1) \qquad (4.2a,b)$$

Then, the system of three singular integral equations, Eqs.(3.21a–c), becomes:

$$\frac{1}{\pi}\int_{-1}^{1}\overline{P_1}(\varphi)\left\{\frac{1}{\varphi-\xi}+\bar{k}_{11}(\xi,\varphi)\right\}d\varphi+\frac{1}{\pi}\int_{-1}^{1}\overline{P_2}(\varphi)\bar{k}_{12}(\xi,\varphi)d\varphi$$
$$+\frac{1}{\pi}\int_{-1}^{1}\overline{m}(\rho)\bar{k}_{13}(\xi,\rho)d\rho=\frac{(\kappa+1)(\kappa-3)}{4\kappa}, \qquad (-1 < \xi < 1)$$

$$\frac{1}{\pi}\int_{-1}^{1}\overline{P_1}(\varphi)\bar{k}_{21}(\xi,\varphi)d\varphi+\frac{1}{\pi}\int_{-1}^{1}\overline{P_2}(\varphi)\left\{\frac{1}{\varphi-\xi}+\bar{k}_{22}(\xi,\varphi)\right\}d\varphi$$
$$+\frac{1}{\pi}\int_{-1}^{1}\overline{m}(\rho)\bar{k}_{23}(\xi,\rho)d\rho=0, \qquad (-1 < \xi < 1)$$

$$\frac{1}{\pi}\int_{-1}^{1}\overline{P_1}(\varphi)\bar{k}_{31}(\eta,\varphi)d\varphi+\frac{1}{\pi}\int_{-1}^{1}\overline{P_2}(\varphi)\bar{k}_{32}(\eta,\varphi)d\varphi$$
$$+\frac{1}{\pi}\int_{-1}^{1}\overline{m}(\rho)\left\{\frac{1}{\rho-\eta}+\frac{1}{\rho+\eta+2g/f}+\bar{k}_{33}(\eta,\rho)\right\}d\rho=-(\kappa+1), \qquad (-1 < \eta < 1)$$

(4.3a–c)

for the non-dimensional unknown functions

$$\overline{P}_i(\varphi) = p_i(c\varphi)/p_0\,, \qquad (i = 1, 2)$$

$$\overline{m}(\rho) = 4\mu m\left(\frac{b-a}{2}\rho + \frac{b+a}{2}\right)\Big/ p_0\,. \tag{4.4a–c}$$

All terms appearing in Eqs.(4.3) are defined in Appendix F and

$$R = L/h\,,$$

$$f = (b-a)/2h\,,$$

$$g = (b+a)/2h\,,$$

$$w = sh\,,$$

$$j = c/h\,. \tag{4.5a–e}$$

Writing

$$\overline{P}_i(\varphi) = G_i(\varphi)\Big/\sqrt{1-\varphi^2}\,, \qquad (i = 1, 2;\ -1 < \varphi < 1)$$

$$\overline{m}(\rho) = Y(\rho)\Big/\sqrt{1-\rho^2}\,, \qquad (-1 < \rho < 1) \tag{4.6a–c}$$

where $G_1(\varphi)$, $G_2(\varphi)$ and $Y(\rho)$ are Hölder-continuous functions by the aid of Eqs.(3.19a,c,d). Eqs.(4.3) can be written as:

$$\frac{1}{\pi}\int_{-1}^{1}\frac{G_1(\varphi)}{\sqrt{1-\varphi^2}}\left\{\frac{1}{\varphi-\xi}+\bar{k}_{11}(\xi,\varphi)\right\}d\varphi+\frac{1}{\pi}\int_{-1}^{1}\frac{G_2(\varphi)}{\sqrt{1-\varphi^2}}\bar{k}_{12}(\xi,\varphi)d\varphi$$

$$+\frac{1}{\pi}\int_{-1}^{1}\frac{Y(\rho)}{\sqrt{1-\rho^2}}\bar{k}_{13}(\xi,\rho)d\rho=\frac{(\kappa+1)(\kappa-3)}{4\kappa}, \qquad (-1<\xi<1)$$

$$\frac{1}{\pi}\int_{-1}^{1}\frac{G_1(\varphi)}{\sqrt{1-\varphi^2}}\bar{k}_{21}(\xi,\varphi)d\varphi+\frac{1}{\pi}\int_{-1}^{1}\frac{G_2(\varphi)}{\sqrt{1-\varphi^2}}\left\{\frac{1}{\varphi-\xi}+\bar{k}_{22}(\xi,\varphi)\right\}d\varphi$$

$$+\frac{1}{\pi}\int_{-1}^{1}\frac{Y(\rho)}{\sqrt{1-\rho^2}}\bar{k}_{23}(\xi,\rho)d\rho=0, \qquad (-1<\xi<1)$$

$$\frac{1}{\pi}\int_{-1}^{1}\frac{G_1(\varphi)}{\sqrt{1-\varphi^2}}\bar{k}_{31}(\eta,\varphi)d\varphi+\frac{1}{\pi}\int_{-1}^{1}\frac{G_2(\varphi)}{\sqrt{1-\varphi^2}}\bar{k}_{32}(\eta,\varphi)d\varphi$$

$$+\frac{1}{\pi}\int_{-1}^{1}\frac{Y(\rho)}{\sqrt{1-\rho^2}}\left\{\frac{1}{\rho-\eta}+\frac{1}{\rho+\eta+2g/f}+\bar{k}_{33}(\eta,\rho)\right\}d\rho=-(\kappa+1), \qquad (-1<\eta<1)$$

(4.7a–c)

As suggested by Krenk (1975), these expressions can be transformed to the following algebraic equations by applying the Gauss-Lobatto integration formula:

$$\sum_{k=1}^{N}C_k\left[\left\{\frac{1}{\varphi_k-\xi_m}+\bar{k}_{11}(\xi_m,\varphi_k)\right\}G_1(\varphi_k)+\bar{k}_{12}(\xi_m,\varphi_k)G_2(\varphi_k)\right.$$

$$\left.+\bar{k}_{13}(\xi_m,\rho_k)Y(\rho_k)\right]=\frac{(\kappa+1)(\kappa-3)}{4\kappa}, \qquad (m=1,\ldots,N-1)$$

$$\sum_{k=1}^{N}C_k\left[\bar{k}_{21}(\xi_m,\varphi_k)G_1(\varphi_k)+\left\{\frac{1}{\varphi_k-\xi_m}+\bar{k}_{22}(\xi_m,\varphi_k)\right\}G_2(\varphi_k)+\bar{k}_{23}(\xi_m,\rho_k)Y(\rho_k)\right]=0,$$

$$(m=1,\ldots,N-1)$$

(4.8a,b)

$$\sum_{k=1}^{N} C_k \left[ \bar{k}_{31}(\eta_m, \varphi_k) G_1(\varphi_k) + \bar{k}_{32}(\eta_m, \varphi_k) G_2(\varphi_k) \right.$$

$$\left. + \left\{ \frac{1}{\rho_k - \eta_m} + \frac{1}{\rho_k + \eta_m + 2g/f} + \bar{k}_{33}(\eta_m, \rho_k) \right\} Y(\rho_k) \right] = -(\kappa + 1), \qquad (m = 1, ..., N-1)$$

(4.8c)

in which integration and collocation points are

$$\varphi_k = \rho_k = \cos\left[(k-1)\pi/(N-1)\right], \qquad (k = 1, 2, ..., N)$$

$$\xi_m = \eta_m = \cos\left[(2m-1)\pi/(2N-2)\right], \qquad (m = 1, 2, ..., N-1)$$

(4.9a–d)

and the weighting constants of the Lobatto polynomials are

$$C_1 = C_N = 1/2(N-1), \; C_k = 1/(N-1). \qquad (k = 2, ..., N-1)$$

(4.10a,b)

The system of Eqs.(4.8) contains 3*(N–1)* equations for the 3*N* unknowns which are $G_1(\varphi_k)$, $G_2(\varphi_k)$ and $Y(\rho_k)$ ($k$=1,2,…,$N$). Therefore, to complete the number of equations to 3*N*, the equilibrium and single-valuedness conditions, Eqs.(3.5) are added to the system after being converted to the following linear algebraic equations:

$$\sum_{k=1}^{N} C_k G_1(\varphi_k) = 0 ,$$

$$\sum_{k=1}^{N} C_k G_2(\varphi_k) = 0 ,$$

$$\sum_{k=1}^{N} C_k Y(\rho_k) = 0 . \qquad (4.11a–c)$$

Determining the unknowns, $G_1(\varphi_k)$, $G_2(\varphi_k)$ and $Y(\rho_k)$ ($k$=1,2,…,$N$) requires computation of the infinite integrals in Fredholm kernels numerically which are given in Appendix F. For this computing process, Laguerre quadrature (Abramowitz and Stegun (1965)) is used and the infinite integrals are computed for every $\varphi_k$, $\rho_k$, $\eta_m$ and $\xi_m$ combination. Then the field quantities can be calculated numerically by determining these unknowns. Behavior of these unknown functions is characterized by the so-called "stress intensity factor" at the edges of the inclusions, $\varphi = \pm 1$ and at the crack tips, $\rho = \pm 1$.

### 4.2 Infinite Strip Having Two Internal Rigid Inclusions (without Cracks)

Consider an infinite strip of width 2$h$ containing two rigid inclusions at $y$=± $L$. The strip is loaded at infinity with uniformly distributed tensile loads (Figure 4.2). In the Section 4.1, Eqs. (4.7a,b) are written for the inclusions where Eq. (4.7c) is written for the cracks.

Therefore the system of algebraic equations Eqs. (4.8a–c), resulting from Eqs. (4.7a–c) will reduce to

$$\sum_{k=1}^{N} C_k \left[ \left\{ \frac{1}{\varphi_k - \xi_m} + \bar{k}_{11}(\xi_m, \varphi_k) \right\} G_1(\varphi_k) + \bar{k}_{12}(\xi_m, \varphi_k) G_2(\varphi_k) \right] = \frac{(\kappa+1)(\kappa-3)}{4\kappa}$$

$$(m = 1, 2, ..., N-1)$$

$$\sum_{k=1}^{N} C_k \left[ \bar{k}_{21}(\xi_m, \varphi_k) G_1(\varphi_k) + \left\{ \frac{1}{\varphi_k - \xi_m} + \bar{k}_{22}(\xi_m, \varphi_k) \right\} G_2(\varphi_k) \right] = 0 \quad (m = 1, 2, ..., N-1)$$

(4.12a,b)

Here, 2*(N–1)* equations exist for the 2$N$ unknowns, $G_1(\varphi_k)$ and $G_2(\varphi_k)$ ($k$=1,2,..,$N$) and to complete the system of equations, two following algebraic equations are added:

$$\sum_{k=1}^{N} C_k G_1(\varphi_k) = 0 \,,$$

$$\sum_{k=1}^{N} C_k G_2(\varphi_k) = 0 \,. \qquad (4.11a,b)$$

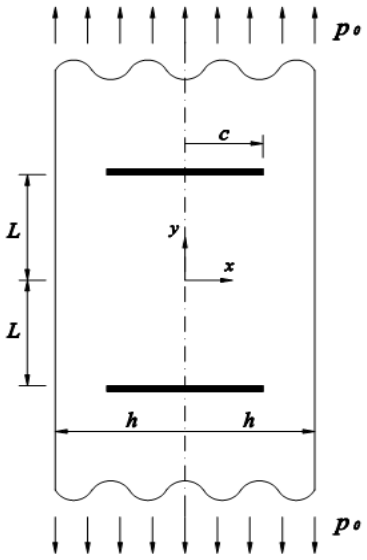


Figure 4.2 Geometry of an infinite strip having two rigid inclusions.

### 4.3 Infinite Strip Having Two Internal Cracks (without Inclusions)

Now consider an infinite strip of width *2h* containing two internal symmetrically located cracks at *y=0* shown in Figure 4.3. Again both ends of the strip are subjected to axial tensile loads of uniform intensity $p_0$ and there is no inclusion in the strip. As mentioned before, the non-dimensional unknown functions related to non-existent parts of the strip will be eliminated which are $\overline{P}_1(\varphi)$ and $\overline{P}_2(\varphi)$ here. So, Eqs. (4.7a,b) and the parts of Eq. (4.7c) containing $G_1(\varphi)$ and $G_2(\varphi)$ will be dismissed.

Remaining equation of Eq. (4.8c), resulting from Eq. (4.7c) will be such that

$$\sum_{k=1}^{N} C_k \left\{ \frac{1}{\rho_k - \eta_m} + \frac{1}{\rho_k + \eta_m + 2g/f} + \bar{k}_{33}(\eta_m, \rho_k) \right\} Y(\rho_k) = -(\kappa + 1)$$

$$(m = 1, 2, ..., N-1)$$

(4.13)

for the infinite strip having just two internal symmetyrical cracks.

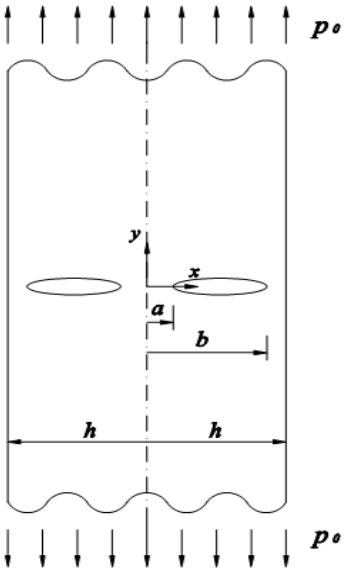


Figure 4.3 Geometry of an infinite strip with two internal symmetrical cracks.

In this case, the following equation will be added to complete the system of ($N$–1) equations for the $N$ unknowns, $Y(\rho_k)$ ($k$=1,2,…,$N$):

$$\sum_{k=1}^{N} C_k Y(\rho_k) = 0 . \qquad (4.11a)$$

### 4.4 Infinite Strip Having Edge Cracks and Two Internal Rigid Inclusions

In this section, an infinite strip of width *2h* containing two edge cracks at *y=0* and two rigid inclusions at *y*=± *L* shown in Figure 4.4 is considered. Again both ends of the strip are subjected to axial tensile loads of uniform intensity $p_0$. In this case, non-dimensional variables of edge cracks are defined as:

$$x=(h-a)\eta+h, \qquad (a<x<h,\ -1<\eta<0)$$

$$t=(h-a)\rho+h. \qquad (a<t<h,\ -1<\rho<0) \qquad (4.14a,b)$$

Instead of Eqs. (4.1), so that the edge crack is modeled as if there is a crack of length 2(*h*–*a*) the other half of which is imagined to extend into the space beyond the free edge of the strip at *x* = *h*. Rearranging Eqs. (4.8) for this case, one can write

$$\sum_{k=1}^{N} C_k \left[ \left\{ \frac{1}{\varphi_k-\xi_m} + \bar{k}_{11}(\xi_m,\varphi_k) \right\} G_1(\varphi_k) + \bar{k}_{12}(\xi_m,\varphi_k) G_2(\varphi_k) \right]$$

$$+ \sum_{k=1}^{(N-1)/2} C_k \left\{ \bar{k}_{13}(\xi_m,\rho_k) - \bar{k}_{13}(\xi_m,-\rho_k) \right\} Y(\rho_k) = \frac{(\kappa+1)(\kappa-3)}{4\kappa}, \quad (m=1,...,N-1)$$

$$\sum_{k=1}^{N} C_k \left[ \bar{k}_{21}(\xi_m,\varphi_k) G_1(\varphi_k) + \left\{ \frac{1}{\varphi_k-\xi_m} + \bar{k}_{22}(\xi_m,\varphi_k) \right\} G_2(\varphi_k) \right],$$

$$+ \sum_{k=1}^{(N-1)/2} C_k \left\{ \bar{k}_{23}(\xi_m,\rho_k) - \bar{k}_{23}(\xi_m,-\rho_k) \right\} Y(\rho_k) = 0, \qquad (m=1,...,N-1)$$

(4.15a,b)

$$\sum_{k=1}^{N} C_k \left[ \bar{k}_{31}(\eta_m, \varphi_k) G_1(\varphi_k) + \bar{k}_{32}(\eta_m, \varphi_k) G_2(\varphi_k) \right]$$

$$+ \sum_{k=1}^{(N-1)/2} C_k \left\{ \frac{1}{\rho_k - \eta_m} + \frac{1}{\rho_k + \eta_m + 2g/f} + \bar{k}_{33}(\eta_m, \rho_k) - \bar{k}_{33}(\eta_m, -\rho_k) \right\} Y(\rho_k) = -(\kappa + 1) ,$$

$$(m = 1, \ldots, (N-1)/2) \qquad (4.15c)$$

where now $N$ is to be chosen odd.

The system of linear algebraic equations, Eqs. (4.15) contain (5$N$–1)/2–2 equations for (5$N$–1)/2 unknowns, $G_i(\varphi_k)$, ($i$=1,2; $k$=1,2,…$N$) and $Y(\rho_k)$, ($k$=1,2,… ($N$–1)/2). In other words, two additional independent equations are necessary and Eqs. (4.11a,b) will complement the system to (5$N$–1)/2 equations.

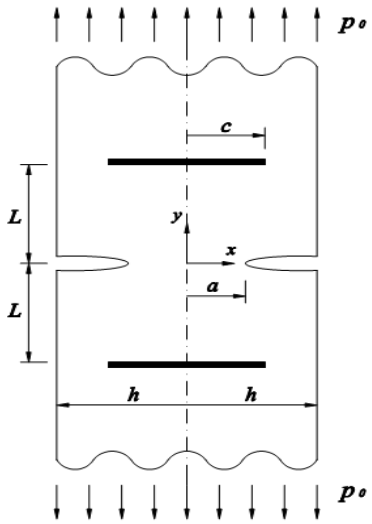


Figure 4.4 Geometry of an infinite strip with two edge cracks and rigid inclusions

### 4.5 Finite Strip Having Two Internal Cracks

When the width of inclusions in infinite strip given in Section 4.1 approaches the width of the strip ($c \to h$), the portion of the infinite strip between the two rigid inclusions becomes a finite strip of length $2L$. The portion between inclusions is subjected to axial tension of uniform intensity at $y = \pm L$ through rigid plates bonded to the strip.

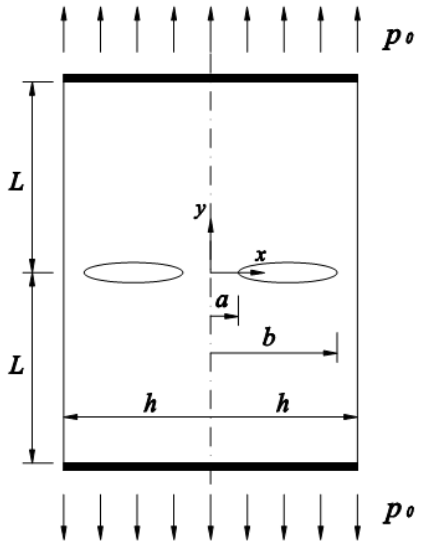


Figure 4.5 Geometry of a finite strip with two internal symmetrical cracks and rigid inclusions.

In this case Eqs. (4.2a,b), (4.4a,b), (4.5e) and (4.6a,b) of Section 4.1 must be replaced by

$$x = h\xi, \qquad (-h < x < h, -1 < \xi < 1)$$

$$r = h\varphi, \qquad (-h < r < h, -1 < \varphi < 1) \qquad (4.16a,b)$$

$$\bar{P}_i(\varphi) = p_i(h\varphi)/p_0\,, \qquad (i = 1, 2) \tag{4.17a,b}$$

$$j=1 \tag{4.18}$$

$$\bar{P}_i(\varphi) = G_i(\varphi)/(1-\varphi^2)^{\alpha}\,, \qquad (i = 1, 2) \tag{4.19a,b}$$

respectively, where $\alpha$ is supposed to be calculated from Eq. (3.19b). Then, instead of Eqs. (4.7a–c), one can write

$$\frac{1}{\pi}\int_{-1}^{1}\frac{G_1(\varphi)}{(1-\varphi^2)^{\alpha}}\left\{\frac{1}{\varphi-\xi}+\bar{k}_{11}(\xi,\varphi)\right\}d\varphi+\frac{1}{\pi}\int_{-1}^{1}\frac{G_2(\varphi)}{(1-\varphi^2)^{\alpha}}\bar{k}_{12}(\xi,\varphi)d\varphi$$
$$+\frac{1}{\pi}\int_{-1}^{1}\frac{Y(\rho)}{\sqrt{1-\rho^2}}\bar{k}_{13}(\xi,\rho)d\rho=\frac{(\kappa+1)(\kappa-3)}{4\kappa}, \qquad (-1<\xi<1)$$

$$\frac{1}{\pi}\int_{-1}^{1}\frac{G_1(\varphi)}{(1-\varphi^2)^{\alpha}}\bar{k}_{21}(\xi,\varphi)d\varphi+\frac{1}{\pi}\int_{-1}^{1}\frac{G_2(\varphi)}{(1-\varphi^2)^{\alpha}}\left\{\frac{1}{\varphi-\xi}+\bar{k}_{22}(\xi,\varphi)\right\}d\varphi$$
$$+\frac{1}{\pi}\int_{-1}^{1}\frac{Y(\rho)}{\sqrt{1-\rho^2}}\bar{k}_{23}(\xi,\rho)d\rho=0, \qquad (-1<\xi<1)$$

$$\frac{1}{\pi}\int_{-1}^{1}\frac{G_1(\varphi)}{(1-\varphi^2)^{\alpha}}\bar{k}_{31}(\eta,\varphi)d\varphi+\frac{1}{\pi}\int_{-1}^{1}\frac{G_2(\varphi)}{(1-\varphi^2)^{\alpha}}\bar{k}_{32}(\eta,\varphi)d\varphi$$
$$+\frac{1}{\pi}\int_{-1}^{1}\frac{Y(\rho)}{\sqrt{1-\rho^2}}\left\{\frac{1}{\rho-\eta}+\frac{1}{\rho+\eta+2g/f}+\bar{k}_{33}(\eta,\rho)\right\}d\rho=-(\kappa+1), \qquad (-1<\eta<1)$$

(4.20a–c)

By using the Gauss-Jacobi (Erdogan, Gupta and Cook (1973)) and the Gauss-Lobatto integration formulas, the following system of algebraic equations are obtained:

$$\sum_{k=1}^{N} W_k \left[ \left\{ \frac{1}{\varphi_k - \xi_m} + \bar{k}_{11}(\xi_m, \varphi_k) \right\} G_1(\varphi_k) + \bar{k}_{12}(\xi_m, \varphi_k) G_2(\varphi_k) \right]$$

$$+ \sum_{k=1}^{N} C_k \bar{k}_{13}(\xi_m, \rho_k) Y(\rho_k) = \frac{(\kappa+1)(\kappa-3)}{4\kappa}, \qquad (m = 1, \ldots, N-1)$$

$$\sum_{k=1}^{N} W_k \left[ \bar{k}_{21}(\xi_m, \varphi_k) G_1(\varphi_k) + \left\{ \frac{1}{\varphi_k - \xi_m} + \bar{k}_{22}(\xi_m, \varphi_k) \right\} G_2(\varphi_k) \right]$$

$$+ \sum_{k=1}^{N} C_k \bar{k}_{23}(\xi_m, \rho_k) Y(\rho_k) = 0, \qquad (m = 1, \ldots, N-1)$$

$$\sum_{k=1}^{N} W_k \left[ \bar{k}_{31}(\eta_m, \varphi_k) G_1(\varphi_k) + \bar{k}_{32}(\eta_m, \varphi_k) G_2(\varphi_k) \right]$$

$$+ \sum_{k=1}^{N} C_k \left\{ \frac{1}{\rho_k - \eta_m} + \frac{1}{\rho_k + \eta_m + 2g/f} + \bar{k}_{33}(\eta_m, \rho_k) \right\} Y(\rho_k) = -(\kappa+1), (m = 1, \ldots, N-1)$$

(4.21a–c)

In this system, $\xi_m$ and $\varphi_k$ are the roots of Jacobi polynomials

$$P_N^{(-\alpha,-\alpha)}(\varphi_k) = 0, \qquad (k = 1, 2, \ldots, N)$$

$$P_{N-1}^{(1-\alpha,1-\alpha)}(\xi_m) = 0, \qquad (m = 1, 2, \ldots, N-1)$$

(4.22a,b)

and $\rho_k$ and $\eta_m$ are still determined from Eqs. (4.9b,d) and $W_k$ are the weighting constants of the Jacobi polynomials. $C_k$ are the weighting constants of the Lobatto polynomials given in Eq.(4.10).

Similarly, as in Section 4.1, 3*(N–1)* equations are to be completed for 3*N* unknowns, $G_1(\varphi_k)$, $G_2(\varphi_k)$ and $Y(\rho_k)$ ($k$=1,2,…$N$) by adding the following equations:

$$\sum_{k=1}^{N} W_k G_1(\varphi_k) = 0\,,$$

$$\sum_{k=1}^{N} W_k G_2(\varphi_k) = 0\,,$$

$$\sum_{k=1}^{N} C_k Y(\rho_k) = 0\,. \qquad (4.23a–c)$$

### 4.6 Finite Strip Having Edge Cracks

Here, a finite strip having a length of 2$L$ and a width of 2$h$ is considered. In the finite strip, there are two edge cracks and both ends of the strip subjected to axial tensile loads of uniform intensity $p_0$ (Figure 4.6). In this case, non-dimensional variables of edge cracks, $\eta$ and $\rho$ are determined from Eqs. (4.14) whereas non-dimensional variables of rigid inclusions, $\xi$ and $\varphi$ are determined from Eqs.(4.16).

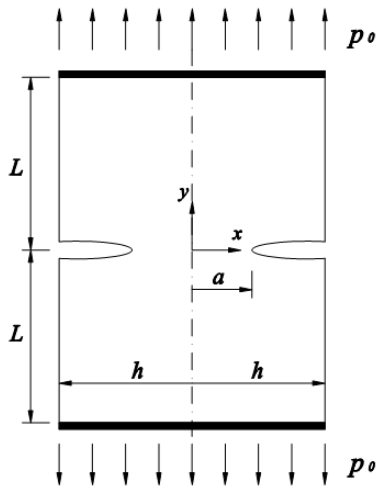


Figure 4.6 Geometry of a finite strip with two edge cracks and rigid inclusions

By using the Gauss-Jacobi and the Gauss-Lobatto integration formulas, Eqs. (4.20) will be converted into the following system of algebraic equations:

$$\sum_{k=1}^{N} W_k \left[ \left\{ \frac{1}{\varphi_k - \xi_m} + \bar{k}_{11}(\xi_m, \varphi_k) \right\} G_1(\varphi_k) + \bar{k}_{12}(\xi_m, \varphi_k) G_2(\varphi_k) \right]$$

$$+ \sum_{k=1}^{(N-1)/2} C_k \left\{ \bar{k}_{13}(\xi_m, \rho_k) - \bar{k}_{13}(\xi_m, -\rho_k) \right\} Y(\rho_k) = \frac{(\kappa+1)(\kappa-3)}{4\kappa} \qquad (m = 1, \ldots, N-1)$$

$$\sum_{k=1}^{N} W_k \left[ \bar{k}_{21}(\xi_m, \varphi_k) G_1(\varphi_k) + \left\{ \frac{1}{\varphi_k - \xi_m} + \bar{k}_{22}(\xi_m, \varphi_k) \right\} G_2(\varphi_k) \right]$$

$$+ \sum_{k=1}^{(N-1)/2} C_k \left\{ \bar{k}_{23}(\xi_m, \rho_k) - \bar{k}_{23}(\xi_m, -\rho_k) \right\} Y(\rho_k) = 0, \qquad (m = 1, \ldots, N-1)$$

$$\sum_{k=1}^{N} W_k \left[ \bar{k}_{31}(\eta_m, \varphi_k) G_1(\varphi_k) + \bar{k}_{32}(\eta_m, \varphi_k) G_2(\varphi_k) \right]$$

$$+ \sum_{k=1}^{(N-1)/2} C_k \left\{ \frac{1}{\rho_k - \eta_m} + \frac{1}{\rho_k + \eta_m + 2g/f} + \bar{k}_{33}(\eta_m, \rho_k) - \bar{k}_{33}(\eta_m, -\rho_k) \right\} Y(\rho_k) = -(\kappa+1), \qquad (m = 1, \ldots, (N-1)/2)$$

(4.24a–c)

where $N$ is to be chosen odd again.

The roots of Jacobi polynomials, $\xi_m$ and $\varphi_k$, are determined from Eqs. (4.22) and $\rho_k$ and $\eta_m$ are still determined from Eqs. (4.9b,d).

Similarly, as in Section 4.4, there are $(5N-1)/2-2$ equations for $(5N-1)/2$ unknowns, $G_i(\varphi_k)$, ($i$=1,2; $k$=1,2,..,$N$) and $Y(\rho_k)$, ($k$=1,2,…,($N$–1)/2) in Eqs. (4.24). Therefore, two additional independent equations, Eqs. (4.23a,b), will complement the system to $(5N-1)/2$ equations.

# CHAPTER V

# STRESS INTENSITY FACTORS

Stress intensity factors have great significance from the fracture mechanics point of view. Stresses become infinite at the edges of the cracks and the inclusions. In this case, stress state around these points can be expressed in terms of the so-called stress intensity factors.

## 5.1 Stress Intensity Factors at the Edges of the Crack

Mode-I stress intensity factors at the edges of the crack may be written as

$$K_{1a} = \lim_{x \to a} \sqrt{2(a-x)}\,\sigma_y(x,0),$$

$$K_{1b} = \lim_{x \to b} \sqrt{2(x-b)}\,\sigma_y(x,0), \qquad (5.1a,b)$$

in which $\sigma_y(x,0)$ may be expressed from Eq.(2.39b) in the form

$$\sigma_y(x,0) = \frac{4\mu}{\pi(\kappa+1)} \int_a^b \frac{m(t)}{t-x} dt + \sigma_{yb}(x,0). \qquad (5.2)$$

The bounded part $\sigma_{yb}(x,0)$ is such that:

$$\sigma_{yb}(x,0) = \frac{4\mu}{\pi(\kappa+1)} \int_a^b m(t) \left\{ \frac{1}{t+x} + A_2^*(t,x,0) \right\} dt. \qquad (5.3)$$

$m(t)$ is expressed as:

$$m(t)=\frac{m^*(t)}{\sqrt{(t-a)(b-t)}}=\begin{cases}\dfrac{m^*(t)(b-t)^{-1/2}}{(t-a)^{1/2}} & , \quad t=a\\ \dfrac{m^*(t)(t-a)^{-1/2}}{(b-t)^{1/2}} & , \quad t=b\end{cases} \tag{5.4}$$

and the integral of the sectionally holomorphic function in Eq. (5.2) is to be calculated by the method given in Muskhelishvili (1953):

$$\frac{1}{\pi}\int_a^b \frac{m(t)}{t-x}dt=\frac{e^{\pi i/2}}{\sin\pi/2}\frac{m^*(a)}{\sqrt{b-a}}\frac{1}{\sqrt{x-a}}-\frac{1}{\sin\pi/2}\frac{m^*(b)}{\sqrt{b-a}}\frac{1}{\sqrt{x-b}}+M^*(x), \tag{5.5}$$

where, $M^*(x)$ is bounded for $a < x < b$.

When Eq. (5.5) is reorganized, the following expression is obtained:

$$\frac{1}{\pi}\int_a^b \frac{m(t)}{t-x}dt=\frac{m^*(a)}{\sqrt{b-a}}\frac{1}{\sqrt{a-x}}-\frac{m^*(b)}{\sqrt{b-a}}\frac{1}{\sqrt{x-b}}+M^*(x). \tag{5.6}$$

If Eq. (5.6) is substituted in Eq. (5.2), $\sigma_y(x,0)$ becomes:

$$\sigma_y(x,0)=\frac{4\mu}{\pi(\kappa+1)}\left[\frac{m^*(a)}{\sqrt{b-a}}\frac{1}{\sqrt{a-x}}-\frac{m^*(b)}{\sqrt{b-a}}\frac{1}{\sqrt{x-b}}+M^*(x)\right]. \tag{5.7}$$

One may get relations between stress intensity factors and $m^*(a)$ and $m^*(b)$ by substituting Eq. (5.7) in Eqs. (5.1):

$$K_{1a}=\frac{4\mu}{\kappa+1}\frac{m^*(a)}{\sqrt{(b-a)/2}},$$

$$K_{1b}=-\frac{4\mu}{\kappa+1}\frac{m^*(b)}{\sqrt{(b-a)/2}}. \tag{5.8a,b}$$

Following relations can be obtained by comparing Eq. (4.4c) and Eq. (4.6c) with Eq. (5.4):

$$m^*(t) = \frac{p_0}{8\mu}(b-a)Y(\rho),$$

$$m^*(a) = \frac{p_0}{8\mu}(b-a)Y(-1),$$

$$m^*(b) = \frac{p_0}{8\mu}(b-a)Y(1). \qquad \text{(5.9a–c)}$$

Substituting Eqs. (5.9b,c) in Eqs. (5.8), the stress intensity factors can be obtained as:

$$K_{1a} = \frac{p_0}{\kappa+1}\sqrt{\frac{b-a}{2}}Y(-1),$$

$$K_{1b} = -\frac{p_0}{\kappa+1}\sqrt{\frac{b-a}{2}}Y(1), \qquad \text{(5.10a,b)}$$

and normalized stress intensity factors may be defined as:

$$\bar{k}_{1a} = \frac{K_{1a}}{p_0\sqrt{(b-a)/2}} = \frac{Y(-1)}{\kappa+1},$$

$$\bar{k}_{1b} = \frac{K_{1b}}{p_0\sqrt{(b-a)/2}} = -\frac{Y(1)}{\kappa+1}. \qquad \text{(5.11a,b)}$$

Note here that when $b \to h$, the stresses at a 90° wedge corner with free edges are finite and $K_{1b}$ would be meaningless.

## 5.2 Stress Intensity Factors at the Edges of the Rigid Inclusions and at the Corners of the Finite Strip

Mode I and II stress intensity factors, $K_{1c}$ and $K_{2c}$ at the edges of the rigid inclusions when $c < h$ are defined and calculated as:

$$K_{1c} = \lim_{x \to c} \sqrt{2(x-c)}\sigma_y(x,L) = \frac{1}{2}\left[\frac{1-\kappa}{1+\kappa}G_1(1) - G_2(1)\right]\sqrt{c}\,p_0,$$

$$K_{2c} = \lim_{x \to c} \sqrt{2(x-c)}\tau_{xy}(x,L) = -\frac{1}{2}\left[G_1(1) + \frac{1-\kappa}{1+\kappa}G_2(1)\right]\sqrt{c}\,p_0. \qquad (5.12a,b)$$

These stress intensity factors may be normalized as follows:

$$\bar{k}_{ic} = K_{ic}/p_0\sqrt{c}, \qquad (i=1,2) \qquad (5.13a,b)$$

In the situation of finite strip, which means $c \to h$, Mode I and II stress intensity factors, $K_{1h}$ and $K_{2h}$ are defined as:

$$K_{1h} = \lim_{x \to h} \sqrt{2}(h-x)^{\alpha}\sigma_y(x,L),$$

$$K_{2h} = \lim_{x \to h} \sqrt{2}(h-x)^{\alpha}\tau_{xy}(x,L), \qquad (5.14a,b)$$

in which α is found from Eq. (3.19a).

From Eqs. (2.39b,c), the following expressions can be written

$$\sigma_y(x,L) = \sigma_{ys}(x,L) + \sigma_{yb}(x,L),$$

$$\tau_{xy}(x,L) = \tau_{xys}(x,L) + \tau_{xyb}(x,L), \qquad (5.15a,b)$$

in which subscripts *s* and *b* refer to the singular and the bounded parts of respective stresses.

By using Eqs. (G.1)−(G.3), in Appendix G, the singular parts can be expressed in the form

$$\sigma_{ys}(x,L)=\frac{\kappa-1}{2\pi(\kappa+1)}\int_{-h}^{h}p_1(r)\frac{1}{r-x}dr+\frac{1}{2\pi(\kappa+1)}\int_{-h}^{h}p_1(r)B_2^*(r,x,L)dr-\frac{1}{2}p_2(x),$$

$$\tau_{ys}(x,L)=\frac{\kappa-1}{2\pi(\kappa+1)}\int_{-h}^{h}p_2(r)\frac{1}{r-x}dr+\frac{1}{2\pi(\kappa+1)}\int_{-h}^{h}p_2(r)C_3^*(r,x,L)dr-\frac{1}{2}p_1(x),$$

(5.16a,b)

or more precisely, in the form

$$\begin{aligned}\sigma_{ys}(x,L)=&\frac{\kappa-1}{2\pi(\kappa+1)}\int_{-h}^{h}p_1(r)\frac{1}{r-x}dr\\&+\frac{1}{2\pi(\kappa+1)}\int_{-h}^{h}p_1(r)\left[\int_0^{\infty}\left\{1-3\kappa+2\kappa s(h-x)-6s(h-r)+4s(h-r)s(h-x)\right\}e^{-s(2h-r-x)}ds\right.\\&\left.\int_0^{\infty}\left\{1-3\kappa+2\kappa s(h+x)-6s(h-r)+4s(h-r)s(h+x)\right\}e^{-s(2h-r+x)}ds\right]dr-\frac{1}{2}p_2(x).\end{aligned}$$

(5.17)

According to Appendix A, definite improper integrals can be calculated and

$$\begin{aligned}\sigma_{ys}(x,L)=&\frac{1}{2\pi(\kappa+1)}\int_{-h}^{h}p_1(r)\left[\frac{\kappa-1}{r-x}-\frac{3\kappa+5}{2h-r-x}+\frac{2(\kappa+7)(h-x)}{(2h-r-x)^2}-\frac{8(h-x)^2}{(2h-r-x)^3}\right.\\&\left.-\frac{3\kappa+5}{2h-r+x}+\frac{2(\kappa+7)(h+x)}{(2h-r+x)^2}-\frac{8(h+x)^2}{(2h-r+x)^3}\right]dr-\frac{1}{2}p_2(x)\end{aligned}\qquad(5.18)$$

or

$$\sigma_{ys}(x,L)=\frac{1}{2\pi(\kappa+1)}\int_{-h}^{h}p_1(r)\left\{\frac{\kappa-1}{r-x}\right.$$
$$+\left[(3\kappa+5)-2(\kappa+7)(h-x)\frac{d}{dx}+4(h-x)^2\frac{d^2}{dx^2}\right]\frac{1}{r-(2h-x)}$$
$$\left.+\left[(3\kappa+5)+2(\kappa+7)(h+x)\frac{d}{dx}+4(h+x)^2\frac{d^2}{dx^2}\right]\frac{1}{r-(2h+x)}\right\}dr-\frac{1}{2}p_2(x) \tag{5.19}$$

can be written.

Eq. (5.19) can be converted into the form given in Eqs. (3.17):

$$\sigma_{ys}(x,L)=\frac{1}{2(\kappa+1)}\left\{(\kappa-1)\left[\frac{P_1(-h)\cot\pi\alpha}{(2h)^\alpha(h+x)^\alpha}-\frac{P_1(h)\cot\pi\alpha}{(2h)^\alpha(h-x)^\alpha}\right]\right.$$
$$+\left[(3\kappa+5)-2\alpha(\kappa+7)+4\alpha(\alpha+1)\right]\frac{-P_1(h)}{(2h)^\alpha\sin\pi\alpha}\frac{1}{(h-x)^\alpha}$$
$$\left.+\left[(3\kappa+5)-2\alpha(\kappa+7)+4\alpha(\alpha+1)\right]\frac{-P_1(-h)}{(2h)^\alpha\sin\pi\alpha}\frac{1}{(h+x)^\alpha}\right\}-\frac{1}{2}\frac{P_2(x)}{(h+x)^\alpha(h-x)^\alpha}. \tag{5.20}$$

Stress intensity factor of Mode I can be determined by substituting Eq. (5.20) in Eq. (5.14a):

$$K_{1h}=\frac{\sqrt{2}}{2}\left\{\frac{1}{1+\kappa}\frac{P_1(h)}{(2h)^\alpha\sin\pi\alpha}\left[(1-\kappa)(\cos\pi\alpha+1)+2(1+\kappa)(\alpha-1)-4(\alpha-1)^2\right]-\frac{P_2(h)}{(2h)^\alpha}\right\}. \tag{5.21}$$

With the help of Eqs. (3.16), (4.4) and (4.6) and the definition of

$$\overline{K}_{ih}=K_{ih}/h^\alpha p_0\,, \qquad (i=1,2) \tag{5.22a,b}$$

normalized stress intensity factor at the rigid corner of the finite strip, $\bar{k}_{1h}$ becomes

$$\bar{k}_{1h} = \frac{\sqrt{2}}{2}\left\{\frac{1}{1+\kappa}\frac{G_1(1)}{2^{\alpha}\sin\pi\alpha}\left[(1-\kappa)(\cos\pi\alpha+1)+2(1+\kappa)(\alpha-1)-4(\alpha-1)^2\right]-\frac{G_2(1)}{2^{\alpha}}\right\}. \tag{5.23}$$

Mode II stress intensity factor can be determined in a similar way such that:

$$\bar{k}_{2h} = \frac{\sqrt{2}}{2}\left\{\frac{1}{1+\kappa}\frac{G_2(1)}{2^{\alpha}\sin\pi\alpha}\left[(\kappa-1)(\cos\pi\alpha+1)+2(\kappa+1)(\alpha-1)+4(\alpha-1)^2\right]-\frac{G_1(1)}{2^{\alpha}}\right\}. \tag{5.24}$$

# CHAPTER VI

# RESULTS AND CONCLUSIONS

## 6.1 Numerical Results

The system of linear algebraic equations is solved numerically for the values of unknown functions, $G_1(\varphi_k)$, $G_2(\varphi_k)$ and $Y(\rho_k)$ ($k$=1,2,...$N$) at discrete collocation points. The numerical solutions are obtained according to the particular problems defined in Chapter 4. Once the values of unknown functions, $G_1(\varphi_k)$, $G_2(\varphi_k)$ and $Y(\rho_k)$ ($k$=1,2,...,$N$) are determined, the stress distributions and stress intensity factors at the edges of the cracks and at the corners of the strip can be calculated numerically.

In this thesis, geometry of the strip is described by geometrical parameters *2a*; distance between inner edges of the cracks, *2b*; distance between outer edges of the cracks, *2c; w*idth of the rigid inclusions, *2h*; width of the strip and *2L*; distance between the rigid inclusions. The material of the strip is described by $\mu$; modulus of rigidity and $v$; Poisson's ratio. The loading is described by $p_0$; uniform intensity of the axial tension. On the other hand, for the sake of generalization of the numerical results, dimensionless geometrical parameters *a/h*, *b/h*, *c/h*, *L/h* normalized by the width of the strip are used. Particular numerical values are not selected for $\mu$ and $p_0$ in the analysis of the problems since the normalized stress distributions and normalized stress intensity factors are used. Here, only Poisson's ratio $v$ is used to describe the material. Some representative calculated results are shown in Figs. 6.1–6.59.

### 6.1.1 Infinite Strip Problem

#### 6.1.1.1 Two Internal Cracks and Internal Inclusions in an Infinite Strip

Consider the problem shown in Fig. 4.1. In this case, the system of equations, Eqs. (4.8) and (4.11) must be solved for the unknown functions $G_1(\varphi_k)$, $G_2(\varphi_k)$ and $Y(\rho_k)$ ($k$=1,2,...$N$). Figures 6.1–6.4 show the normalized Mode I stress intensity factor $\bar{k}_{1a}$ at the inner edge of the crack. Figure 6.1 shows variation of $\bar{k}_{1a}$ with $a/h$ when $b/h$ = 0.9, $L/h$ = 0.5 and $c/h$ = 0.5 for several values of $v$. In Figure 6.1, it is seen that $\bar{k}_{1a}$ decreases with increasing $a/h$. In Figure 6.2, variation of $\bar{k}_{1a}$ with $b/h$ when $a/h$ = 0.1, $L/h$ = 0.5 and $c/h$ = 0.5 is given for same values of $v$ shown in Fig. 6.1. Here, $\bar{k}_{1a}$ increases with increasing $b/h$. Figures 6.1 and 6.2 show that $\bar{k}_{1a}$ decreases with decreasing crack width.

Figure 6.3 shows variation of $\bar{k}_{1a}$ with $c/h$ when $a/h$ = 0.1, $b/h$ = 0.9 and $L/h$ = 0.5 for several values of $v$. Here, $\bar{k}_{1a}$ decreases with increasing $c/h$ which means when the edge of the rigid inclusion gets away from $a$, the value of $\bar{k}_{1a}$ becomes smaller. It is also noted that larger value of $v$ has a significant role in decrease of $\bar{k}_{1a}$.

Figure 6.4 shows again variation of $\bar{k}_{1a}$ with $c/h$ when $a/h$ = 0.1, $b/h$ = 0.9 and $v$ = 0.3 for several values of $L/h$. $\bar{k}_{1a}$ decreases significantly with increasing $c/h$ especially for smaller values of $L/h$ which means the inclusion has a great role in decrease of $\bar{k}_{1a}$ when it becomes closer to the crack.

Figures 6.5–6.8 show the normalized Mode I stress intensity factor $\bar{k}_{1b}$ at the outer edge of the crack and have behavior similar to $\bar{k}_{1a}$ as given in Figures 6.1–6.4.

Figures 6.9–6.12 show the normalized Mode I stress intensity factor $\bar{k}_{1c}$ at the edge of the internal inclusion. Figure 6.9 shows variation of $\bar{k}_{1c}$ with $a/h$ when $b/h$ = 0.9, $L/h$ = 0.5 and $c/h$ = 0.5 for several values of $v$. $\bar{k}_{1c}$ decreases as $a/h$ increases until ~ 0.3. After this value of $a/h$, $\bar{k}_{1c}$ increases.

Figure 6.10 shows variation of $\bar{k}_{1c}$ with *b/h* when *a/h* = 0.1, *L/h* = 0.5 and *c/h* = 0.5. Here, $\bar{k}_{1c}$ increases with increasing *b/h* until ~ 0.5. After this value of *b/h*, $\bar{k}_{1c}$ decreases.

Figure 6.11 shows variation of $\bar{k}_{1c}$ with *c/h* when *a/h* = 0.1, *b/h* = 0.9 and *L/h* = 0.5 for several values of *v*. Here, $\bar{k}_{1c}$ decreases with increasing *c/h* until ~ 0.3. After this value of *c/h*, $\bar{k}_{1c}$ increases until ~ 0.9 and then decreases again.

Figure 6.12 shows the effect of *L/h* on the variation of $\bar{k}_{1c}$ with *c/h* when *a/h* = 0.1, *b/h* = 0.9 and *v* = 0.3. Here, it is seen that when *L/h* = 1 and 2, $\bar{k}_{1c}$ decreases smoothly as the inclusion gets larger. When the inclusions are closer to the cracks on the other hand, e.g., when *L/h* = 0.5 or 0.75, $\bar{k}_{1c}$ first decreases with increasing *c/h* and after some particular value of *c/h* it starts to increase and then decreases again.

Figures 6.13–6.16 show the normalized Mode II stress intensity factor $\bar{k}_{2c}$ at the edge of the internal inclusion. In Figure 6.13, $\bar{k}_{2c}$ increases with increasing *a/h* when *b/h* = 0.9, *L/h* = 0.5 and *c/h* = 0.5. After the value of *a/h* = 0.5, $\bar{k}_{2c}$ decreases slightly.

Figure 6.14 shows variation of $\bar{k}_{2c}$ with *b/h* when *a/h* = 0.1, *L/h* = 0.5 and *c/h* = 0.5. In this case, $\bar{k}_{2c}$ decreases very little with increasing *b/h* and then starts to increase smoothly after some particular value of *b/h.*

Figure 6.15 shows variation of $\bar{k}_{2c}$ with *c/h* when *a/h* = 0.1, *b/h* = 0.9 and *L/h* = 0.5 for several values of *v*. Here, $\bar{k}_{2c}$ decreases with increasing *c/h*, variation being magnified for larger values of *v*.

Figure 6.16 shows the effect of *L/h* on the variation of $\bar{k}_{2c}$ with *c/h* when *a/h* = 0.1, *b/h* = 0.9 and *v* = 0.3. In this figure, $\bar{k}_{2c}$ decreases with increasing *c/h*

and when inclusion is closer to the crack, the magnitude of $\bar{k}_{2c}$ has a remarkable change.

#### 6.1.1.2 Edge Cracks and Internal Inclusions in an Infinite Strip

Consider the problem shown in Fig. 4.4. In this case, the system in, Eqs.(4.15) and (4.11a,b) must be solved for the unknown functions $G_1(\varphi_k)$, $G_2(\varphi_k)$ and $Y(\rho_k)$ ($k$=1,2,...$N$). Figures 6.17 and 6.18 show the normalized Mode I stress intensity factor $\bar{k}_{1a}$ for the edge crack. Figure 6.17 shows variation of $\bar{k}_{1a}$ with $a/h$ when $L/h$ = 0.5 and $c/h$ = 0.5 for several values of $v$. Here, $\bar{k}_{1a}$ decreases with increasing $a/h$. After the value of $a/h$ = 0.2, the slope of the $\bar{k}_{1a}$ diminishes remarkably for all $v$ values.

In Figure 6.18, $\bar{k}_{1a}$ decreases with increasing $c/h$ when $a/h$ = 0.5 and $L/h$ = 0.5. As the value of $v$ increases, relatively larger decrease of $\bar{k}_{1a}$ is observed.

Figures 6.19 and 6.20 show the normalized Mode I stress intensity factor $\bar{k}_{1c}$ at the edge of the inclusion. In Figure 6.19, $\bar{k}_{1c}$ increases with increasing $a/h$ when $L/h$ = 0.5 and $c/h$ = 0.5.

Figure 6.20 shows variation of $\bar{k}_{1c}$ with $c/h$ when $a/h$ = 0.5 and $L/h$ = 0.5. As can be seen from this figure, $\bar{k}_{1c}$ decreases with increasing $c/h$ until ~ 0.7. After this value of $c/h$, $\bar{k}_{1c}$ increases as the inclusion gets larger.

Figures 6.21 and 6.22 show the normalized Mode II stress intensity factor $\bar{k}_{2c}$ at the edge of the inclusion. In Figure 6.21, $\bar{k}_{2c}$ increases slightly until some particular value of $a/h$ and then decreases smoothly with increasing $a/h$ in the case of $L/h$ = 0.5 and $c/h$ = 0.5.

Figure 6.22 shows variation of $\bar{k}_{2c}$ with *c/h* when *a/h* = 0.5 and *L/h* = 0.5. Here, $\bar{k}_{2c}$ increases slightly first, and then decreases with further increase in *c/h*.

### 6.1.2 Finite Strip Problem

#### 6.1.2.1 Two Internal Cracks in a Finite Strip

When the width of rigid inclusions approach the width of the strip, $c \rightarrow h$, the portion of the infinite strip between the inclusions becomes identical with the finite strip problem. For this problem Eqs. (4.21) and (4.23) must be solved for the unknown functions $G_1(\varphi_k)$, $G_2(\varphi_k)$ and $Y(\rho_k)$ ($k$=1,2,...$N$).

Figures 6.23–6.27 show the normalized Mode I stress intensity factor $\bar{k}_{1a}$ at the inner edge of the crack. Figure 6.23 shows variation of $\bar{k}_{1a}$ with *a/h* when *b/h* = 0.9 and *L/h* = 1 for several values of *v*. In this figure, $\bar{k}_{1a}$ decreases with increasing *a/h*.

Figure 6.24 shows variation of $\bar{k}_{1a}$ with *a/h* when *b/h* = 0.9 and *L/h* =0.5. Here, $\bar{k}_{1a}$ again decreases with increasing *a/h*. As can be seen in these figures, $\bar{k}_{1a}$ has close ranges of values in both cases which means that the interaction between the rigid inclusions and the cracks has a similar effect on $\bar{k}_{1a}$ at the levels of *L/h* =0.5 and 1.

In Figure 6.25, $\bar{k}_{1a}$ increases with increasing *b/h* when *a/h* = 0,1 and *L/h* =0.5. At *b/h* = 1 which means the internal crack becomes edge crack, $\bar{k}_{1a}$ shows a remarkable increase for all values of *v*.

Figure 6.26 shows the effect of *L/h* on the variation of $\bar{k}_{1a}$ with *a/h* when *b/h* = 0.9 and *v* = 0.3. Here, $\bar{k}_{1a}$ decreases with increasing *a/h*.

Figure 6.27 shows the effect of *L/h* on the variation of $\bar{k}_{1a}$ with *b/h* when *a/h* = 0.1 and *v* = 0.3. As expected $\bar{k}_{1a}$ increases with increasing *b/h*.

Figures 6.28–6.32 show the normalized Mode I stress intensity factor $\bar{k}_{1b}$ at the outer edge of the crack which has similar behavior as $\bar{k}_{1a}$ given in Figures 6.23–6.27.

Figures 6.33–6.38 show the normalized Mode I stress intensity factor $\bar{k}_{1h}$ at the corner of the finite strip. Figure 6.33 shows variation of $\bar{k}_{1h}$ with *b/h* when *a/h* = 0.1 and *L/h* = 1 for several values of *v*. Here, no significant variation with *b/h* is observed until the point of *b/h* = ~ 0.6. After this point $\bar{k}_{1h}$ decreases while it first increases slightly. It should be also noted that $\bar{k}_{1h}$ starts to decrease dramatically as $b \rightarrow h$.

In Figure 6.34, $\bar{k}_{1h}$ first decreases with increasing *a/h* when *b/h* = 0.9 and *L/h* =1 and then increases slightly.

Figure 6.35 shows variation of $\bar{k}_{1h}$ with *a/h* when *b/h* = 0.9 and *L/h* = 0.5 for several values of *v*. Similar to behavior in Fig. 6.34, $\bar{k}_{1h}$ first decreases with increasing *a/h* and then increases slightly.

Figure 6.36 shows variation of $\bar{k}_{1h}$ with *b/h* when *a/h* = 0.1 and *L/h* = 0.5 for several values of *v*. Here, $\bar{k}_{1h}$ first increases with increasing *b/h*, experiences a maximum around *b/h* = 0.7 and then decreases. It is also seen that $\bar{k}_{1h}$ shows a remarkable decrease as $b \rightarrow h$.

Figure 6.37 shows the effect of $L/h$ on the variation of $\bar{k}_{1h}$ with $a/h$ when $b/h$ = 0.9 and $\nu$ = 0.3. As can be realized from this figure, when the rigid inclusions go away from the cracks, $L/h$ = 2, $\bar{k}_{1h}$ first increases and then starts to decrease. On the other hand, in the cases of $L/h$ = 0.5 and $L/h$ = 1, $\bar{k}_{1h}$ first decreases and then increases with increasing $a/h$ . It should be also noted that when the inclusions are close to the cracks, the variation of $\bar{k}_{1h}$ becomes considerably significant.

Figure 6.38 shows the effect of $L/h$ on the variation of $\bar{k}_{1h}$ with $b/h$ when $a/h$ = 0.1 and $\nu$ = 0.3. Compared to Figure 6.37, Figure 6.38 shows reverse behavior for the same values of $L/h$. This time $\bar{k}_{1h}$ first increases and then starts to decrease for $L/h$ = 0.5 and $L/h$ = 1 where it first decreases and then increases for $L/h$ = 2.

Figures 6.39–6.44 show the normalized Mode II stress intensity factor $\bar{k}_{2h}$ at the corner of the finite strip. Figure 6.39 shows variation of $\bar{k}_{2h}$ with $b/h$ when $a/h$ = 0.1 and $L/h$ = 1. Here, no significant variation with $b/h$ is observed except when $b \rightarrow h$. As the value of $\nu$ decreases, the magnitude of the $\bar{k}_{2h}$ decreases.

In Figures 6.40 and 6.41, variation of $\bar{k}_{2h}$ with $a/h$ is given when $L/h$ = 1 and $L/h$ = 0.5, respectively. In both Figures, $b/h$= 0.9 and $\bar{k}_{2h}$ first decreases and then increases slightly with increasing $a/h$.

Figure 6.42 shows variation of $\bar{k}_{2h}$ with $b/h$ when $a/h$ = 0.1 and $L/h$ = 0.5. Similar to the behavior in Fig. 6.36, $\bar{k}_{2h}$ first increases with increasing $b/h$ and then starts to decrease and contrary to Fig. 6.36, the magnitude of the $\bar{k}_{2h}$ decreases as the value of $\nu$ decreases.

Figure 6.43 shows variation of $\bar{k}_{2h}$ with $a/h$ in the case of $b/h$= 0.9 and $\nu$ = 0.3 whereas Figure 6.44 shows variation of $\bar{k}_{2h}$ with $b/h$ in the case of $a/h$= 0.1

and $v$ = 0.3 for several values of *L/h*. Both figures show similar behavior as in Figs. 6.37 and 6.38.

### 6.1.2.2 Edge Cracks in a Finite Strip

Consider the problem shown in Fig. 4.6. In this case, the system of equations, Eqs.(4.24) and (4.23a,b) must be solved for the unknown functions $G_1(\varphi_k)$, $G_2(\varphi_k)$ and $Y(\rho_k)$ ($k$=1,2,...,$N$).

Figures 6.45–6.51 show the normalized Mode I stress intensity factor $\bar{k}_{1a}$ for the edge crack in the finite strip. In Figures 6.45 and 6.46, variation of $\bar{k}_{1a}$ with *a/h* is given when *L/h* = 1 and *L/h* = 2, respectively. Both cases show decrease in $\bar{k}_{1a}$ with increasing *a/h*.

In Figures 6.47 and 6.48, variation of $\bar{k}_{1a}$ with *a/h* is given when $v$ = 0.3 and $v$ = 0.45, respectively. In both figures, $\bar{k}_{1a}$ decreases with increasing *a/h* for particular values of *L/h*. It is seen that as the rigid inclusions go away from the cracks, the magnitude of $\bar{k}_{1a}$ increases.

Figure 6.49 shows variation of $\bar{k}_{1a}$ with *L/h* when $v$ = 0.3 for several values of *a/h*. Here, in general $\bar{k}_{1a}$ increases with increasing *L/h*.

In Figures 6.50 and 6.51, variation of $\bar{k}_{1a}$ with *L/h* is given when *a/h* = 0.1 and *a/h* = 0.5, respectively. In both cases, $\bar{k}_{1a}$ decreases with increasing *L/h* until *L/h* = ~ 0.35 and then starts increasing smoothly.

Figures 6.52–6.55 show the normalized Mode I stress intensity factor $\bar{k}_{1h}$ at the corner of the finite strip. Figure 52 shows variation of $\bar{k}_{1h}$ with *a/h* when *L/h* =

0.5. $\bar{k}_{1h}$ increases with increasing *a/h* and then becomes stationary after *a/h* =~ 0.95 for fixed values of *v*.

In Figure 6.53 variation of $\bar{k}_{1h}$ with *a/h* is given when *v* = 0.3. For *L/h* = 0.5 and *L/h* = 1, $\bar{k}_{1h}$ increases with increasing *a/h* and then becomes stationary for *a/h* > ~0.95. However, for *L/h* = 2, $\bar{k}_{1h}$ decreases slightly and then becomes stationary for the same range of *a/h*.

Figure 6.54 shows variation of $\bar{k}_{1h}$ with *L/h* when *v* = 0.3 for several values of *a/h*. In this figure, $\bar{k}_{1h}$ increases with increasing *L/h* and after *L/h* = ~1.4, the values of $\bar{k}_{1h}$ become almost constant for all fixed values of *a/h*, 0.1−0.9.
Figure 6.55 shows variation of $\bar{k}_{1h}$ with *L/h* when *a/h* = 0.5 for several values of *v*. Here, $\bar{k}_{1h}$ increases with increasing *L/h* and then decreases slightly.

Figures 6.56–6.59 show the normalized Mode II stress intensity factor $\bar{k}_{2h}$ at the corner of the finite strip. Figure 6.56 shows variation of $\bar{k}_{2h}$ with *a/h* when *L/h* = 0.5. $\bar{k}_{2h}$ increases with increasing *a/h.* As can be realized from the figure the magnitude of $\bar{k}_{2h}$ increases with increasing *v* also.

Figures 6.57–6.59 show similar behavior as in Figs. 6.53–6.55 for variations of $\bar{k}_{2h}$.

## 6.2 Conclusions

This study considers the analysis of a symmetrical finite strip containing two symmetrical collinear edge cracks (notches) located at the middle of the strip. Two ends of the finite strip are bonded to two rigid plates and both ends are subjected to axial tension. The material of the strip is assumed to be linearly elastic and isotropic.

For the solution of the finite strip problem, an infinite strip of width *2h* containing two internal cracks of width *b–a* at *y=0* and two rigid inclusions of width *2c* at $y=\pm L$ is considered. When the width of rigid inclusions approach the width of the strip, the portion of the infinite strip between the inclusions becomes identical with the finite strip problem. When the outer edges of the internal cracks approach the edge of the strip, they become edge cracks. Therefore, the results for internal cracks and/or internal rigid inclusions are also given.

General expressions of stresses and displacements for the perturbation problem are obtained by solving Navier equations using Fourier transforms and these expressions are forced to satisfy the boundary conditions. Satisfying the homogeneous boundary conditions at the edges of the strip, the general expressions for an infinite medium become expressions for a strip with free edges. By the use of remaining conditions on the cracks and the inclusions, a system of three singular integral equations is obtained. By using Gauss-Lobatto and Gauss-Jacobi integration formulas, these three singular integral equations are converted into a system of linear algebraic equations. To obtain numerical results, the system of linear algebraic equations is solved with a Fortran program.

The normalized Mode I stress intensity factors $\bar{k}_{1a}$ and $\bar{k}_{1b}$, at the edges of the cracks and the normalized Mode I and II stress intensity factors, $\bar{k}_{1c}$ and $\bar{k}_{2c}$, at the edge of the inclusion and at the corner of the finite strip are presented in graphical form in Figs. 6.1–6.59. From the formulation and the presented figures, following conclusions may be deduced:

1. There is considerable interaction between the cracks and the rigid inclusions when inclusions become closer to the cracks.
2. As the value of *v* increases, the effect of *v* on $\bar{k}_{1a}$ and $\bar{k}_{1b}$ increases in the case of infinite strip.

3. In finite strip, $\bar{k}_{1b}$ increases dramatically when the outer edges of internal cracks tend to open.
4. No remarkable variations are observed for $\bar{k}_{2h}$ when $L/h$ = 1 for all values of $v$.
5. In finite strip in the case of edge crack, $\bar{k}_{1a}$ has close values for all $v$ values when $L/h$ = 2.

### 6.3 Suggestion for Further Studies

Results and methods used in this study can be applied in many engineering problems by considering various applications:

1. Thermal loads can be added to finite and infinite problems.
2. The material of the strip may be assumed to be composite.

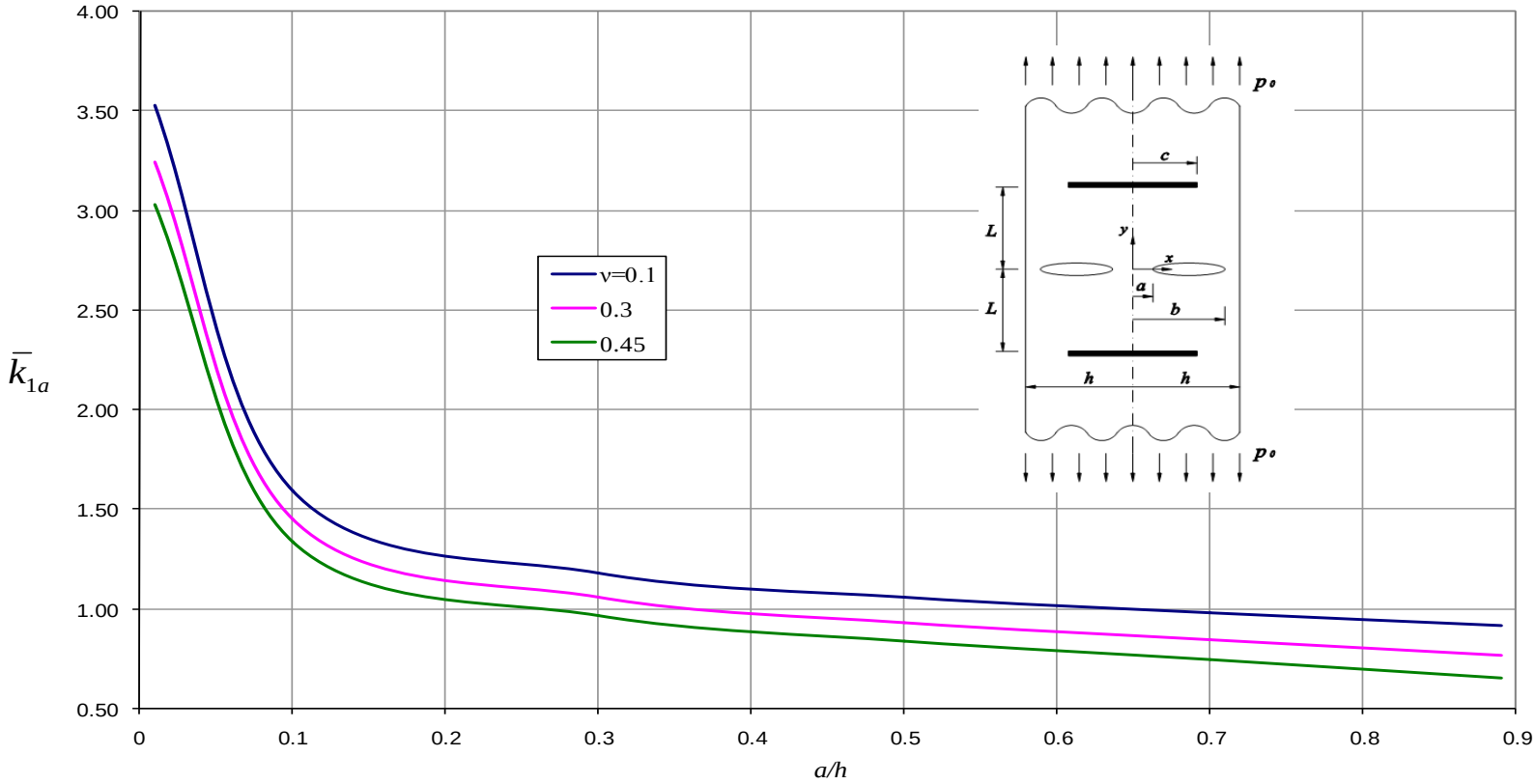


Figure 6.1 Normalized Mode I stress intensity factor $\bar{k}_{1a}$ at inner edge of crack when $b/h = 0.9$ $L/h = 0.5$ $c/h = 0.5$ (Plane strain).

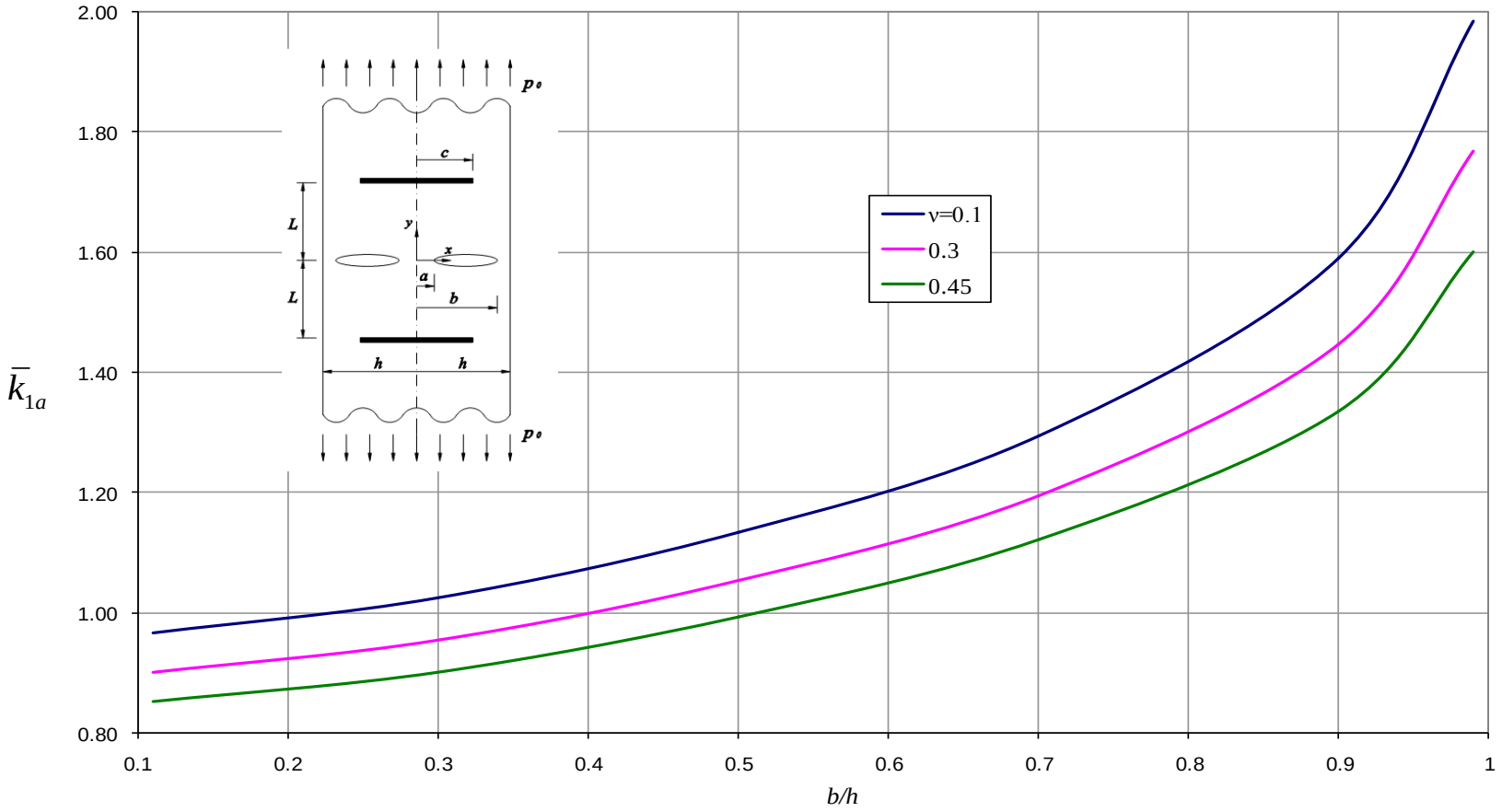


Figure 6.2 Normalized Mode I stress intensity factor $\bar{k}_{1a}$ at inner edge of crack when $a/h$ = 0.1 $L/h$ = 0.5 $c/h$ = 0.5 (Plane strain).

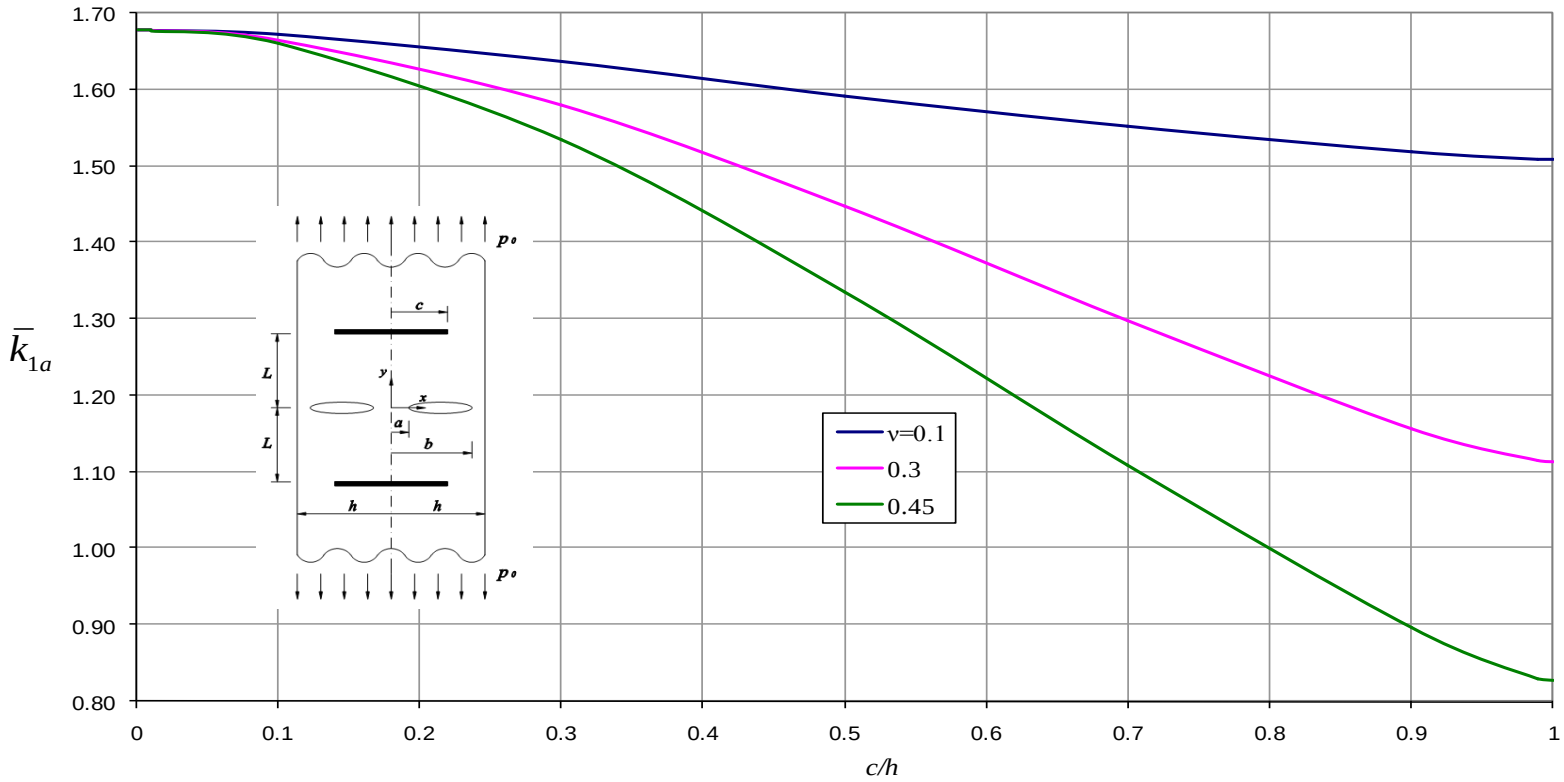


Figure 6.3 Normalized Mode I stress intensity factor $\bar{k}_{1a}$ at inner edge of crack when $a/h = 0.1$ $b/h = 0.9$ $L/h = 0.5$ (Plane strain).

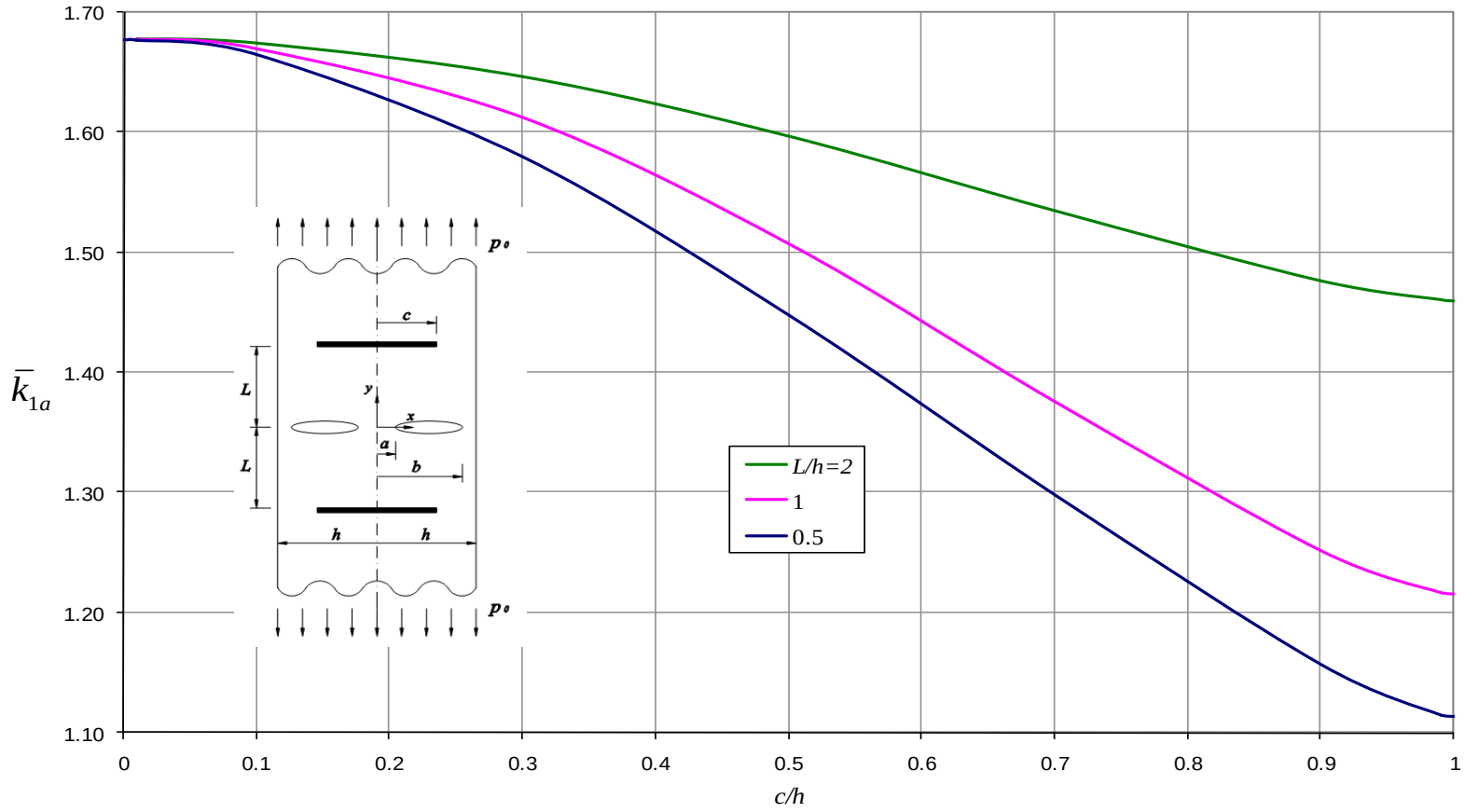


Figure 6.4 Normalized Mode I stress intensity factor $\bar{k}_{1a}$ at inner edge of crack when $a/h = 0.1$ $b/h = 0.9$ $\nu = 0.3$ (Plane strain).

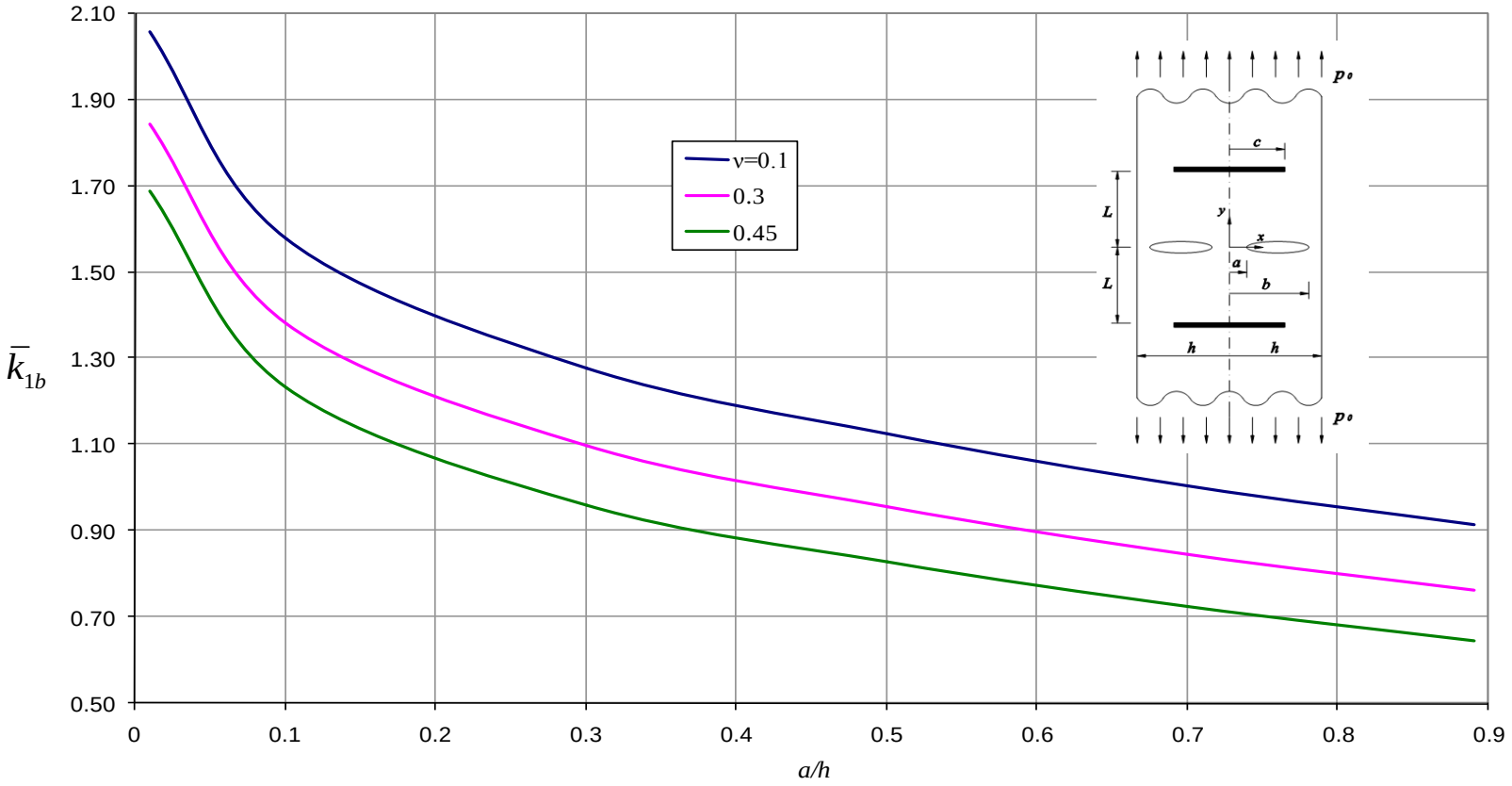


Figure 6.5 Normalized Mode I stress intensity factor $\bar{k}_{1b}$ at outer edge of crack when $b/h = 0.9$ $L/h = 0.5$ $c/h = 0.5$ (Plane strain).

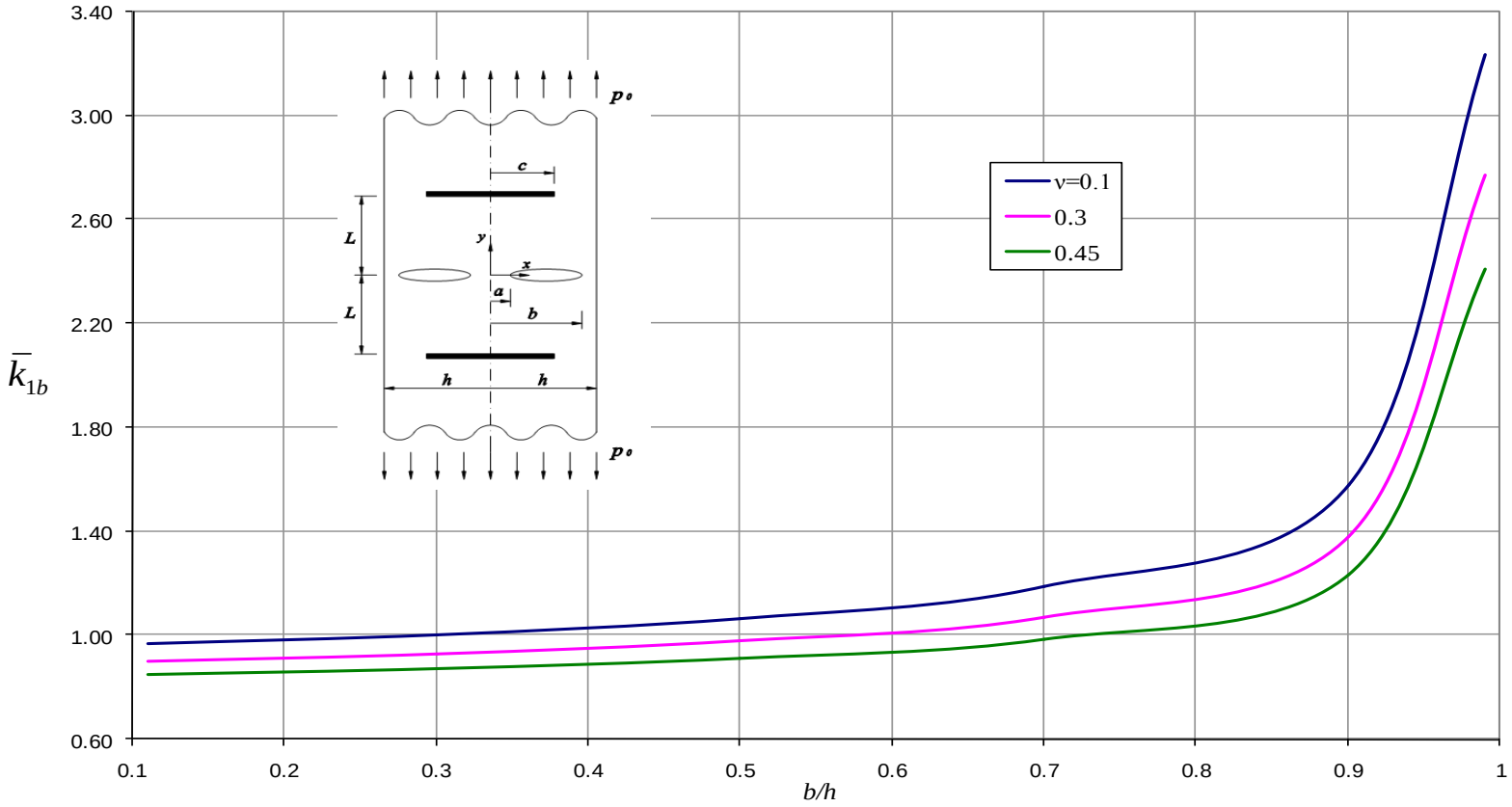


Figure 6.6 Normalized Mode I stress intensity factor $\bar{k}_{1b}$ at outer edge of crack when $a/h = 0.1$ $L/h = 0.5$ $c/h = 0.5$ (Plane strain).

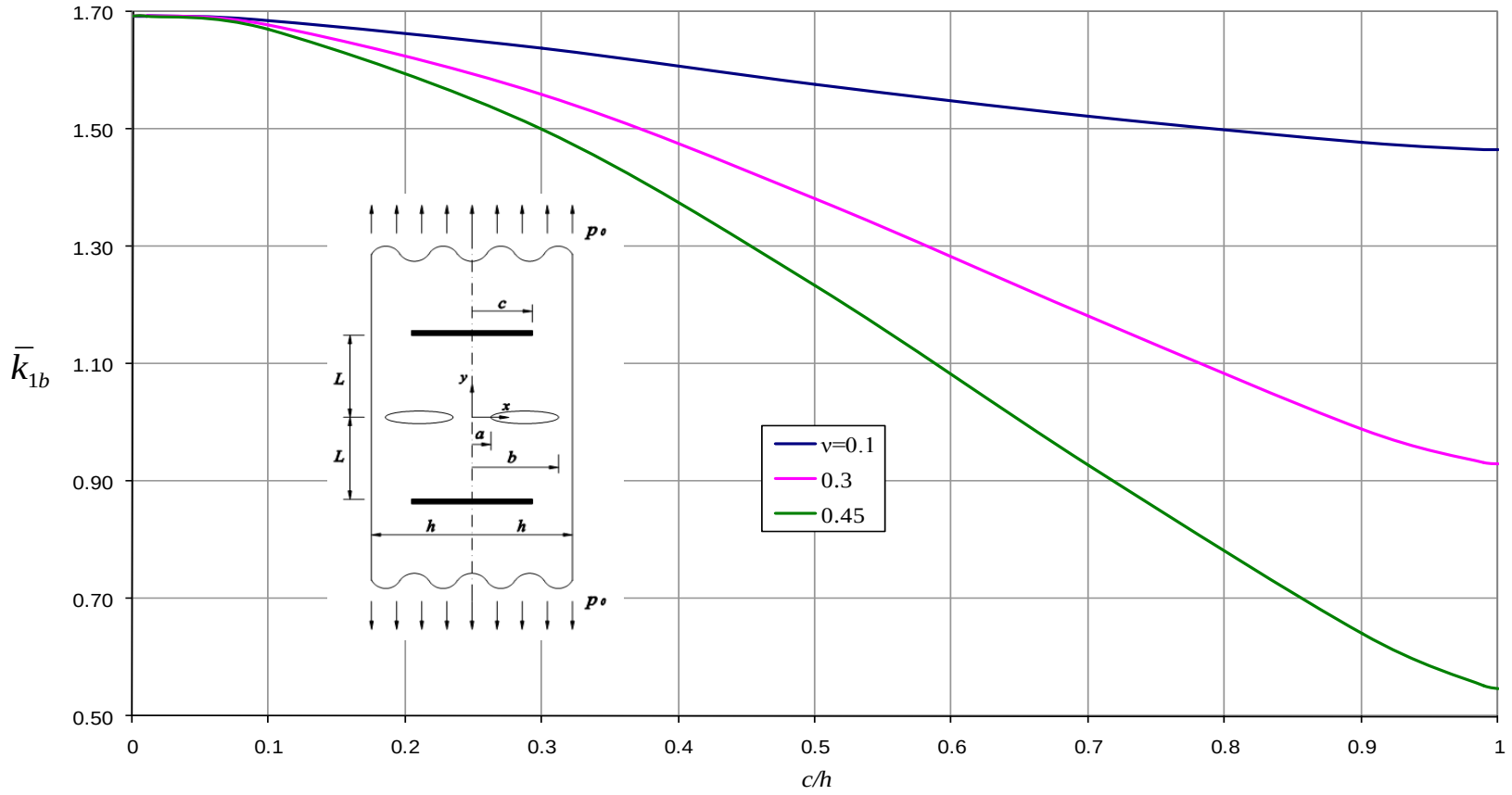


Figure 6.7 Normalized Mode I stress intensity factor $\bar{k}_{1b}$ at outer edge of crack when $a/h = 0.1$ $b/h = 0.9$ $L/h = 0.5$ (Plane strain).

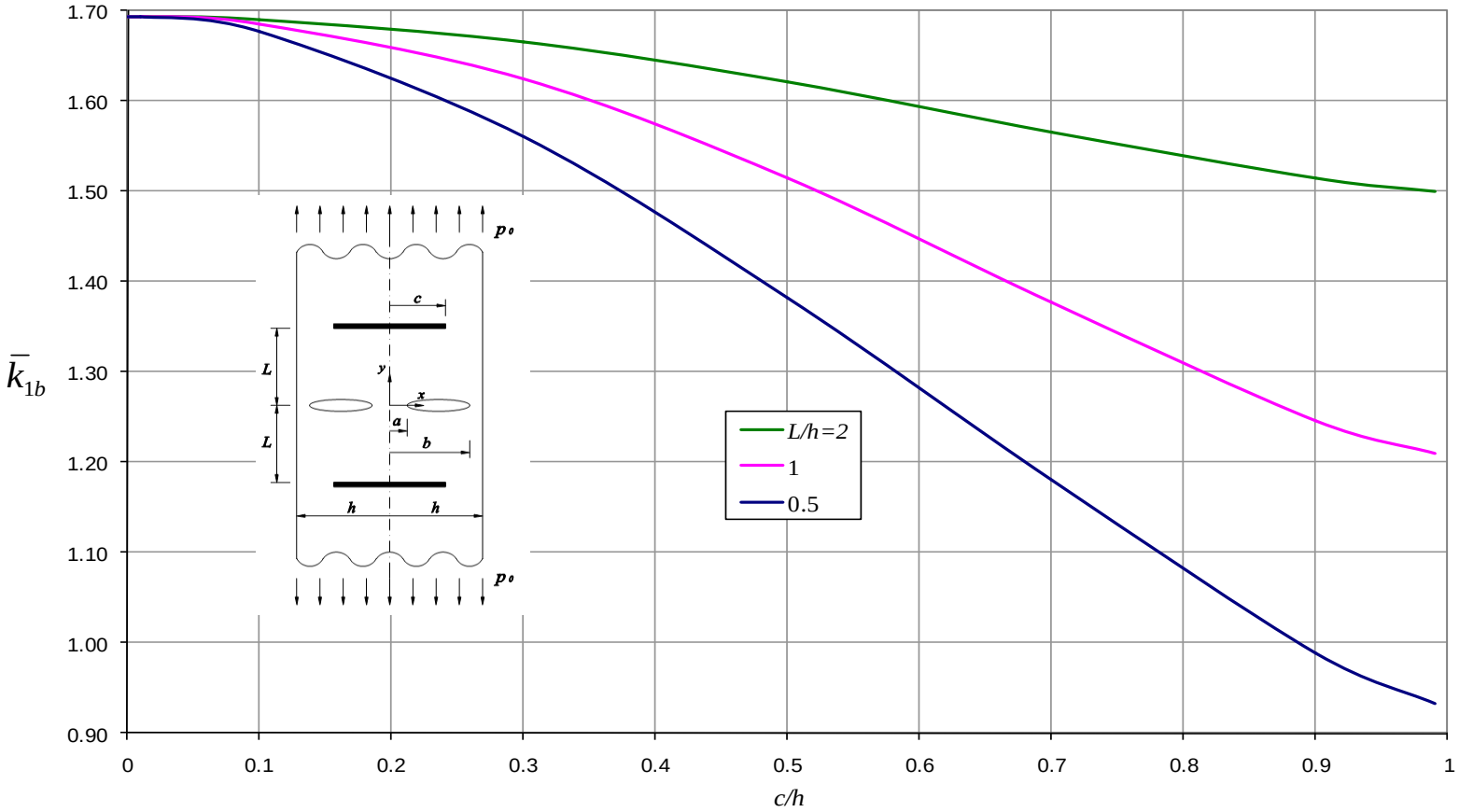


Figure 6.8 Normalized Mode I stress intensity factor $\bar{k}_{1b}$ at outer edge of crack when $a/h = 0.1$ $b/h = 0.9$ $v = 0.3$ (Plane strain).

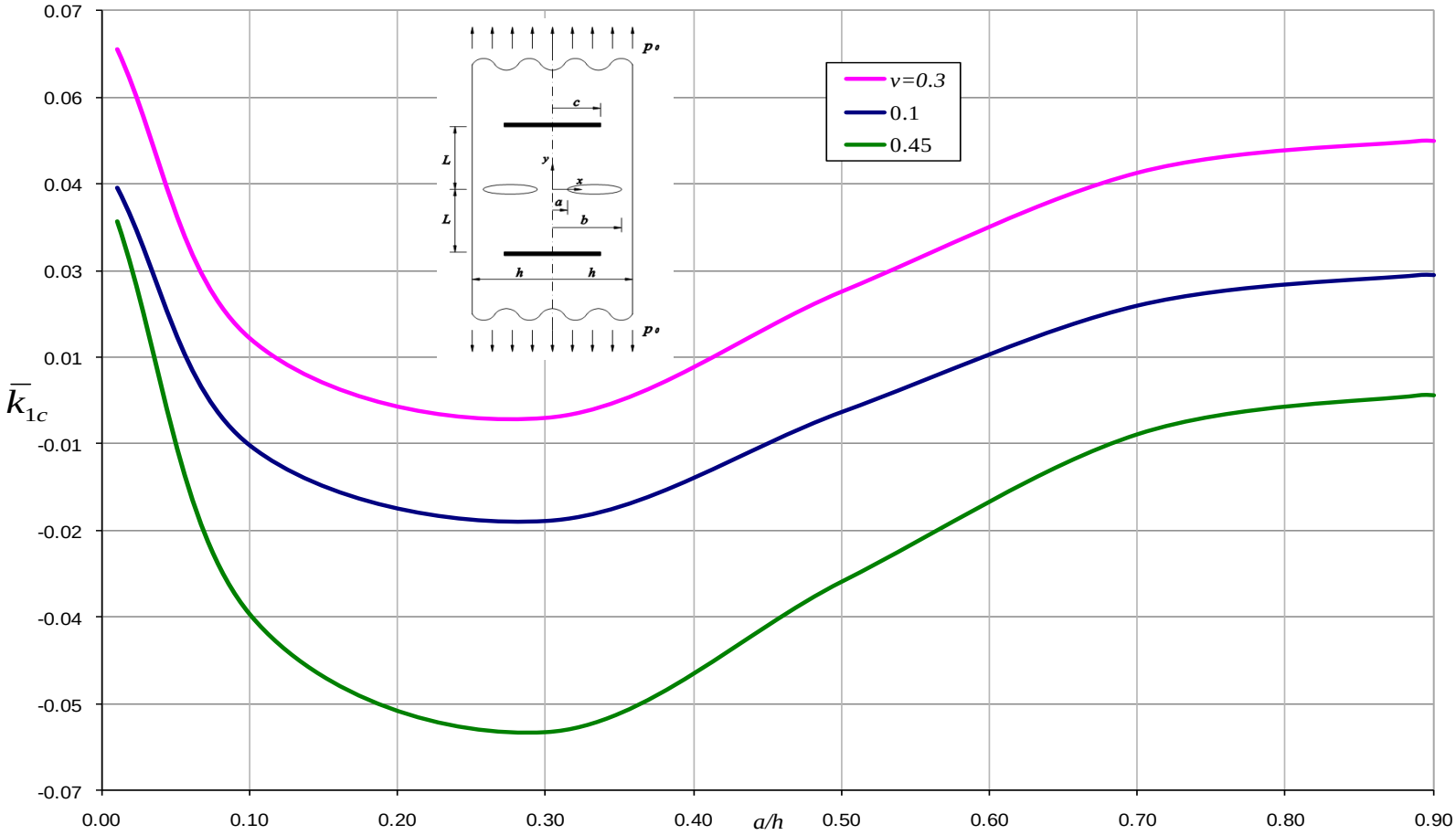


Figure 6.9 Normalized Mode I stress intensity factor $\bar{k}_{1c}$ at edge of inclusion when $b/h = 0.9$ $L/h = 0.5$ $c/h = 0.5$ (Plane strain).

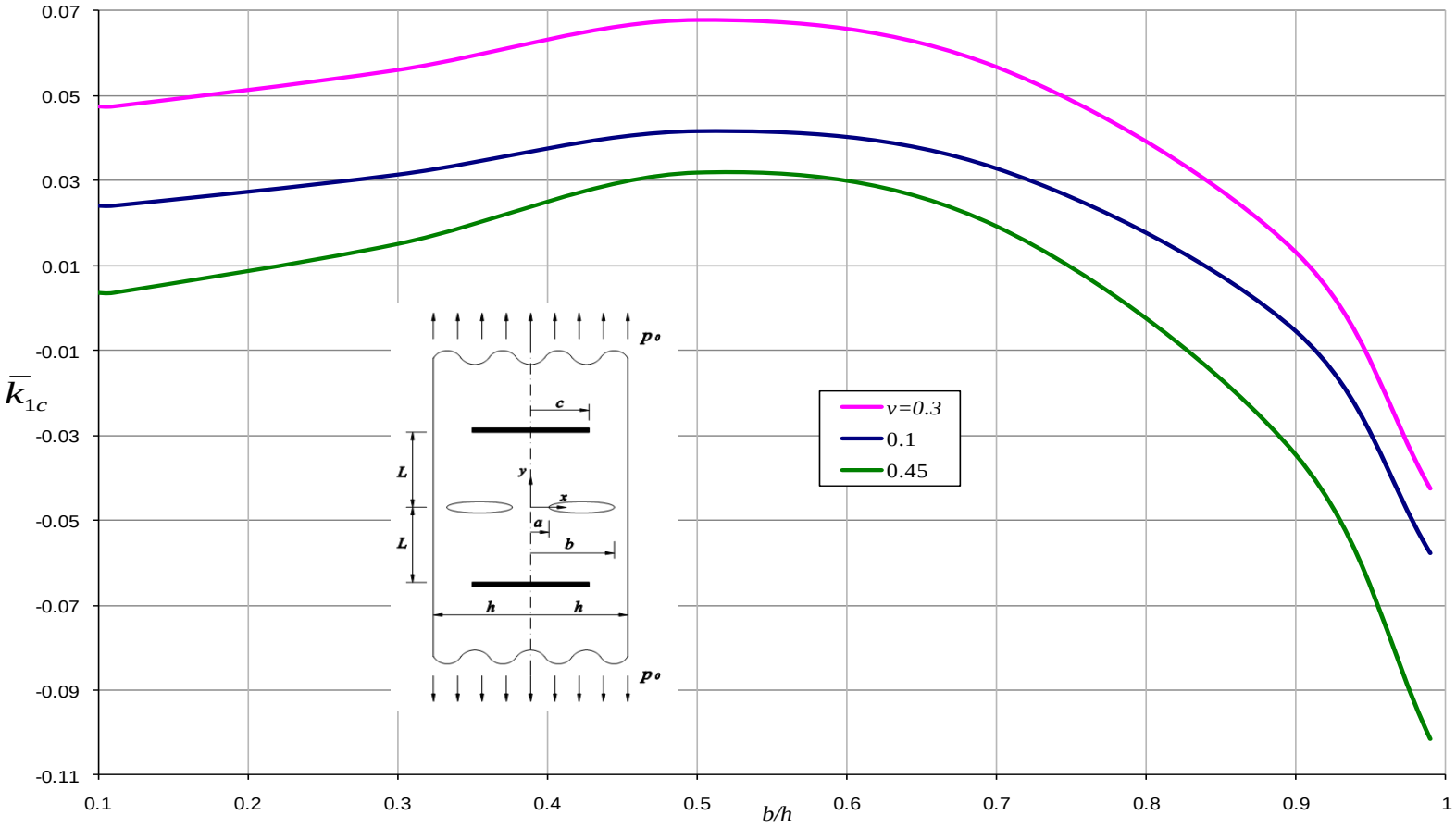


Figure 6.10 Normalized Mode I stress intensity factor $\bar{k}_{1c}$ at edge of inclusion when $a/h$ = 0.1 $L/h$ = 0.5 $c/h$ = 0.5 (Plane strain).

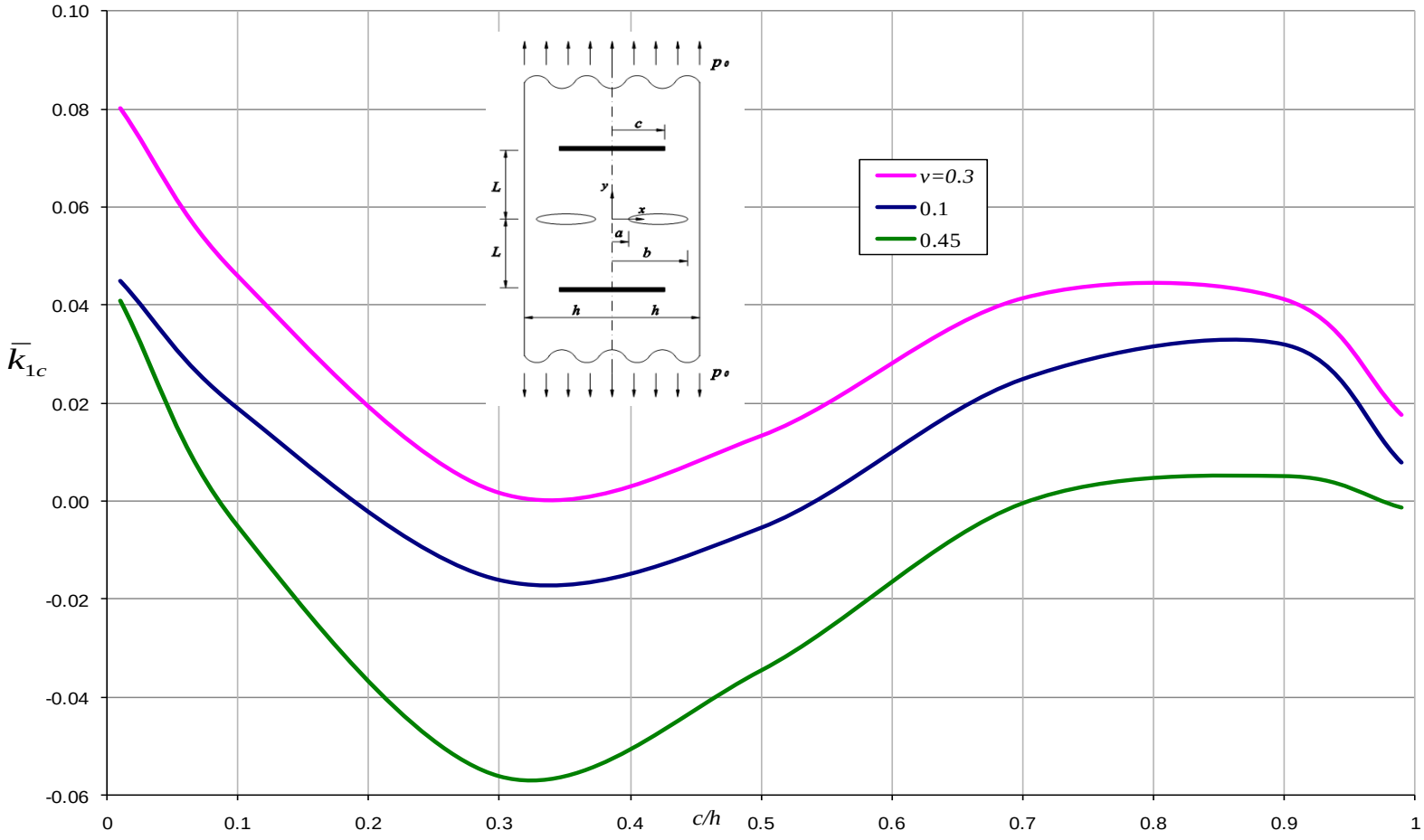


Figure 6.11 Normalized Mode I stress intensity factor $\bar{k}_{1c}$ at edge of inclusion when $a/h = 0.1$ $b/h = 0.9$ $L/h = 0.5$ (Plane strain).

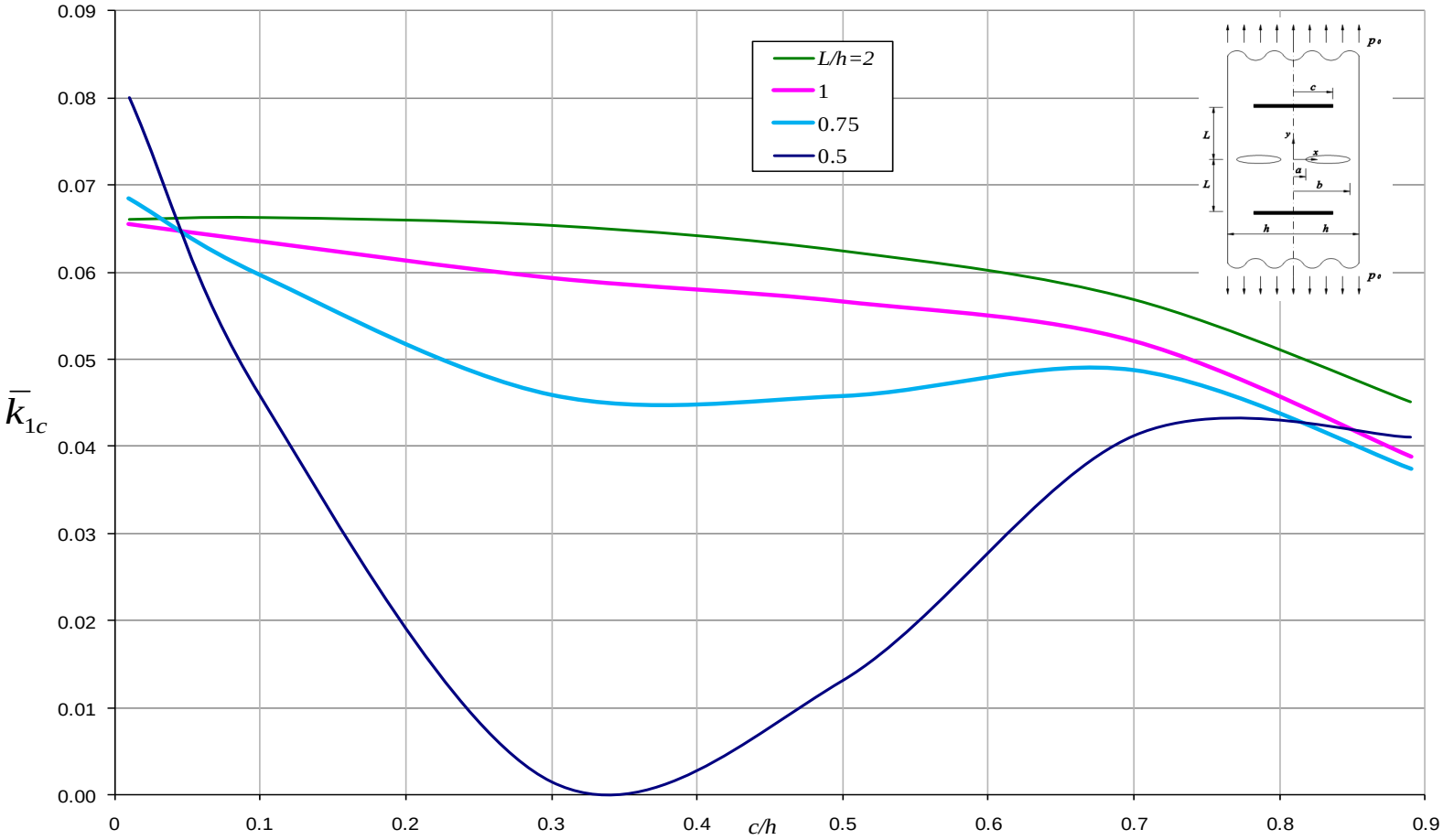


Figure 6.12 Normalized Mode I stress intensity factor $\bar{k}_{1c}$ at edge of inclusion when $a/h$ = 0.1 $b/h$ = 0.9 $\nu$ = 0.3 (Plane strain).

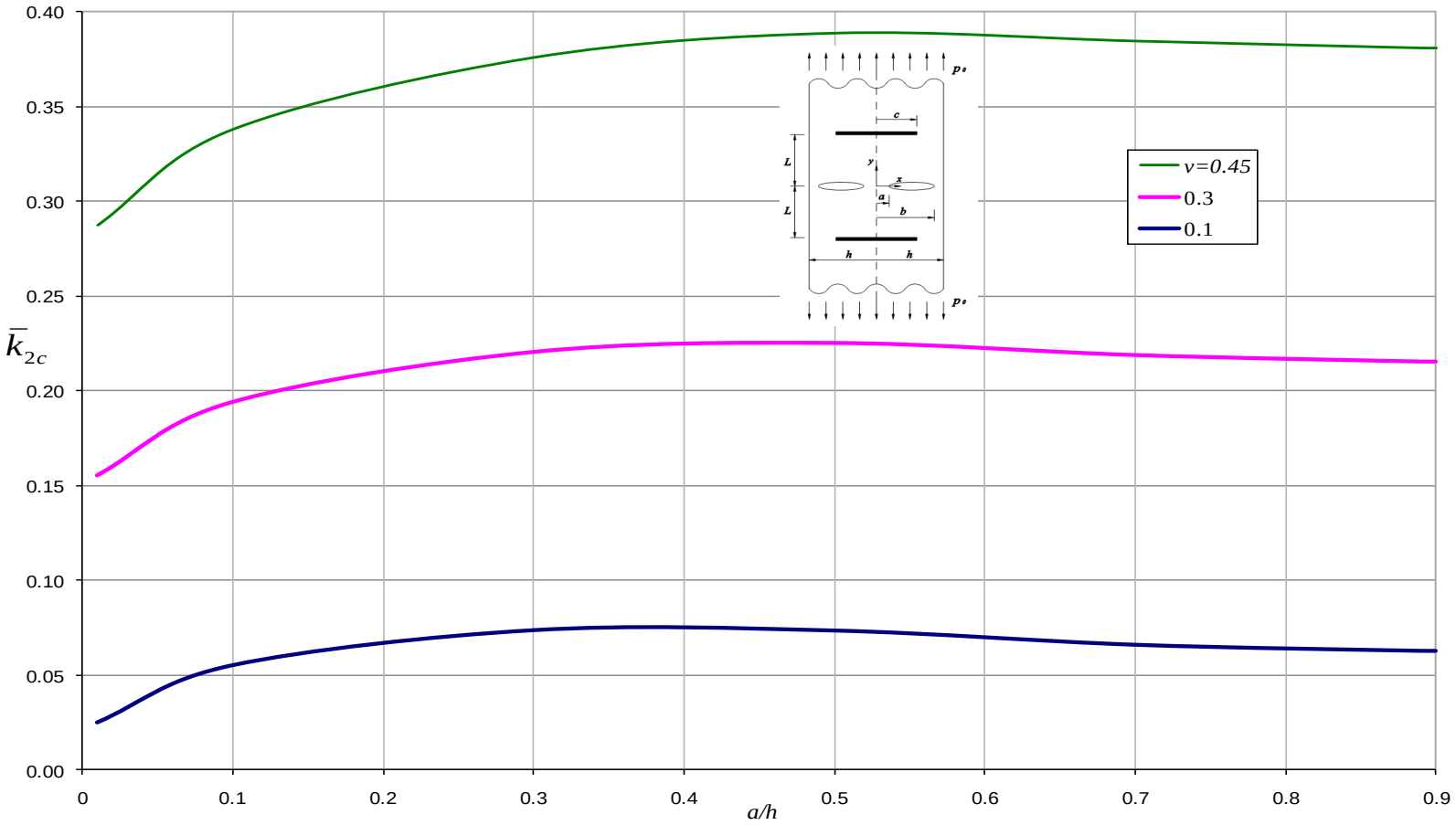


Figure 6.13 Normalized Mode II stress intensity factor $\bar{k}_{2c}$ at edge of inclusion when $b/h$ = 0.9 $L/h$ = 0.5 $c/h$ = 0.5 (Plane strain).

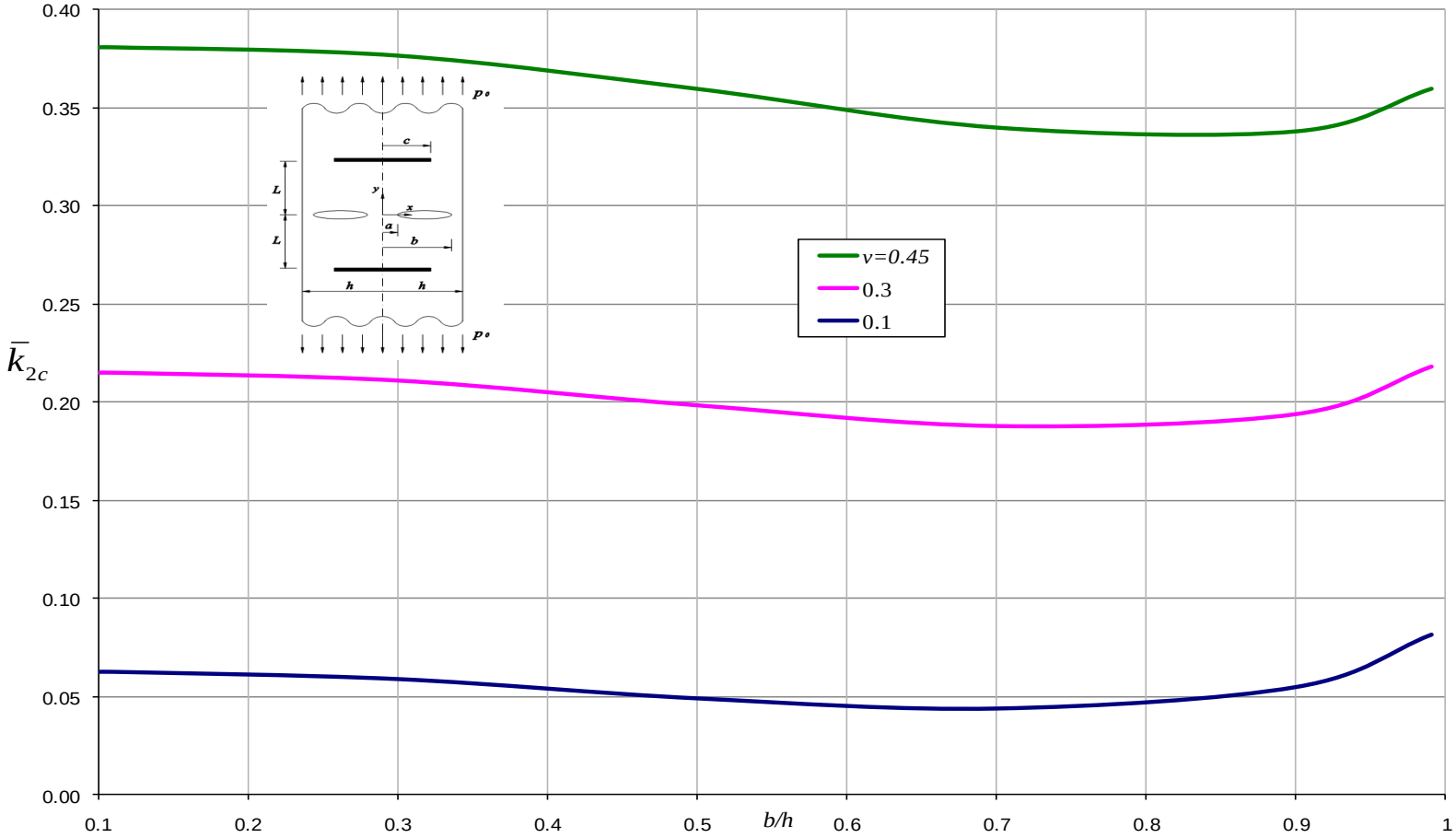


Figure 6.14 Normalized Mode II stress intensity factor $\bar{k}_{2c}$ at edge of inclusion when $a/h$ = 0.1 $L/h$ = 0.5 $c/h$ = 0.5 (Plane strain).

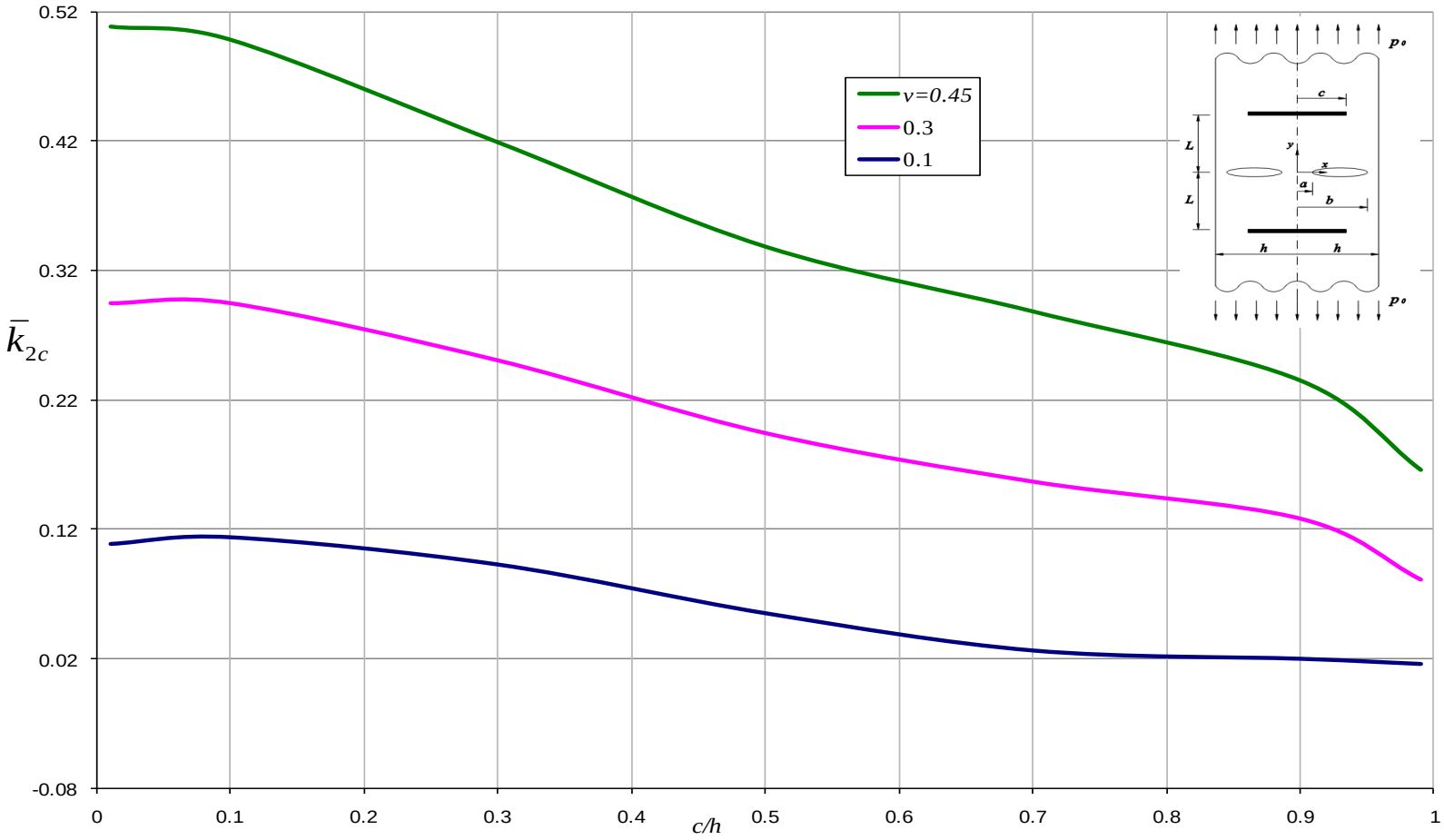


Figure 6.15 Normalized Mode II stress intensity factor $\bar{k}_{2c}$ at edge of inclusion when $a/h = 0.1$ $b/h = 0.9$ $L/h = 0.5$ (Plane strain).

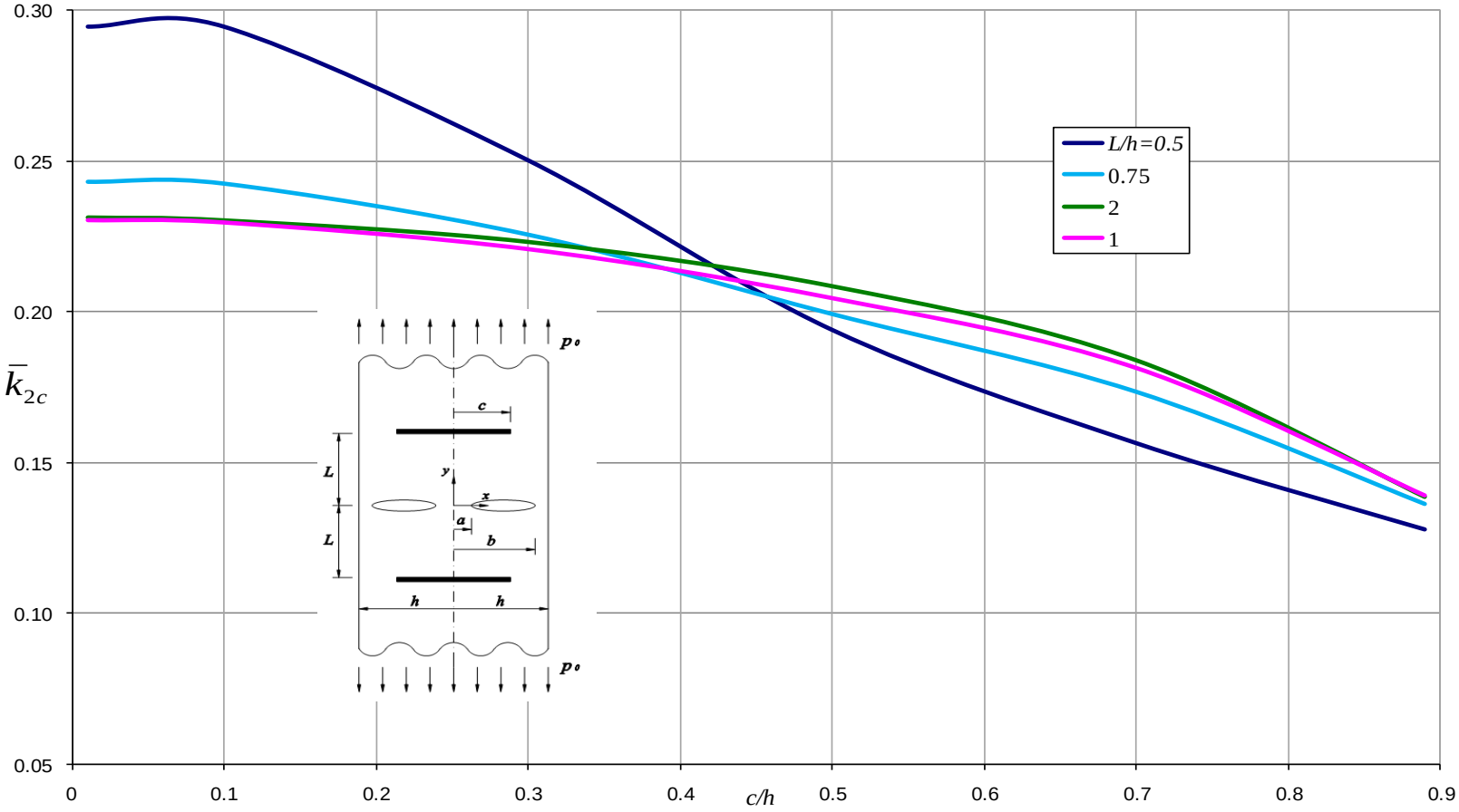


Figure 6.16 Normalized Mode II stress intensity factor $\bar{k}_{2c}$ at edge of inclusion when $a/h = 0.1$ $b/h = 0.9$ $v = 0.3$ (Plane strain).

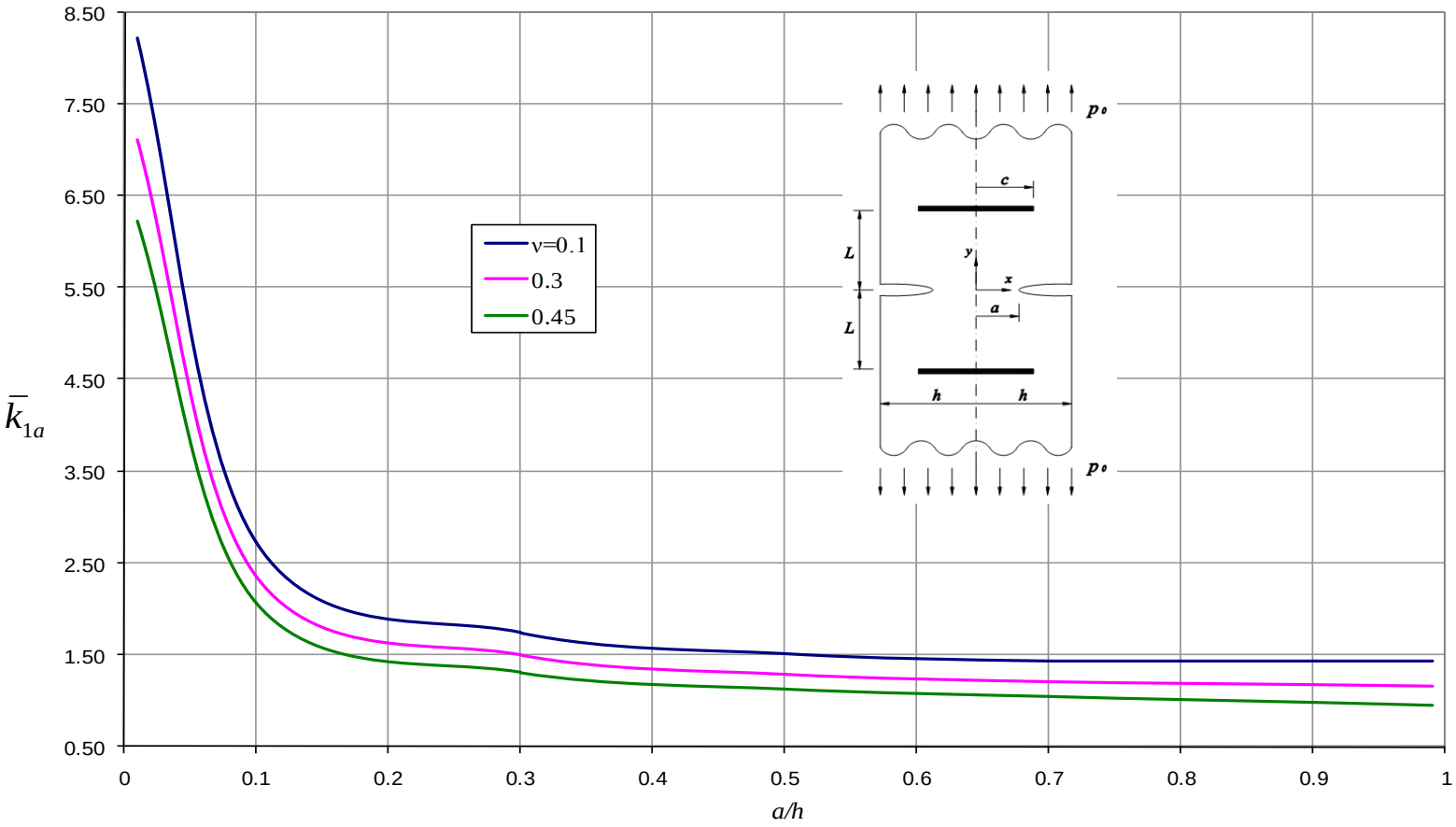


Figure 6.17 Normalized Mode I stress intensity factor $\bar{k}_{1a}$ for edge crack when $L/h$ = 0.5 and $c/h$ = 0.5 (Plane strain).

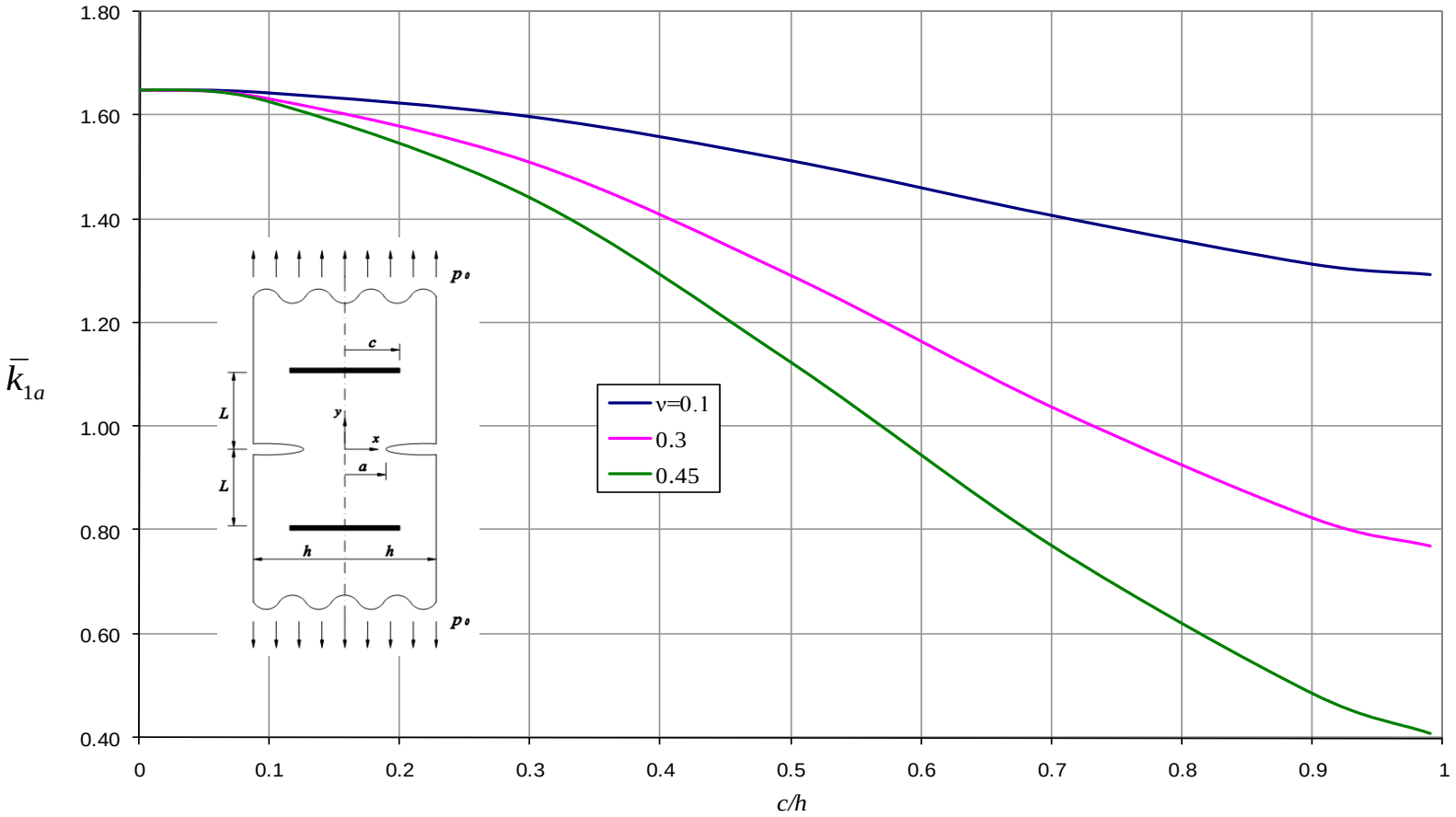


Figure 6.18 Normalized Mode I stress intensity factor $\bar{k}_{1a}$ for edge crack when $a/h$ = 0.5 and $L/h$ = 0.5 (Plane strain).

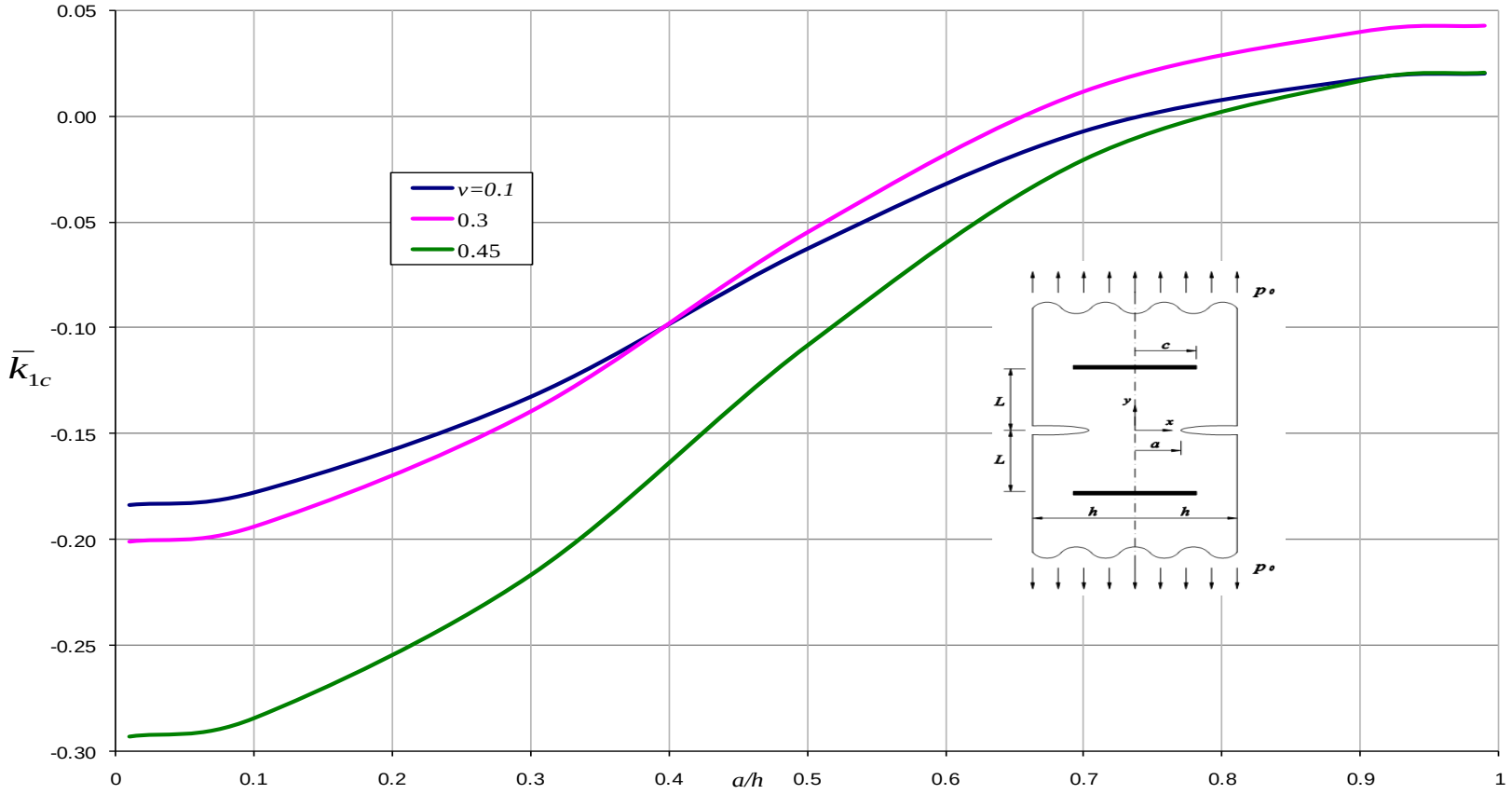


Figure 6.19 Normalized Mode I stress intensity factor $\bar{k}_{1c}$ at edge of inclusion when $L/h$ = 0.5 and $c/h$ = 0.5 (Plane strain).

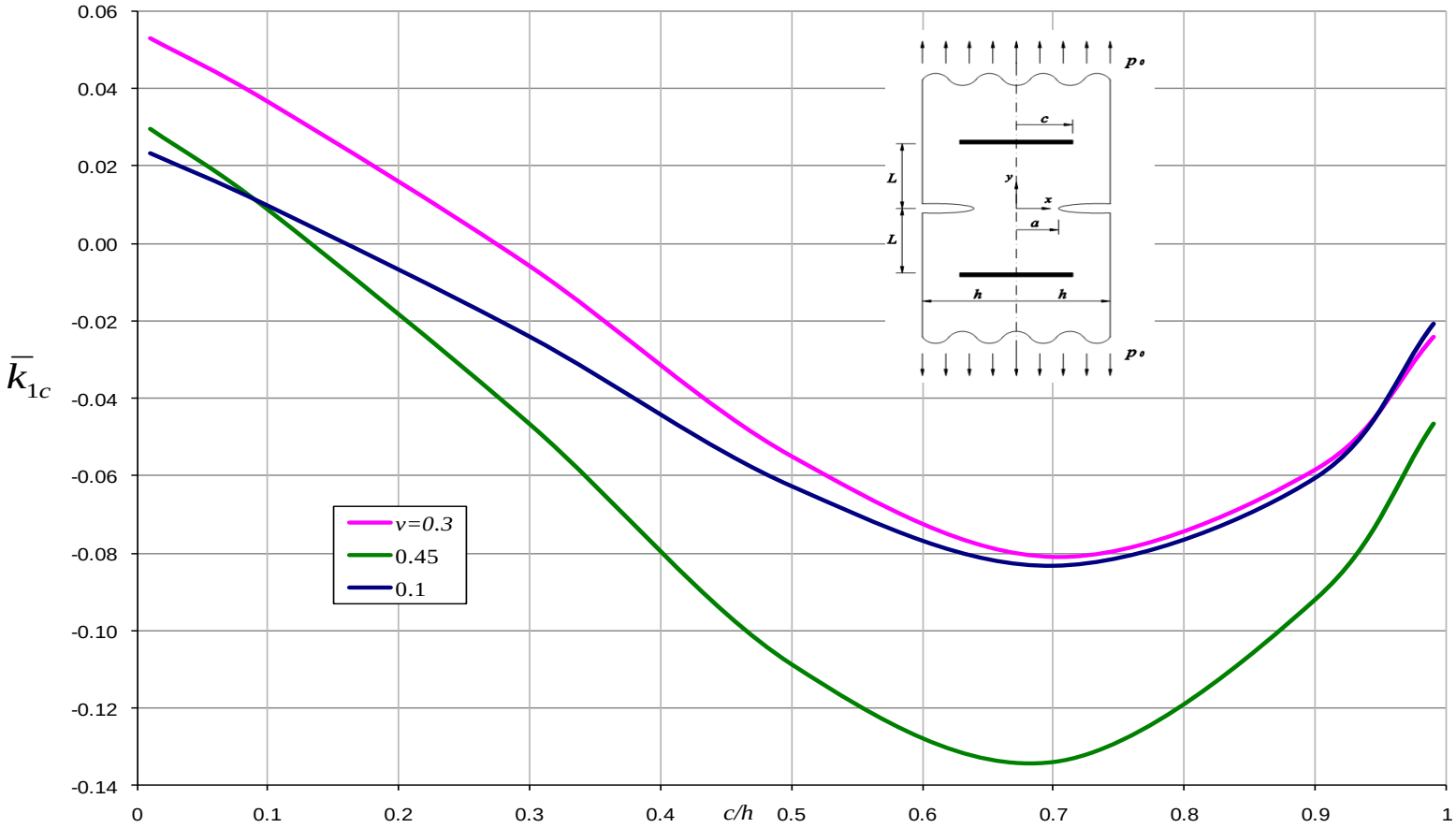


Figure 6.20 Normalized Mode I stress intensity factor $\bar{k}_{1c}$ at edge of inclusion when $a/h$ = 0.5 and $L/h$ = 0.5 (Plane strain).

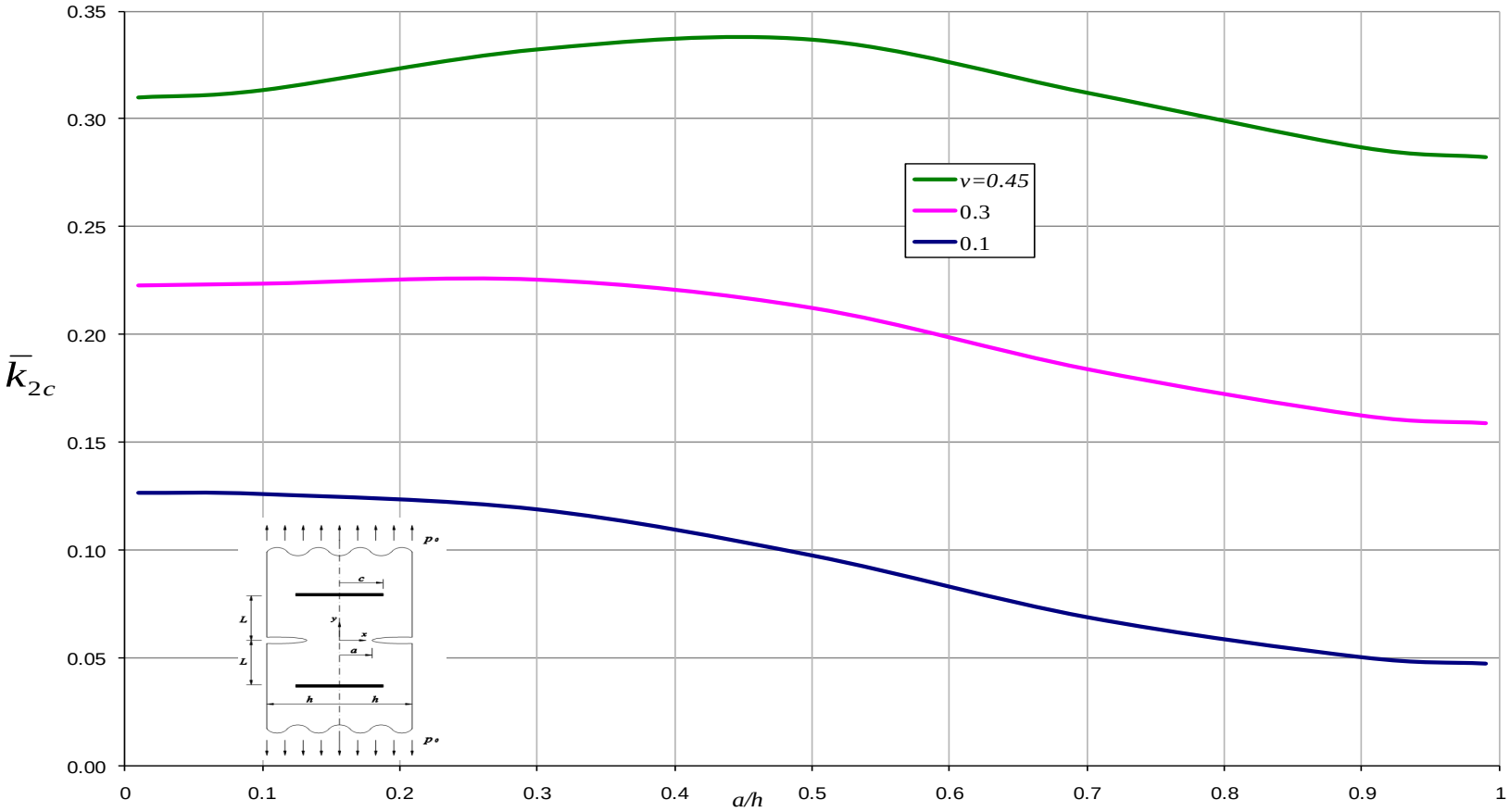


Figure 6.21 Normalized Mode II stress intensity factor $\bar{k}_{2c}$ at edge of inclusion when $L/h$ = 0.5 and $c/h$ = 0.5 (Plane strain).

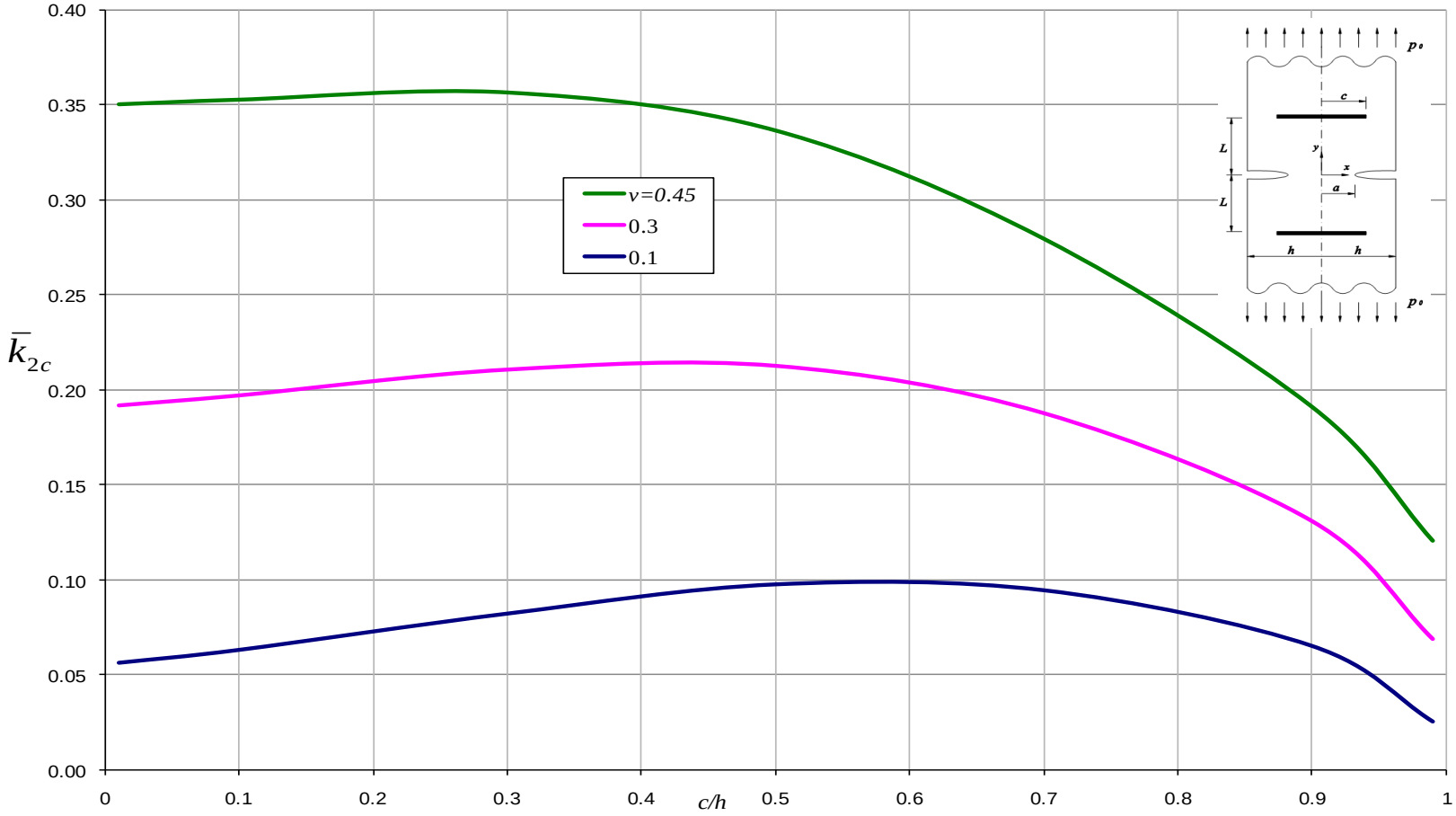


Figure 6.22 Normalized Mode II stress intensity factor $\bar{k}_{2c}$ at edge of inclusion when $a/h$ = 0.5 and $L/h$ = 0.5 (Plane strain).

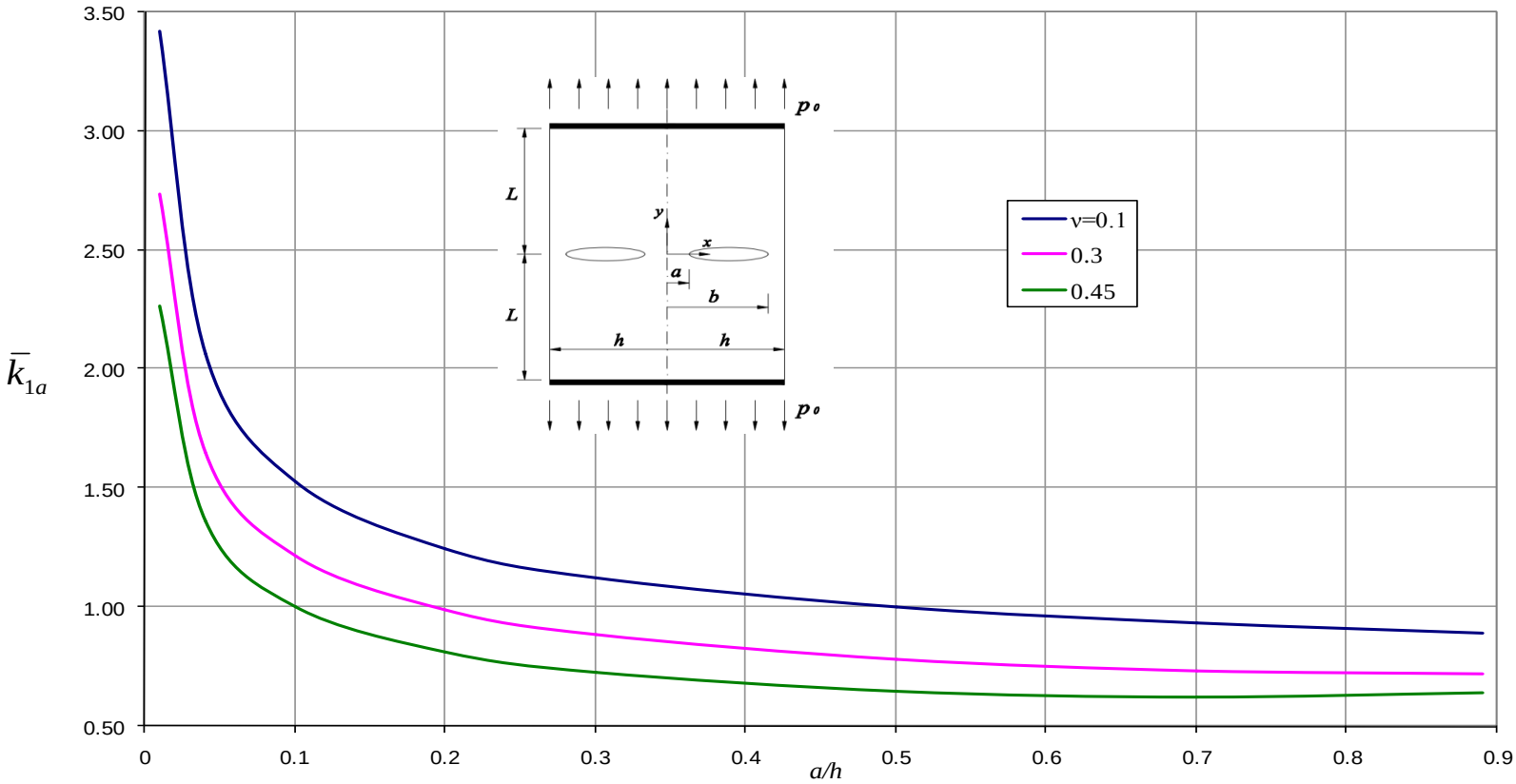


Figure 6.23 Normalized Mode I stress intensity factor $\bar{k}_{1a}$ at inner edge of crack in finite strip when $b/h$ = 0.9 and $L/h$ = 1 (Plane strain).

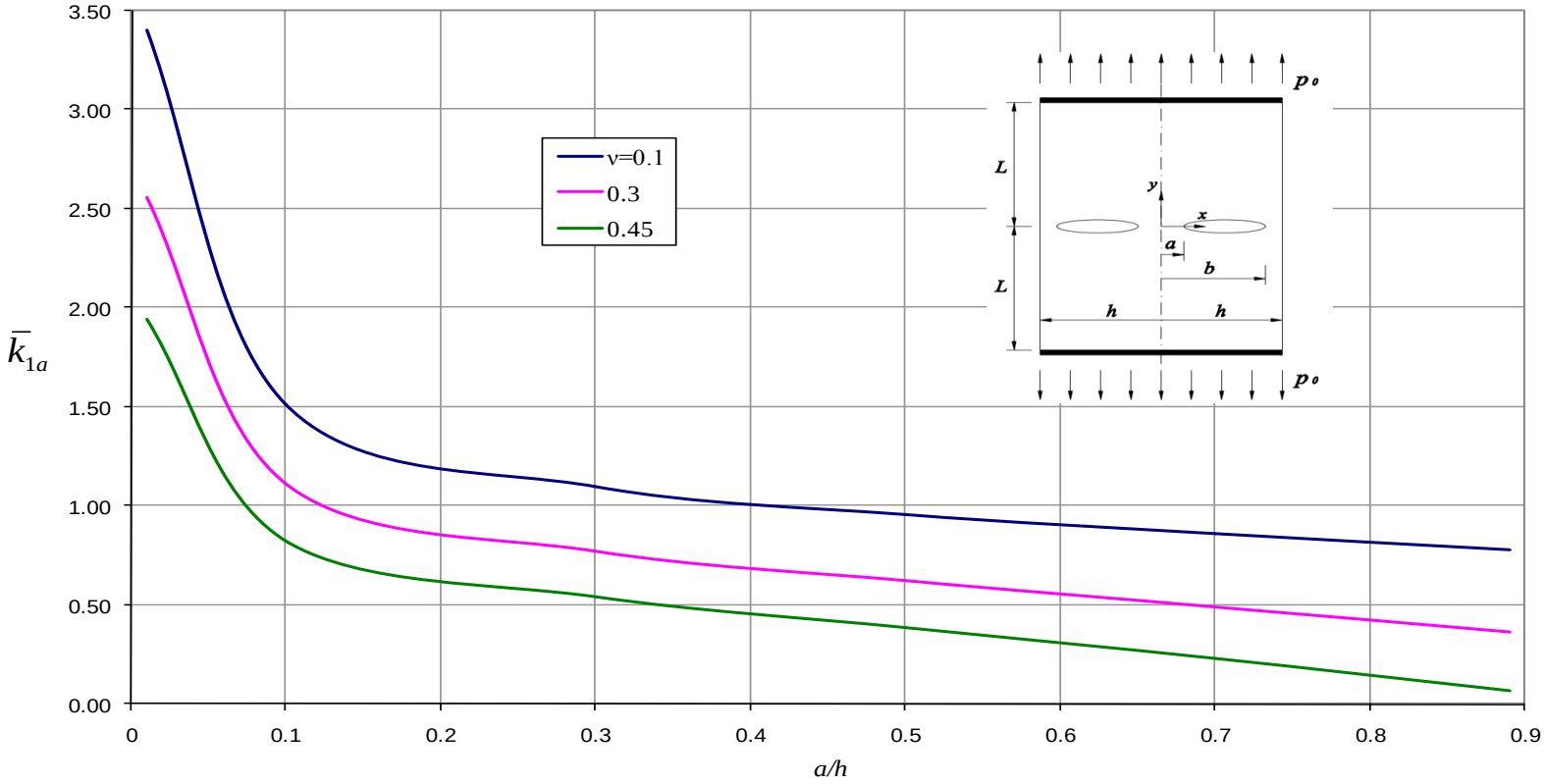


Figure 6.24 Normalized Mode I stress intensity factor $\bar{k}_{1a}$ at inner edge of crack in finite strip when $b/h$ = 0.9 and $L/h$ = 0.5 (Plane strain).

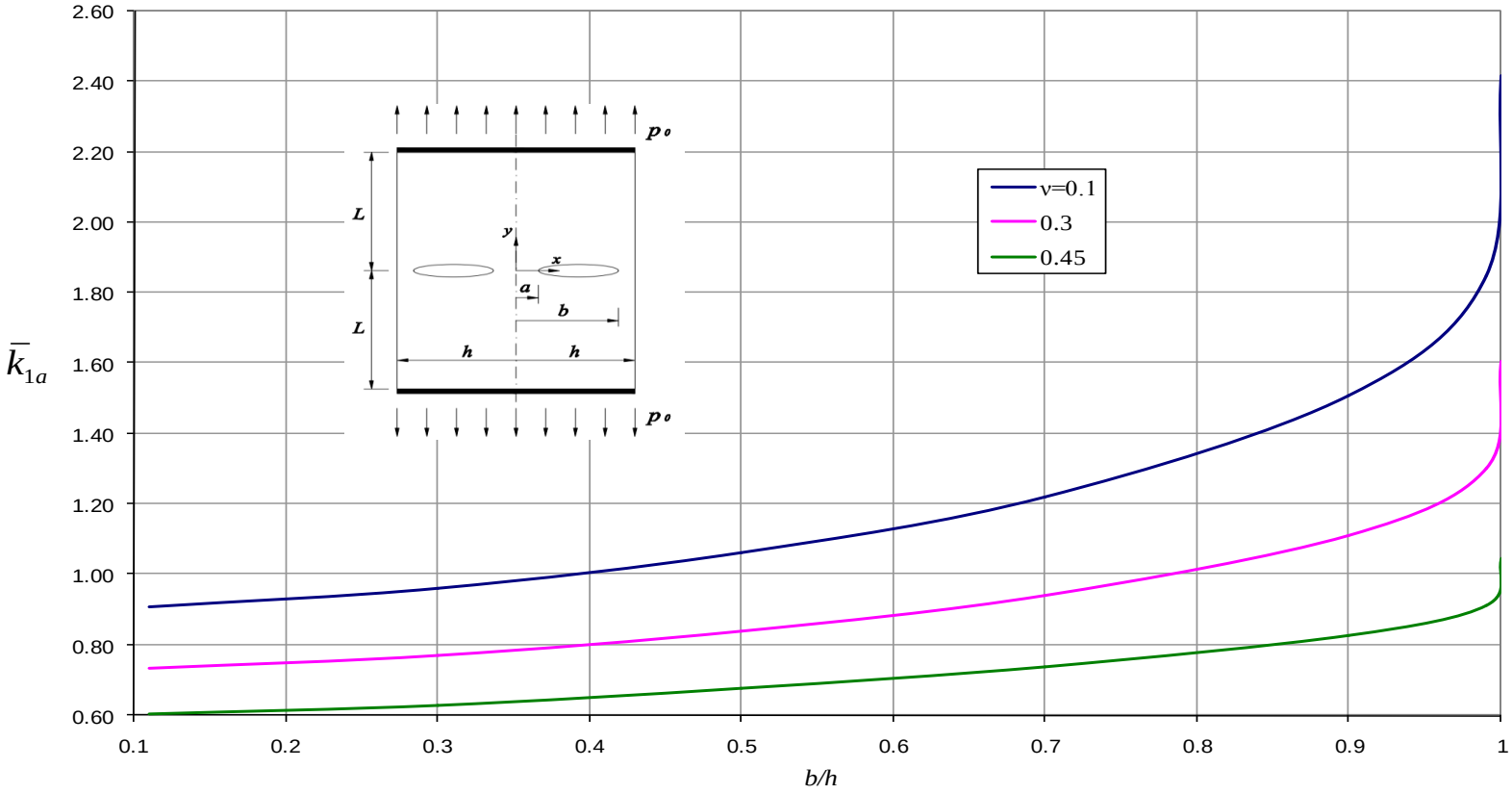


Figure 6.25 Normalized Mode I stress intensity factor $\bar{k}_{1a}$ at inner edge of crack in finite strip when $a/h$ = 0.1 and $L/h$ = 0.5 (Plane strain).

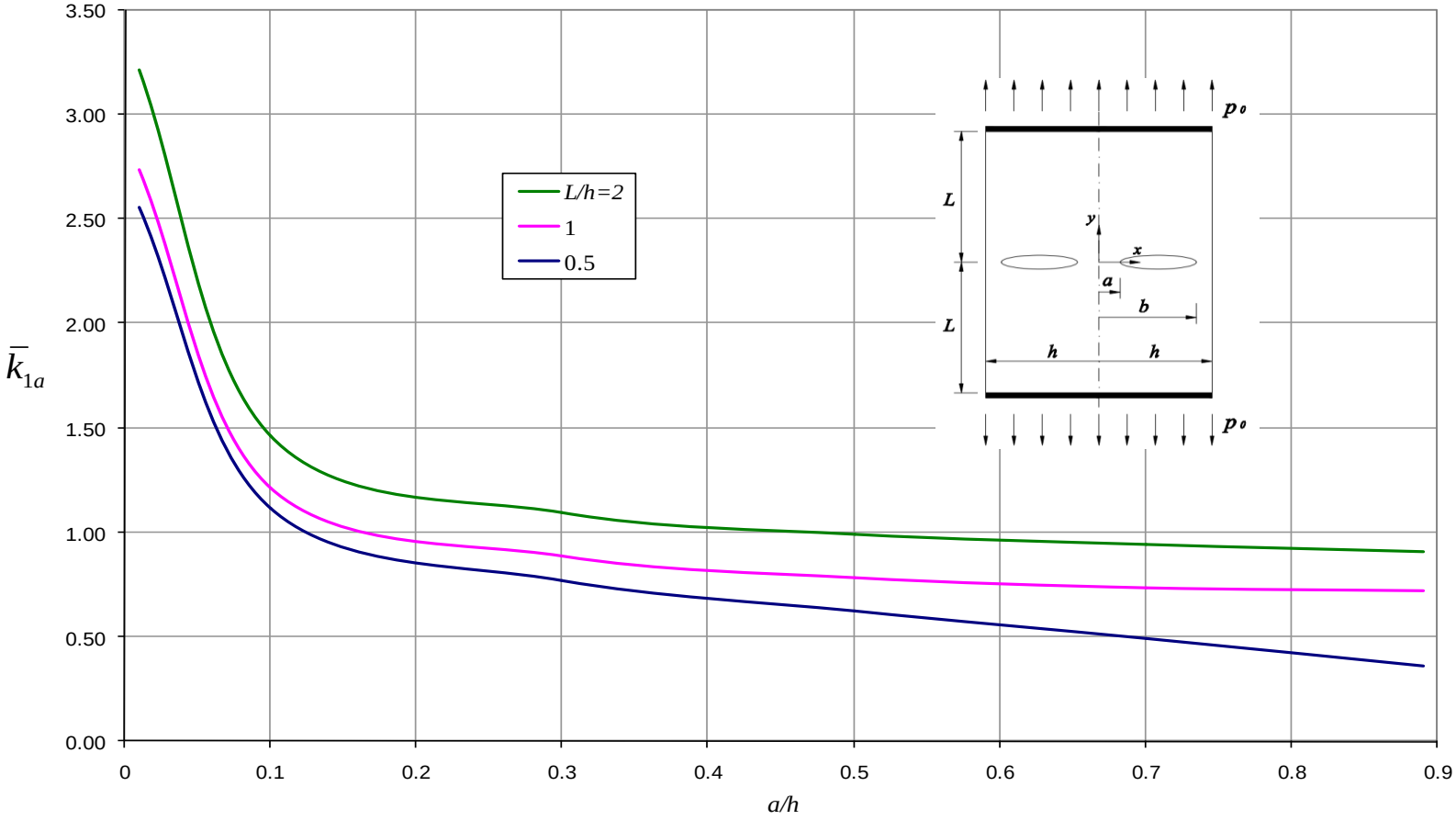


Figure 6.26 Normalized Mode I stress intensity factor $\bar{k}_{1a}$ at inner edge of crack in finite strip when $b/h$ = 0.9 and $\nu$ = 0.3 (Plane strain).

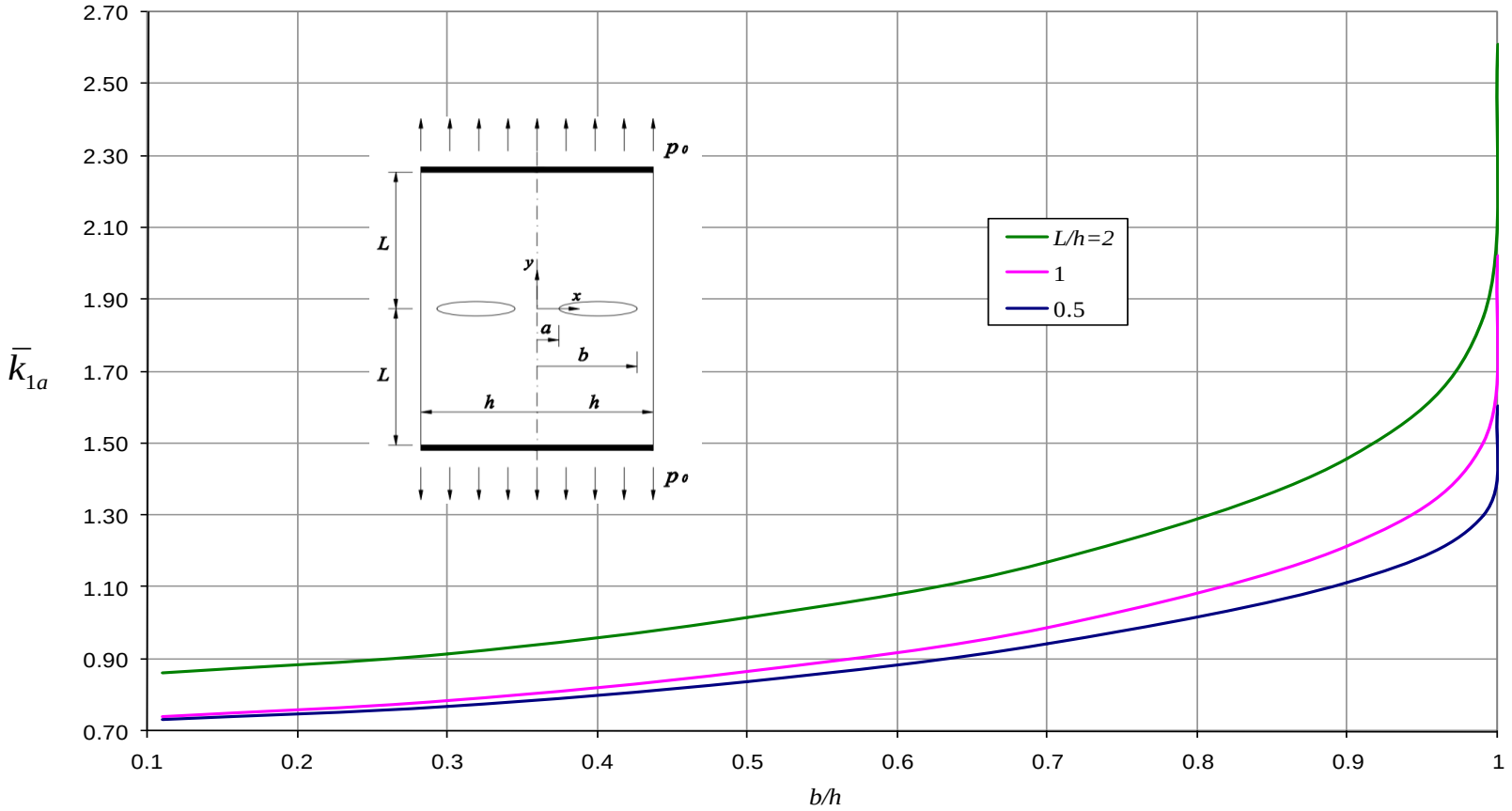


Figure 6.27 Normalized Mode I stress intensity factor $\bar{k}_{1a}$ at inner edge of crack in finite strip when $a/h$ = 0.1 and $\nu$ = 0.3 (Plane strain).

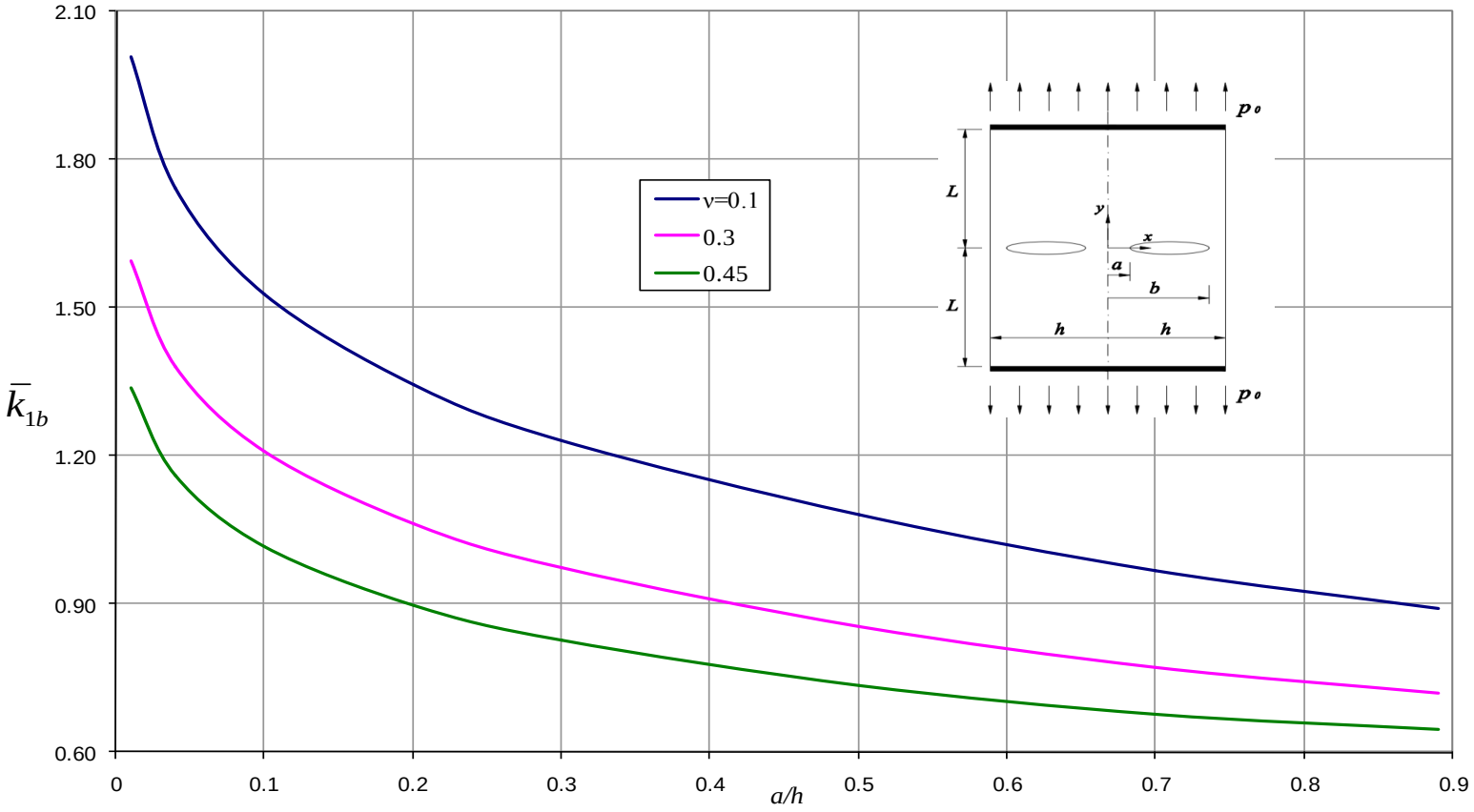


Figure 6.28 Normalized Mode I stress intensity factor $\bar{k}_{1b}$ at outer edge of crack in finite strip when $b/h$ = 0.9 and $L/h$ = 1 (Plane strain).

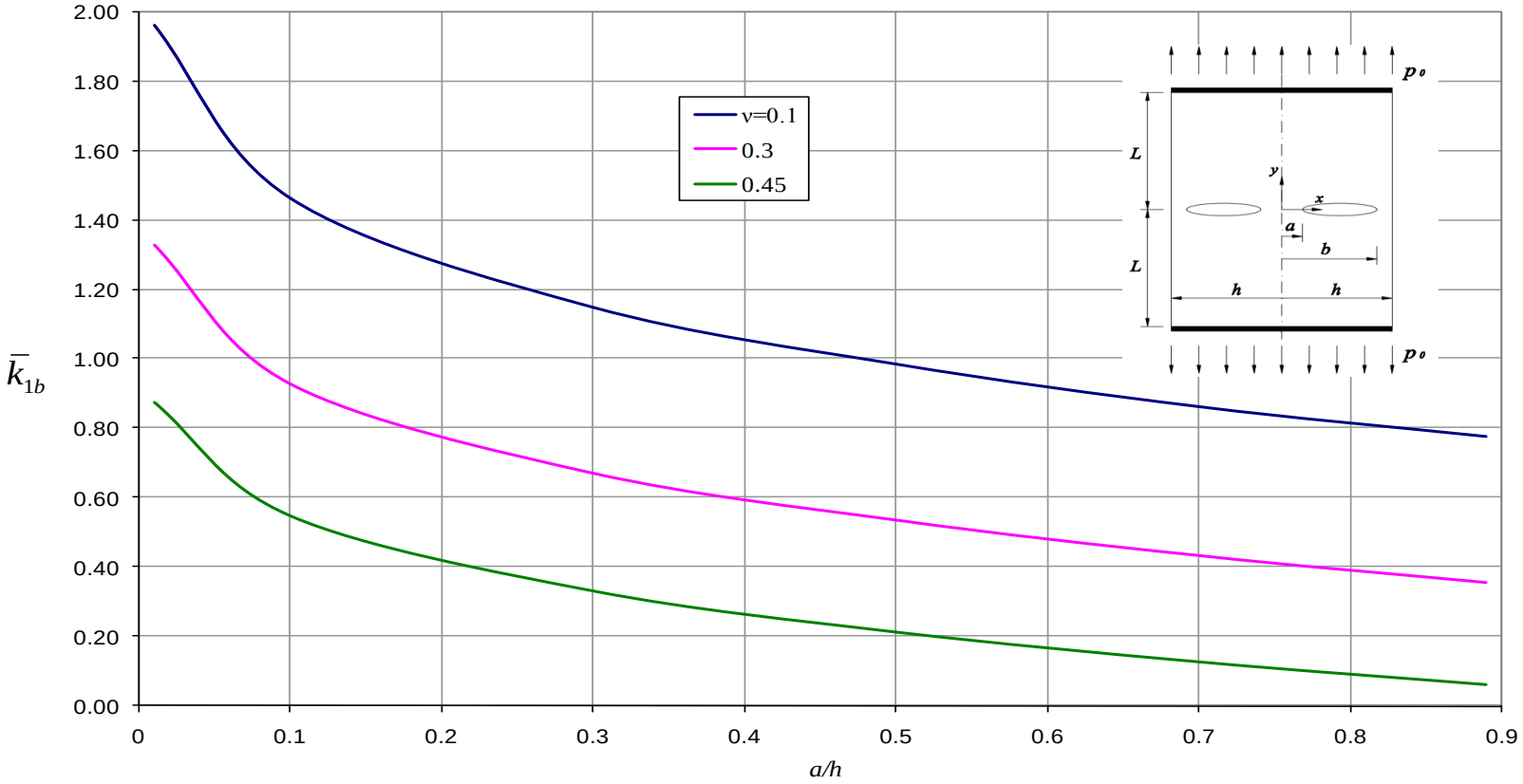


Figure 6.29 Normalized Mode I stress intensity factor $\bar{k}_{1b}$ at outer edge of crack in finite strip when $b/h$ = 0.9 and $L/h$ = 0.5 (Plane strain).

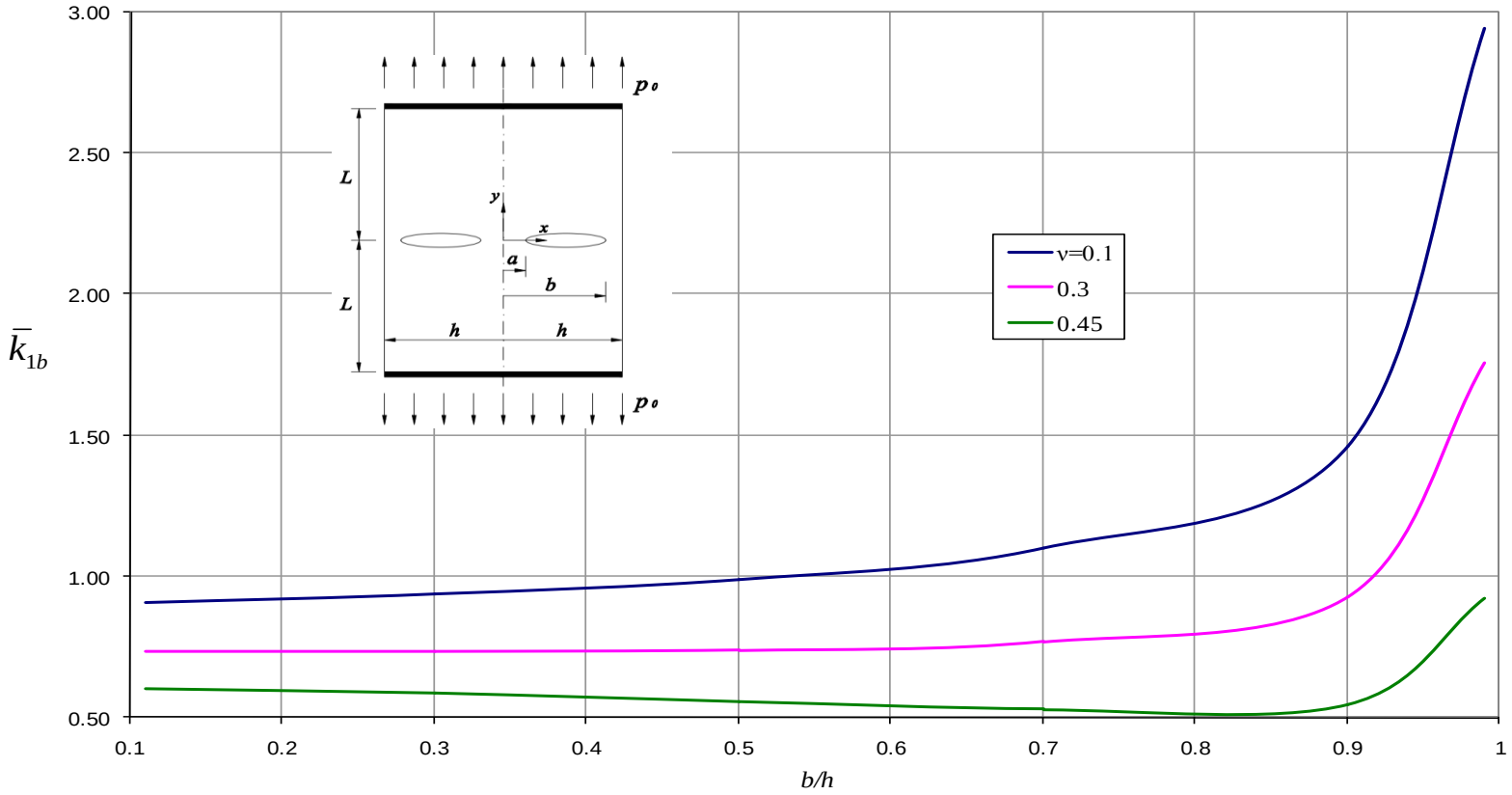


Figure 6.30 Normalized Mode I stress intensity factor $\bar{k}_{1b}$ at outer edge of crack in finite strip when $a/h$ = 0.1 and $L/h$ = 0.5 (Plane strain).

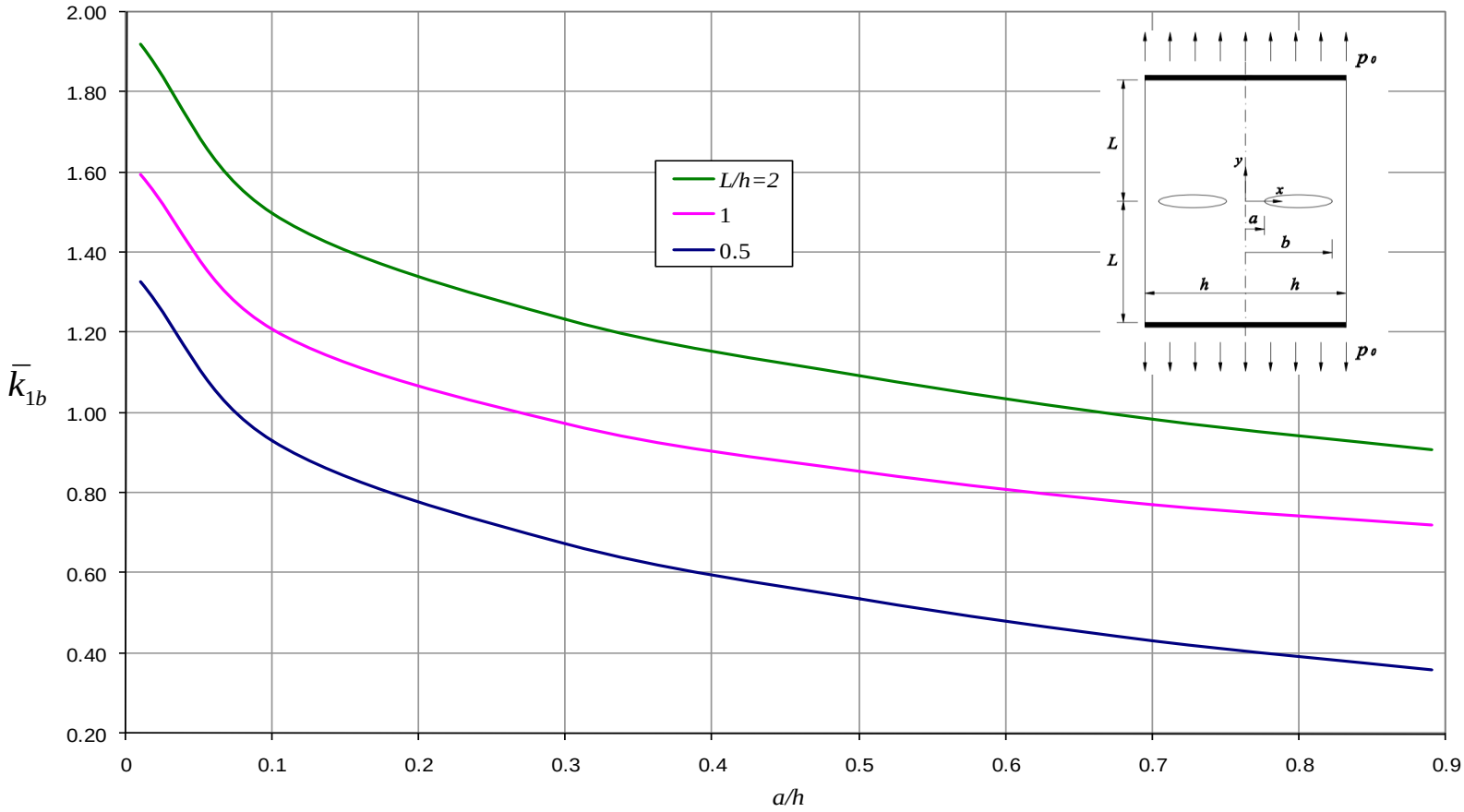


Figure 6.31 Normalized Mode I stress intensity factor $\bar{k}_{1b}$ at outer edge of crack in finite strip when $b/h$ = 0.9 and $\nu$ = 0.3 (Plane strain).

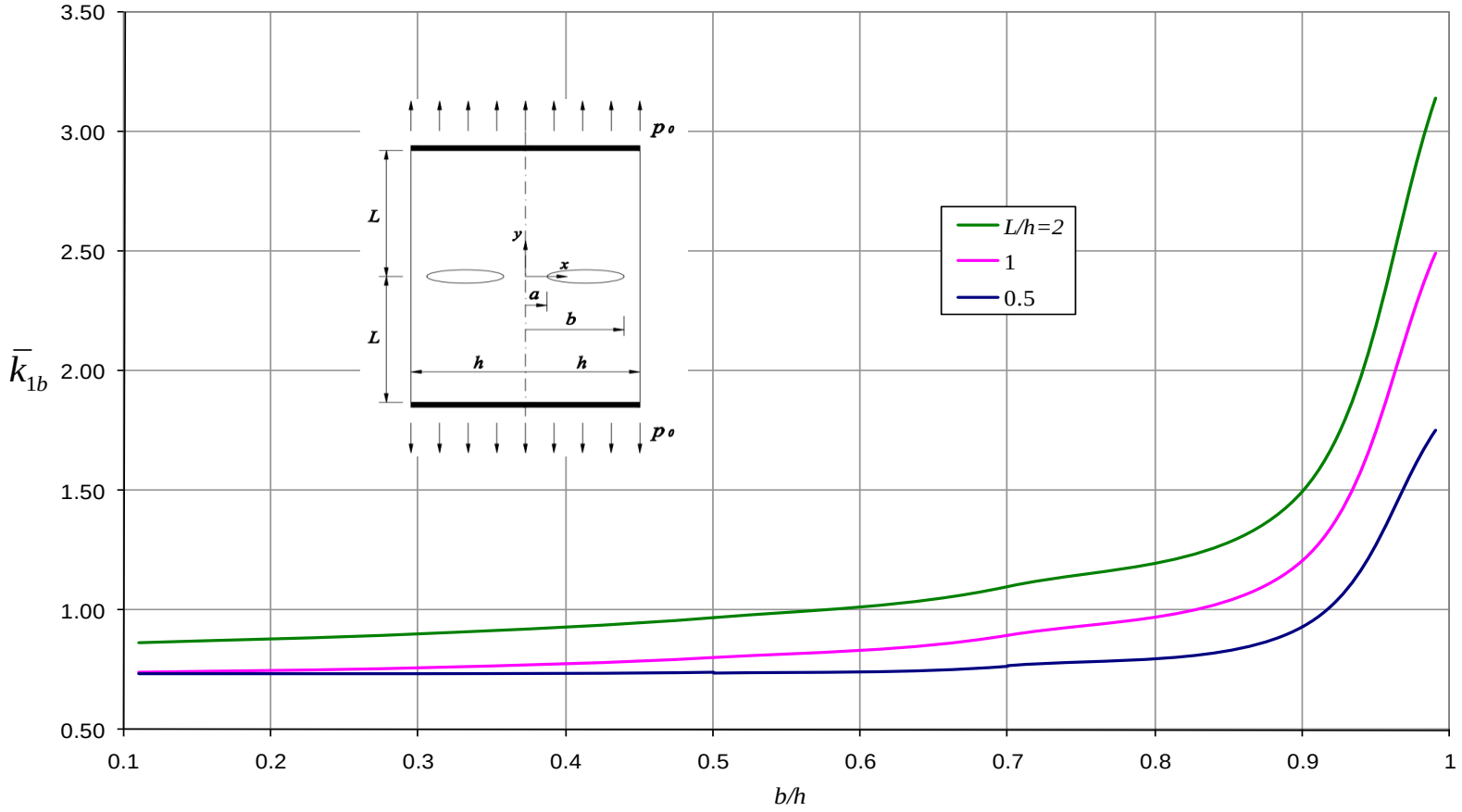


Figure 6.32 Normalized Mode I stress intensity factor $\bar{k}_{1b}$ at outer edge of crack in finite strip when $a/h$ = 0.1 and $\nu$ = 0.3 (Plane strain).

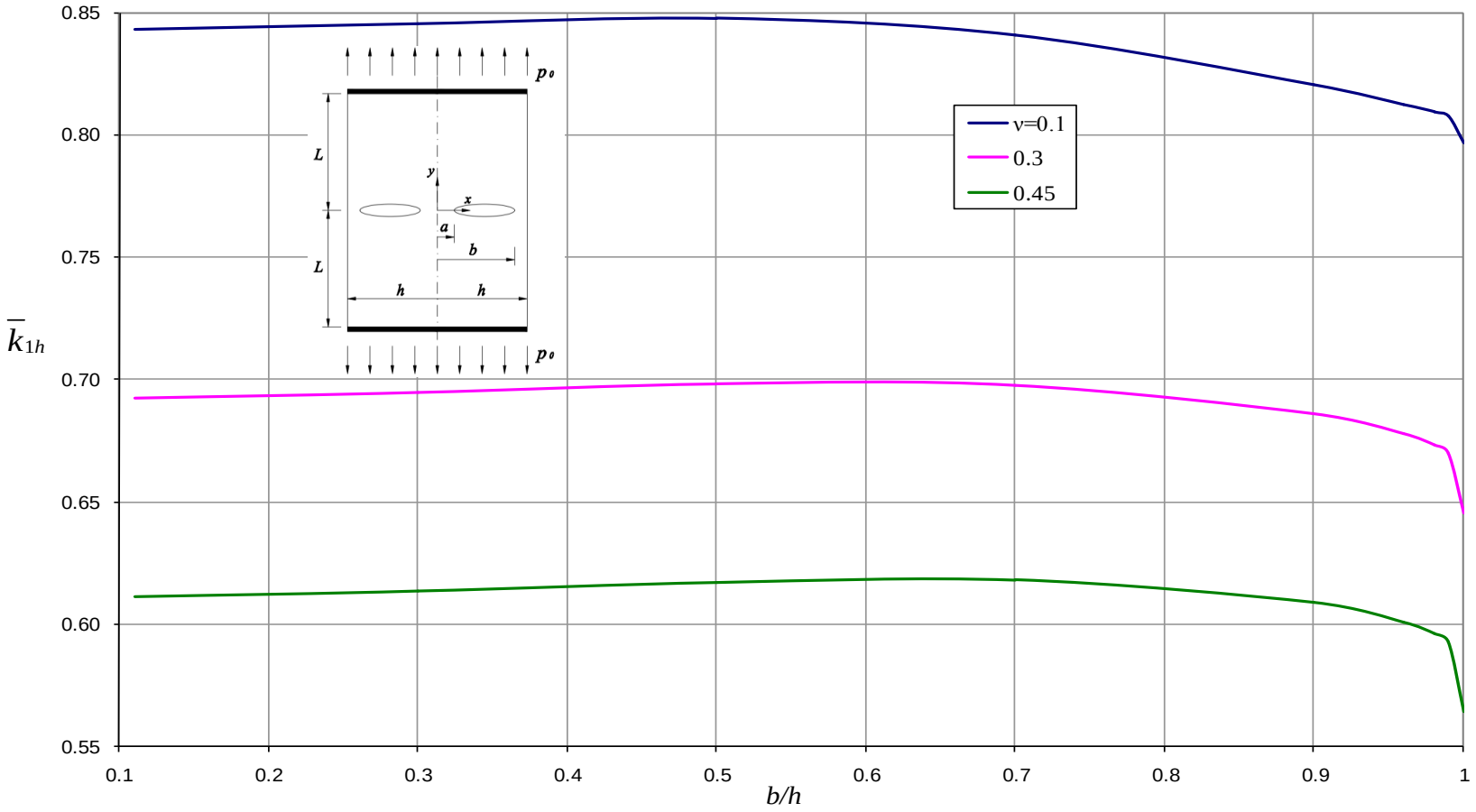


Figure 6.33 Normalized Mode I stress intensity factor $\bar{k}_{1h}$ at corner of finite strip when $a/h$ = 0.1 and $L/h$ = 1 (Plane strain).

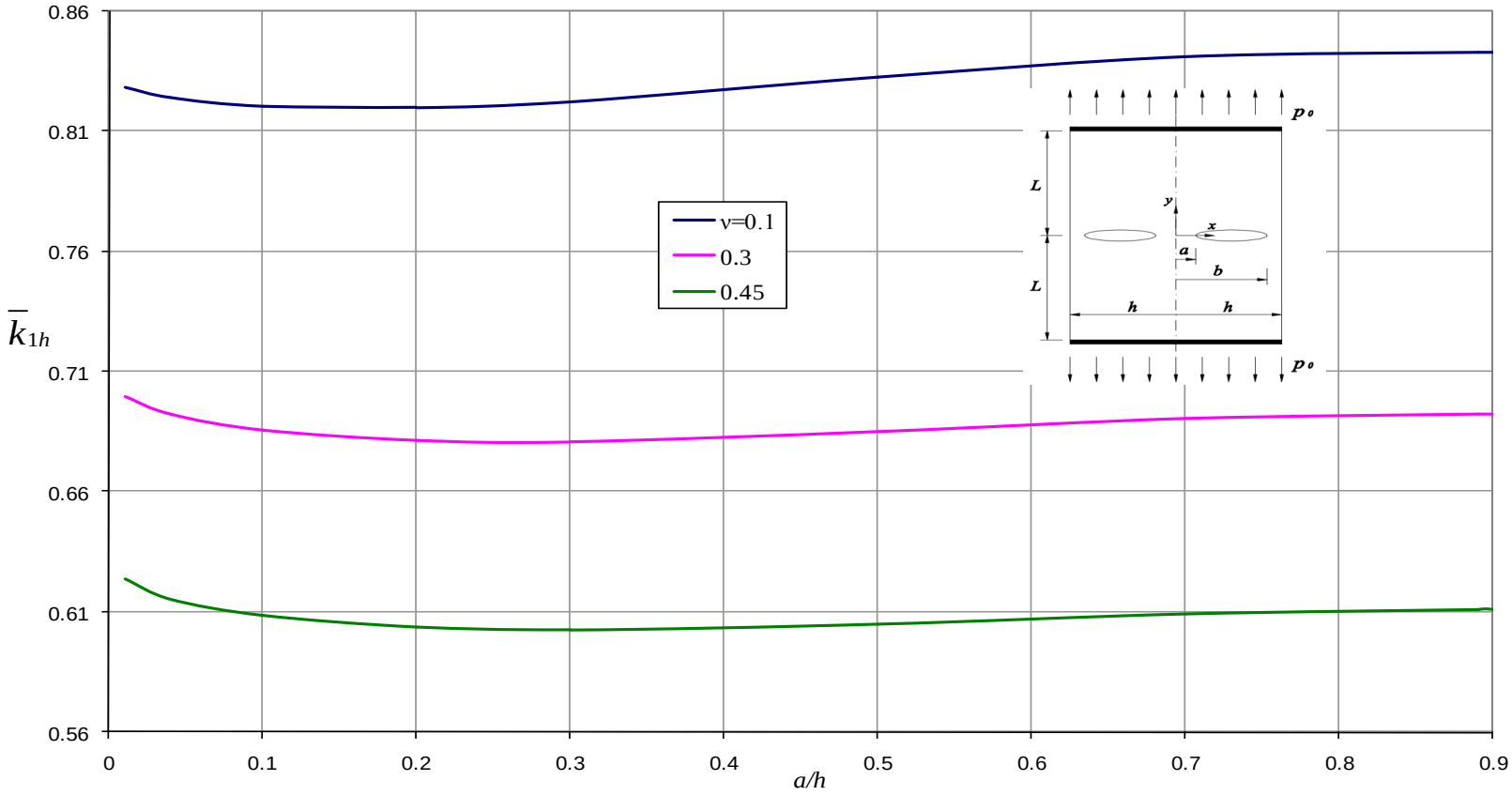


Figure 6.34 Normalized Mode I stress intensity factor $\overline{k}_{1h}$ at corner of finite strip when $b/h$ = 0.9 and $L/h$ = 1 (Plane strain).

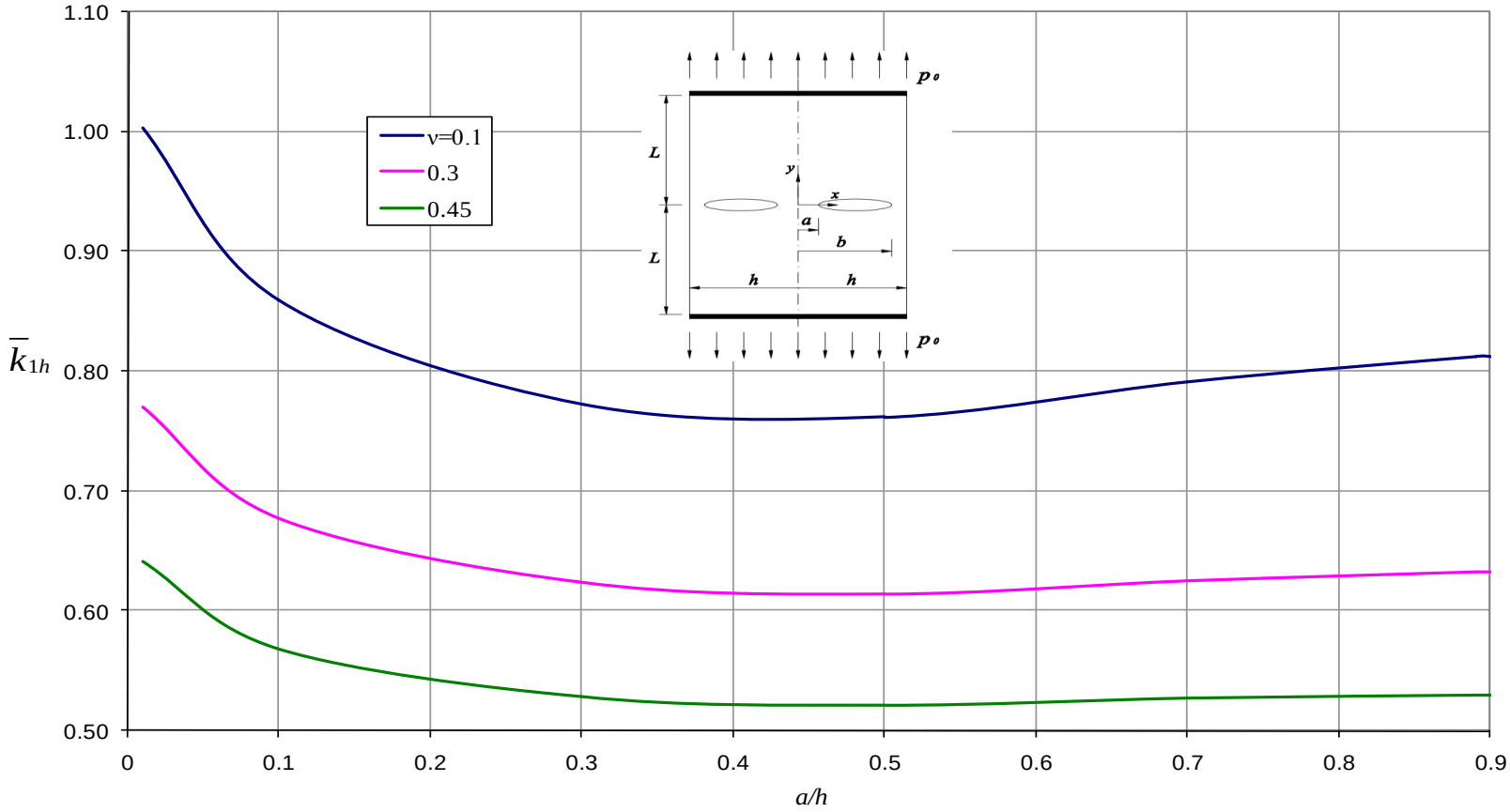


Figure 6.35 Normalized Mode I stress intensity factor $\overline{k}_{1h}$ at corner of finite strip when $b/h$ = 0.9 and $L/h$ = 0.5 (Plane strain).

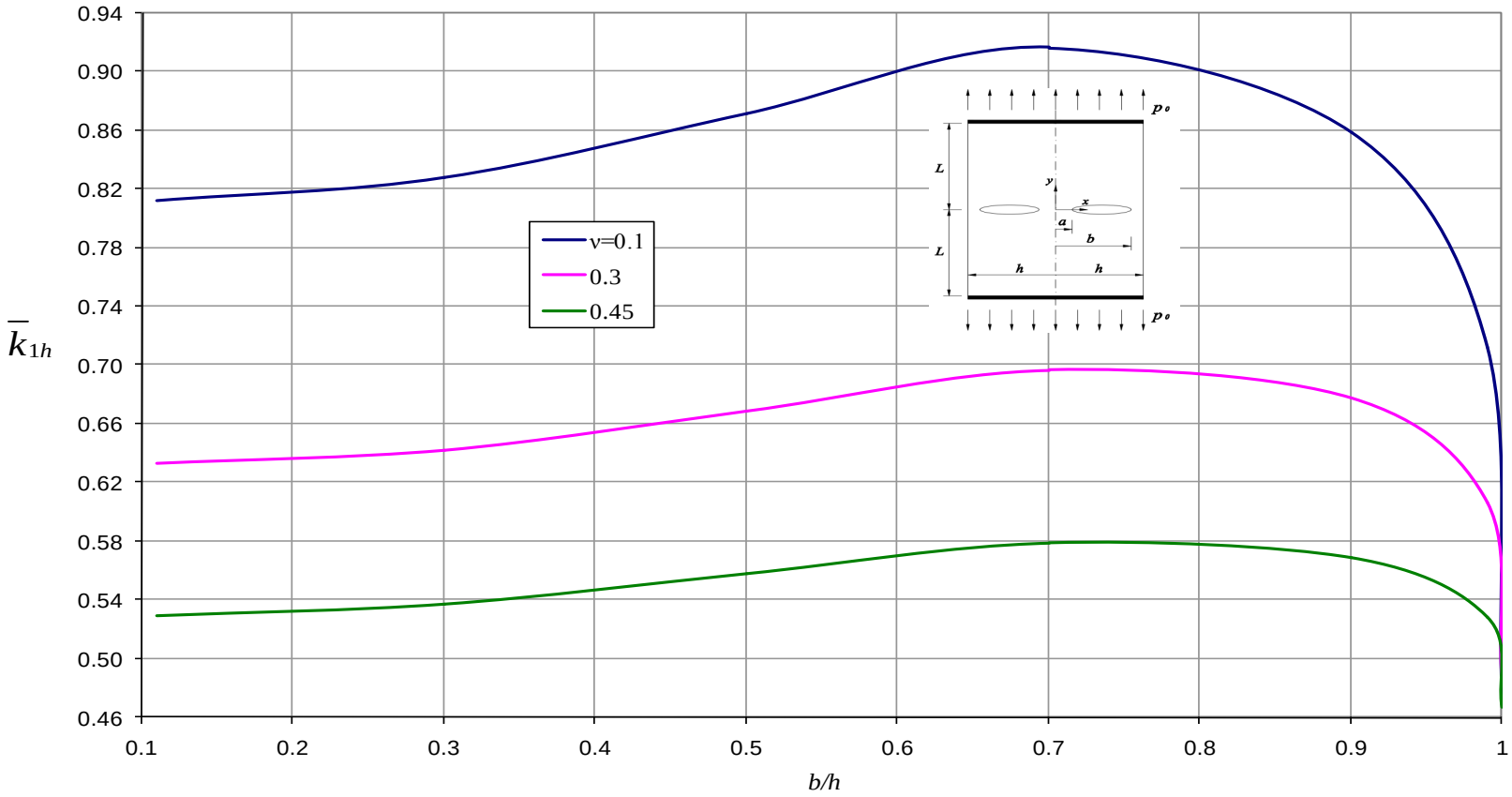


Figure 6.36 Normalized Mode I stress intensity factor $\overline{k}_{1h}$ at corner of finite strip when $a/h$ = 0.1 and $L/h$ = 0.5 (Plane strain).

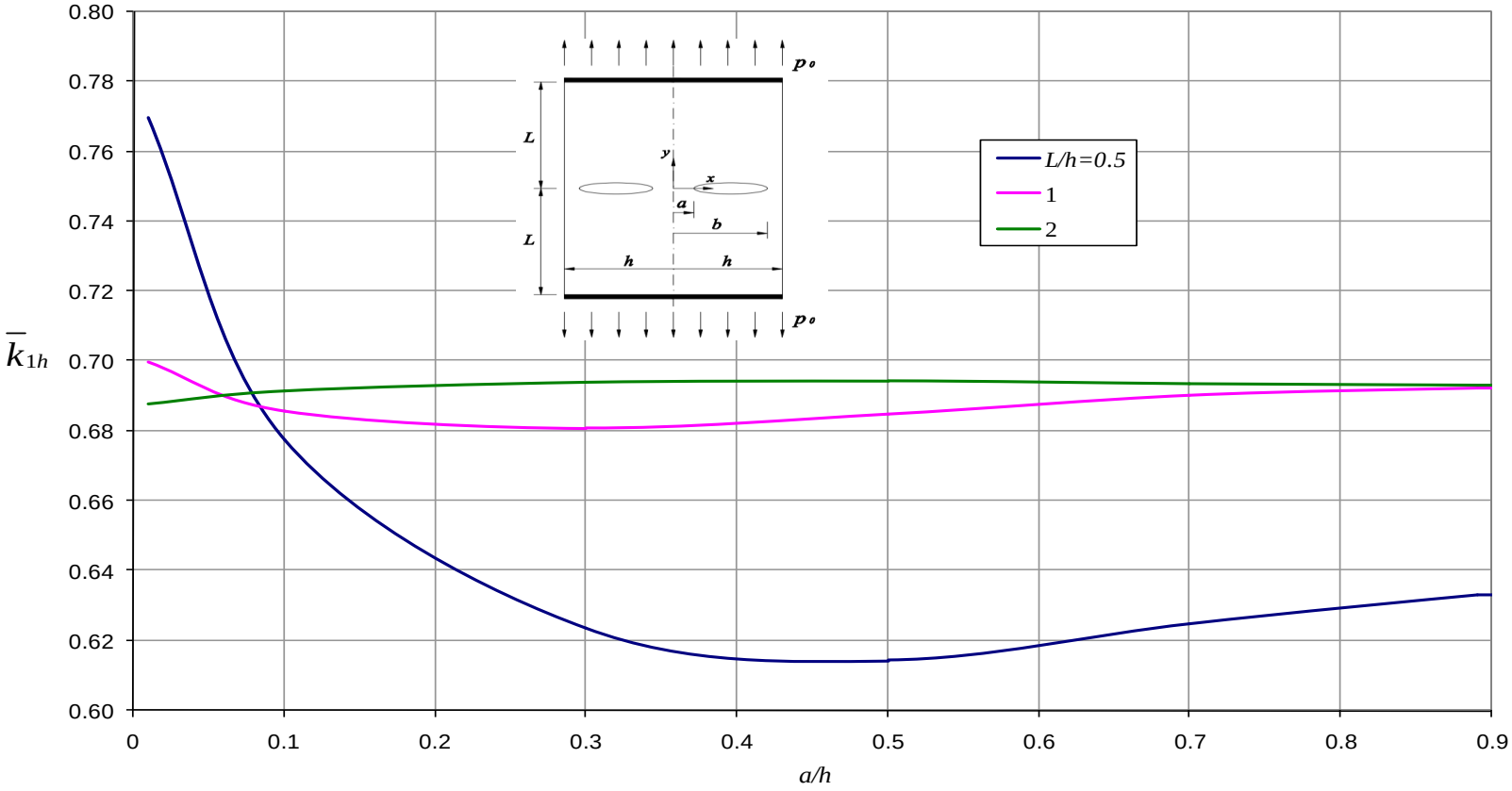


Figure 6.37 Normalized Mode I stress intensity factor $\bar{k}_{1h}$ at corner of finite strip when $b/h$ = 0.9 and $v$= 0.3 (Plane strain).

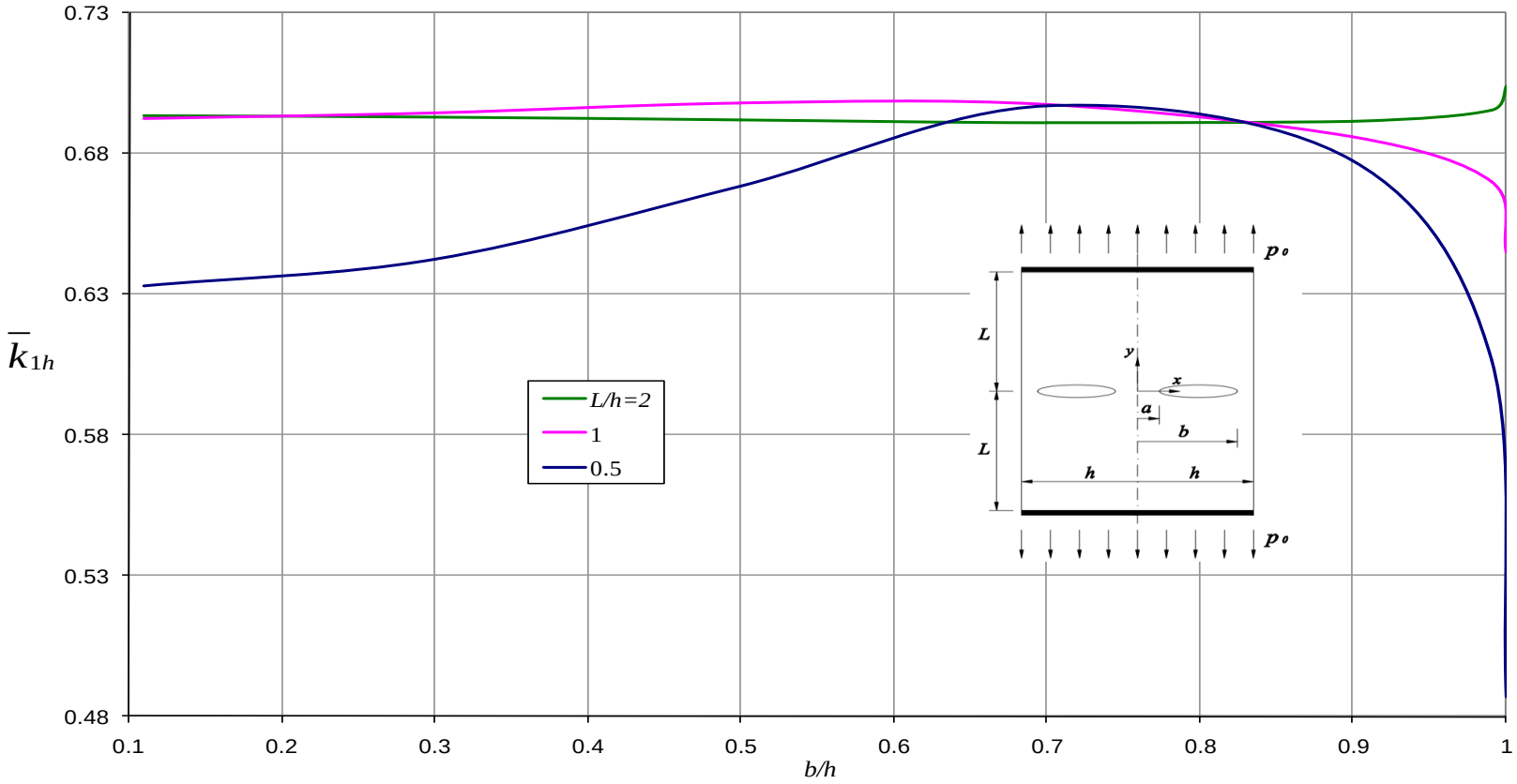


Figure 6.38 Normalized Mode I stress intensity factor $\overline{k}_{1h}$ at corner of finite strip when $a/h$ = 0.1 and $v$= 0.3 (Plane strain).

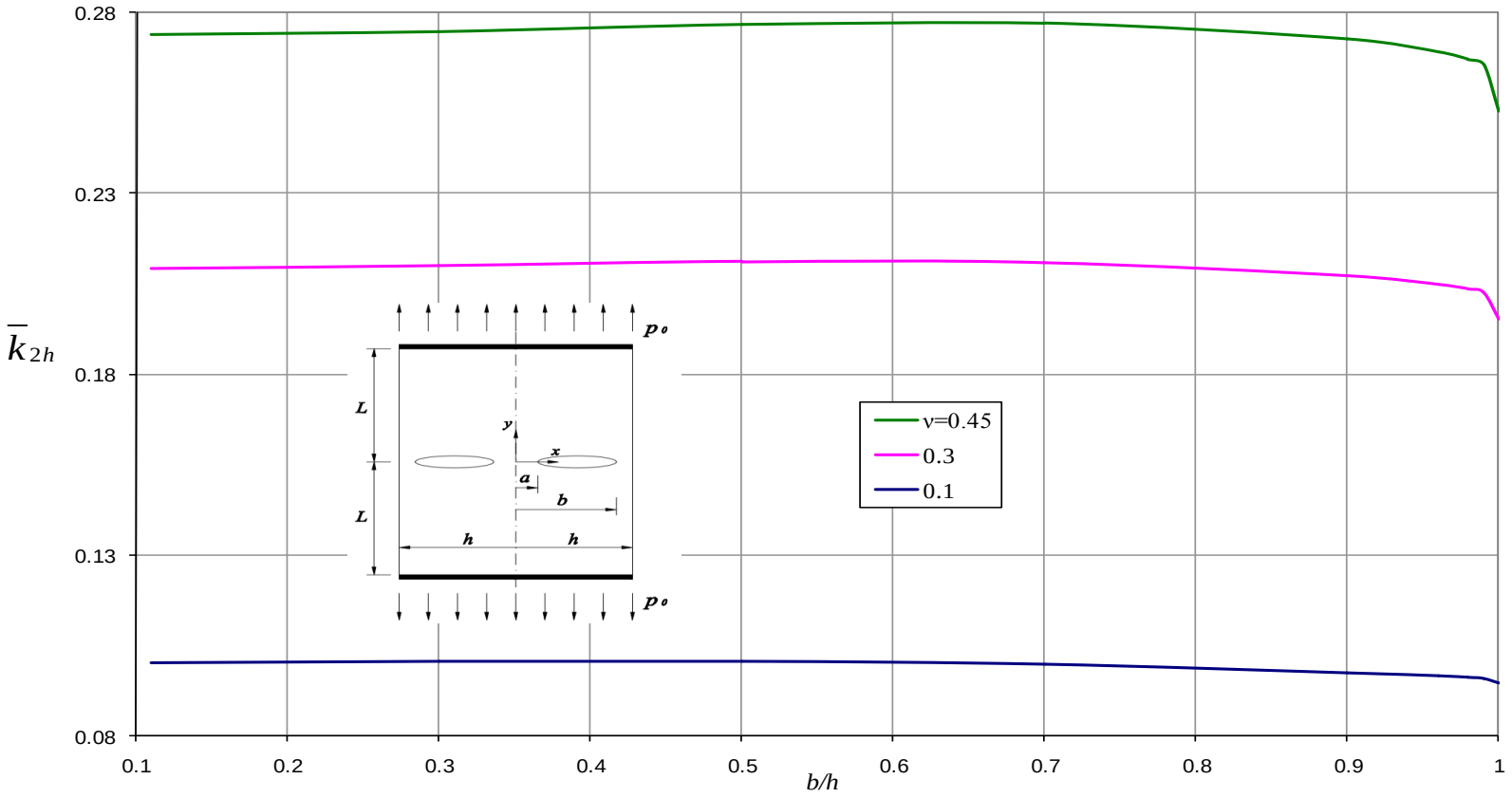


Figure 6.39 Normalized Mode II stress intensity factor $\bar{k}_{2h}$ at corner of finite strip when $a/h = 0.1$ and $L/h = 1$ (Plane strain).

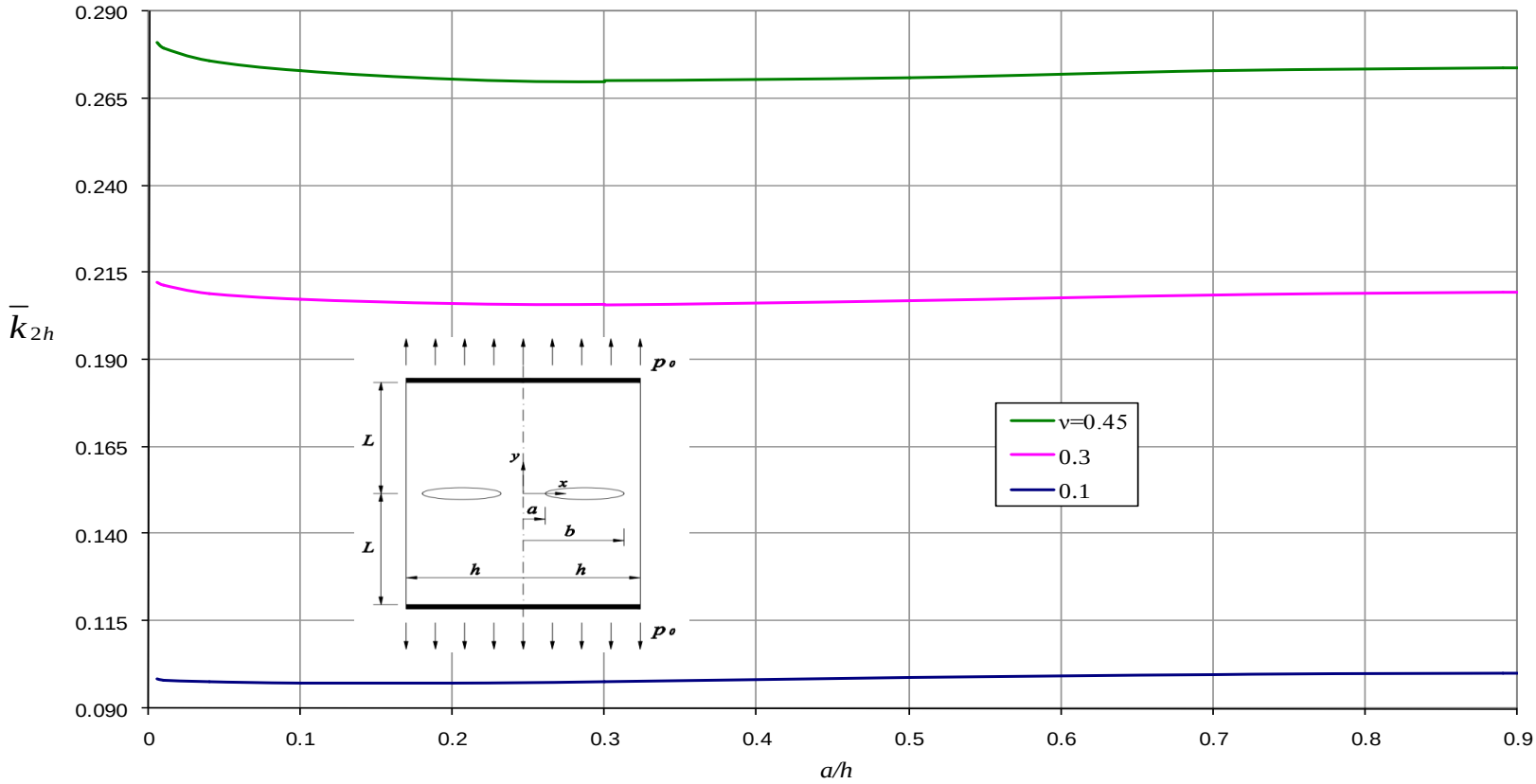


Figure 6.40 Normalized Mode II stress intensity factor $\overline{k}_{2h}$ at corner of finite strip when $b/h = 0.9$ and $L/h = 1$ (Plane strain).

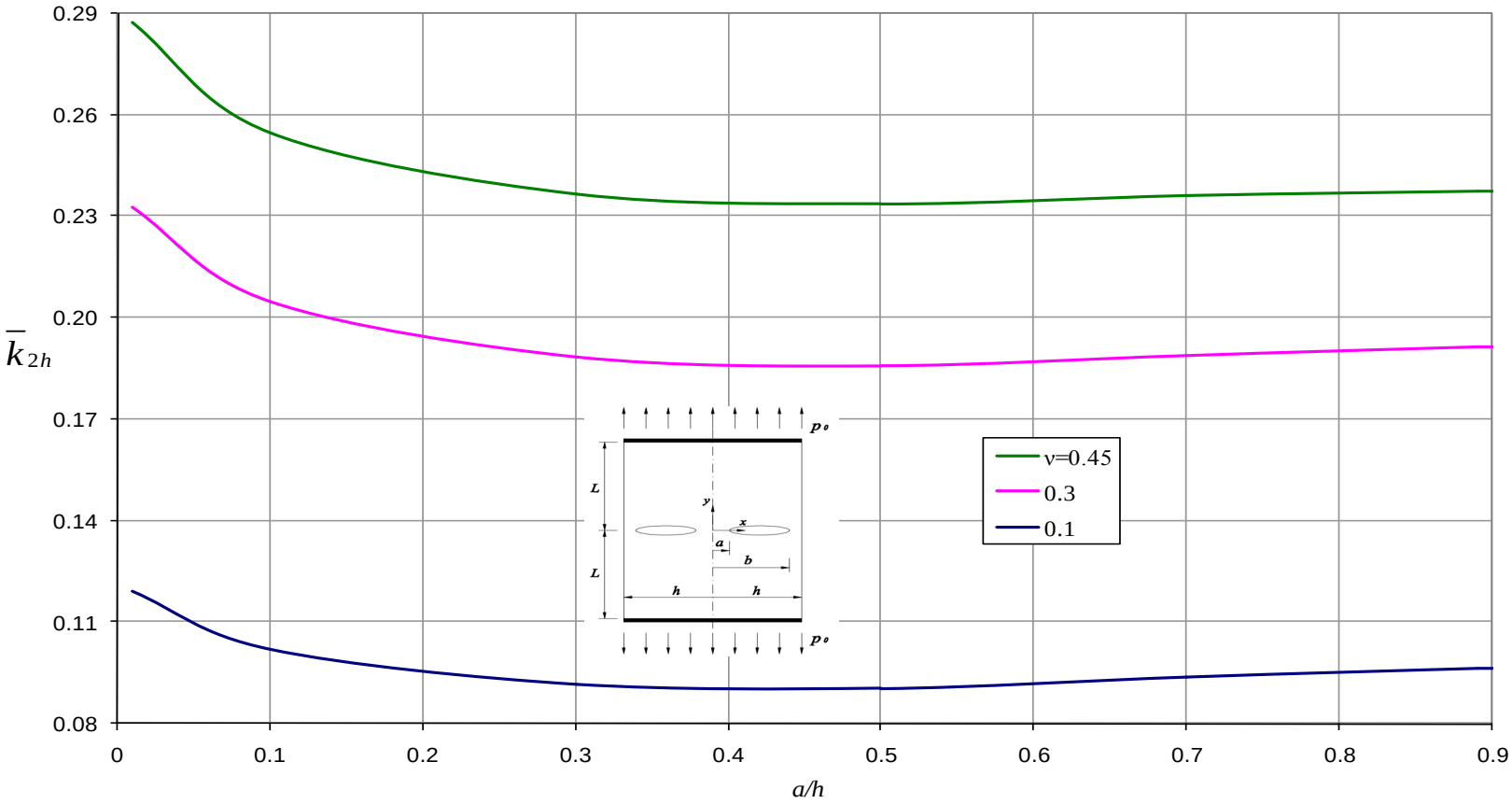


Figure 6.41 Normalized Mode II stress intensity factor $\bar{k}_{2h}$ at corner of finite strip when $b/h$ = 0.9 and $L/h$ = 0.5 (Plane strain).

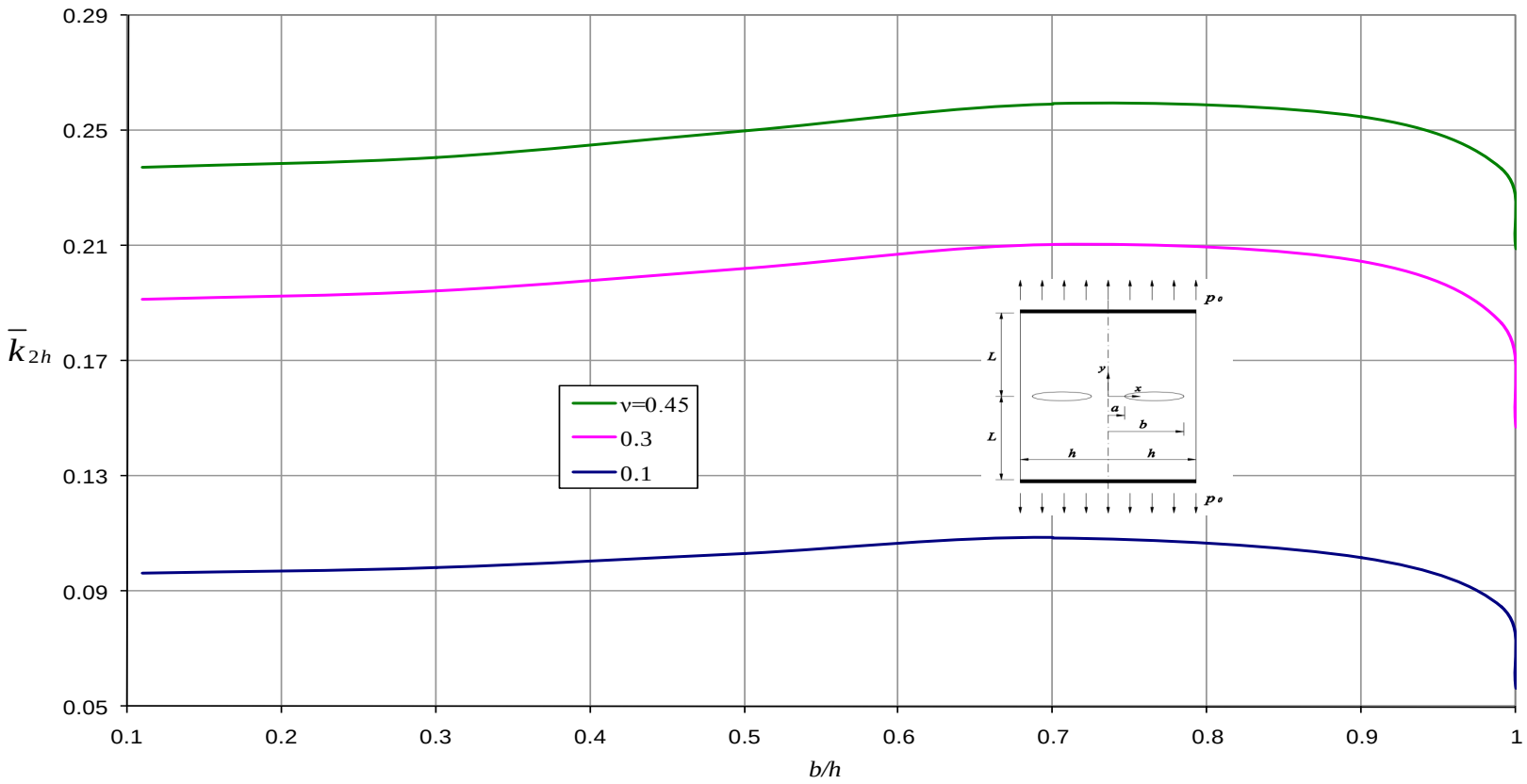


Figure 6.42 Normalized Mode II stress intensity factor $\bar{k}_{2h}$ at corner of finite strip when $a/h$ = 0.1 and $L/h$ = 0.5 (Plane strain).

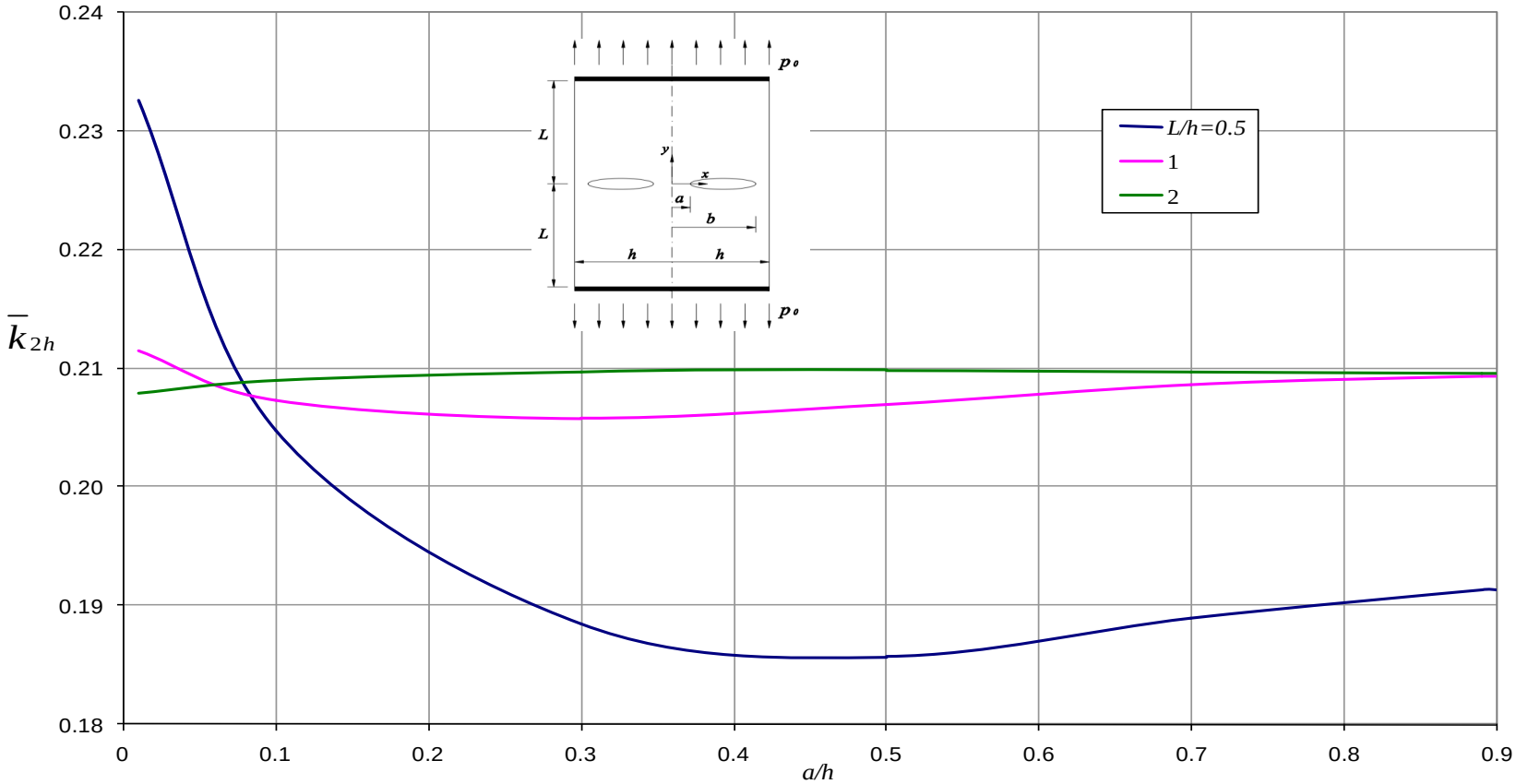


Figure 6.43 Normalized Mode II stress intensity factor $\bar{k}_{2h}$ at corner of finite strip when $b/h$ = 0.9 and $v$ = 0.3 (Plane strain).

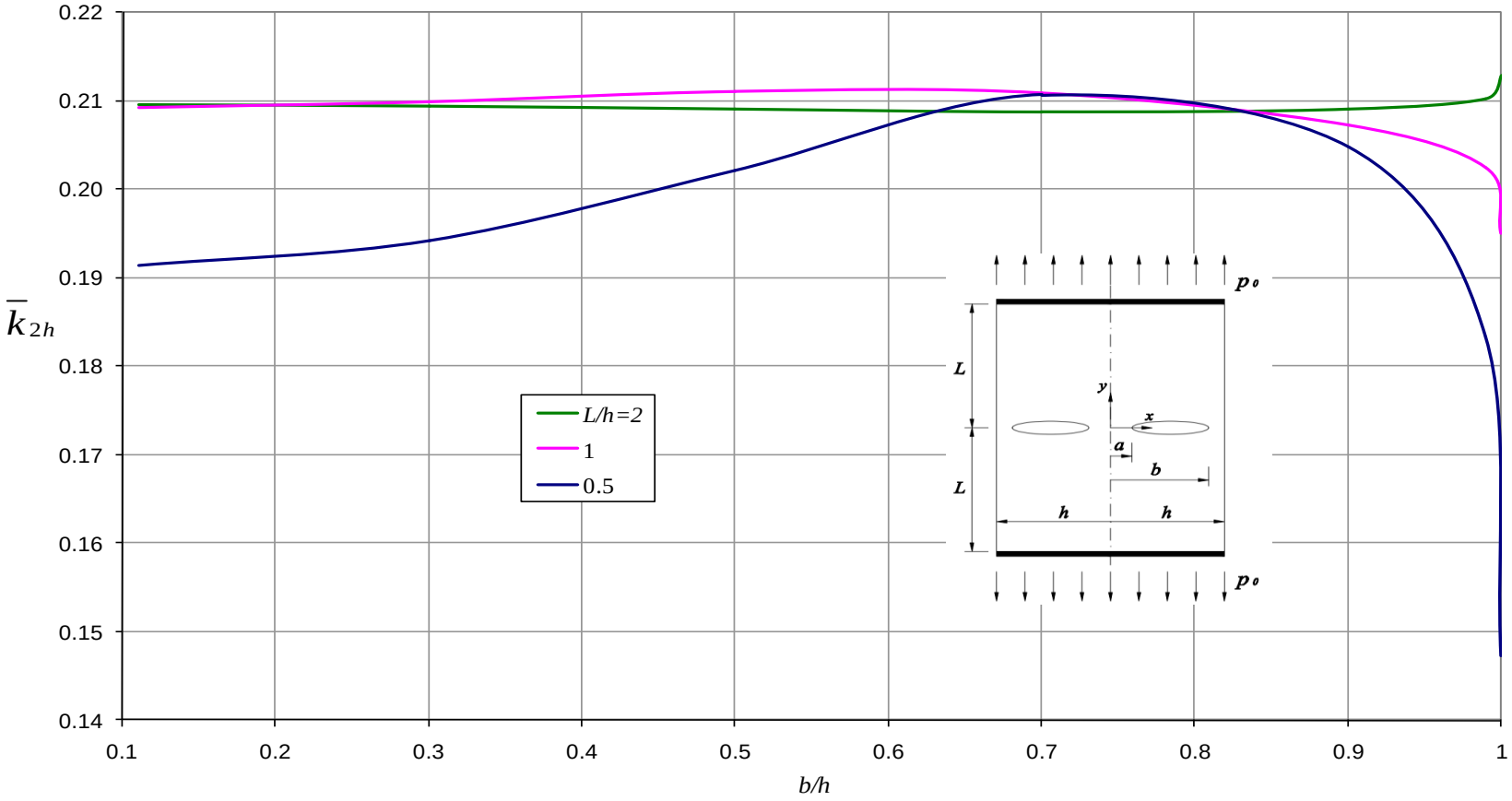


Figure 6.44 Normalized Mode II stress intensity factor $\bar{k}_{2h}$ at corner of finite strip when $a/h$ = 0.1 and $\nu$ = 0.3 (Plane strain).

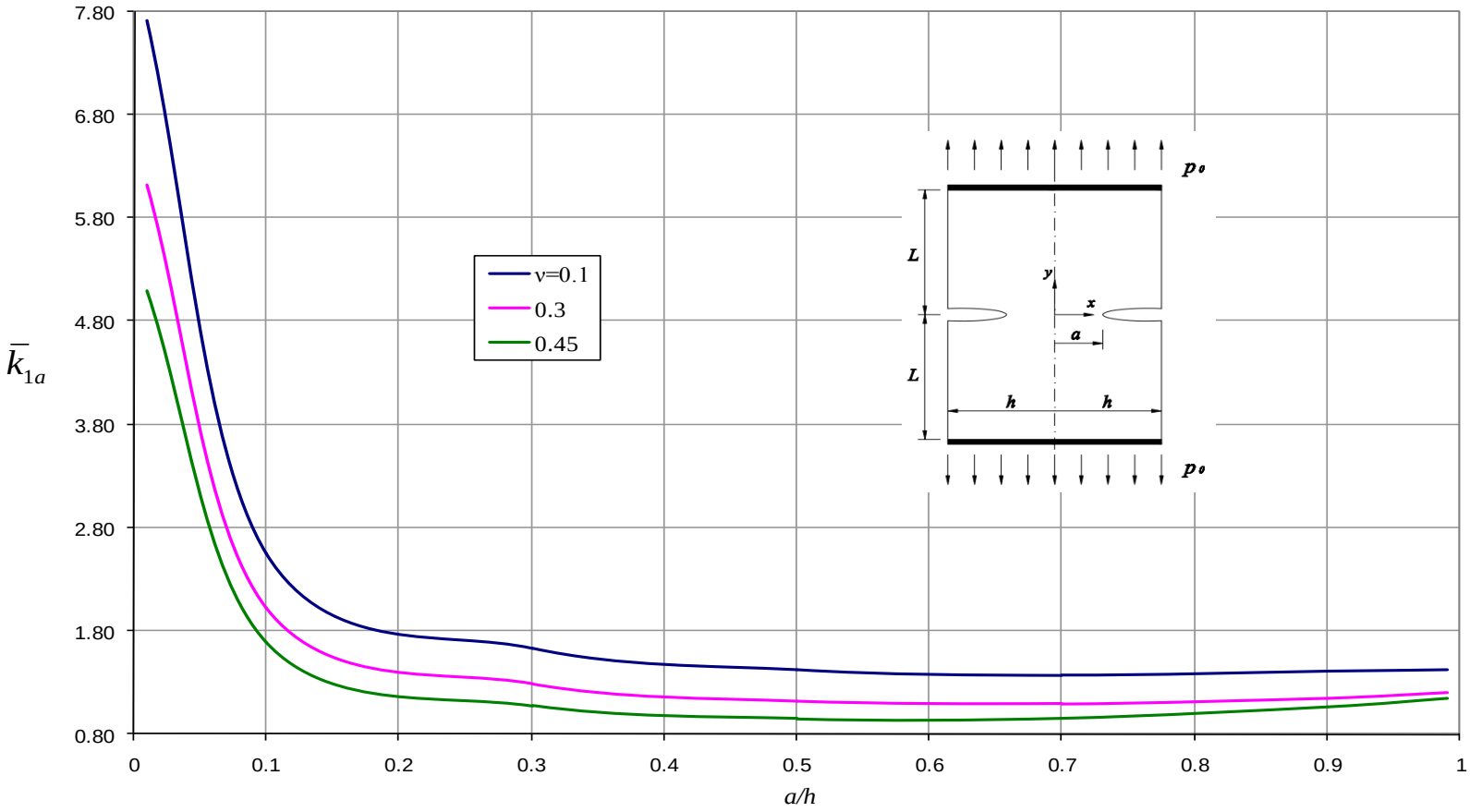


Figure 6.45 Normalized Mode I stress intensity factor $\bar{k}_{1a}$ for edge crack in finite strip when $L/h$ = 1 (Plane strain).

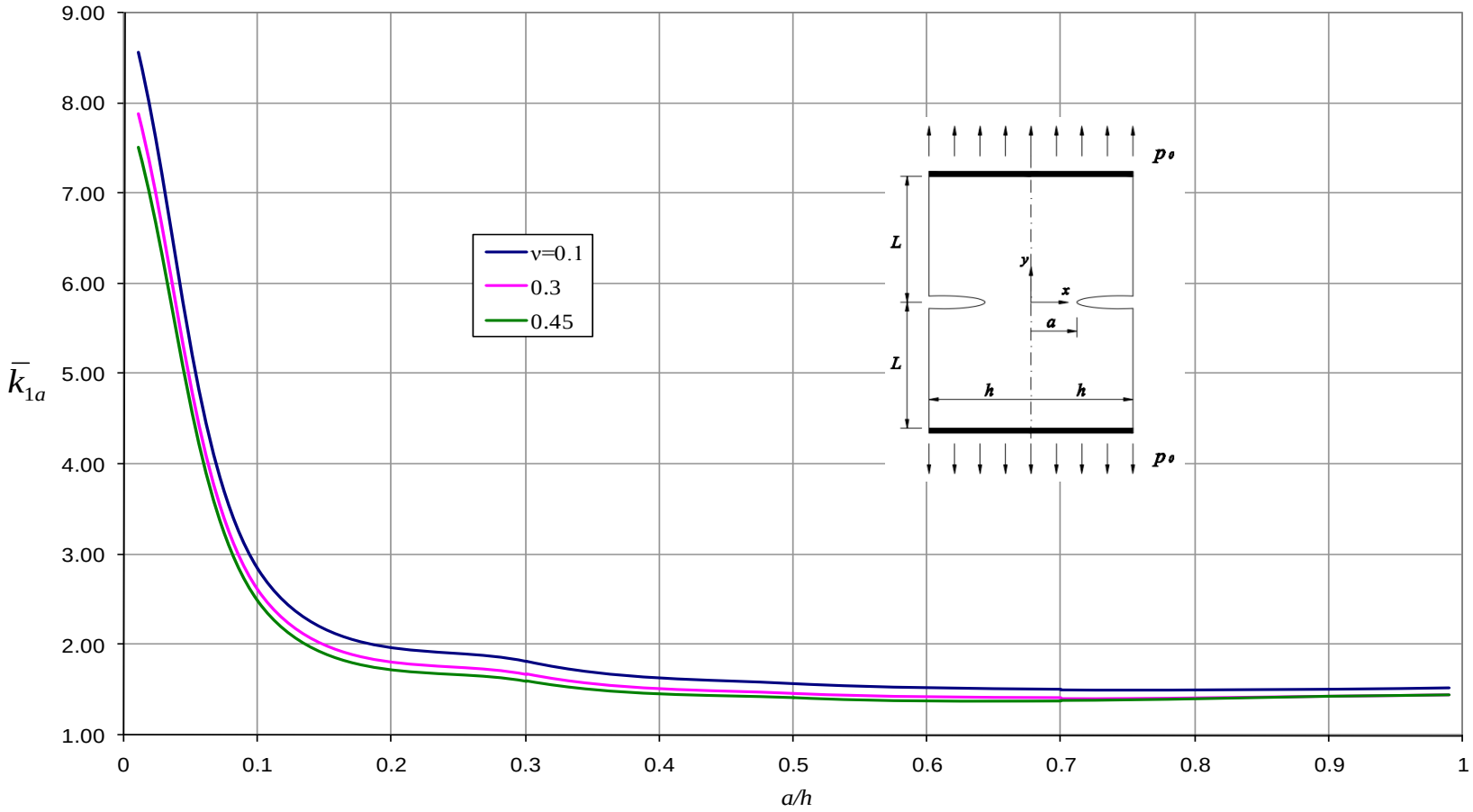


Figure 6.46 Normalized Mode I stress intensity factor $\bar{k}_{1a}$ for edge crack in finite strip when $L/h$ = 2 (Plane strain).

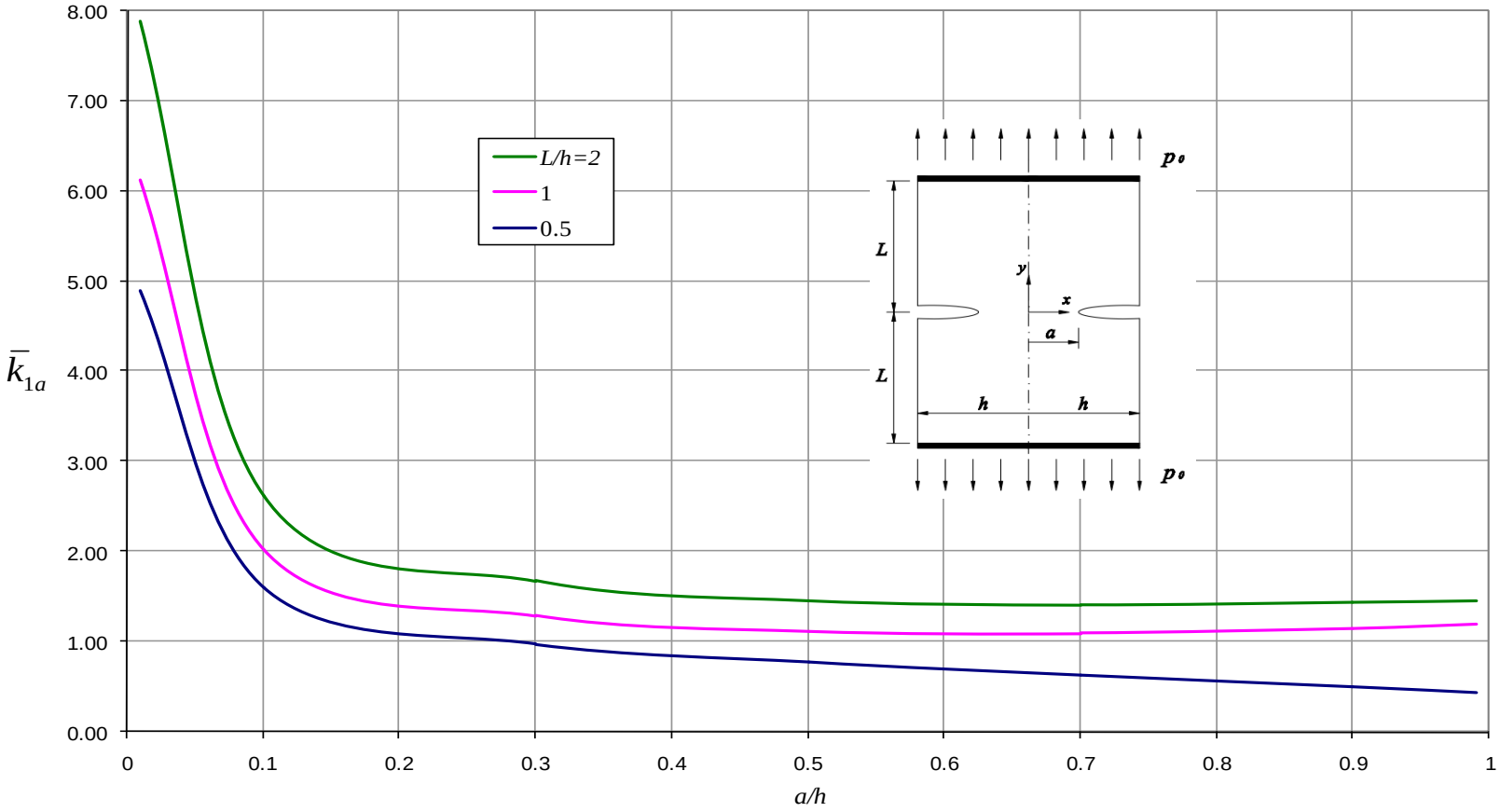


Figure 6.47 Normalized Mode I stress intensity factor $\bar{k}_{1a}$ for edge crack in finite strip when $\nu$ = 0.3 (Plane strain).

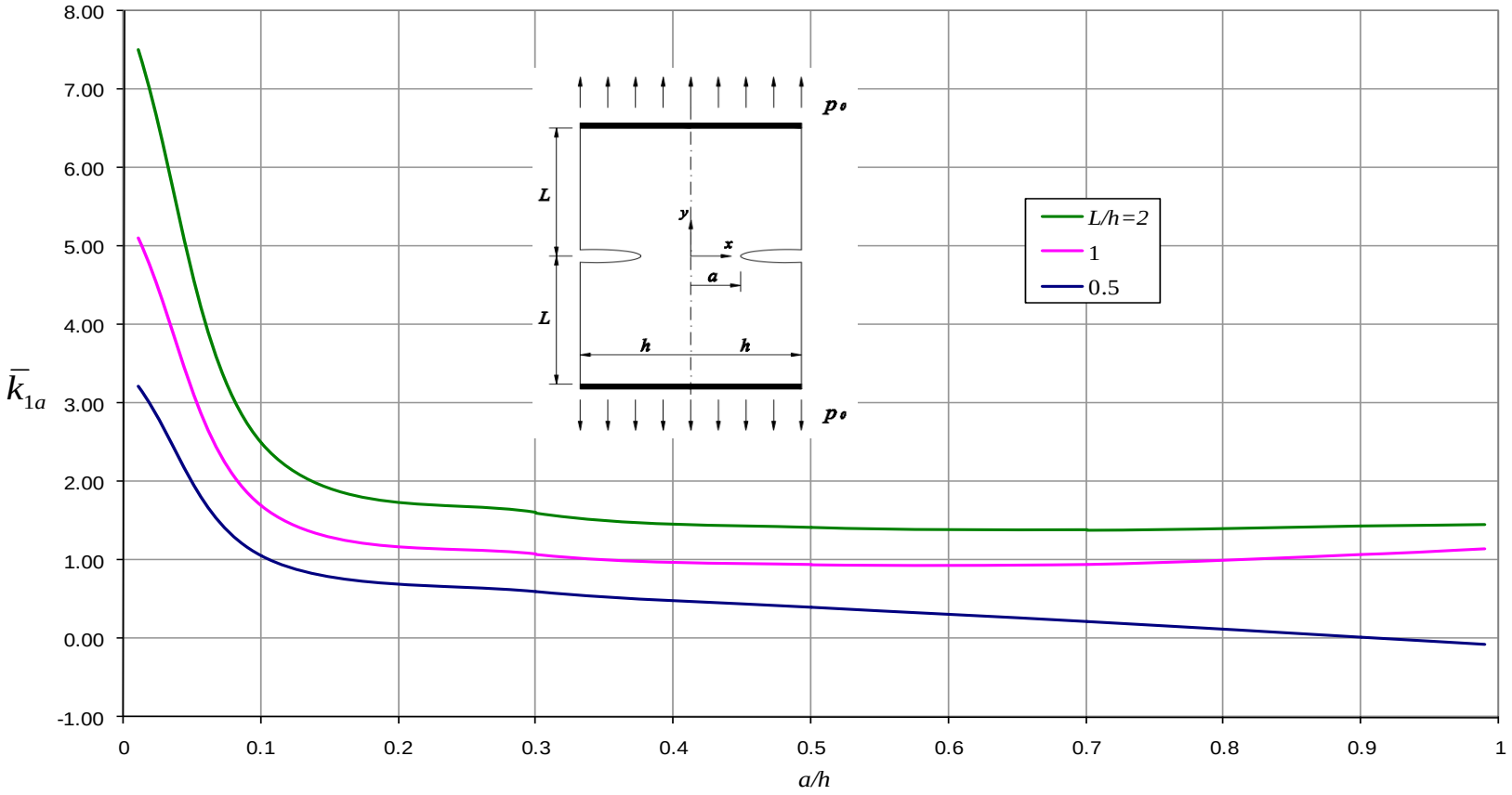


Figure 6.48 Normalized Mode I stress intensity factor $\bar{k}_{1a}$ for edge crack in finite strip when $\nu$ = 0.45 (Plane strain).

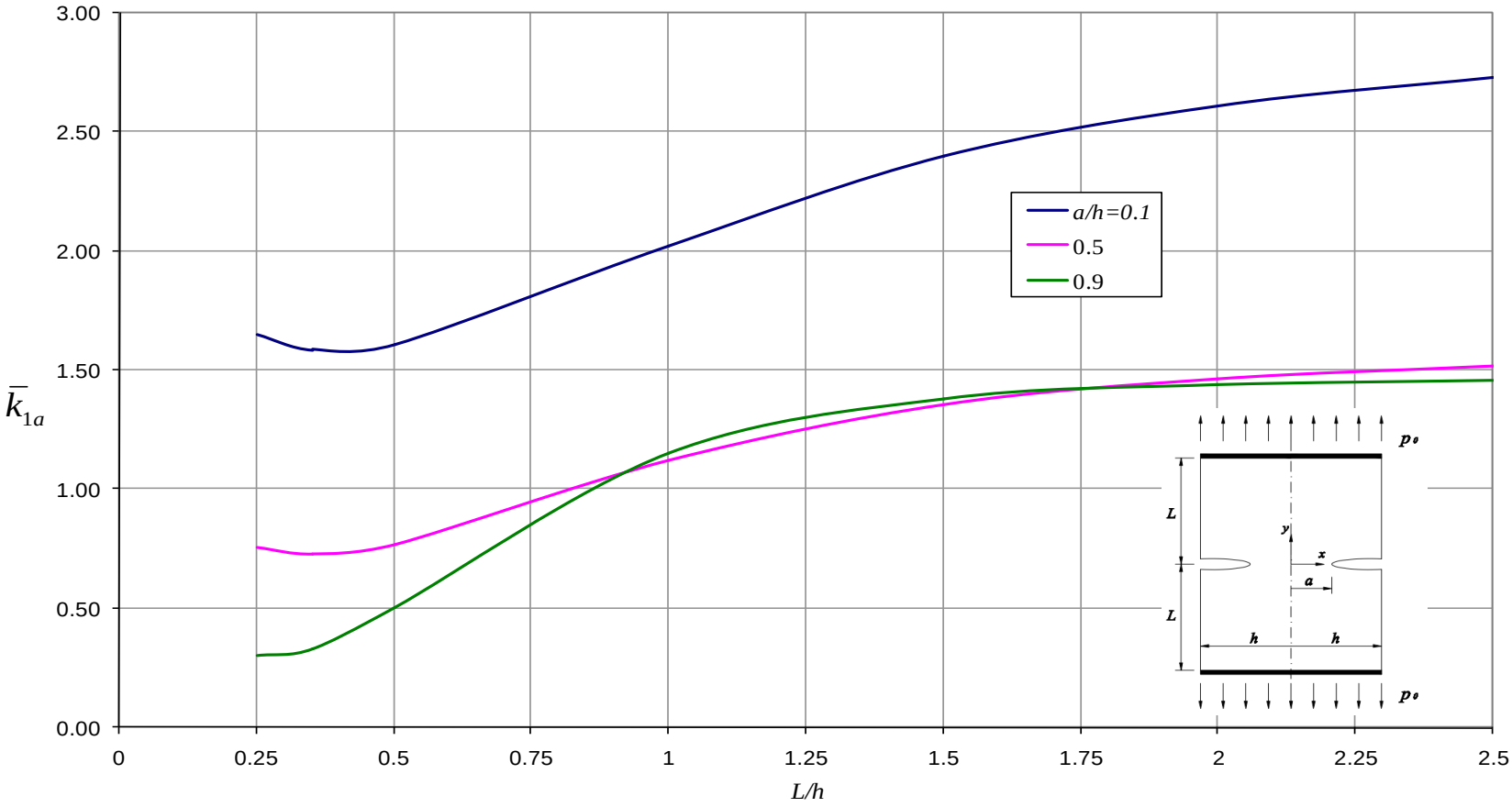


Figure 6.49 Normalized Mode I stress intensity factor $\bar{k}_{1a}$ for edge crack in finite strip when $\nu$ = 0.3 (Plane strain).

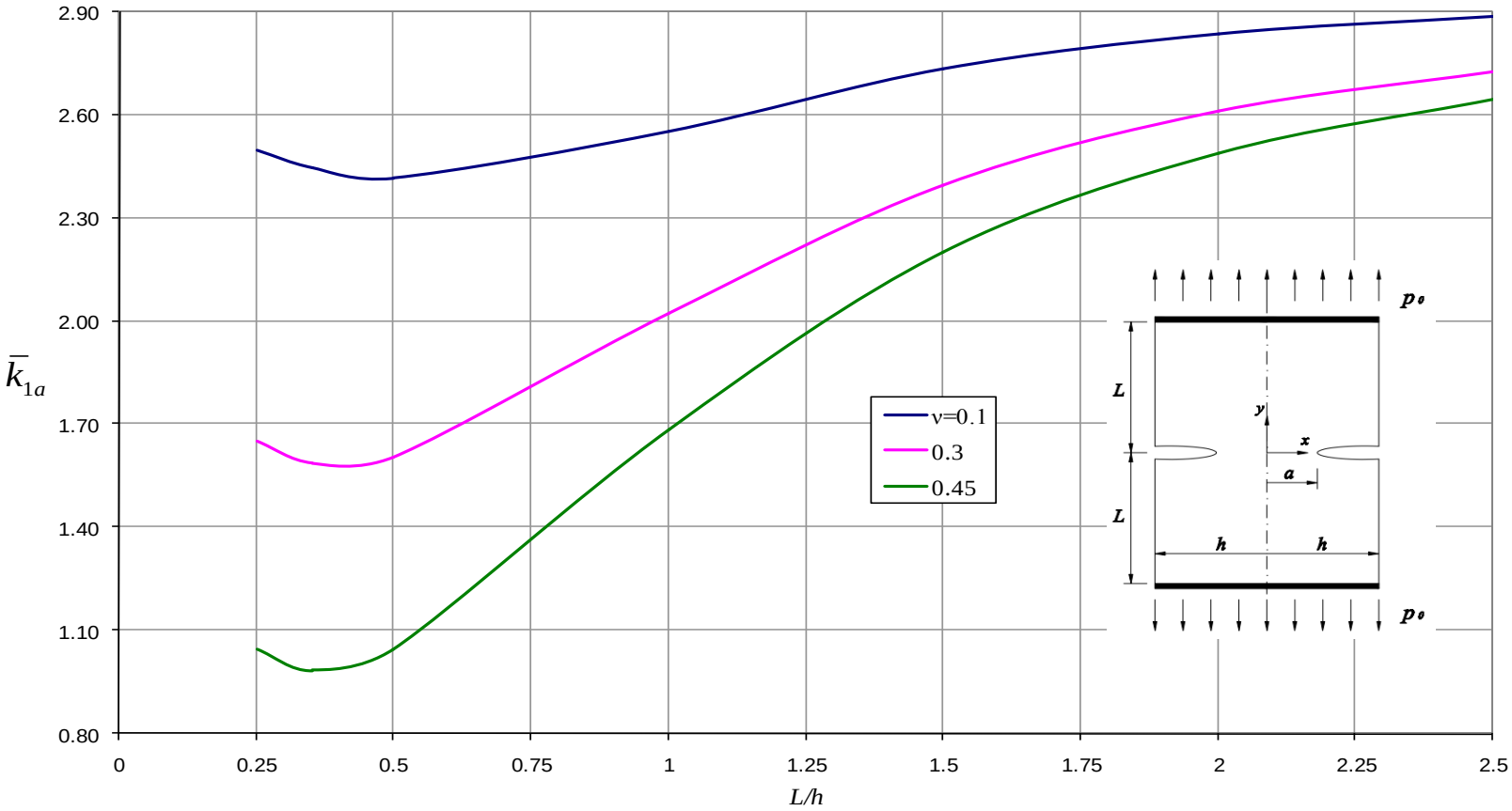


Figure 6.50 Normalized Mode I stress intensity factor $\bar{k}_{1a}$ for edge crack in finite strip when $a/h$ = 0.1 (Plane strain).

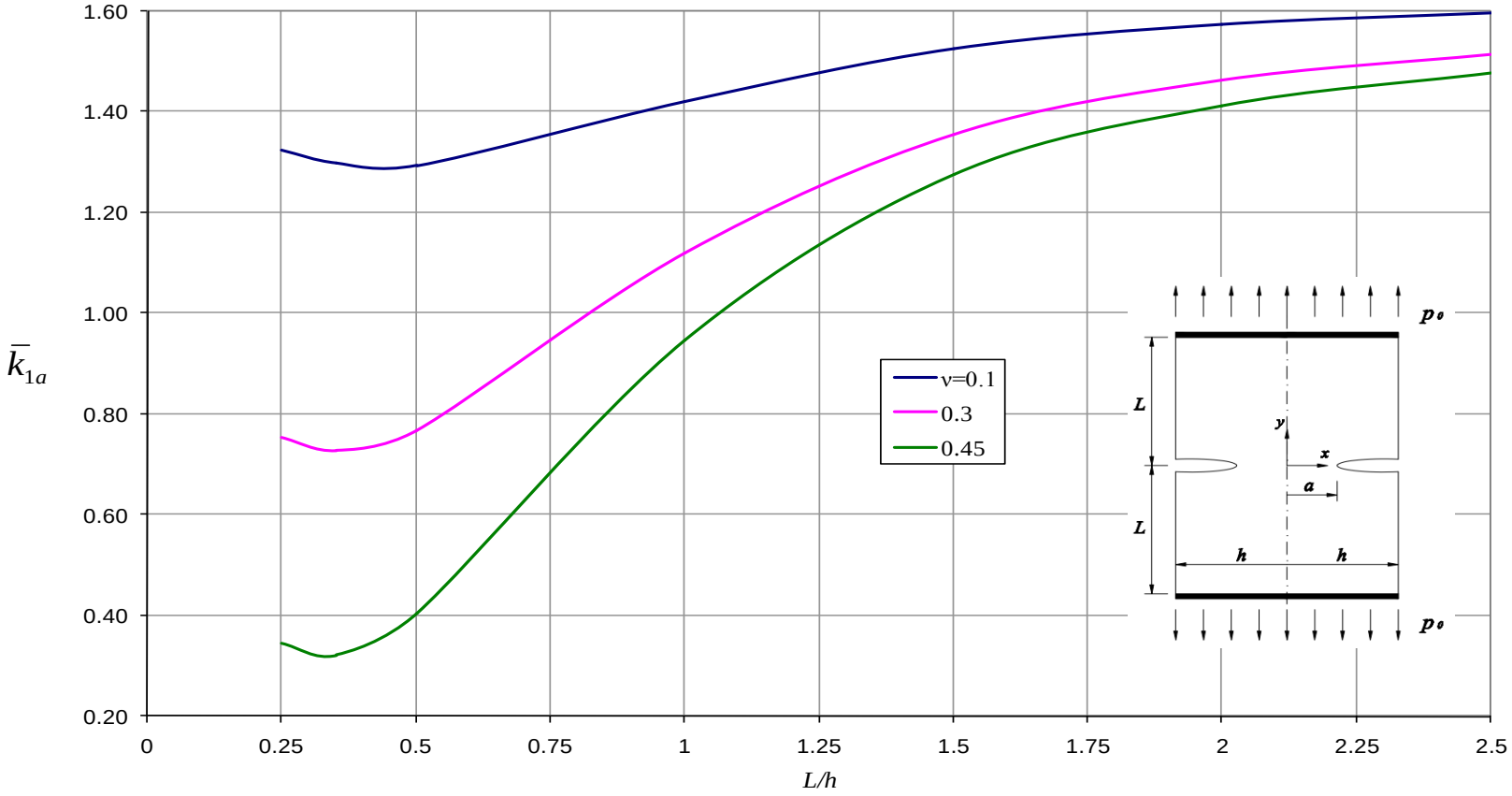


Figure 6.51 Normalized Mode I stress intensity factor $\bar{k}_{1a}$ for edge crack in finite strip when $a/h$ = 0.5 (Plane strain).

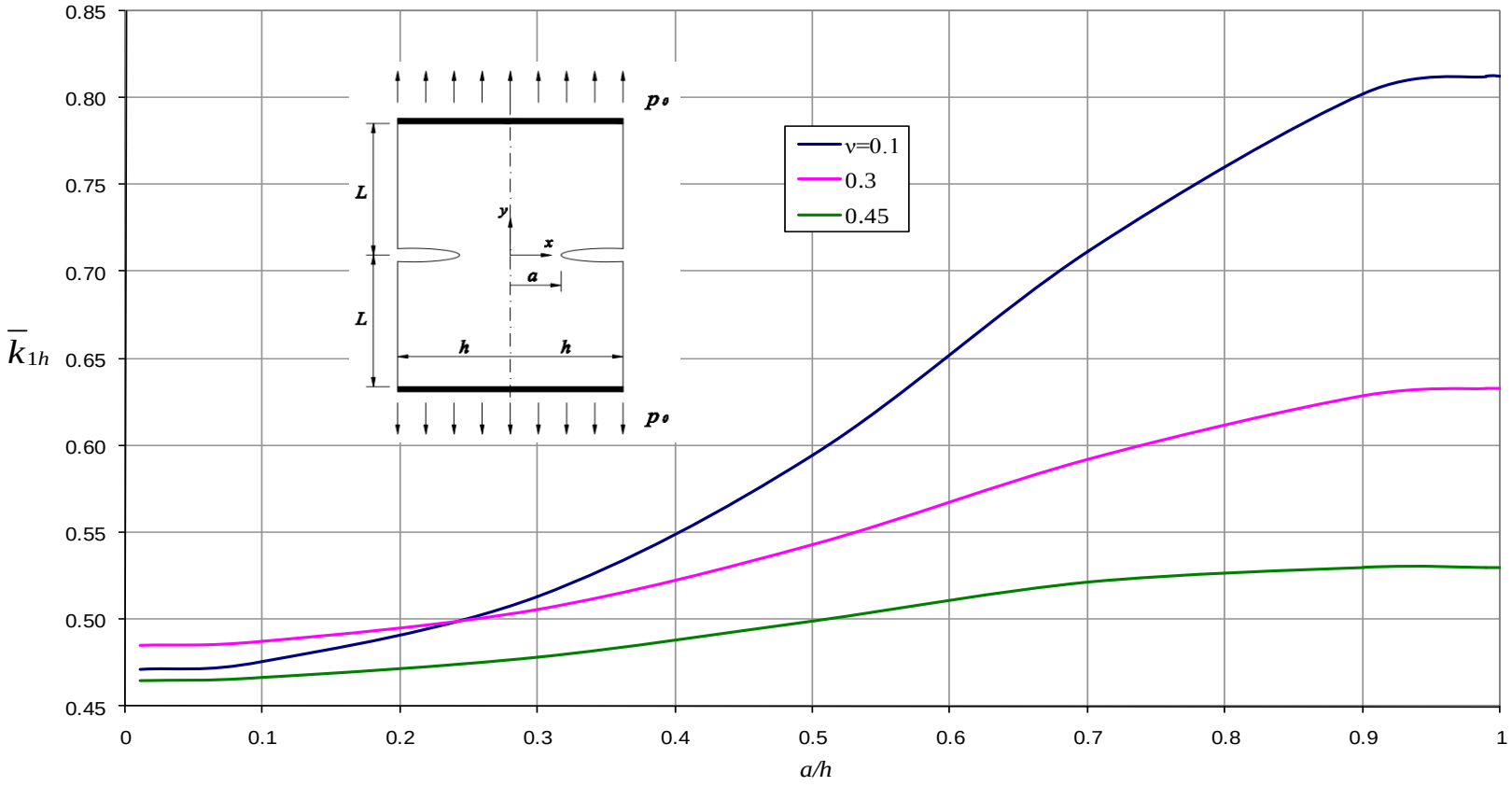


Figure 6.52 Normalized Mode I stress intensity factor $\bar{k}_{1h}$ at corner of finite strip when $L/h$ = 0.5 (Plane strain).

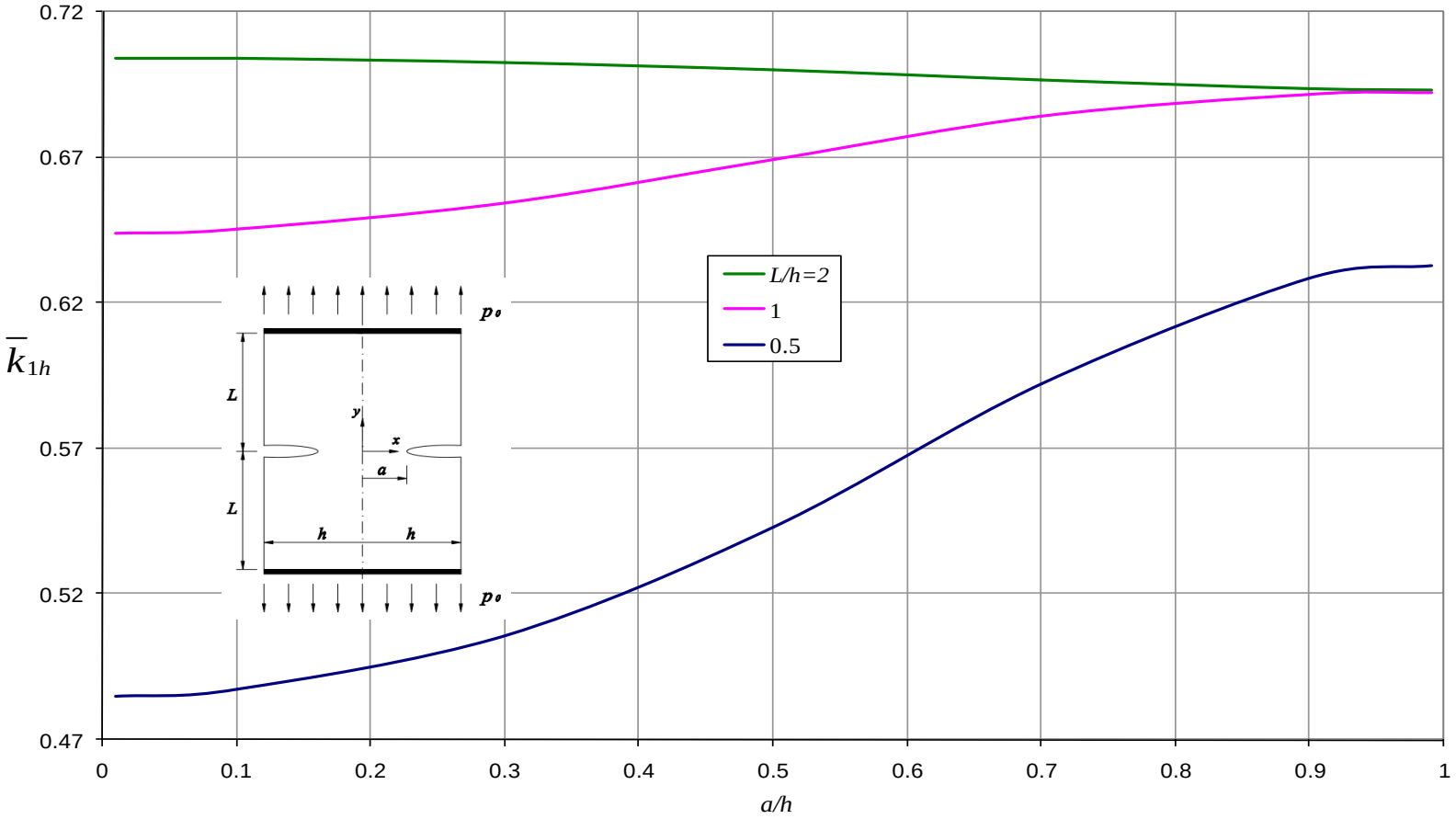


Figure 6.53 Normalized Mode I stress intensity factor $\overline{k}_{1h}$ at corner of finite strip when $\nu$ = 0.3 (Plane strain).

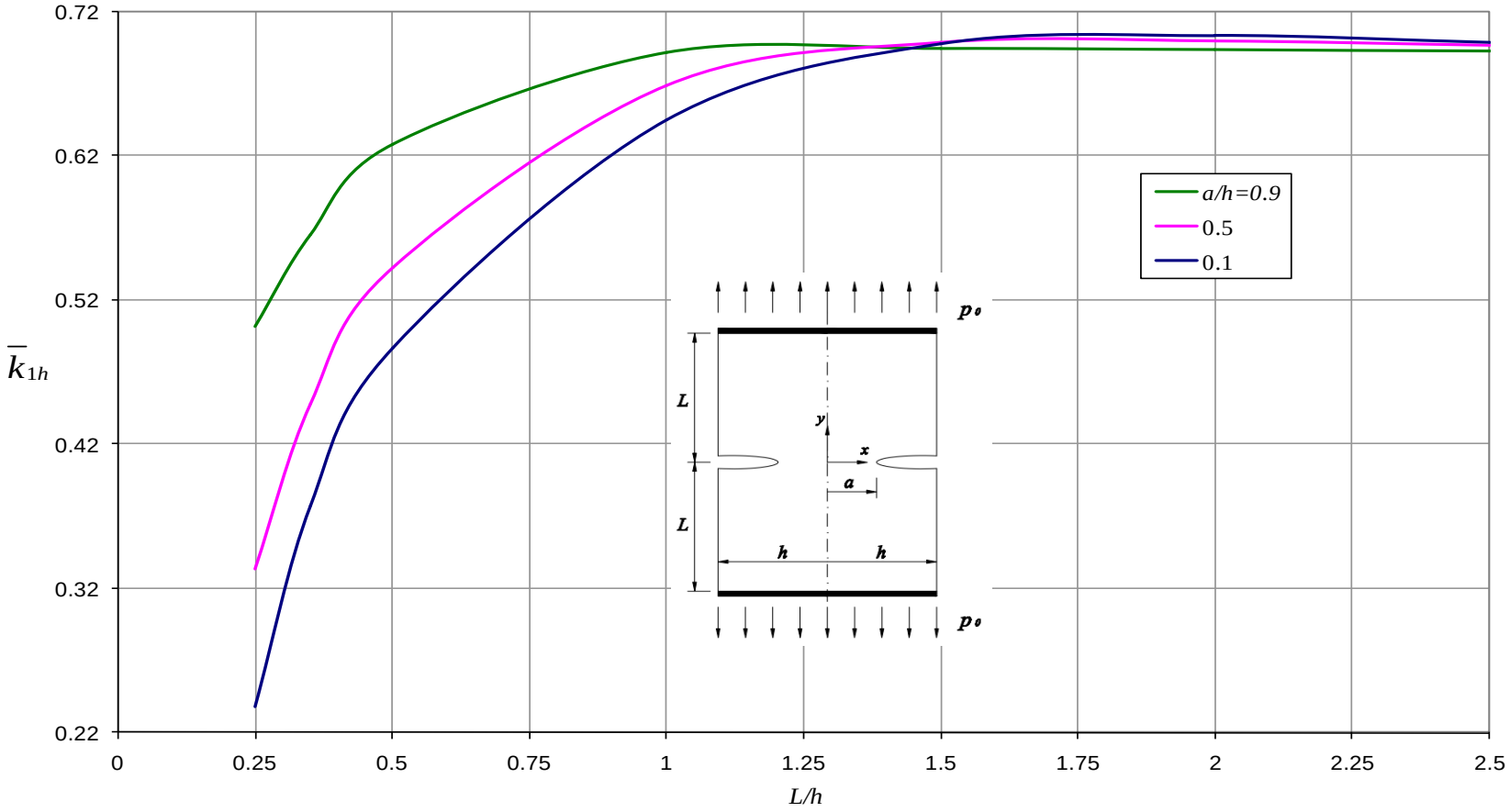


Figure 6.54 Normalized Mode I stress intensity factor $\bar{k}_{1h}$ at corner of finite strip when $\nu$ = 0.3 (Plane strain).

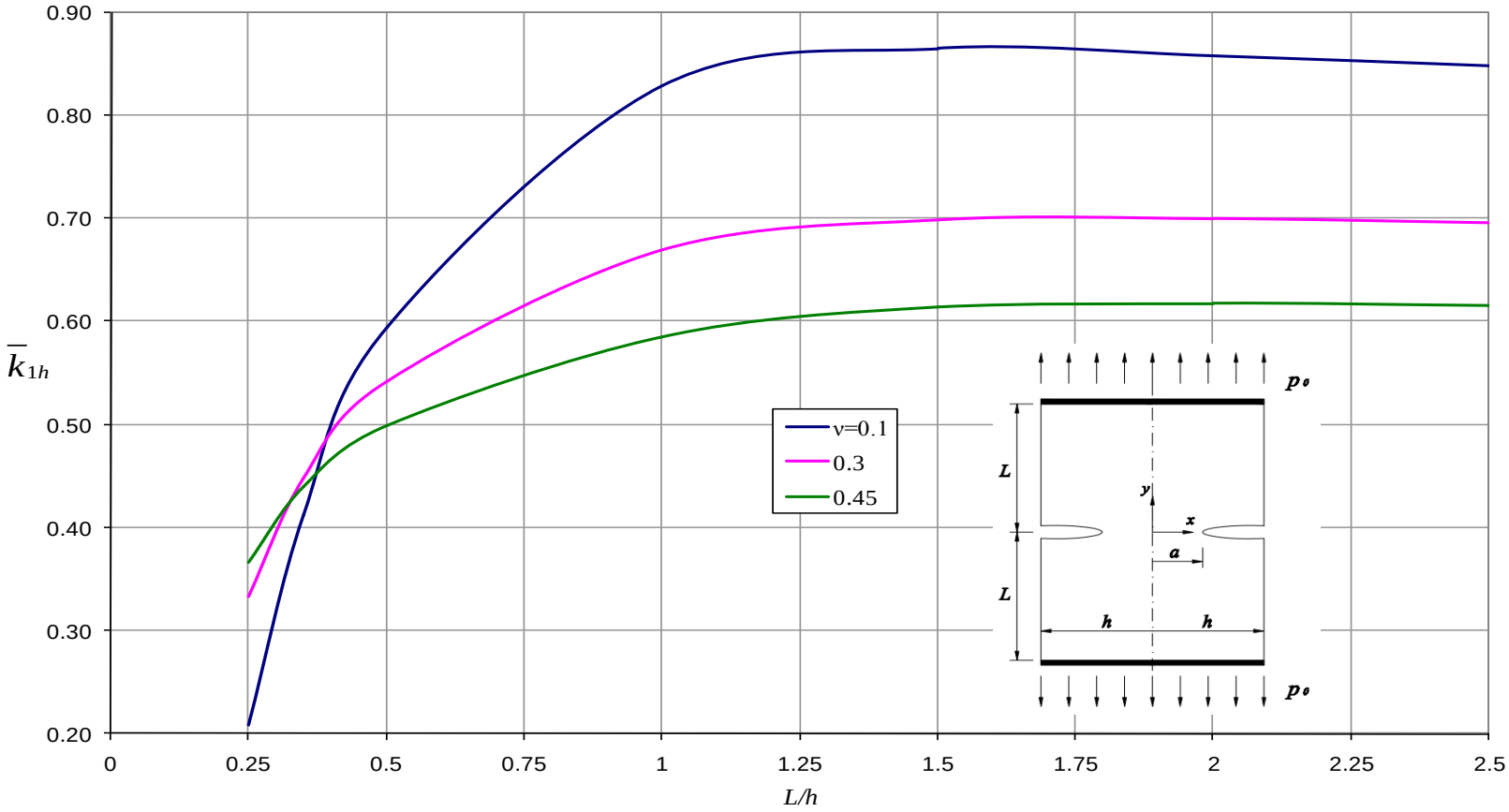


Figure 6.55 Normalized Mode I stress intensity factor $\bar{k}_{1h}$ at corner of finite strip when $a/h$ = 0.5 (Plane strain).

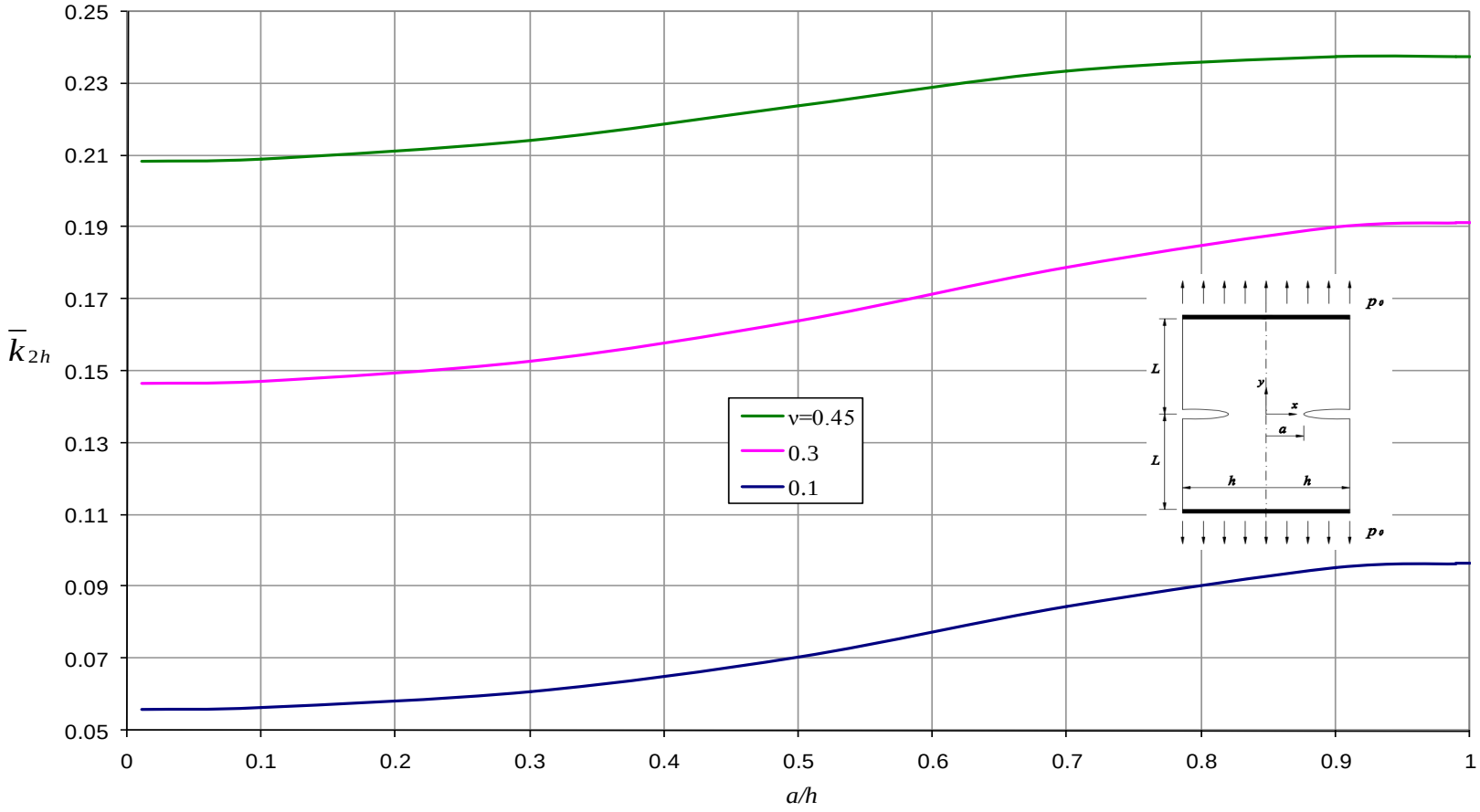


Figure 6.56 Normalized Mode II stress intensity factor $\overline{k}_{2h}$ at corner of finite strip when $L/h$ = 0.5 (Plane strain).

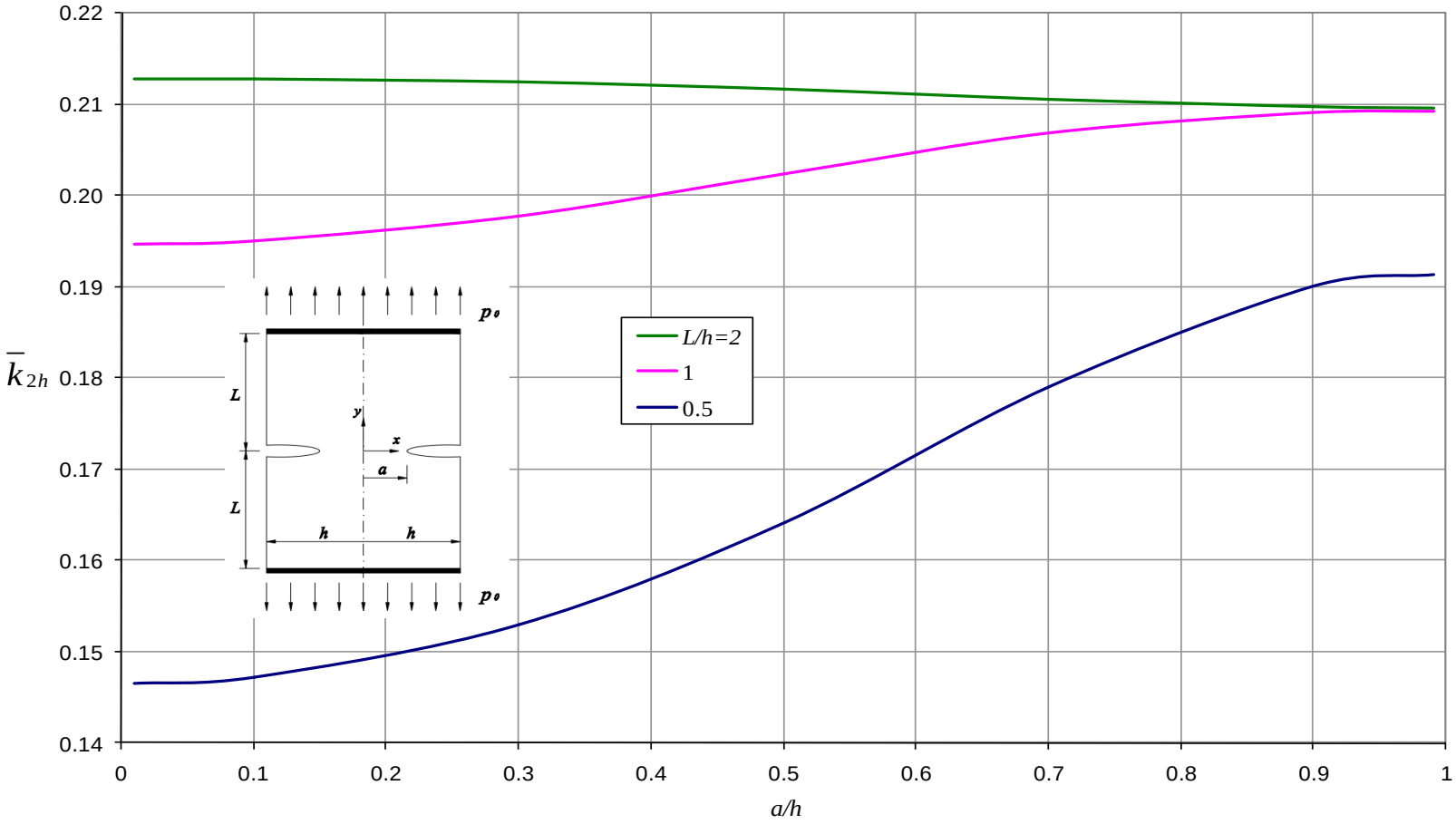


Figure 6.57 Normalized Mode II stress intensity factor $\bar{k}_{2h}$ at corner of finite strip when $v$ = 0.3 (Plane strain).

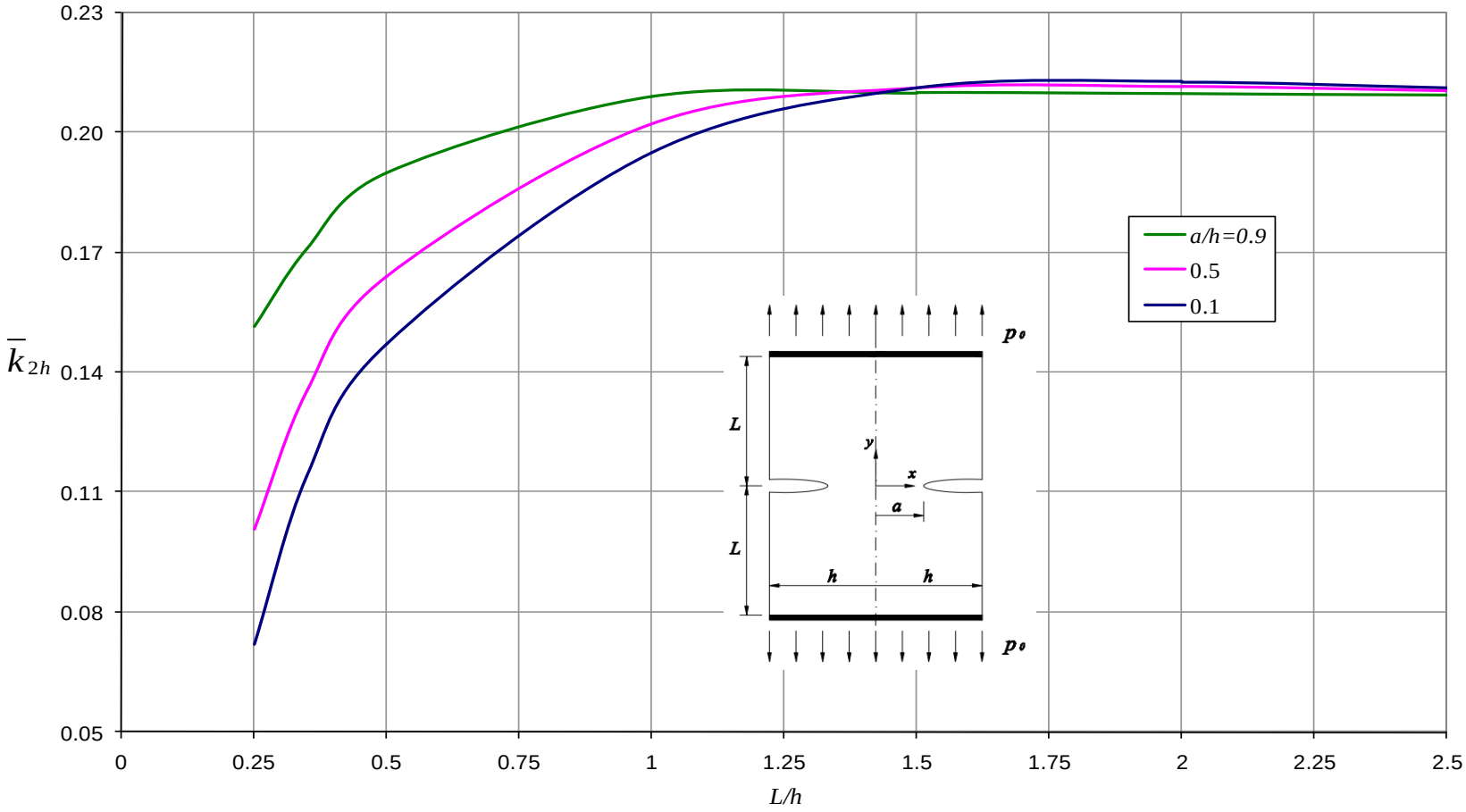


Figure 6.58 Normalized Mode II stress intensity factor $\bar{k}_{2h}$ at corner of finite strip when $\nu$ = 0.3 (Plane strain).

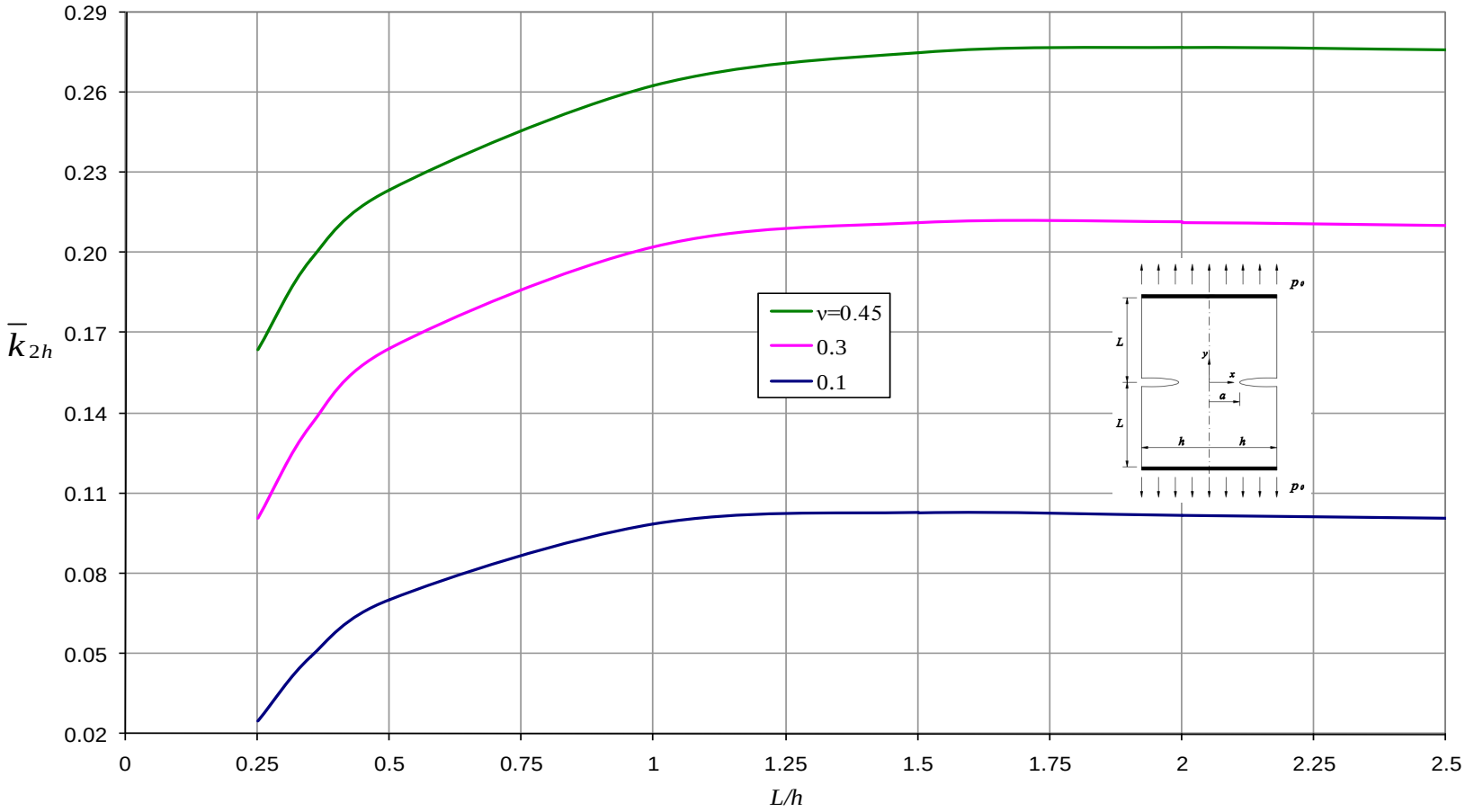


Figure 6.59 Normalized Mode II stress intensity factor $\overline{k}_{2h}$ at corner of finite strip when $a/h$ = 0.5 (Plane strain).

## REFERENCES


Abramowitz, M. and Stegun, I.A., Handbook of Mathematical Functions, Dover, 1965.

Adams, G.G. and Bogy, D.B., "A Note on a Paper by G. D. Gupta", Journal of Applied Mechanics, 42, 224–225 (1975).

Adams, G.G., "A A Semi-Infinite Elastic Strip Bonded to an Infinite Strip", Journal of Applied Mechanics, 47, 789–794 (1980).

Artem, H.S.A. and Geçit, M.R., "An Elastic Hollow Cylinder Under Axial Tension Containing a Crack and Two Rigid Inclusions of Ring Shape", Computers and Structures, 80, 2277–2287 (2002).

Blaibel, A.F.H. and Geçit M.R., "Bending of a Semi-Infinite Elastic Strip Bonded to an Infinite Strip", International Journal of Engineering Science, 27, 793–807 (1989).

Civelek, M.B. and Erdoğan, F., "Crack Problems for a Rectangular Plate and an Infinite Strip", International Journal of Fracture, 19, 139–159 (1982).

Cook, T.S. and Erdoğan, F., "Stresses in Bonded Materials with a Crack Perpendicular to the Interface", International Journal of Engineering Science, 10, 677–697 (1972).

Erdelyi, A., Ed., Tables of Integral Transforms, Vol. 1, McGraw-Hill, NY, 1953.

Erdoğan, F., "Simultaneous Dual Integral Equations with Trigonometric and Bessel Kernels", Zeitschrift für Angewandte Mathematik und Mechanik, 48, 217–225 (1968).

Erdoğan, F., Gupta, G.D. and Cook, T.S., "Numerical Solution of Singular Integral Equations", Methods of Analysis and Solutions of Crack Problems, G.C. Sih, Ed., Noordhoff International Publishing, Chapter 7, 414–420 (1973).

Geçit, M.R., "Antiplane Shear in Adhesively Bonded Semi-Infinite Media with Transverse Cracks", International Journal of Fracture, 24, 163–178 (1984).

Geçit, M.R., and Turgut A., "Extension of a Finite Strip Bonded to a Rigid Support", Computational Mechanics, 3, 398–410 (1988).

Gupta, G.D., "An Integral Approach to the Semi-Infinite Strip Problem", Journal of Applied Mechanics, Transactions of the ASME, 40, 948–954 (1973).

Gupta, G.D., and Erdoğan, F., "The Problem of Edge Cracks in an Infinite Strip", Journal of Applied Mechanics, Transactions of the ASME, 41, 1–6 (1974).

Gupta, G.D., "The Problem of a Finite Strip Compressed between Rough Rigid Stamps", Journal of Applied Mechanics, Transactions of the ASME, 42, 81–87 (1975).

Griffith, A.A., "The Phenomena of Rapture and Flow in Solids", Philosophical Transactions of the Royal Society of London, Series A, Mathematical and Physical Sciences, A221, 163–198 (1920).

Kaman, M.O., and Geçit, M.R., "Cracked Semi-Infinite Cylinder and Finite Cylinder Problems", International Journal of Engineering Science, 44, 1534–1555 (2006).

Krenk, S., "On the Elastic Strip with an Internal Crack", International Journal of Solids and Structures, 11, 693–708 (1975).

Muskhelishvili, N.I., Singular Integral Equations, P. Noordhoff, Gröningen, Holland, 1953.

Oberhettinger, F., Tabellen zur Fourier Transformation, Springer-Verlag, Germany, 1957.

Sneddon, I.N., and Srivastav, R.P., "The Stress Field in the Vicinity of a Griffith Crack in a Strip of Finite Width", International Journal of Engineering Science, 9, 479–488 (1971).

Toygar, M.E., and Geçit, M.R., "Cracked Infinite Cylinder with Two Rigid Inclusions Under Axisymmetric Tension", International Journal of Solids and Structures, 43, 4777–4794 (2006).

Turgut, A., and Geçit, M.R., "A Semi-Infinite Elastic Strip Containing a Transverse Crack", The Arabian Journal for Science and Engineering, 13, 71–80 (1988).

Yetmez, M., and Geçit, M.R., "Finite Strip with a Central Crack Under Tension", International Journal of Engineering Science, 43, 472–493 (2005).

Zhou, Z.G., Bai, Y.Y., Zhang, X.W., "Two Collinear Griffith Cracks Subjected to Uniform Tension in Infinitely Long Strip", International Journal of Solids and Structures, 36, 5597–5609 (1999).

## APPENDIX A

FORMULAE INVOLVING DEFINITE INTEGRALS

Evaluation of some definite integrals from Erdelyi and Magnus (1953):

$$\int_0^\infty e^{-ax}dx = \frac{1}{a},$$

$$\int_0^\infty xe^{-ax}dx = \frac{1}{a^2},$$

$$\int_0^\infty x^2e^{-ax}dx = \frac{2}{a^3},$$

$$\int_0^\infty e^{-ax}\sin(bx)dx = \frac{b}{a^2+b^2},$$

$$\int_0^\infty xe^{-ax}\sin(bx)dx = \frac{2ab}{\left[a^2+b^2\right]^2},$$

$$\int_0^\infty x^2e^{-ax}\sin(bx)dx = \frac{2b\left(3a^2-b^2\right)}{\left[a^2+b^2\right]^3},$$

$$\int_0^\infty e^{-ax}\cos(bx)dx = \frac{a}{a^2+b^2},$$

$$\int_0^\infty xe^{-ax}\cos(bx)dx = \frac{a^2-b^2}{\left[a^2+b^2\right]^2},$$

$$\int_0^\infty x^2e^{-ax}\cos(bx)dx = \frac{2a\left(a^2-3b^2\right)}{\left[a^2+b^2\right]^3}. \qquad \text{(A.1a–i)}$$

## APPENDIX B

DEFINITIONS APPEARING IN EQS. (2.24) AND (2.25)

$$SL_{11}^{1}(\gamma, y_1) = \{-\kappa - 3 + 2\gamma(L + y_1)\} e^{-\gamma(L+y_1)},$$

$$SL_{12}^{1}(\gamma, y_1) = \{\kappa - 3 + 2\gamma(L + y_1)\} e^{-\gamma(L+y_1)},$$

$$SL_{21}^{1}(\gamma, y_1) = \{-\kappa - 3 + 2\gamma(L - y_1)\} e^{-\gamma(L-y_1)},$$

$$SL_{22}^{1}(\gamma, y_1) = \{\kappa - 3 + 2\gamma(L - y_1)\} e^{-\gamma(L-y_1)}. \quad \text{(B.1a–d)}$$

$$ST_{11}^{1}(\gamma, y_1) = \{\kappa - 1 - 2\gamma(L + y_1)\} e^{-\gamma(L+y_1)},$$

$$ST_{12}^{1}(\gamma, y_1) = \{-\kappa - 1 - 2\gamma(L + y_1)\} e^{-\gamma(L+y_1)},$$

$$ST_{21}^{1}(\gamma, y_1) = \{\kappa - 1 - 2\gamma(L - y_1)\} e^{-\gamma(L-y_1)},$$

$$ST_{22}^{1}(\gamma, y_1) = \{-\kappa - 1 - 2\gamma(L - y_1)\} e^{-\gamma(L-y_1)}. \quad \text{(B.2a–d)}$$

$$SS_{11}^{1}(\gamma, y_1) = \{\kappa + 1 - 2\gamma(L + y_1)\} e^{-\gamma(L+y_1)},$$

$$SS_{12}^{1}(\gamma, y_1) = \{-\kappa + 1 - 2\gamma(L + y_1)\} e^{-\gamma(L+y_1)},$$

$$SS_{21}^{1}(\gamma, y_1) = \{-\kappa - 1 + 2\gamma(L - y_1)\} e^{-\gamma(L-y_1)},$$

$$SS_{22}^{1}(\gamma, y_1) = \{\kappa - 1 + 2\gamma(L - y_1)\} e^{-\gamma(L-y_1)}. \quad \text{(B.3a–d)}$$

$$SL_{11}^{2}(\gamma, y_2) = \{4\gamma L + (1 + e^{2L\gamma})(-\kappa - 3 + 2\gamma y_2)\} e^{-\gamma(2L+y_2)},$$

$$SL_{12}^{2}(\gamma, y_2) = \{4\gamma L + (1 - e^{2L\gamma})(\kappa - 3 + 2\gamma y_2)\} e^{-\gamma(2L+y_2)}. \quad \text{(B.4a,b)}$$

$$ST_{11}^{2}(\gamma, y_2) = \{-4\gamma L + (1 + e^{2L\gamma})(\kappa - 1 - 2\gamma y_2)\} e^{-\gamma(2L+y_2)},$$

$$ST_{12}^{2}(\gamma, y_2) = \{-4\gamma L + (1 - e^{2L\gamma})(-\kappa - 1 - 2\gamma y_2)\} e^{-\gamma(2L+y_2)}, \quad \text{(B.5a,b)}$$

$$SS_{11}^{2}(\gamma, y_2) = \left\{-4\gamma L + (1+e^{2L\gamma})(\kappa + 1 - 2\gamma y_2)\right\} e^{-\gamma(2L+y_2)},$$

$$SS_{12}^{2}(\gamma, y_2) = \left\{-4\gamma L + (1-e^{2L\gamma})(-\kappa + 1 - 2\gamma y_2)\right\} e^{-\gamma(2L+y_2)}. \qquad \text{(B.6a,b)}$$

$$DL_{11}^{1}(\gamma, y_1) = \left\{L + y_1 - \kappa/\gamma\right\} e^{-\gamma(L+y_1)},$$

$$DL_{12}^{1}(\gamma, y_1) = \left\{L + y_1\right\} e^{-\gamma(L+y_1)},$$

$$DL_{21}^{1}(\gamma, y_1) = \left\{L - y_1 - \kappa/\gamma\right\} e^{-\gamma(L-y_1)},$$

$$DL_{22}^{1}(\gamma, y_1) = \left\{L - y_1\right\} e^{-\gamma(L-y_1)}. \qquad \text{(B.7a–b)}$$

$$DT_{11}^{1}(\gamma, y_1) = \left\{L + y_1\right\} e^{-\gamma(L+y_1)},$$

$$DT_{12}^{1}(\gamma, y_1) = \left\{L + y_1 + \kappa/\gamma\right\} e^{-\gamma(L+y_1)},$$

$$DT_{21}^{1}(\gamma, y_1) = \left\{-L + y_1\right\} e^{-\gamma(L-y_1)},$$

$$DT_{22}^{1}(\gamma, y_1) = \left\{-L + y_1 - \kappa/\gamma\right\} e^{-\gamma(L-y_1)}. \qquad \text{(B.8a–b)}$$

$$DL_{11}^{2}(\gamma, y_2) = \left\{2L + (1+e^{2L\gamma})(y_2 - \kappa/\gamma)\right\} e^{-\gamma(2L+y_2)},$$

$$DL_{12}^{2}(\gamma, y_2) = \left\{2L + (1-e^{2L\gamma})y_2\right\} e^{-\gamma(2L+y_2)}. \qquad \text{(B.9a,b)}$$

## APPENDIX C

INTEGRATION FORMULAS FOR FOURIER TRANSFORMATION

Evaluation of some definite integrals for Fourier transformation from Oberhettinger (1957):

$$\int_0^\infty \frac{\cos\psi y}{y^2+a^2}dy = \frac{\pi}{2a}e^{-\psi a},$$

$$\int_0^\infty \frac{y\sin\psi y}{y^2+a^2}dy = \frac{\pi}{2}e^{-\psi a},$$

$$\int_0^\infty \frac{y^2\cos\psi y}{y^2+a^2}dy = -\frac{\pi a}{2}e^{-\psi a},$$

$$\int_0^\infty \frac{y^3\sin\psi y}{y^2+a^2}dy = -\frac{\pi a^2}{2}e^{-\psi a}. \qquad \text{(C.1a–d)}$$

$$\int_0^\infty \frac{\cos\psi y}{\left[y^2+a^2\right]^2}dy = \frac{\pi}{4a^3}\left(a\psi+1\right)e^{-\psi a},$$

$$\int_0^\infty \frac{y\sin\psi y}{\left[y^2+a^2\right]^2}dy = \frac{\pi}{4a}\psi e^{-\psi a},$$

$$\int_0^\infty \frac{y^2\cos\psi y}{\left[y^2+a^2\right]^2}dy = \frac{\pi}{4a}\left(1-a\psi\right)e^{-\psi a},$$

$$\int_0^\infty \frac{y^3\sin\psi y}{\left[y^2+a^2\right]^2}dy = \frac{\pi}{4}\left(2-a\psi\right)e^{-\psi a}. \qquad \text{(C.2a–d)}$$

$$\int_0^\infty \left\{ \frac{1}{(y-L)^2+(h-r)^2} + \frac{1}{(y+L)^2+(h-r)^2} \right\} \cos\psi y dy = \frac{\pi}{h-r} e^{-\psi(h-r)} \cos\psi L ,$$

$$\int_0^\infty \left\{ \frac{y-L}{(y-L)^2+(h-r)^2} - \frac{y+L}{(y+L)^2+(h-r)^2} \right\} \cos\psi y dy = -\pi e^{-\psi(h-r)} \sin\psi L ,$$

$$\int_0^\infty \left\{ \frac{1}{\left[(y-L)^2+(h-r)^2\right]^2} + \frac{1}{\left[(y+L)^2+(h-r)^2\right]^2} \right\} \cos\psi y dy$$

$$= \frac{\pi\left[\psi(h-r)+1\right]}{2(h-r)^3} e^{-\psi(h-r)} \cos\psi L ,$$

$$\int_0^\infty \left\{ \frac{y-L}{\left[(y-L)^2+(h-r)^2\right]^2} - \frac{y+L}{\left[(y+L)^2+(h-r)^2\right]^2} \right\} \cos\psi y dy$$

$$= -\frac{\pi\psi}{2(h-r)} e^{-\psi(h-r)} \sin\psi L.$$

(C.3a–d)

$$\int_0^\infty \left\{ \frac{1}{(y-L)^2+(h-r)^2} - \frac{1}{(y+L)^2+(h-r)^2} \right\} \sin\psi y dy = \frac{\pi}{h-r} e^{-\psi(h-r)} \sin\psi L ,$$

$$\int_0^\infty \left\{ \frac{y-L}{(y-L)^2+(h-r)^2} + \frac{y+L}{(y+L)^2+(h-r)^2} \right\} \sin\psi y dy = \pi e^{-\psi(h-r)} \cos\psi L ,$$

$$\int_0^\infty \left\{ \frac{1}{\left[(y-L)^2+(h-r)^2\right]^2} - \frac{1}{\left[(y+L)^2+(h-r)^2\right]^2} \right\} \sin\psi y dy$$

$$= \frac{\pi\left[\psi(h-r)+1\right]}{2(h-r)^3} e^{-\psi(h-r)} \sin\psi L,$$

$$\int_0^\infty \left\{ \frac{y-L}{\left[\left(y-L\right)^2+\left(h-r\right)^2\right]^2} + \frac{y+L}{\left[\left(y+L\right)^2+\left(h-r\right)^2\right]^2} \right\} \sin\psi y dy = \frac{\pi\psi}{2\left(h-r\right)} e^{-\psi\left(h-r\right)} \cos\psi L.$$

(C.4a–d)

## APPENDIX D

TERMS FOR EQS. (2.39) AND (2.40)

$$A_1(t,x,y)=\int_0^\infty \frac{\cos sy}{1+4she^{-2sh}-e^{-4sh}}\left\{Z_{a11}e^{-s(2h-t-x)}+Z_{a12}e^{-s(2h-t+x)}\right.$$
$$\left.+Z_{a13}e^{-s(2h+t-x)}+Z_{a14}e^{-s(2h+t+x)}\right\}ds,$$
$$Z_{a11}=2s(t+x)e^{-2sh}+\{1-2s(h-t)\}\{-1-2s(h-x)\}+1,$$
$$Z_{a12}=2s(t-x)e^{-2sh}+\{1-2s(h-t)\}\{-1-2s(h+x)\}+1,$$
$$Z_{a13}=2s(t-x)e^{-2sh}+\{1-2s(h+t)\}\{1+2s(h-x)\}-1,$$
$$Z_{a14}=2s(t+x)e^{-2sh}+\{1-2s(h+t)\}\{-1+2s(h+x)\}+1,$$

$$B_1(r,x,y)=\int_0^\infty \frac{\cos sL\cos sy}{1+4she^{-2sh}-e^{-4sh}}\left\{Z_{b11}e^{-s(2h-r-x)}+Z_{b12}e^{-s(2h-r+x)}\right\}ds,$$
$$Z_{b11}=2\left[\{\kappa-2s(r+x)+1\}e^{-2sh}+\{\kappa+2s(h-r)\}\{-1-2s(h-x)\}-1\right],$$
$$Z_{b12}=2\left[\{\kappa-2s(r-x)+1\}e^{-2sh}+\{\kappa+2s(h-r)\}\{-1-2s(h+x)\}-1\right],$$

$$C_1(r,x,y)=\int_0^\infty \frac{\sin sL\cos sy}{1+4she^{-2sh}-e^{-4sh}}\left\{Z_{c11}e^{-s(2h-r-x)}+Z_{c12}e^{-s(2h-r+x)}\right\}ds,$$
$$Z_{c11}=2\left[\{\kappa+2s(r+x)-1\}e^{-2sh}+\{-\kappa+2s(h-r)\}\{1+2s(h-x)\}+1\right],$$
$$Z_{c12}=2\left[\{\kappa+2s(r-x)-1\}e^{-2sh}+\{-\kappa+2s(h-r)\}\{1+2s(h+x)\}+1\right].$$

(D.1a–l)

$$A_2(t,x,y)=\int_0^\infty \frac{\cos sy}{1+4she^{-2sh}-e^{-4sh}}\left\{Z_{a21}e^{-s(2h-t-x)}+Z_{a22}e^{-s(2h-t+x)}\right.$$
$$\left.+Z_{a23}e^{-s(2h+t-x)}+Z_{a24}e^{-s(2h+t+x)}\right\}ds,$$
$$Z_{a21}=\{-4-2s(t+x)\}e^{-2sh}+\{1-2s(h-t)\}\{-3+2s(h-x)\}-1,$$
$$Z_{a22}=\{-4-2s(t-x)\}e^{-2sh}+\{1-2s(h-t)\}\{-3+2s(h+x)\}-1,$$

$$Z_{a23} = \{4-2s(t-x)\}e^{-2sh} + \{1-2s(h+t)\}\{3-2s(h-x)\}+1,$$
$$Z_{a24} = \{4-2s(t+x)\}e^{-2sh} + \{1-2s(h+t)\}\{3-2s(h+x)\}+1,$$

$$B_2(r,x,y) = \int_0^\infty \frac{\cos sL \cos sy}{1+4she^{-2sh}-e^{-4sh}} \{Z_{b21}e^{-s(2h-r-x)} + Z_{b22}e^{-s(2h-r+x)}\}ds,$$
$$Z_{b21} = 2\Big[\{-\kappa+2s(r+x)+3\}e^{-2sh} + \{\kappa+2s(h-r)\}\{-3+2s(h-x)\}+1\Big],$$
$$Z_{b22} = 2\Big[\{-\kappa+2s(r-x)+3\}e^{-2sh} + \{\kappa+2s(h-r)\}\{-3+2s(h+x)\}+1\Big],$$

$$C_2(r,x,y) = \int_0^\infty \frac{\sin sL \cos sy}{1+4she^{-2sh}-e^{-4sh}} \{Z_{c21}e^{-s(2h-r-x)} + Z_{c22}e^{-s(2h-r+x)}\}ds,$$
$$Z_{c21} = 2\Big[\{-\kappa-2s(r+x)-3\}e^{-2sh} + \{\kappa-2s(h-r)\}\{-3+2s(h-x)\}-1\Big],$$
$$Z_{c22} = 2\Big[\{-\kappa-2s(r-x)-3\}e^{-2sh} + \{\kappa-2s(h-r)\}\{-3+2s(h+x)\}-1\Big].$$

(D.2a–l)

$$A_3(t,x,y) = \int_0^\infty \frac{\sin sy}{1+4she^{-2sh}-e^{-4sh}} \{Z_{a31}e^{-s(2h-t-x)} + Z_{a32}e^{-s(2h-t+x)} + Z_{a33}e^{-s(2h+t-x)} + Z_{a34}e^{-s(2h+t+x)}\}ds,$$
$$Z_{a31} = \{-2-2s(t+x)\}e^{-2sh} + \{1-2s(h-t)\}\{-1+2s(h-x)\}-1,$$
$$Z_{a32} = \{2+2s(t-x)\}e^{-2sh} + \{1-2s(h-t)\}\{1-2s(h+x)\}+1,$$
$$Z_{a33} = \{2-2s(t-x)\}e^{-2sh} + \{1-2s(h+t)\}\{1-2s(h-x)\}+1,$$
$$Z_{a34} = \{-2+2s(t+x)\}e^{-2sh} + \{1-2s(h+t)\}\{-1+2s(h+x)\}-1,$$

$$B_3(r,x,y) = \int_0^\infty \frac{\cos sL \sin sy}{1+4she^{-2sh}-e^{-4sh}} \{Z_{b31}e^{-s(2h-r-x)} + Z_{b32}e^{-s(2h-r+x)}\}ds,$$
$$Z_{b31} = 2\Big[\{-\kappa+2s(r+x)+1\}e^{-2sh} + \{\kappa+2s(h-r)\}\{-1+2s(h-x)\}+1\Big],$$
$$Z_{b32} = 2\Big[\{\kappa-2s(r-x)-1\}e^{-2sh} + \{\kappa+2s(h-r)\}\{1-2s(h+x)\}-1\Big],$$

$$C_3(r,x,y)=\int_0^\infty \frac{\sin sL\sin sy}{1+4she^{-2sh}-e^{-4sh}}\left\{Z_{c31}e^{-s(2h-r-x)}+Z_{c32}e^{-s(2h-r+x)}\right\}ds,$$

$$Z_{c31}=2\Big[\left\{-\kappa-2s(r+x)-1\right\}e^{-2sh}+\left\{\kappa-2s(h-r)\right\}\left\{-1+2s(h-x)\right\}-1\Big],$$

$$Z_{c32}=2\Big[\left\{\kappa+2s(r-x)+1\right\}e^{-2sh}+\left\{\kappa-2s(h-r)\right\}\left\{1-2s(h+x)\right\}+1\Big].$$

(D.3a–l)

$$A_4(t,x,y)=\int_0^\infty \frac{\cos sy}{1+4she^{-2sh}-e^{-4sh}}\left\{Z_{a41}e^{-s(2h-t-x)}+Z_{a42}e^{-s(2h-t+x)}\right.$$

$$\left.+Z_{a43}e^{-s(2h+t-x)}+Z_{a44}e^{-s(2h+t+x)}\right\}ds,$$

$$Z_{a41}=\left\{-\kappa+2s(t+x)+3\right\}e^{-2sh}+\left\{-1+2s(h-t)\right\}\left\{\kappa+2s(h-x)-2\right\}+1,$$

$$Z_{a42}=\left\{-\kappa+2s(t-x)+3\right\}e^{-2sh}+\left\{-1+2s(h-t)\right\}\left\{\kappa+2s(h+x)-2\right\}+1,$$

$$Z_{a43}=\left\{\kappa+2s(t-x)-3\right\}e^{-2sh}+\left\{1-2s(h+t)\right\}\left\{\kappa+2s(h-x)-2\right\}-1,$$

$$Z_{a44}=\left\{\kappa+2s(t+x)-3\right\}e^{-2sh}+\left\{1-2s(h+t)\right\}\left\{\kappa+2s(h+x)-2\right\}-1,$$

$$B_4(r,x,y)=\int_0^\infty \frac{\cos sL\cos sy}{1+4she^{-2sh}-e^{-4sh}}\left\{Z_{b41}e^{-s(2h-r-x)}+Z_{b42}e^{-s(2h-r+x)}\right\}ds,$$

$$Z_{b41}=\left\{2\kappa-2s(r+x)-2\right\}e^{-2sh}+\left\{\kappa+2s(h-r)\right\}\left\{-\kappa-2s(h-x)+2\right\}-1,$$

$$Z_{b42}=\left\{2\kappa-2s(r-x)-2\right\}e^{-2sh}+\left\{\kappa+2s(h-r)\right\}\left\{-\kappa-2s(h+x)+2\right\}-1,$$

$$C_4(r,x,y)=\int_0^\infty \frac{\sin sL\cos sy}{1+4she^{-2sh}-e^{-4sh}}\left\{Z_{c41}e^{-s(2h-r-x)}+Z_{c42}e^{-s(2h-r+x)}\right\}ds,$$

$$Z_{c41}=\left\{2+2s(r+x)\right\}e^{-2sh}+\left\{-\kappa+2s(h-r)\right\}\left\{\kappa+2s(h-x)-2\right\}+1,$$

$$Z_{c42}=\left\{2+2s(r-x)\right\}e^{-2sh}+\left\{-\kappa+2s(h-r)\right\}\left\{\kappa+2s(h+x)-2\right\}+1.$$

(D.4a–l)

$$A_5(t,x,y)=\int_0^\infty \frac{\sin sy}{1+4she^{-2sh}-e^{-4sh}}\left\{Z_{a51}e^{-s(2h-t-x)}+Z_{a52}e^{-s(2h-t+x)}\right.$$

$$\left.+Z_{a53}e^{-s(2h+t-x)}+Z_{a54}e^{-s(2h+t+x)}\right\}ds,$$

$$Z_{a51} = \{-\kappa - 2s(t+x) - 3\}e^{-2sh} + \{1 - 2s(h-t)\}\{-\kappa + 2s(h-x) - 2\} - 1,$$

$$Z_{a52} = \{\kappa + 2s(t-x) + 3\}e^{-2sh} + \{1 - 2s(h-t)\}\{\kappa - 2s(h+x) + 2\} + 1,$$

$$Z_{a53} = \{\kappa - 2s(t-x) + 3\}e^{-2sh} + \{1 - 2s(h+t)\}\{\kappa - 2s(h-x) + 2\} + 1,$$

$$Z_{a54} = \{-\kappa + 2s(t+x) - 3\}e^{-2sh} + \{1 - 2s(h+t)\}\{-\kappa + 2s(h+x) - 2\} - 1,$$

$$B_5(r,x,y) = \int_0^\infty \frac{\cos sL \sin sy}{1 + 4she^{-2sh} - e^{-4sh}} \{Z_{b51}e^{-s(2h-r-x)} + Z_{b52}e^{-s(2h-r+x)}\} ds,$$

$$Z_{b51} = \{2s(r+x) + 2\}e^{-2sh} + \{\kappa + 2s(h-r)\}\{-\kappa + 2s(h-x) - 2\} + 1,$$

$$Z_{b52} = \{-2s(r-x) - 2\}e^{-2sh} + \{\kappa + 2s(h-r)\}\{\kappa - 2s(h+x) + 2\} - 1,$$

$$C_5(r,x,y) = \int_0^\infty \frac{\sin sL \sin sy}{1 + 4she^{-2sh} - e^{-4sh}} \{Z_{c51}e^{-s(2h-r-x)} + Z_{c52}e^{-s(2h-r+x)}\} ds,$$

$$Z_{c51} = \{-2\kappa - 2s(r+x) - 2\}e^{-2sh} + \{\kappa - 2s(h-r)\}\{-\kappa + 2s(h-x) - 2\} - 1,$$

$$Z_{c52} = \{2\kappa + 2s(r-x) + 2\}e^{-2sh} + \{\kappa - 2s(h-r)\}\{\kappa - 2s(h+x) + 2\} + 1.$$

(D.5a–l)

## APPENDIX E

SINGULAR KERNELS OF EQS. (3.6)−(3.8)

$K_{ij\infty}$, $K_{ijb,}$ $k_{ijs}$ $(i, j = 1–3)$ appearing Eqs. (3.6)–(3.8):

$$\begin{aligned}K_{11\infty}(x,r,s) = \frac{1}{2}\Big\{e^{-s(2h-r-x)}\Big[&-(\kappa-1)^2 - 2\kappa s(h-x) - 2(\kappa-2)s(h-r) - 4s(h-r)s(h-x)\\ &+\Big\{-(\kappa-1)^2 - 2\kappa s(h-x) - 2(\kappa-2)s(h-r) - 4s(h-r)s(h-x)\Big\}\cos(2Ls)\Big]\\ &+e^{-s(2h-r+x)}\Big[-(\kappa-1)^2 - 2\kappa s(h+x) - 2(\kappa-2)s(h-r) - 4s(h-r)s(h+x)\\ &+\Big\{-(\kappa-1)^2 - 2\kappa s(h+x) - 2(\kappa-2)s(h-r) - 4s(h-r)s(h+x)\Big\}\cos(2Ls)\Big]\Big\}.\end{aligned} \tag{E.1}$$

$$K_{11b}(x,r,s) = \frac{1}{2\kappa}\frac{\{1+\cos 2Ls\}e^{-s(2h-r)}}{1+4sh e^{-2sh} - e^{-4sh}}\left\{V_{11}e^{-s(2h-x)} + V_{12}e^{-s(2h+x)}\right\},$$

$$\begin{aligned}V_{11} = {}&2s(h-r)\Big\{(2sh+\kappa-2)(e^{-2sh}-4sh)-1\Big\} + 2\Big[\{\kappa+2s(h-r)\}(4sh-e^{-2sh})+1\Big]sx\\ &+\Big[(1-\kappa)^2 + 2\kappa sh\Big](e^{-2sh}-4sh) + 2(1-\kappa+sh),\end{aligned}$$

$$\begin{aligned}V_{12} = {}&2s(h-r)\Big\{(2sh+\kappa-2)(e^{-2sh}-4sh)-1\Big\} + 2\Big[\{\kappa+2s(h-r)\}(e^{-2sh}-4sh)-1\Big]sx\\ &+\Big[(1-\kappa)^2 + 2\kappa sh\Big](e^{-2sh}-4sh) + 2(1-\kappa+sh).\end{aligned}$$

(E.2a–c)

$$\begin{aligned}K_{12\infty}(x,r,s) = \frac{\sin 2Ls}{2}\Big\{e^{-s(2h-r-x)}&\big[1-\kappa(\kappa-2) - 2\kappa s(h-x) + 2(\kappa-2)s(h-r)\\ &+4s(h-r)s(h-x)\big] + e^{-s(2h-r+x)}\big[1-\kappa(\kappa-2) - 2\kappa s(h+x)\\ &+2(\kappa-2)s(h-r) + 4s(h-r)s(h+x)\big]\Big\}.\end{aligned} \tag{E.3}$$

$$K_{12b}(x,r,s) = \frac{1}{2\kappa}\frac{\{\sin 2Ls\}e^{-s(2h-r)}}{1+4sh e^{-2sh} - e^{-4sh}}\left\{V_{21}e^{-s(2h-x)} + V_{22}e^{-s(2h+x)}\right\},$$

$$\begin{aligned}V_{21} = {}&2s(h-r)\Big\{\big[2s(h-x)+\kappa-2\big](4sh-e^{-2sh})+1\Big\} - 2 - 2s(h+x)\\ &+\Big[1+2\kappa-\kappa^2 - 2\kappa s(h-x)\Big](4sh-e^{-2sh}).\end{aligned}$$

$$\begin{aligned}V_{22} = {}&2s(h-r)\Big\{\big[2s(h+x)+\kappa-2\big](4sh-e^{-2sh})+1\Big\} - 2 - 2s(h-x)\\ &+\Big[1+2\kappa-\kappa^2 - 2\kappa s(h+x)\Big](4sh-e^{-2sh}).\end{aligned} \tag{E.4a–c}$$

$$K_{13\infty}(x,t,s)=\cos(Ls)\Big\{e^{-s(2h-t-x)}\big[-\kappa+3-2s(h-x)+2(\kappa-2)s(h-t)$$
$$+4s(h-t)s(h-x)\big]+e^{-s(2h-t+x)}\big[-\kappa+3-2s(h+x)+2(\kappa-2)s(h-t)$$
$$+4s(h-t)s(h+x)\big]+e^{-s(2h+t-x)}\big[\kappa-3+2s(h-x)-2(\kappa-2)s(h+t)$$
$$-4s(h+t)s(h-x)\big]+e^{-s(2h+t+x)}\big[\kappa-3+2s(h+x)-2(\kappa-2)s(h+t)$$
$$-4s(h+t)s(h+x)\big]\Big\}. \qquad \text{(E.5)}$$

$$K_{13b}(x,t,s)=\frac{1}{2\kappa}\frac{\{\cos Ls\}}{1+4she^{-2sh}-e^{-4sh}}\Big[e^{-s(2h-t)}\Big\{V_{31}e^{-s(2h-x)}+V_{32}e^{-s(2h+x)}\Big\}$$
$$+e^{-s(2h+t)}\Big\{V_{33}e^{-s(2h-x)}+V_{34}e^{-s(2h+x)}\Big\}\Big],$$

$$V_{31}=2s(h-t)\Big\{\big[2s(h-x)+\kappa-2\big](4sh-e^{-2sh})+1\Big\}-4sh$$
$$+\big[\kappa-3+2s(h-x)\big](1-4sh+e^{-2sh}),$$

$$V_{32}=2s(h-t)\Big\{\big[2s(h+x)+\kappa-2\big](4sh-e^{-2sh})+1\Big\}-4sh$$
$$+\big[\kappa-3+2s(h+x)\big](1-4sh+e^{-2sh}),$$

$$V_{33}=2s(h+t)\Big\{\big[2s(h-x)+\kappa-2\big](e^{-2sh}-4sh)+1\Big\}+4sh$$
$$+\big[-\kappa+3-2s(h-x)\big](1-4sh+e^{-2sh}),$$

$$V_{34}=2s(h+t)\Big\{\big[2s(h+x)+\kappa-2\big](e^{-2sh}-4sh)+1\Big\}+4sh$$
$$+\big[-\kappa+3-2s(h+x)\big](1-4sh+e^{-2sh}). \qquad \text{(E.6a–e)}$$

$$K_{21\infty}(x,r,s)=\frac{\sin 2Ls}{2}\Big\{e^{-s(2h-r-x)}\big[1-\kappa(\kappa+2)+2\kappa s(h-x)-2(\kappa+2)s(h-r)$$
$$+4s(h-r)s(h-x)\big]+e^{-s(2h-r+x)}\big[-1+\kappa(\kappa+2)-2\kappa s(h+x)$$
$$+2(\kappa+2)s(h-r)-4s(h-r)s(h+x)\big]\Big\}. \qquad \text{(E.7)}$$

$$K_{21b}(x,r,s)=\frac{1}{2\kappa}\frac{\{\sin 2Ls\}e^{-s(2h-r)}}{1+4she^{-2sh}-e^{-4sh}}\Big\{V_{41}e^{-s(2h-x)}+V_{42}e^{-s(2h+x)}\Big\},$$

$$V_{41}=\Big\{2s(h-r)\big[2s(h-x)-\kappa-2\big]+2\kappa s(h-x)+1-2\kappa-\kappa^2\Big\}(4sh-e^{-2sh})$$
$$+2s(h-r)-2-2s(h+x),$$

$$V_{42}=-\Big\{2s(h-r)\big[2s(h+x)-\kappa-2\big]+2\kappa s(h+x)+1-2\kappa-\kappa^2\Big\}(4sh-e^{-2sh})$$
$$-2s(h-r)+2+2s(h-x). \qquad \text{(E.8a–c)}$$

$$K_{22\infty}(x,r,s)=\frac{1}{2}\Big\{e^{-s(2h-r-x)}\Big[-(\kappa+1)^2+2\kappa s(h-x)+2(\kappa+2)s(h-r)$$
$$-4s(h-r)s(h-x)+\Big\{(\kappa+1)^2-2\kappa s(h-x)-2(\kappa+2)s(h-r)$$
$$+4s(h-r)s(h-x)\Big\}\cos(2Ls)\Big]+e^{-s(2h-r+x)}\Big[(\kappa+1)^2-2\kappa s(h+x)$$
$$-2(\kappa+2)s(h-r)+4s(h-r)s(h+x)+\Big\{-(\kappa+1)^2+2\kappa s(h+x)$$
$$+2(\kappa+2)s(h-r)-4s(h-r)s(h+x)\Big\}\cos(2Ls)\Big]\Big\}. \qquad \text{(E.9)}$$

$$K_{22b}(x,r,s)=\frac{1}{2\kappa}\frac{\{1-\cos 2Ls\}e^{-s(2h-r)}}{1+4she^{-2sh}-e^{-4sh}}\left\{V_{51}e^{-s(2h-x)}+V_{52}e^{-s(2h+x)}\right\},$$

$$V_{51}=2s(h-r)\Big\{\Big[2s(h-x)-\kappa-2\Big](e^{-2sh}-4sh)-1\Big\}+2\Big[\kappa+1+s(h+x)\Big]$$
$$+\Big[(1+\kappa)^2-2\kappa s(h-x)\Big](e^{-2sh}-4sh),$$

$$V_{52}=2s(h-r)\Big\{\Big[-2s(h+x)+\kappa+2\Big](e^{-2sh}-4sh)+1\Big\}+2\Big[-\kappa-1-s(h-x)\Big]$$
$$+\Big[-(1+\kappa)^2+2\kappa s(h+x)\Big](e^{-2sh}-4sh). \qquad \text{(E.10a–c)}$$

$$K_{23\infty}(x,t,s)=\sin(Ls)\Big\{e^{-s(2h-t-x)}\Big[-\kappa-3+2s(h-x)+2(\kappa+2)s(h-t)$$
$$-4s(h-t)s(h-x)\Big]+e^{-s(2h-t+x)}\Big[\kappa+3-2s(h+x)-2(\kappa+2)s(h-t)$$
$$+4s(h-t)s(h+x)\Big]+e^{-s(2h+t-x)}\Big[\kappa+3-2s(h-x)-2(\kappa+2)s(h+t)$$
$$+4s(h+t)s(h-x)\Big]+e^{-s(2h+t+x)}\Big[-\kappa-3+2s(h+x)+2(\kappa+2)s(h+t)$$
$$-4s(h+t)s(h+x)\Big]\Big\}. \qquad \text{(E.11)}$$

$$K_{23b}(x,t,s)=\frac{1}{2\kappa}\frac{\{\sin Ls\}}{1+4she^{-2sh}-e^{-4sh}}\Big[e^{-s(2h-t)}\left\{V_{61}e^{-s(2h-x)}+V_{62}e^{-s(2h+x)}\right\}$$
$$+e^{-s(2h+t)}\left\{V_{63}e^{-s(2h-x)}+V_{64}e^{-s(2h+x)}\right\}\Big],$$

$$V_{61}=2s(h-t)\Big\{\Big[-2s(h-x)+\kappa+2\Big](4sh-e^{-2sh})-1\Big\}+4sh$$
$$+\Big[\kappa+3-2s(h-x)\Big](1-4sh+e^{-2sh}),$$

$$V_{62}=2s(h-t)\Big\{\Big[2s(h+x)-\kappa-2\Big](4sh-e^{-2sh})+1\Big\}-4sh$$
$$+\Big[\kappa+3-2s(h+x)\Big](-1+4sh-e^{-2sh}),$$

$$V_{63}=2s(h+t)\Big\{\Big[2s(h-x)-\kappa-2\Big](4sh-e^{-2sh})+1\Big\}-4sh$$
$$+\Big[\kappa+3-2s(h-x)\Big](-1+4sh-e^{-2sh}),$$

$$V_{64}=2s(h+t)\Big\{\Big[-2s(h+x)+\kappa+2\Big](4sh-e^{-2sh})-1\Big\}+4sh$$
$$+\Big[\kappa+3-2s(h+x)\Big](1-4sh+e^{-2sh}). \qquad \text{(E.12a–e)}$$

$$K_{31\infty}(x,r,s)=\cos(Ls)\Big\{e^{-s(2h-r-x)}\big[3\kappa-1-2\kappa s(h-x)+6s(h-r)-4s(h-r)s(h-x)\big]$$
$$+e^{-s(2h-r+x)}\big[3\kappa-1-2\kappa s(h+x)+6s(h-r)-4s(h-r)s(h+x)\big]\Big\}.$$

(E.13)

$$K_{31b}(x,r,s)=\frac{\{\cos Ls\}e^{-s(2h-r)}}{1+4she^{-2sh}-e^{-4sh}}\Big\{V_{71}e^{-s(2h-x)}+V_{72}e^{-s(2h+x)}\Big\},$$

$$V_{71}=2s(h-r)\Big\{\big[3-2s(h-x)\big](4sh-e^{-2sh})-1\Big\}+\big[3-2s(h-x)\big]\Big\{1+\kappa(4sh-e^{-2sh})\Big\}$$
$$+e^{-2sh}-\kappa,$$

$$V_{72}=2s(h-r)\Big\{\big[3-2s(h+x)\big](4sh-e^{-2sh})-1\Big\}+\big[3-2s(h+x)\big]\Big\{1+\kappa(4sh-e^{-2sh})\Big\}$$
$$+e^{-2sh}-\kappa.$$ (E.14a–c)

$$K_{32\infty}(x,r,s)=\sin(Ls)\Big\{e^{-s(2h-r-x)}\big[3\kappa+1-2\kappa s(h-x)-6s(h-r)+4s(h-r)s(h-x)\big]$$
$$+e^{-s(2h-r+x)}\big[3\kappa+1-2\kappa s(h+x)-6s(h-r)+4s(h-r)s(h+x)\big]\Big\}.$$

(E.15)

$$K_{32b}(x,r,s)=\frac{\{\sin Ls\}e^{-s(2h-r)}}{1+4she^{-2sh}-e^{-4sh}}\Big\{V_{81}e^{-s(2h-x)}+V_{82}e^{-s(2h+x)}\Big\},$$

$$V_{81}=2s(h-r)\Big\{\big[-3+2s(h-x)\big](4sh-e^{-2sh})+1\Big\}-e^{-2sh}-\kappa$$
$$+\big[3-2s(h-x)\big]\Big\{-1+\kappa(4sh-e^{-2sh})\Big\},$$

$$V_{82}=2s(h-r)\Big\{\big[-3+2s(h+x)\big](4sh-e^{-2sh})+1\Big\}-e^{-2sh}-\kappa$$
$$+\big[3-2s(h+x)\big]\Big\{-1+\kappa(4sh-e^{-2sh})\Big\}.$$ (E.16a–c)

$$K_{33\infty}(x,t,s)=2\Big\{e^{-s(2h-t-x)}\big[2-s(h-x)-3s(h-t)+2s(h-t)s(h-x)\big]$$
$$+e^{-s(2h-t+x)}\big[2-s(h+x)-3s(h-t)+2s(h-t)s(h+x)\big]$$
$$+e^{-s(2h+t-x)}\big[-2+s(h-x)+3s(h+t)-2s(h+t)s(h-x)\big]$$
$$+e^{-s(2h+t+x)}\big[-2+s(h+x)+3s(h+t)-2s(h+t)s(h+x)\big]\Big\}.$$

(E.17)

$$K_{33b}(x,t,s)=\frac{1}{1+4she^{-2sh}-e^{-4sh}}\Big[e^{-s(2h-t)}\left\{V_{91}e^{-s(2h-x)}+V_{92}e^{-s(2h+x)}\right\}$$
$$+e^{-s(2h+t)}\left\{V_{93}e^{-s(2h-x)}+V_{94}e^{-s(2h+x)}\right\}\Big],$$

$$V_{91}=s(h-t)\left\{\left[-3+2s(h-x)\right](4sh-e^{-2sh})+1\right\}-2sh$$
$$+\left[2-s(h-x)\right]\left\{-1+4sh-e^{-2sh}\right\},$$

$$V_{92}=s(h-t)\left\{\left[-3+2s(h+x)\right](4sh-e^{-2sh})+1\right\}-2sh$$
$$+\left[2-s(h+x)\right]\left\{-1+4sh-e^{-2sh}\right\},$$

$$V_{93}=s(h+t)\left\{\left[3-2s(h-x)\right](4sh-e^{-2sh})-1\right\}+2sh$$
$$+\left[-2+s(h-x)\right]\left\{-1+4sh-e^{-2sh}\right\},$$

$$V_{94}=s(h+t)\left\{\left[3-2s(h+x)\right](4sh-e^{-2sh})-1\right\}+2sh$$
$$+\left[-2+s(h+x)\right]\left\{-1+4sh-e^{-2sh}\right\}. \qquad \text{(E.18a–e)}$$

$$k_{11s}(r,x)=\frac{1}{2\kappa}\left\{\frac{\kappa^2-3}{2h-r-x}+\frac{12(h-x)}{(2h-r-x)^2}-\frac{8(h-x)^2}{(2h-r-x)^3}\right.$$
$$+\frac{\kappa^2-3}{2h-r+x}+\frac{12(h+x)}{(2h-r+x)^2}-\frac{8(h+x)^2}{(2h-r+x)^3}$$
$$+(1-\kappa)^2\frac{2h-r-x}{(2h-r-x)^2+4L^2}$$
$$+2\left[\kappa(2h-r-x)-2(h-r)\right]\frac{(2h-r-x)^2-4L^2}{\left[(2h-r-x)^2+4L^2\right]^2}$$
$$+8(2h-r-x)(h-x)(h-r)\frac{(2h-r-x)^2-12L^2}{\left[(2h-r-x)^2+4L^2\right]^3}$$
$$+(1-\kappa)^2\frac{2h-r+x}{(2h-r+x)^2+4L^2}$$
$$+2\left[\kappa(2h-r+x)-2(h-r)\right]\frac{(2h-r+x)^2-4L^2}{\left[(2h-r+x)^2+4L^2\right]^2}$$
$$+8(2h-r+x)(h+x)(h-r)\frac{(2h-r+x)^2-12L^2}{\left[(2h-r+x)^2+4L^2\right]^3}$$
$$\left.+2\kappa\frac{r-x}{(r-x)^2+4L^2}-16L^2\frac{r-x}{\left[(r-x)^2+4L^2\right]^2}\right\}. \qquad \text{(E.19)}$$

$$k_{12s}(r,x)=\frac{1}{2\kappa}\Bigg\{-(1+2\kappa-\kappa^2)\frac{2L}{(2h-r-x)^2+4L^2}$$
$$+2\left[\kappa(h-x)+(2-\kappa)(h-r)\right]\frac{4L(2h-r-x)}{\left[(2h-r-x)^2+4L^2\right]^2}$$
$$-16L(h-x)(h-r)\frac{3(2h-r-x)^2-4L^2}{\left[(2h-r-x)^2+4L^2\right]^3}$$
$$-(1+2\kappa-\kappa^2)\frac{2L}{(2h-r+x)^2+4L^2}$$
$$+2\left[\kappa(h+x)+(2-\kappa)(h-r)\right]\frac{4L(2h-r+x)}{\left[(2h-r+x)^2+4L^2\right]^2}$$
$$-16L(h+x)(h-r)\frac{3(2h-r+x)^2-4L^2}{\left[(2h-r+x)^2+4L^2\right]^3}+\frac{4L}{(r-x)^2+4L^2}-\frac{32L^3}{\left[(r-x)^2+4L^2\right]^2}\Bigg\}$$

(E.20)

$$k_{13s}(t,x)=\frac{1}{2\kappa}\Bigg\{(\kappa-1)\frac{t-x}{(2h-t-x)^2+L^2}$$
$$+4\left[L^2(\kappa-1)(h-t)+\left\{-2(h-x)(h-t)-L^2\right\}(2h-t-x)\right]\frac{1}{\left[(2h-t-x)^2+L^2\right]^2}$$
$$+32L^2(h-x)(h-t)\frac{2h-t-x}{\left[(2h-t-x)^2+L^2\right]^3}+(\kappa-1)\frac{t+x}{(2h-t+x)^2+L^2}$$
$$+4\left[L^2(\kappa-1)(h-t)+\left\{-2(h+x)(h-t)-L^2\right\}(2h-t+x)\right]\frac{1}{\left[(2h-t+x)^2+L^2\right]^2}$$
$$+32L^2(h+x)(h-t)\frac{2h-t+x}{\left[(2h-t+x)^2+L^2\right]^3}+(\kappa-1)\frac{t+x}{(2h+t-x)^2+L^2}$$
$$-4\left[L^2(\kappa-1)(h+t)+\left\{-2(h-x)(h+t)-L^2\right\}(2h+t-x)\right]\frac{1}{\left[(2h+t-x)^2+L^2\right]^2}$$
$$-32L^2(h-x)(h+t)\frac{2h+t-x}{\left[(2h+t-x)^2+L^2\right]^3}+(\kappa-1)\frac{t-x}{(2h+t+x)^2+L^2}$$
$$-4\left[L^2(\kappa-1)(h+t)+\left\{-2(h+x)(h+t)-L^2\right\}(2h+t+x)\right]\frac{1}{\left[(2h+t+x)^2+L^2\right]^2}$$
$$-32L^2(h+x)(h+t)\frac{2h+t+x}{\left[(2h+t+x)^2+L^2\right]^3}$$

$$-(\kappa-1)\frac{t-x}{(t-x)^2+L^2}+4L^2\frac{t-x}{\left[(t-x)^2+L^2\right]^2}$$
$$-(\kappa-1)\frac{t+x}{(t+x)^2+L^2}+4L^2\frac{t+x}{\left[(t+x)^2+L^2\right]^2}\Bigg\}. \qquad \text{(E.21)}$$

$$k_{21s}(r,x)=\frac{1}{2\kappa}\Bigg\{(\kappa^2+2\kappa-1)\frac{2L}{(2h-r-x)^2+4L^2}$$
$$+4\left[(\kappa+2)(h-r)-\kappa(h-x)\right]\frac{2L(2h-r-x)}{\left[(2h-r-x)^2+4L^2\right]^2}$$
$$-8(h-x)(h-r)\frac{2L\left\{3(2h-r-x)^2-4L^2\right\}}{\left[(2h-r-x)^2+4L^2\right]^3}$$
$$-(\kappa^2+2\kappa-1)\frac{2L}{(2h-r+x)^2+4L^2}$$
$$-4\left[(\kappa+2)(h-r)-\kappa(h+x)\right]\frac{2L(2h-r+x)}{\left[(2h-r+x)^2+4L^2\right]^2}$$
$$+8(h+x)(h-r)\frac{2L\left\{3(2h-r+x)^2-4L^2\right\}}{\left[(2h-r+x)^2+4L^2\right]^3}$$
$$-\frac{4L}{(r-x)^2+4L^2}+\frac{32L^3}{\left[(r-x)^2+4L^2\right]^2}\Bigg\}. \qquad \text{(E.22)}$$

$$k_{22s}(r,x)=\frac{1}{2\kappa}\Bigg\{\frac{\kappa^2-3}{2h-r-x}+\frac{12(h-x)}{(2h-r-x)^2}-\frac{8(h-x)^2}{(2h-r-x)^3}$$
$$-\frac{\kappa^2-3}{2h-r+x}-\frac{12(h+x)}{(2h-r+x)^2}+\frac{8(h+x)^2}{(2h-r+x)^3}-(1+\kappa)^2\frac{(2h-r-x)}{(2h-r-x)^2+4L^2}$$
$$+2\left[(\kappa+2)(h-r)+\kappa(h-x)\right]\frac{(2h-r-x)^2-4L^2}{\left[(2h-r-x)^2+4L^2\right]^2}$$
$$-8(2h-r-x)(h-x)(h-r)\frac{(2h-r-x)^2-12L^2}{\left[(2h-r-x)^2+4L^2\right]^3}$$
$$+(1+\kappa)^2\frac{(2h-r+x)}{(2h-r+x)^2+4L^2}-2\left[(\kappa+2)(h-r)+\kappa(h+x)\right]\frac{(2h-r+x)^2-4L^2}{\left[(2h-r+x)^2+4L^2\right]^2}$$

$$+8(2h-r+x)(h+x)(h-r)\frac{(2h-r+x)^2-12L^2}{\left[(2h-r+x)^2+4L^2\right]^3}$$
$$-2\kappa\frac{r-x}{(r-x)^2+4L^2}-16L^2\frac{r-x}{\left[(r-x)^2+4L^2\right]^2}\Bigg\}. \tag{E.23}$$

$$k_{23s}(t,x)=\frac{1}{2\kappa}\Bigg\{(\kappa+3)\frac{L}{(2h-t-x)^2+L^2}-32L^2(h-t)(h-x)\frac{L}{\left[(2h-t-x)^2+L^2\right]^3}$$
$$+4\left[-(\kappa+2)(h-t)(2h-t-x)+\{5(h-t)-(h-x)\}(h-x)\right]\frac{L}{\left[(2h-t-x)^2+L^2\right]^2}$$
$$-(\kappa+3)\frac{L}{(2h-t+x)^2+L^2}+32L^2(h-t)(h+x)\frac{L}{\left[(2h-t+x)^2+L^2\right]^3}$$
$$+4\left[(\kappa+2)(h-t)(2h-t+x)+\{-5(h-t)+(h+x)\}(h+x)\right]\frac{L}{\left[(2h-t+x)^2+L^2\right]^2}$$
$$-(\kappa+3)\frac{L}{(2h+t-x)^2+L^2}+32L^2(h+t)(h-x)\frac{L}{\left[(2h+t-x)^2+L^2\right]^3}$$
$$+4\left[(\kappa+2)(h+t)(2h+t-x)+\{-5(h+t)+(h-x)\}(h-x)\right]\frac{L}{\left[(2h+t-x)^2+L^2\right]^2}$$
$$+(\kappa+3)\frac{L}{(2h+t+x)^2+L^2}-32L^2(h+t)(h+x)\frac{L}{\left[(2h+t+x)^2+L^2\right]^3}$$
$$+4\left[-(\kappa+2)(h+t)(2h+t+x)+\{5(h+t)-(h+x)\}(h+x)\right]\frac{L}{\left[(2h+t+x)^2+L^2\right]^2}$$
$$-(\kappa-1)\frac{L}{(t-x)^2+L^2}-4L^2\frac{L}{\left[(t-x)^2+L^2\right]^2}$$
$$+(\kappa-1)\frac{L}{(t+x)^2+L^2}+4L^2\frac{L}{\left[(t+x)^2+L^2\right]^2}\Bigg\}. \tag{E.24}$$

$$k_{31s}(r,x)=\{-(\kappa-1)(2h-r-x)-2(\kappa+3)(h-r)\}\frac{1}{(2h-r-x)^2+L^2}$$
$$+4\left[2(h-x)(h-r)(2h-r-x)+L^2\{3(h-r)-\kappa(h-x)\}\right]\frac{1}{\left[(2h-r-x)^2+L^2\right]^2}$$
$$-32L^2(h-x)(h-r)(2h-r-x)\frac{1}{\left[(2h-r-x)^2+L^2\right]^3}$$
$$+\{-(\kappa-1)(2h-r+x)-2(\kappa+3)(h-r)\}\frac{1}{(2h-r+x)^2+L^2}$$

$$+4\left[2(h+x)(h-r)(2h-r+x)+L^2\left\{3(h-r)-\kappa(h+x)\right\}\right]\frac{1}{\left[(2h-r+x)^2+L^2\right]^2}$$
$$-32L^2(h+x)(h-r)(2h-r+x)\frac{1}{\left[(2h-r+x)^2+L^2\right]^3}$$
$$+(\kappa-1)\frac{r-x}{(r-x)^2+L^2}-4L^2\frac{r-x}{\left[(r-x)^2+L^2\right]^2}. \qquad \text{(E.25)}$$

$$k_{32s}(r,x)=-(1+3\kappa)\frac{L}{(2h-r-x)^2+L^2}$$
$$+4\left\{\kappa(h-x)(2h-r-x)-3(h-r)(r-x)\right\}\frac{L}{\left[(2h-r-x)^2+L^2\right]^2}$$
$$+32L^2(h-x)(h-r)\frac{L}{\left[(2h-r-x)^2+L^2\right]^3}-(1+3\kappa)\frac{L}{(2h-r+x)^2+L^2}$$
$$+4\left\{\kappa(h+x)(2h-r+x)-3(h-r)(r+x)\right\}\frac{L}{\left[(2h-r+x)^2+L^2\right]^2}$$
$$+32L^2(h+x)(h-r)\frac{L}{\left[(2h-r+x)^2+L^2\right]^3}$$
$$-(\kappa+3)\frac{L}{(r-x)^2+L^2}+\frac{4L(r-x)^2}{\left[(r-x)^2+L^2\right]^2}. \qquad \text{(E.26)}$$

$$k_{33s}(t,x)=\frac{1}{2h-t-x}-6(h-x)\frac{1}{(2h-t-x)^2}+4(h-x)^2\frac{1}{(2h-t-x)^3}$$
$$+\frac{1}{2h-t+x}-6(h+x)\frac{1}{(2h-t+x)^2}+4(h+x)^2\frac{1}{(2h-t+x)^3}$$
$$-\frac{1}{2h+t-x}+6(h-x)\frac{1}{(2h+t-x)^2}-4(h-x)^2\frac{1}{(2h+t-x)^3}$$
$$-\frac{1}{2h+t+x}+6(h+x)\frac{1}{(2h+t+x)^2}-4(h+x)^2\frac{1}{(2h+t+x)^3}. \qquad \text{(E.27)}$$

## APPENDIX F

NON-DIMENSIONAL KERNELS OF EQS. (4.3)

$$\bar{k}_{11}(\xi,\varphi)=\bar{k}_{11s}(\xi,\varphi)+\int_0^\infty \overline{K}_{11b}(\xi,\varphi,w)dw. \tag{F.1}$$

$$\begin{aligned}\bar{k}_{11s}(\xi,\varphi)=\frac{j}{2\kappa}\Bigg\{&\frac{\kappa^2-3}{2-j\varphi-j\xi}+\frac{12(1-j\xi)}{(2-j\varphi-j\xi)^2}-\frac{8(1-j\xi)^2}{(2-j\varphi-j\xi)^3}\\&+\frac{\kappa^2-3}{2-j\varphi+j\xi}+\frac{12(1+j\xi)}{(2-j\varphi+j\xi)^2}-\frac{8(1+j\xi)^2}{(2-j\varphi+j\xi)^3}\\&+(1-\kappa)^2\frac{2-j\varphi-j\xi}{(2-j\varphi-j\xi)^2+4R^2}+(1-\kappa)^2\frac{2-j\varphi+j\xi}{(2-j\varphi+j\xi)^2+4R^2}\\&+2\left[\kappa(2-j\varphi-j\xi)-2(1-j\varphi)\right]\frac{(2-j\varphi-j\xi)^2-4R^2}{\left[(2-j\varphi-j\xi)^2+4R^2\right]^2}\\&+2\left[\kappa(2-j\varphi+j\xi)-2(1-j\varphi)\right]\frac{(2-j\varphi+j\xi)^2-4R^2}{\left[(2-j\varphi+j\xi)^2+4R^2\right]^2}\\&+8(2-j\varphi-j\xi)(1-j\xi)(1-j\varphi)\frac{(2-j\varphi-j\xi)^2-12R^2}{\left[(2-j\varphi-j\xi)^2+4R^2\right]^3}\\&+8(2-j\varphi+j\xi)(1+j\xi)(1-j\varphi)\frac{(2-j\varphi+j\xi)^2-12R^2}{\left[(2-j\varphi+j\xi)^2+4R^2\right]^3}\\&+2\kappa\frac{j\varphi-j\xi}{(j\varphi-j\xi)^2+4R^2}-16R^2\frac{j\varphi-j\xi}{\left[(j\varphi-j\xi)^2+4R^2\right]^2}\Bigg\}.\end{aligned} \tag{F.2}$$

$$\overline{K}_{11b}(\xi,\varphi,w)=\frac{j}{2\kappa}\frac{\{1+\cos 2Rw\}e^{-w(2-j\varphi)}}{1+4we^{-2w}-e^{-4w}}\left\{e^{-w(2-j\xi)}\overline{V}_{11}+e^{-w(2+j\xi)}\overline{V}_{12}\right\},$$

$$\begin{aligned}\overline{V}_{11}=&\,2w(1-j\varphi)\left\{(2w+\kappa-2)(e^{-2w}-4w)-1\right\}\\&+2\left[\left\{\kappa+2w(1-j\varphi)\right\}(4w-e^{-2w})+1\right]wj\xi\\&+\left[(1-\kappa)^2+2\kappa w\right](e^{-2w}-4w)+2(1-\kappa+w),\end{aligned}$$

$$\begin{aligned}\overline{V}_{12} &= 2w(1-j\varphi)\left\{(2w+\kappa-2)(e^{-2w}-4w)-1\right\}\\ &\quad +2\left[\left\{\kappa+2w(1-j\varphi)\right\}(e^{-2w}-4w)-1\right]wj\xi\\ &\quad +\left[(1-\kappa)^2+2\kappa w\right](e^{-2w}-4w)+2(1-\kappa+w)\,.\end{aligned} \tag{F.3a–c}$$

$$\overline{k}_{12}(\xi,\varphi)=\overline{k}_{12s}(\xi,\varphi)+\int_0^\infty \overline{K}_{12b}(\xi,\varphi,w)dw\,. \tag{F.4}$$

$$\begin{aligned}\overline{k}_{11s}(\xi,\varphi) &= \frac{j}{2\kappa}\left\{-(1+2\kappa-\kappa^2)\frac{2R}{(2-j\varphi-j\xi)^2+4R^2}\right.\\ &\quad -(1+2\kappa-\kappa^2)\frac{2R}{(2-j\varphi+j\xi)^2+4R^2}\\ &\quad +2\left[\kappa(1-j\xi)+(2-\kappa)(1-j\varphi)\right]\frac{4R(2-j\varphi-j\xi)}{\left[(2-j\varphi-j\xi)^2+4R^2\right]^2}\\ &\quad +2\left[\kappa(1+j\xi)+(2-\kappa)(1-j\varphi)\right]\frac{4R(2-j\varphi+j\xi)}{\left[(2-j\varphi+j\xi)^2+4R^2\right]^2}\\ &\quad -16R(1-j\xi)(1-j\varphi)\frac{3(2-j\varphi-j\xi)^2-4R^2}{\left[(2-j\varphi-j\xi)^2+4R^2\right]^3}\\ &\quad -16R(1+j\xi)(1-j\varphi)\frac{3(2-j\varphi+j\xi)^2-4R^2}{\left[(2-j\varphi+j\xi)^2+4R^2\right]^3}\\ &\quad \left.+\frac{4R}{(j\varphi-j\xi)^2+4R^2}-\frac{32R^3}{\left[(j\varphi-j\xi)^2+4R^2\right]^2}\right\}.\end{aligned} \tag{F.5}$$

$$\overline{K}_{12b}(\xi,\varphi,w)=\frac{j}{2\kappa}\frac{\{\sin 2Rw\}e^{-w(2-j\varphi)}}{1+4we^{-2w}-e^{-4w}}\left\{e^{-w(2-j\xi)}\overline{V}_{21}+e^{-w(2+j\xi)}\overline{V}_{22}\right\},$$

$$\begin{aligned}\overline{V}_{21} &= 2w(1-j\varphi)\left\{1-\left[2-\kappa-2w(1-j\xi)\right](4w-e^{-2w})\right\}-2-2w(1+j\xi)\\ &\quad +\left[1+2\kappa-\kappa^2-2\kappa w(1-j\xi)\right](4w-e^{-2w}),\\ \overline{V}_{22} &= 2w(1-j\varphi)\left\{1-\left[2-\kappa-2w(1+j\xi)\right](4w-e^{-2w})\right\}-2-2w(1-j\xi)\\ &\quad +\left[1+2\kappa-\kappa^2-2\kappa w(1+j\xi)\right](4w-e^{-2w}).\end{aligned} \tag{F.6a–c}$$

$$\overline{k}_{13}(\xi,\rho)=\overline{k}_{13s}(\xi,\rho)+\int_0^\infty \overline{K}_{13b}(\xi,\rho,w)dw\,. \tag{F.7}$$

$$\bar{k}_{13s}(\xi,\rho)=\frac{f}{2\kappa}\Bigg[(\kappa-1)\Bigg\{\frac{f\rho+g-j\xi}{(2-f\rho-g-j\xi)^2+R^2}+\frac{f\rho+g+j\xi}{(2-f\rho-g+j\xi)^2+R^2}$$
$$+\frac{f\rho+g+j\xi}{(2+f\rho+g-j\xi)^2+R^2}+\frac{f\rho+g-j\xi}{(2+f\rho+g+j\xi)^2+R^2}$$
$$-\frac{f\rho+g-j\xi}{(f\rho+g-j\xi)^2+R^2}-\frac{f\rho+g+j\xi}{(f\rho+g+j\xi)^2+R^2}\Bigg\}$$
$$+4\Big[R^2(\kappa-1)(1-f\rho-g)$$
$$+\Big\{-2(1-j\xi)(1-f\rho-g)-R^2\Big\}(2-f\rho-g-j\xi)\Big]\frac{1}{\Big[(2-f\rho-g-j\xi)^2+R^2\Big]^2}$$
$$+4\Big[R^2(\kappa-1)(1-f\rho-g)$$
$$+\Big\{-2(1+j\xi)(1-f\rho-g)-R^2\Big\}(2-f\rho-g+j\xi)\Big]\frac{1}{\Big[(2-f\rho-g+j\xi)^2+R^2\Big]^2}$$
$$-4\Big[R^2(\kappa-1)(1+f\rho+g)$$
$$+\Big\{-2(1-j\xi)(1+f\rho+g)-R^2\Big\}(2+f\rho+g-j\xi)\Big]\frac{1}{\Big[(2+f\rho+g-j\xi)^2+R^2\Big]^2}$$
$$-4\Big[R^2(\kappa-1)(1+f\rho+g)$$
$$+\Big\{-2(1+j\xi)(1+f\rho+g)-R^2\Big\}(2+f\rho+g+j\xi)\Big]\frac{1}{\Big[(2+f\rho+g+j\xi)^2+R^2\Big]^2}$$
$$+32(1-j\xi)(1-f\rho-g)\frac{R^2(2-f\rho-g-j\xi)}{\Big[(2-f\rho-g-j\xi)^2+R^2\Big]^3}$$
$$+32(1+j\xi)(1-f\rho-g)\frac{R^2(2-f\rho-g+j\xi)}{\Big[(2-f\rho-g+j\xi)^2+R^2\Big]^3}$$
$$-32(1-j\xi)(1+f\rho+g)\frac{R^2(2+f\rho+g-j\xi)}{\Big[(2+f\rho+g-j\xi)^2+R^2\Big]^3}$$
$$-32(1+j\xi)(1+f\rho+g)\frac{R^2(2+f\rho+g+j\xi)}{\Big[(2+f\rho+g+j\xi)^2+R^2\Big]^3}$$
$$+4\frac{R^2(f\rho+g-j\xi)}{\Big[(f\rho+g-j\xi)^2+R^2\Big]^2}+4\frac{R^2(f\rho+g+j\xi)}{\Big[(f\rho+g+j\xi)^2+R^2\Big]^2}\Bigg]. \qquad \text{(F.8)}$$

$$\overline{K}_{13b}(\xi,\rho,w)=\frac{f}{2\kappa}\frac{\{\cos Rw\}}{1+4we^{-2w}-e^{-4w}}\Big[e^{-w(2-f\rho-g)}\left\{e^{-w(2-j\xi)}\overline{V}_{31}+e^{-w(2+j\xi)}\overline{V}_{32}\right\}$$
$$+e^{-w(2+f\rho+g)}\left\{e^{-w(2-j\xi)}\overline{V}_{33}+e^{-w(2+j\xi)}\overline{V}_{34}\right\}\Big],$$

$$\overline{V}_{31}=2w(1-f\rho-g)\left\{\left[\kappa-2+2w(1-j\xi)\right](4w-e^{-2w})+1\right\}-4w$$
$$+\left[\kappa-3+2w(1-j\xi)\right](1-4w+e^{-2w}),$$

$$\overline{V}_{32}=2w(1-f\rho-g)\left\{\left[\kappa-2+2w(1+j\xi)\right](4w-e^{-2w})+1\right\}-4w$$
$$+\left[\kappa-3+2w(1+j\xi)\right](1-4w+e^{-2w}),$$

$$\overline{V}_{33}=2w(1+f\rho+g)\left\{\left[\kappa-2+2w(1-j\xi)\right](e^{-2w}-4w)+1\right\}+4w$$
$$+\left[-\kappa+3-2w(1-j\xi)\right](1-4w+e^{-2w}),$$

$$\overline{V}_{34}=2w(1+f\rho+g)\left\{\left[\kappa-2+2w(1+j\xi)\right](e^{-2w}-4w)+1\right\}+4w$$
$$+\left[-\kappa+3-2w(1+j\xi)\right](1-4w+e^{-2w}).$$

(F.9a–e)

$$\overline{k}_{21}(\xi,\varphi)=\overline{k}_{21s}(\xi,\varphi)+\int_0^\infty\overline{K}_{21b}(\xi,\varphi,w)dw. \tag{F.10}$$

$$\overline{k}_{21s}(\xi,\varphi)=\frac{j}{2\kappa}\Bigg\{(-1+2\kappa+\kappa^2)\frac{2R}{(2-j\varphi-j\xi)^2+4R^2}$$
$$+(1-2\kappa-\kappa^2)\frac{2R}{(2-j\varphi+j\xi)^2+4R^2}$$
$$+2\left[-\kappa(1-j\xi)+(2+\kappa)(1-j\varphi)\right]\frac{4R(2-j\varphi-j\xi)}{\left[(2-j\varphi-j\xi)^2+4R^2\right]^2}-\frac{4R}{(j\varphi-j\xi)^2+4R^2}$$
$$+2\left[\kappa(1+j\xi)-(2+\kappa)(1-j\varphi)\right]\frac{4R(2-j\varphi+j\xi)}{\left[(2-j\varphi+j\xi)^2+4R^2\right]^2}+\frac{32R^3}{\left[(j\varphi-j\xi)^2+4R^2\right]^2}$$
$$-16R(1-j\xi)(1-j\varphi)\frac{3(2-j\varphi-j\xi)^2-4R^2}{\left[(2-j\varphi-j\xi)^2+4R^2\right]^3}$$
$$+16R(1+j\xi)(1-j\varphi)\frac{3(2-j\varphi+j\xi)^2-4R^2}{\left[(2-j\varphi+j\xi)^2+4R^2\right]^3}\Bigg\}. \tag{F.11}$$

$$\overline{K}_{21b}(\xi,\varphi,w)=\frac{j}{2\kappa}\frac{\{\sin 2Rw\}e^{-w(2-j\varphi)}}{1+4we^{-2w}-e^{-4w}}\left\{e^{-w(2-j\xi)}\overline{V}_{41}+e^{-w(2+j\xi)}\overline{V}_{42}\right\},$$

$$\overline{V}_{41} = \left\{2w(1-j\varphi)\left[-2-\kappa+2w(1-j\xi)\right]+2\kappa w(1-j\xi)+1-2\kappa-\kappa^2\right\}(4w-e^{-2w})$$
$$+2w(1-j\varphi)-2-2w(1+j\xi),$$

$$\overline{V}_{42} = \left\{2w(1-j\varphi)\left[2+\kappa-2w(1+j\xi)\right]-2\kappa w(1+j\xi)-1+2\kappa+\kappa^2\right\}(4w-e^{-2w})$$
$$-2w(1-j\varphi)+2+2w(1-j\xi).$$

(F.12a–c)

$$\overline{k}_{22}(\xi,\varphi) = \overline{k}_{22s}(\xi,\varphi) + \int_0^\infty \overline{K}_{22b}(\xi,\varphi,w)dw. \tag{F.13}$$

$$\begin{aligned}\overline{k}_{22s}(\xi,\varphi) = \frac{j}{2\kappa}\Bigg\{ & \frac{\kappa^2-3}{2-j\varphi-j\xi}+\frac{12(1-j\xi)}{(2-j\varphi-j\xi)^2}-\frac{8(1-j\xi)^2}{(2-j\varphi-j\xi)^3} \\ & -\frac{\kappa^2-3}{2-j\varphi+j\xi}-\frac{12(1+j\xi)}{(2-j\varphi+j\xi)^2}+\frac{8(1+j\xi)^2}{(2-j\varphi+j\xi)^3} \\ & -(1+\kappa)^2\frac{(2-j\varphi-j\xi)}{(2-j\varphi-j\xi)^2+4R^2}+(1+\kappa)^2\frac{(2-j\varphi+j\xi)}{(2-j\varphi+j\xi)^2+4R^2} \\ & +2\left[(2+\kappa)(1-j\varphi)+\kappa(1-j\xi)\right]\frac{(2-j\varphi-j\xi)^2-4R^2}{\left[(2-j\varphi-j\xi)^2+4R^2\right]^2} \\ & -2\left[(2+\kappa)(1-j\varphi)+\kappa(1+j\xi)\right]\frac{(2-j\varphi+j\xi)^2-4R^2}{\left[(2-j\varphi+j\xi)^2+4R^2\right]^2} \\ & -8(2-j\varphi-j\xi)(1-j\xi)(1-j\varphi)\frac{(2-j\varphi-j\xi)^2-12R^2}{\left[(2-j\varphi-j\xi)^2+4R^2\right]^3} \\ & +8(2-j\varphi+j\xi)(1+j\xi)(1-j\varphi)\frac{(2-j\varphi+j\xi)^2-12R^2}{\left[(2-j\varphi+j\xi)^2+4R^2\right]^3} \\ & -2\kappa\frac{j\varphi-j\xi}{(j\varphi-j\xi)^2+4R^2}-16R^2\frac{j\varphi-j\xi}{\left[(j\varphi-j\xi)^2+4R^2\right]^2}\Bigg\}. \end{aligned} \tag{F.14}$$

$$\overline{K}_{22b}(\xi,\varphi,w) = \frac{j}{2\kappa}\frac{\{1-\cos 2Rw\}e^{-w(2-j\varphi)}}{1+4we^{-2w}-e^{-4w}}\left\{e^{-w(2-j\xi)}\overline{V}_{51}+e^{-w(2+j\xi)}\overline{V}_{52}\right\},$$

$$\overline{V}_{51} = 2w(1-j\varphi)\left\{\left[2w(1-j\xi)-2-\kappa\right](e^{-2w}-4w)-1\right\}+2\left[1+\kappa+w(1+j\xi)\right]$$
$$+\left[2\kappa w(1-j\xi)-(1+\kappa)^2\right](4w-e^{-2w}),$$

$$\overline{V}_{52} = 2w(1-j\varphi)\left\{\left[-2w(1+j\xi)+2+\kappa\right](e^{-2w}-4w)+1\right\}-2\left[1+\kappa+w(1-j\xi)\right]$$
$$+\left[-2\kappa w(1+j\xi)+(1+\kappa)^2\right](4w-e^{-2w})\,. \qquad \text{(F.15a–c)}$$

$$\overline{k}_{23}(\xi,\rho) = \overline{k}_{23s}(\xi,\rho)+\int_0^\infty \overline{K}_{23b}(\xi,\rho,w)dw\,. \qquad \text{(F.16)}$$

$$\begin{aligned}
\overline{k}_{23S}(\xi,\rho) = \frac{f}{2\kappa}\Bigg[ & (\kappa+3)\left\{\frac{R}{(2-f\rho-g-j\xi)^2+R^2}-\frac{R}{(2-f\rho-g+j\xi)^2+R^2}\right.\\
& \left.-\frac{R}{(2+f\rho+g-j\xi)^2+R^2}+\frac{R}{(2+f\rho+g+j\xi)^2+R^2}\right\}\\
& +4\left[-(\kappa+2)(1-f\rho-g)(2-f\rho-g-j\xi)\right.\\
& \left.+\left\{5(1-f\rho-g)-(1-j\xi)\right\}(1-j\xi)\right]\frac{R}{\left[(2-f\rho-g-j\xi)^2+R^2\right]^2}\\
& +4\left[(\kappa+2)(1-f\rho-g)(2-f\rho-g+j\xi)\right.\\
& \left.+\left\{-5(1-f\rho-g)+(1+j\xi)\right\}(1+j\xi)\right]\frac{R}{\left[(2-f\rho-g+j\xi)^2+R^2\right]^2}\\
& +4\left[(\kappa+2)(1+f\rho+g)(2+f\rho+g-j\xi)\right.\\
& \left.+\left\{-5(1+f\rho+g)+(1-j\xi)\right\}(1-j\xi)\right]\frac{R}{\left[(2+f\rho+g-j\xi)^2+R^2\right]^2}\\
& +4\left[-(\kappa+2)(1+f\rho+g)(2+f\rho+g+j\xi)\right.\\
& \left.+\left\{5(1+f\rho+g)-(1+j\xi)\right\}(1+j\xi)\right]\frac{R}{\left[(2+f\rho+g+j\xi)^2+R^2\right]^2}\\
& -32R^2(1-f\rho-g)(1-j\xi)\frac{R}{\left[(2-f\rho-g-j\xi)^2+R^2\right]^3}\\
& +32R^2(1-f\rho-g)(1+j\xi)\frac{R}{\left[(2-f\rho-g+j\xi)^2+R^2\right]^3}\\
& +32R^2(1+f\rho+g)(1-j\xi)\frac{R}{\left[(2+f\rho+g-j\xi)^2+R^2\right]^3}\\
& -32R^2(1+f\rho+g)(1+j\xi)\frac{R}{\left[(2+f\rho+g+j\xi)^2+R^2\right]^3}\\
& -(\kappa-1)\frac{R}{(f\rho+g-j\xi)^2+R^2}+(\kappa-1)\frac{R}{(f\rho+g+j\xi)^2+R^2}\\
& -4R^2\frac{R}{\left[(f\rho+g-j\xi)^2+R^2\right]^2}+4R^2\frac{R}{\left[(f\rho+g+j\xi)^2+R^2\right]^2}\Bigg]\,. \qquad \text{(F.17)}
\end{aligned}$$

$$\overline{K}_{23b}(\xi,\rho,w)=\frac{f}{2\kappa}\frac{\{\sin Rw\}}{1+4we^{-2w}-e^{-4w}}\Big[e^{-w(2-f\rho-g)}\left\{e^{-w(2-j\xi)}\overline{V}_{61}+e^{-w(2+j\xi)}\overline{V}_{62}\right\}$$
$$+e^{-w(2+f\rho+g)}\left\{e^{-w(2-j\xi)}\overline{V}_{63}+e^{-w(2+j\xi)}\overline{V}_{64}\right\}\Big],$$

$$\overline{V}_{61}=2w(1-f\rho-g)\left\{\left[2+\kappa-2w(1-j\xi)\right](4w-e^{-2w})-1\right\}+4w$$
$$+\left[\kappa+3-2w(1-j\xi)\right](1-4w+e^{-2w}),$$

$$\overline{V}_{62}=2w(1-f\rho-g)\left\{\left[-2-\kappa+2w(1+j\xi)\right](4w-e^{-2w})+1\right\}-4w$$
$$+\left[\kappa+3-2w(1+j\xi)\right](-1+4w-e^{-2w}),$$

$$\overline{V}_{63}=2w(1+f\rho+g)\left\{\left[-2-\kappa+2w(1-j\xi)\right](4w-e^{-2w})+1\right\}-4w$$
$$+\left[\kappa+3-2w(1-j\xi)\right](-1+4w-e^{-2w}),$$

$$\overline{V}_{64}=2w(1+f\rho+g)\left\{\left[2+\kappa-2w(1+j\xi)\right](4w-e^{-2w})-1\right\}+4w$$
$$+\left[\kappa+3-2w(1+j\xi)\right](1-4w+e^{-2w}).$$

(F.18a–e)

$$\overline{k}_{31}(\eta,\varphi)=\overline{k}_{31s}(\eta,\varphi)+\int_0^\infty\overline{K}_{31b}(\eta,\varphi,w)dw. \qquad \text{(F.19)}$$

$$\overline{k}_{31s}(\eta,\varphi)=j\Bigg[\left\{-(\kappa-1)(2-j\varphi-f\eta-g)-2(\kappa+3)(1-j\varphi)\right\}\frac{1}{(2-j\varphi-f\eta-g)^2+R^2}$$
$$+\left\{-(\kappa-1)(2-j\varphi+f\eta+g)-2(\kappa+3)(1-j\varphi)\right\}\frac{1}{(2-j\varphi+f\eta+g)^2+R^2}$$
$$+4\Big[2(1-f\eta-g)(1-j\varphi)(2-j\varphi-f\eta-g)$$
$$+R^2\left\{3(1-j\varphi)-\kappa(1-f\eta-g)\right\}\Big]\frac{1}{\left[(2-j\varphi-f\eta-g)^2+R^2\right]^2}$$
$$+4\Big[2(1+f\eta+g)(1-j\varphi)(2-j\varphi+f\eta+g)$$
$$+R^2\left\{3(1-j\varphi)-\kappa(1+f\eta+g)\right\}\Big]\frac{1}{\left[(2-j\varphi+f\eta+g)^2+R^2\right]^2}$$
$$-32R^2(1-f\eta-g)(1-j\varphi)(2-j\varphi-f\eta-g)\frac{1}{\left[(2-j\varphi-f\eta-g)^2+R^2\right]^3}$$

$$-32R^2(1+f\eta+g)(1-j\varphi)(2-j\varphi+f\eta+g)\frac{1}{\left[(2-j\varphi+f\eta+g)^2+R^2\right]^3}$$
$$+(\kappa-1)\frac{j\varphi-f\eta-g}{(j\varphi-f\eta-g)^2+R^2}-4\frac{R^2(j\varphi-f\eta-g)}{\left[(j\varphi-f\eta-g)^2+R^2\right]^2}\Bigg].$$

(F.20)

$$\overline{K}_{31b}(\eta,\varphi,w)=j\frac{\{\cos Rw\}e^{-w(2-j\varphi)}}{1+4we^{-2w}-e^{-4w}}\left\{e^{-w(2-f\eta-g)}\overline{V}_{71}+e^{-w(2+f\eta+g)}\overline{V}_{72}\right\},$$

$$\overline{V}_{71}=2w(1-j\varphi)\left\{\left[3-2w(1-f\eta-g)\right](4w-e^{-2w})-1\right\}+e^{-2w}-\kappa$$
$$+\left[3-2w(1-f\eta-g)\right]\left\{1+\kappa(4w-e^{-2w})\right\},$$

$$\overline{V}_{72}=2w(1-j\varphi)\left\{\left[3-2w(1+f\eta+g)\right](4w-e^{-2w})-1\right\}+e^{-2w}-\kappa$$
$$+\left[3-2w(1+f\eta+g)\right]\left\{1+\kappa(4w-e^{-2w})\right\}.$$

(F.21a–c)

$$\overline{k}_{32}(\eta,\varphi)=\overline{k}_{32s}(\eta,\varphi)+\int_0^\infty\overline{K}_{32b}(\eta,\varphi,w)dw.$$ (F.22)

$$\overline{k}_{32S}(\eta,\varphi)=j\Bigg[-(1+3\kappa)\left\{\frac{R}{(2-j\varphi-f\eta-g)^2+R^2}+\frac{R}{(2-j\varphi+f\eta+g)^2+R^2}\right\}$$
$$+4\{\kappa(1-f\eta-g)(2-j\varphi-f\eta-g)$$
$$-3(1-j\varphi)(j\varphi-f\eta-g)\}\frac{R}{\left[(2-j\varphi-f\eta-g)^2+R^2\right]^2}$$
$$+4\{\kappa(1+f\eta+g)(2-j\varphi+f\eta+g)$$
$$-3(1-j\varphi)(j\varphi+f\eta+g)\}\frac{R}{\left[(2-j\varphi+f\eta+g)^2+R^2\right]^2}$$
$$+32R^2(1-f\eta-g)(1-j\varphi)\frac{R}{\left[(2-j\varphi-f\eta-g)^2+R^2\right]^3}$$
$$+32R^2(1+f\eta+g)(1-j\varphi)\frac{R}{\left[(2-j\varphi+f\eta+g)^2+R^2\right]^3}$$

$$-(\kappa+3)\frac{R}{(j\varphi-f\eta-g)^2+R^2}+4(j\varphi-f\eta-g)^2\frac{R}{\left[(j\varphi-f\eta-g)^2+R^2\right]^2}\Bigg].$$

(F.23)

$$\overline{K}_{32b}(\eta,\varphi,w)=j\frac{\{\sin Rw\}e^{-w(2-j\varphi)}}{1+4we^{-2w}-e^{-4w}}\left\{e^{-w(2-f\eta-g)}\overline{V}_{81}+e^{-w(2+f\eta+g)}\overline{V}_{82}\right\},$$

$$\begin{aligned}\overline{V}_{81}&=2w(1-j\varphi)\left\{\left[-3+2w(1-f\eta-g)\right](4w-e^{-2w})+1\right\}-e^{-2w}-\kappa\\&\quad+\left[3-2w(1-f\eta-g)\right]\left\{-1+\kappa(4w-e^{-2w})\right\},\\\overline{V}_{82}&=2w(1-j\varphi)\left\{\left[-3+2w(1+f\eta+g)\right](4w-e^{-2w})+1\right\}-e^{-2w}-\kappa\\&\quad+\left[3-2w(1+f\eta+g)\right]\left\{-1+\kappa(4w-e^{-2w})\right\}.\end{aligned}$$

(F.24a–c)

$$\overline{k}_{33}(\eta,\rho)=\overline{k}_{33s}(\eta,\rho)+\int_0^\infty\overline{K}_{33b}(\eta,\rho,w)dw.$$

(F.25)

$$\begin{aligned}\overline{k}_{33s}(\eta,\rho)&=\frac{f}{2-f\rho-f\eta-2g}-6(1-f\eta-g)\frac{f}{(2-f\rho-f\eta-2g)^2}\\&\quad+4(1-f\eta-g)^2\frac{1}{(2-f\rho-f\eta-2g)^3}+\frac{f}{2-f\rho+f\eta}\\&\quad-6(1+f\eta+g)\frac{f}{(2-f\rho+f\eta)^2}+4(1+f\eta+g)^2\frac{f}{(2-f\rho+f\eta)^3}\\&\quad-\frac{f}{2+f\rho-f\eta}+6(1-f\eta-g)\frac{f}{(2+f\rho-f\eta)^2}\\&\quad-4(1-f\eta-g)^2\frac{f}{(2+f\rho-f\eta)^3}-\frac{f}{2+f\rho+f\eta+2g}\\&\quad+6(1+f\eta+g)\frac{f}{(2+f\rho+f\eta+2g)^2}-4(1+f\eta+g)^2\frac{f}{(2+f\rho+f\eta+2g)^3}\end{aligned}$$

.

(F.26)

$$\begin{aligned}\overline{K}_{33b}(\eta,\rho,w)=\frac{f}{1+4we^{-2w}-e^{-4w}}\Big[&e^{-w(2-f\rho-g)}\left\{e^{-w(2-f\eta-g)}\overline{V}_{91}+e^{-w(2+f\eta+g)}\overline{V}_{92}\right\}\\&+e^{-w(2+f\rho+g)}\left\{e^{-w(2-f\eta-g)}\overline{V}_{93}+e^{-w(2+f\eta+g)}\overline{V}_{94}\right\}\Big],\end{aligned}$$

$$\bar{V}_{91} = w(1-f\rho-g)\{[-3+2w(1-f\eta-g)](4w-e^{-2w})+1\}-2w$$
$$+[2-w(1-f\eta-g)]\{-1+4w-e^{-2w}\},$$

$$\bar{V}_{92} = w(1-f\rho-g)\{[-3+2w(1+f\eta+g)](4w-e^{-2w})+1\}-2w$$
$$+[2-w(1+f\eta+g)]\{-1+4w-e^{-2w}\},$$

$$\bar{V}_{93} = w(1+f\rho+g)\{[3-2w(1-f\eta-g)](4w-e^{-2w})-1\}+2w$$
$$+[-2+w(1-f\eta-g)]\{-1+4w-e^{-2w}\},$$

$$\bar{V}_{94} = w(1+f\rho+g)\{[3-2w(1+f\eta+g)](4w-e^{-2w})-1\}+2w$$
$$+[-2+w(1+f\eta+g)]\{-1+4w-e^{-2w}\}.$$

(F.27a–e)

## APPENDIX G

LIMITS OF CERTAIN INTEGRALS

Evaluation of the limits of certain integrals from Erdogan (1968):

Let $f(t)$ be continuous and satisfying Hölder condition in the relevant interval, then

$$\lim_{L-y\to 0}\int_0^{\infty} f(t)\left(\frac{L-y}{(L-y)^2+(t-x)^2}\pm\frac{L-y}{(L-y)^2+(t+x)^2}\right)dt$$

$$=\lim_{L-y\to 0}\int_{x-\varepsilon}^{x+\varepsilon}(L-y)\,f(t)\left(\frac{1}{(L-y)^2+(t-x)^2}\pm\frac{1}{(L-y)^2+(t+x)^2}\right)dt,$$

$$=\lim_{L-y\to 0}\int_{x-\varepsilon}^{x+\varepsilon} f(t)\frac{L-y}{(L-y)^2+(t-x)^2}dt=\pi f(x). \qquad \text{(G.1)}$$

$$\lim_{L-y\to 0}\int_0^{\infty} f(t)\left\{\frac{(L-y)^3-(L-y)(t-x)^2}{\left[(L-y)^2+(t-x)^2\right]^2}\pm\frac{(L-y)^3-(L-y)(t+x)^2}{\left[(L-y)^2+(t+x)^2\right]^2}\right\}dt$$

$$=\lim_{L-y\to 0}\int_{x-\varepsilon}^{x+\varepsilon} f(t)\frac{(L-y)^3-(L-y)(t-x)^2}{\left[(L-y)^2+(t-x)^2\right]^2}dt,$$

$$=f(x)\left\{\frac{\pi}{2}-\frac{\pi}{2}\right\}=0. \qquad \text{(G.2)}$$

$$\lim_{L-y\to 0}\int_0^{\infty} f(t)\left\{\frac{(L-y)^3(t+x)}{\left[(L-y)^2+(t+x)^2\right]^2}-\frac{(L-y)^3(t-x)}{\left[(L-y)^2+(t-x)^2\right]^2}\right\}dt$$

$$=\lim_{L-y\to 0}\int_{x-\varepsilon}^{x+\varepsilon} f(t)\frac{-(L-y)^2(t-x)}{\left[(L-y)^2+(t-x)^2\right]^2}dt$$

$$=-\lim_{L-y\to 0}\int_{-\varepsilon}^{\varepsilon} f(x+a)\frac{(L-y)^2\alpha}{\left[(L-y)^2+\alpha^2\right]^2}d\alpha=0. \qquad \text{(G.3)}$$